UNIVERSITY OF VENDA

REMEDIATION OF ACID MINE DRAINAGE USING MAGNESITE AND ITS BENTONITE CLAY COMPOSITE

By

Vhahangwele Masindi (***Pr. Sci. Nat.***)

Senior Researcher

Council for Scientific and Industrial Research (CSIR)

A thesis submitted to the University of Venda, School of Environmental Sciences, Department of Ecology and Resource Management in partial fulfilment of the requirements for degree of **Doctor of Philosophy in Environmental Science**.

Promoter: Prof. Mugera Wilson Gitari

Co-promoters: Prof. Hlanganani Tutu

Dr. Marinda De Beer

2015

DEDICATION

I dedicate this part of work to my family:

1 Gundo Masindi
2 Murangi Precious Masindi
3 Vhuthuhawe Junior Masindi
4 Vhudihawe Masindi
5 Murudzi Masindi

These people are wonderful; they are the reason why I keep on smiling and working extra hard every day. I love them unconditionally. May God keep us together till end of time.

DECLARATION

I declare that "**Remediation of acid mine drainage using magnesite and its bentonite clay composite"** is my own work in execution and design, that it has not been submitted for any degree or examination in any other university and that all the sources I have used have been indicated and duly acknowledged by complete references. It is being submitted for the Degree of Doctor of Philosophy in Environmental Science to the University of the Venda, Limpopo Province, South Africa.

Signature: ..... Date: 20-11-2015

Masindi Vhahangwele (Pr. Sci. Nat.)

University of Venda (UNIVEN)

Council for Scientific and Industrial Research (CSIR)

This thesis is submitted after examination and approval by the following supervisors

Signature: ... . Date: 20-11-2015

Prof Mugera Wilson Gitari (University of Venda)

Signature: .... Date: 20-11-2015

Prof Hlanganani Tutu (University of the Witwatersrand)

Signature: ..... Date: 20-11-2015

Dr Marinda De Beer (Council for Scientific and Industrial Research)

ACKNOWLEDGEMENTS

I would like to convey my sincere gratitude to the **Research and Innovation Directorate**, **Department of Ecology and Resource management**, **School of Environmental Sciences**, **University of Venda**, **Council for Scientific and Industrial Research (CSIR)**, **SASOL-INZALO**, the **National Research Foundation (NRF)**, the **Department of Science and Technology (DST) and ESKOM-TESP** for funding this project.

The following Institutions are acknowledged for collaboration work and the people that we worked with that led to achieving most of the objectives:

My supervisors **Prof Mugera Wilson Gitari** (Environmental Remediation and Water Pollution Chemistry Group, Department of Ecology and Resources Management, University of Venda, P/bag X5050, Thohoyandou, 0950, South Africa), **Prof Hlanganani Tutu** (Molecular Sciences Institute, School of Chemistry, University of the Witwatersrand, P/Bag X4, WITS, 2050, Johannesburg, South Africa) and **Dr Marinda de Beer** (DST/CSIR National Centre for Nano-structured Materials, Council for Scientific and Industrial Research, P.O Box 395, Pretoria, 0001, South Africa) for their advice and support throughout this work.

I would like to extend my sincere thanks to my research assistant **Glynn K. Pindihama** for his assistance, encouragement and stimulating discussions.

To the real treasure in my life, my beloved wife. There are no single words that could ever express what she did and always does for me and how much appreciation I have for her. She has always been there for me throughout my studies.

I wish to thank all faculty members and support staff of the Department of Ecology and Resource Management and postgraduate students, for their continuous support, constant help and extending the departmental facilities for my project work.

I would also like to thank my family for the roles they played in my life. For the special love and care they gave me. Your love is indispensable and immeasurable.

At last but not the least, I would like to thank the Almighty God for giving me life and energy.

ACADEMIC AND TECHNICAL OUTPUTS

PATENTS

Masindi V and Gitari W.M (2015) Treatment of wastewater using cryptocrystalline magnesite, filed in Canada, USA, Argentina, Australia and South Africa.

Masindi V and Gitari W.M (2015) Treatment of wastewater using mechanochemically synthesized magnesite and bentonite clay composite, filed in Canada, USA, Argentina, Australia and South Africa.

PUBLICATIONS

Masindi, V., Gitari, W., Tutu, H. & Debeer, M. 2015. Passive remediation of acid mine drainage using cryptocrystalline magnesite: A batch experimental and geochemical modelling approach. *Water SA,* 41**,** 677 - 682.

Masindi, V., Gitari, W., Tutu, H. & Debeer, M. 2015. Fate of inorganic contaminants post treatment of acid mine drainage with cryptocrystalline magnesite: A batch experimental and geochemical modelling approach. *Journal of Environmental Chemical Engineering*. http://dx.doi.org/10.1016/j.jece.2016.03.020.

Masindi, V., Gitari, M. W., Tutu, H. & Debeer, M. 2015. Efficiency of ball milled South African bentonite clay for remediation of acid mine drainage. *Journal of Water Process Engineering,* 8**,** 227-240.

Masindi, V., Gitari, W. M., Tutu, H. & De Beer, M. 2015. Synthesis of cryptocrystalline magnesite-bentonite clay composite and its application for neutralization and attenuation of inorganic contaminants in acidic and metalliferous mine drainage. *Water Process Engineering,* http://dx.doi.org/10.1016/j.jwpe.2015.11.007.

CONFERENCE PROCEEDINGS

Masindi V., Gitari W.M., Tutu H., De Beer M., Nekhwevha N., 2014. Neutralization and attenuation of inorganic contaminants from acid mine drainage and mine leachates using cryptocrystalline magnesite: A batch experimental approach: An Interdisciplinary Response to Mine Water Challenges - Sui, Sun & Wang (eds) China University of Mining and Technology Press, Xuzhou, ISBN 978-7-5646-2437-8

Masindi V., Gitari W.M., Tutu H., De Beer M., 2015. Synthesis of a porous magnesite-bentonite clay composite and its application for neutralisation and attenuation of inorganic contaminants in acidic and metalliferous mine drainage, Green and innovative technologies and engineering solutions for environmental issue, 5th International Conference on Environment 2015 (ICENV 2015) 18th – 19th August, 2015 Penang, Malaysia, ISBN 978-967-394-219-0

Masindi V., Gitari W.M., Tutu H., De Beer M., 2015. Efficiency of ball milled South African Bentonite Clay for remediation of acid mine drainage. 1st UNIVEN-WSU International Research Conference, 2 - 4 September 2015

Masindi V., Gitari W.M., Tutu H., De Beer M., 2015. Treatment of acid mine drainage using cryptocrystalline magnesite: An experimental and geochemical modelling approach, 4th YWP-ZA Biennial Conference and 1st Africa-wide YWP Conference, 16-18 November 2015 at the CSIR International Convention Centre in Pretoria, South Africa.

Masindi V., Gitari W.M., Tutu H., De Beer M., 2015. Integration of geochemical modelling and experimental results to establish fates of inorganic contaminants during the treatment of acid mine drainage with cryptocrystalline magnesite, CSIR Emerging Researcher Symposium, 16-18 October 2015 at the CSIR International Convention Centre in Pretoria, SA.

OTHER PUBLICATIONS RELATED TO THIS WORK

Masindi, V. 2016. A novel technology for neutralizing acidity and attenuating toxic chemical species from acid mine drainage using cryptocrystalline magnesite tailings. *Journal of Water Process Engineering,* 10**,** 67-77.

Masindi, V. & Gitari Mugera, W. 2015. The potential of ball-milled South African bentonite clay for attenuation of heavy metals from acidic wastewaters: Simultaneous sorption of Co^{2+}, Cu^{2+}, Ni^{2+}, Pb^{2+}, and Zn^{2+} ions. *Journal of Environmental Chemical Engineering,* 3**,** 2416-2425.

Masindi, V., Gitari Mugera, W., Tutu, H. & De Beer, M. 2014a. Removal of selenium from wastewater by using magnesite-bentonite clay composite: Kinetics and Equilibrium studies *The North American Conference on Sustainability, Energy & the Environment***,** 227 - 245.

Masindi, V., Gitari, M. W., Tutu, H. & De Beer, M. 2014b. Application of magnesite–bentonite clay composite as an alternative technology for removal of arsenic from industrial effluents. *Toxicological and Environmental Chemistry,* 96**,** 1435-1451.

Masindi, V., Gitari, M. W., Tutu, H. & Debeer, M. 2015a. Removal of boron from aqueous solution using magnesite and bentonite clay composite. *Desalination and Water Treatment***,** 1-11.

Masindi, V. & Gitari, W. M. 2016a. Removal of arsenic from wastewaters by cryptocrystalline magnesite: complimenting experimental results with modelling. *Journal of Cleaner Production,* 113**,** 318-324.

Masindi, V. & Gitari, W. M. 2016b. Simultaneous removal of metal species from acidic aqueous solutions using cryptocrystalline magnesite/bentonite clay composite: an experimental and modelling approach. *Journal of Cleaner Production,* 112, Part 1**,** 1077-1085.

Masindi, V., Gitari, W. M. & Ngulube, T. 2015b. Kinetics and equilibrium studies for removal of fluoride from underground water using cryptocrystalline magnesite. *Journal of Water Reuse and Desalination,* 5**,** 282-292.

Masindi, V., Gitari, W. M. & Pindihama, K. G. 2015c. Adsorption of phosphate from municipal effluents using cryptocrystalline magnesite: complementing laboratory results with geochemical modelling. *Desalination and Water Treatment*.

Masindi, V., Gitari, W. M. & Pindihama, K. G. 2015d. Synthesis of nanocomposite of cryptocrystalline magnesite-bentonite clay and its application for phosphate removal from municipal effluents. *Environ Technol,* 24**,** 1-27.

TABLE OF CONTENTS

LIST OF FIGURES

LIST OF TABLES

ABSTRACT

Wastewaters originating from mining activities are usually acidic and often contain high concentrations of Fe, Mn, Al and SO_4^{2-} in addition to traces of Pb, Co, Ni, Cu, Zn, Mg, Ca and Na. This wastewater impacts surface and subsurface water resources negatively and has to be treated before release to receiving aquatic ecosystems. Numerous wastewater treatment technologies have been developed and implemented. However, cost implications, ineffectiveness, selective treatment capabilities and generation of secondary sludge that is toxic and expensive to dispose-off to the environment due to stringent environmental regulations often limit their application. As such, mining companies are in a search for cheaper, brine free, effective and efficient mine water treatment technology. This study assessed the potential of applying mechanochemically modified cryptocrystalline magnesite-bentonite clay composite for acid mine drainage (AMD) treatment. To accomplish this, neutralization of acidity and removal of inorganic contaminants from mine effluents were studied using batch laboratory experiments and precipitation of chemical species was determined using pH Redox Equilibrium (in C language) (PHREEQC) geochemical modelling. The present study was divided into three parts which includes: (1) the application of magnesite for remediation of AMD, (2) the application of ball milled bentonite clay for remediation of AMD and (3) the application of magnesite-bentonite clay composite for remediation of AMD.

In the first part of the study, AMD was reacted with cryptocrystalline magnesite. The reaction of AMD with magnesite at an optimum solid: liquid ratio of 1:100 and contact time of 60 min led to an increase in pH, reaching a maximum pH of 10, resulting in significant precipitation of most metal species. Increase of pH in solution with contact time caused the removal of the metal ions mainly by precipitation, co-precipitation and adsorption. SO_4^{2-} concentration was lowered from 4640 to 1910 mg/L. Fe was mainly removed as $Fe(OH)_3$, goethite, and jarosite, Al as basaluminite, boehmite and jurbanite, $Al(OH)_3$ and as gibbsite and diaspore. Al and Fe precipitated as iron (oxy)-hydroxides and aluminium (oxy)-hydroxides. Mn precipitated as rhodochrosite and manganite. Ca was removed as gypsum. Sulphate was removed as gypsum, and Fe, Al hydroxyl sulphate minerals. Mg was removed as brucite and dolomite. These would explain the decrease in the metal species and SO_4^{2-} concentration in the product water. Cryptocrystalline magnesite effectively neutralized AMD and attenuated concentration of

inorganic species to within Department of Water and Sanitation (DWS) water quality guidelines for 1997. Though > 60% SO_4^{2-} removal was achieved, a polishing technology will be required to remove alkali and alkaline earth metal species and remaining SO_4^{2-} from the aqueous system.

In the second part of this study, AMD was reacted with ball milled bentonite clay. The contact of AMD with bentonite clay led to an increase in pH and a significant reduction in concentrations of metal species. At constant agitation time of 30 mins, the pH increased with the increase in dosage of bentonite clay. Removal of Mn^{2+}, Al^{3+}, and Fe^{3+} was greatest after 30 min of agitation. The adsorption affinity obeyed the sequence: Fe > Al > Mn > SO_4^{2-}. The pH of reacted AMD was > 6. Bentonite clay showed high adsorption capacities for Al and Fe at concentration < 500 mg/L, while the capacity for Mn was lower. Adsorption efficiency for SO_4^{2-} was > 50%. Adsorption kinetics revealed that the suitable kinetic model describing data was pseudo-second-order hence confirming chemisorption. Adsorption isotherms indicated that removal of metals fitted the Langmuir adsorption isotherm for Fe and SO_4^{2-} and the Freundlich adsorption isotherm for Al and Mn, respectively. Gibbs free energy model predicted that the reaction is not spontaneous in nature for Al, Fe and Mn except for SO_4^{2-}. Ball-milled bentonite clay showed an excellent capacity in neutralising acidity and lowering the levels of inorganic contaminants in acidic mine effluents. A polishing technology will be required to remove alkali and alkaline earth metal species and remaining SO_4^{2-} from the aqueous system.

The third part of the study evaluated the reaction of magnesite-bentonite clay composite in neutralisation of the acidity and attenuates levels of inorganic contaminants in metalliferous effluents. The interaction of the composite with AMD led to an increase in pH (pH >11) and lowering of metal concentrations. The removal of Al^{3+}, $Fe^{3+/2+}$, Mn^{2+} and SO_4^{2-} was optimum at 20 min of equilibration and 1g of adsorbent dosage. The composite removed ≈99% (Al^{3+}, Fe^{3+}, and Mn^{2+}) and ≈90% (SO_4^{2-}) from raw mine effluent. Minor elements such as Co, Cu, Zn, Ni and Pb were also removed significantly. The synthesized composite showed a significantly better heavy metals and SO_4^{2-} removal ability of from highly acidic solutions as compared to that obtained by cryptocrystalline magnesite and bentonite clay when used individually. Adsorption kinetics fitted better to pseudo-second-order kinetic than pseudo-first-order kinetic and intra-particle diffusion model hence confirming chemisorption. Adsorption data fitted better to Freundlich adsorption isotherm than Langmuir hence

confirming multisite adsorption. Gibbs free energy model predicted that the reaction is spontaneous in nature for Al, Fe and SO_4^{2-} except for Mn. Geochemical model indicated that Fe was removed as $Fe(OH)_3$, goethite, and jarosite, Al as basaluminite, boehmite and jurbanite, $Al(OH)_3$ and as gibbsite and diaspore. Al and Fe precipitated as iron (oxy)-hydroxides and aluminium (oxy)-hydroxides. Mn precipitated as rhodochrosite and manganite. Ca was removed as gypsum. Sulphate (SO_4^{2-}) was removed as gypsum, and Fe, Al hydroxyl sulphate minerals. Mg was removed as brucite and dolomite. This would explain the decrease in the metal species and SO_4^{2-} concentration in the product water. The composite removed the contaminants to below South African legal requirements for water use. It was concluded that the composite has the potential to neutralize acidity and attenuate potentially toxic chemical species from acidic and metalliferous mine drainage as compared to cryptocrystalline magnesite and bentonite clay when used individually. As such, it can be concluded that the new synthesized composite has a synergetic potential in wastewater treatment.

Keywords: Acid mine drainage; cryptocrystalline magnesite; bentonite clay; cryptocrystalline magnesite-bentonite clay composite; chemical species; batch experiments; adsorption; precipitation; geochemical modelling

CHAPTER ONE

INTRODUCTION

1.1 Background information

Mining of coal and gold has left serious environmental pollution in its awake (Gitari et al., 2006, Tutu et al., 2008). Mineral extraction processes expose sulphide bearing minerals such as pyrite (FeS_2), pyrrhotite (Fe_xS_x), chalcocite (Cu_2S), Covellite (CuS), chalcopyrite ($CuFeS_2$), molybdenite (MoS_2), millerite (NiS), galena (PbS), sphelerite (ZnS) and arsenoprite (FeAsS) to oxidizing conditions. During rainfall and underground mine workings, those minerals react with water and oxygen to form sulphuric acid (Wang, 2010, Simate and Ndlovu, 2014). The resultant acid leaches out metals from the surrounding geology (Sracek et al., 2004). Formation of acidic and metalliferous drainage is also mediated by oxidizing bacterial species which include such as: *Thiobacillus ferrooxidans, Ferrobacillus sulphooxidans* and *Thiobacillus thiooxidans* (Baker and Banfield, 2003, Akcil and Koldas, 2006, Abreu et al., 2011, Bálintová and Singovszká, 2011, Butler, 2011).

The potential of the surrounding geology to generate acid mine drainage (AMD) is governed by numerous factors such as the sulphur content in the surrounding geology and associated strata, hydrology and geology of the area (Valente and Leal Gomes, 2009, Vazquez, 2009, Wang, 2010, Van Vuuren, 2011, Zhang et al., 2013, Wildeman et al., 2014). Physically, the colour of AMD is determined by the dominant metals. Iron rich AMD is characterized by a yellowish to reddish colour, Aluminium rich AMD is characterized by a white colour and manganese rich AMD is characterized by a black colour (Hedin et al., 2005, Hallberg, 2010, Figueiredo and da Silva, 2011, Ghosh et al., 2012, Equeenuddin et al., 2013, Grawunder et al., 2014). Chemically, AMD is characterized by acidic pH and toxic chemical species such as Al, Fe, and Mn, anions of SO_4^{2-} and traces of As, B, Ba, Co, Cr, Cu, Mo, Ni, Sr and Zn. On dissolution, those chemical species are transported downstream to receiving aquatic ecosystems or leached to underground water resources (Gitari et al., 2006, Wade et al., 2006, Wisskirchen et al., 2006, Xu et al., 2007, Tutu et al., 2008, Xu et al., 2009, Wang, 2010, Gitari et al., 2011, Van Vuuren, 2011, Sun et al., 2012, Zvimba et al., 2012, Gitari et al.,

2013, Oberholster et al., 2013, Park et al., 2013, Torres and Auleda, 2013, Ntuli et al., 2014, Rimstidt and Vaughan, 2014, Simate and Ndlovu, 2014, Suponik and Blanco, 2014, Wildeman et al., 2014).

This alters the chemical profile of surface and underground water resources and its suitability to cater for variety of defined uses. An array of scientific studies have documented that AMD is hazardous to terrestrial and aquatic organisms (Gitari *et al.*, 2013). On exposure, AMD can cause skin irritation to human skin and killing of fish and other aquatic organisms. It can also cause blindness on contact with eyes and variety of cancers and other diseases because it contains potentially toxic chemical species from ore and tailings or parent rock (Botz and Mason, 1990, Bortnikova et al., 2001, Achterberg et al., 2003, Akcil and Koldas, 2006, Dsa et al., 2008, Morais et al., 2008, Da Silveira et al., 2009, Afriyie-Debrah et al., 2010, Behum et al., 2010, Abreu et al., 2011, Cormier, 2011, Borrego et al., 2012, Boukhalfa and Chaguer, 2012, Ekemen Keskin et al., 2013).

Considering the potential impacts that AMD can impose to terrestrial and aquatic ecosystems, this wastewater originating from mining activities need to be contained, managed and treated prior to discharge. A number of technologies have been developed and used for treatment of AMD and they include precipitation (Mayo et al., 2000, Watten et al., 2005, Pérez-López et al., 2010, Macingova and Luptakova, 2011, Madzivire et al., 2011, Luptakova et al., 2012, Labastida et al., 2013, Heviánková et al., 2014), ion-exchange (Cheng et al., 2009, Gaikwad, 2010, Buzzi et al., 2013, Torres and Auleda, 2013, Martí-Calatayud et al., 2014), adsorption (Mohan and Chander, 2006, Gitari et al., 2008, Motsi et al., 2009, Sarmiento et al., 2009, Zhang, 2011, Chen et al., 2013, Falayi and Ntuli, 2014), coagulation (Dong et al., 2011, Ruihua et al., 2011, Radić et al., 2014), and bio-sorption (Demchak et al., 2001, Brenner, 2004, Johnson and Hallberg, 2005, Whitehead and Prior, 2005, Tutu et al., 2008, White et al., 2011, Sheridan et al., 2013). Moreover, cost factors, inefficiencies, selective adsorption, inconveniences and generation of secondary sludge, limit their adoption (Johnson and Hallberg, 2005). From the stated reasons, it is clear that there is a need for a low cost and effective method which can neutralize and remove toxic chemical species from AMD.

Due to high adsorption capacity, magnificent ion exchange and swelling properties, high surface area, leafy or lamella morphology, abundance and low cost clay minerals have been

received vast applications in depollution science (Zhao et al., 2011). To improve the adsorption and depollution properties, clay needs to be modified to improve its adsorption capacity which is dependent on pH and concentration of pollutants in aqueous solution. Commonly used methods for clay modification include:

- Intercalation and pillaring (Bhattacharyya and Gupta, 2006, Masindi et al., 2014b, Masindi et al., 2015a, Masindi et al., 2015b),
- Acid activation (Bhattacharyya and Gupta, 2006, Bhattacharyya and Gupta, 2008b, Bhattacharyya and Gupta, 2008a, Bhattacharyya and Gupta, 2011),
- Mechanochemical activation (Masindi et al., 2014a, Dukić et al., 2015, Masindi and Gitari Mugera, 2015, Masindi et al., 2015a, Masindi and Gitari, 2015, Masindi et al., 2015c)
- and Organoclays (Lepoitevin et al., 2014).

Amongst all clay modifications and composite synthesis science, mechanochemical activation has been recommended by numerous studies due to high metals attenuation potentials. Nevertheless, mechanochemical modification is economic viable and environmental friendly as compared to other modification techniques. Documented literature has revealed that mechanochemical modification lead to improved physiochemical properties of clay that makes it the best material for water decontamination (Masindi and Gitari Mugera, 2015, Masindi et al., 2015a). Moreover, limited studies have evaluated the use of mechanical milling on improving the adsorption properties of clay for pollutants in wastewater (Dukić et al., 2015, Masindi and Gitari Mugera, 2015).

The use of vibratory ball mill for synthesizing and pulverization clay minerals may lead to fragmentation, distortion, breakage of crystalline network and particle size reduction. It also lead to increased surface area, and trigger the exfoliation and amorphization of particles hence enhancing the removal efficiencies of the pollutants by fabricated composites and clay minerals (Dukić et al., 2015). On the other hand, longer milling times lead to the agglomeration of finer particles that result in the decrease of the cation exchange capacity (CEC) (Dukić et al., 2015, Masindi and Gitari Mugera, 2015), as such, milling need to be medium enough to maintain high cation exchange capacity of clay. Moreover, the metals attenuation ability of clay is limited by pH of the solution, at pH < 4 the metal removal efficiencies of clay is poor (Gitari, 2014). In the quest to find pragmatic ways that will improve the limitations of virgin raw and modified clays as adsorbents, the adsorbents can be

prepared in a composite form with some metal oxides or carbonates (Dukić et al., 2015, Masindi et al., 2015a, Masindi and Gitari, 2015).

To respond to the challenges that are been presented by current technologies, government, mining houses, and scientific communities are seeking for innovative and locally available technologies for remediating AMD. The present study was designed with the aim of synthesizing mechanochemically modified bentonite clay using a vibratory ball mill and evaluate its application for neutralization and attenuation of inorganic contaminants in metalliferous and acidic mine effluents.

1.2 Problem statement

Discharge of highly acidic effluent from abandoned gold mines on the Witwatersrand goldfields, South Africa has led to pollution of surface and subsurface aquatic ecosystems (Tutu et al., 2008). AMD pollution can degrade the habitats of aquatic organisms, causes safety problems, ruins the natural aesthetics and impacts the economy of the country negatively (Maree et al., 2004, Ntuli et al., 2014, Simate and Ndlovu, 2014). Acidity and heavy loads of metals inhibit plants growth, corrodes infrastructure and kills intolerant species. It degrades the water quality rendering it unfit for multitudes defined uses . Numerous wastewater treatment technologies have been developed to decontaminate mine wastewaters in an attempt to produce safe drinking water but very few of them have been reported to produce water that is within the legal requirement. The majority of AMD treatment technologies are species selective and some require two steps of pretreatment. South Africa primarily relies on the use of lime ($CaCO_3$) for neutralizing or raising the pH of AMD.

During liming of AMD to neutralize the pH, metals precipitate as hydroxides and the final product of the neutralization reaction is calcium sulphate dehydrate (gypsum), and produces waters, compositions of which exceed the Department of Water and Sanitation (DWS) (previously known as Department of Water Affairs and Forestry, DWAF) stipulated water guidelines for Domestic Water Use (Gitari et al., 2006, Madzivire et al., 2010, Madzivire et al., 2014). The mainly gypsum sludge may also contain toxic metal species, which require proper disposal and frequent long-term environmental hazard monitoring which is unsatisfactory. Chemical treatment of mine wastewater by neutralization produces

voluminous sludge that is expensive to store and dispose-off (Madzivire et al., 2011). Consequently, there is a need to devise an alternative technology that can neutralize AMD and remove inorganic contaminants in a single treatment step, if possible.

The results of this investigation will assist in solving the challenge of AMD pollution by formulating cryptocrystalline magnesite-bentonite clay composite that can neutralize AMD and remove inorganic contaminants in a single step. It will also reveal conditions that will be useful in designing a pilot AMD treatment plant.

1.3 Objective

1.3.1 Main objective

The overall aim of this study was to assess cryptocrystalline magnesite, bentonite clay and magnesite-bentonite clay blends/composites as treatment agents for acid mine drainage.

1.3.2 Specific objectives

To achieve the above overall aim, the following specific objectives were pursued;

- Determination of the physicochemical and mineralogical properties of cryptocrystalline magnesite, bentonite clay and the composite.
- Identification of the chemical composition of AMD from the Witwatersrand Western Basin, Gauteng, South Africa
- Assessment of the optimum conditions for treatment of AMD using cryptocrystalline magnesite, bentonite clay and their composite in batch tests, and explore the chemistry of the resultant residue and processed water;
- Investigation of the mineralogical transformation and chemical characterization of resultant solid residues and geochemical modelling of process water.

1.4 Research questions

In order to address the main and specific objectives of this project, specific questions were formulated. These led to tasks that had to be accomplished to achieve the objectives of this project. The research questions were as follows:

- What are the physicochemical and mineralogical properties of cryptocrystalline magnesite, bentonite clay and the composite?
- What are the chemical compositions of AMD from the Witwatersrand Western Basin, Gauteng, South Africa?
- What is the chemistry of processed water and the resultant solid residues after interacting AMD with the cryptocrystalline magnesite and bentonite clay?
- What is the chemistry of the processed water and the resultant solid residues after interacting AMD with magnesite/bentonite clay composite?
- How does the quality of treated water compare with the South African water quality guidelines?

1.5 Hypothesis

Magnesite and bentonite clay treatment techniques alone are not as efficient as their composite material in terms of AMD treatment.

1.6 Novelty of the work

Cryptocrystalline magnesite, vibratory ball milled bentonite clay and magnesite-bentonite clay composite have, to the author's knowledge, never been used for treatment of AMD, therefore, this is the first study to evaluate the feasibility of applying cryptocrystalline magnesite, bentonite clay and magnesite-bentonite clay composite for neutralisation and attenuation of inorganic contaminants from metalliferous and acidic mine effluents.

This study identified optimum conditions required to treat AMD using magnesite and ball milled bentonite clay, and the prevailing chemistry thereof. A new mechanochemical synthesis was also developed using a vibratory ball mill and evaluated for neutralization of acidity and attenuate inorganic contaminants in a single step evaluated.

The results from this study will assist in the scaling up of the process from laboratory to pilot-plant scale with the aim of constructing a full-scale treatment plant.

1.7 Thesis structure

This thesis is divided into six chapters, each explaining different aspects of the investigation. A summary of each chapter is given below.

CHAPTER 1: Introduction

A brief background of the AMD problem is given together with different attempted solutions to the problem. The magnitude of AMD problem in South Africa and the need for a solution for AMD to be treated prior to release to avoid surface and subsurface water contamination is also reported. An outline of the objectives, research questions, study significance, hypothesis and novelty of the study are briefly discussed.

CHAPTER 2: Literature review

An in-depth explanation of the AMD problem and solutions is given: The formation process, its sources, environmental impacts, and the available treatment technologies. The physicochemical properties of magnesite and bentonite clay and their applications in wastewater treatment are investigated. The geochemical model employed to predict speciation, mechanisms of metal attenuation and for complementing experimental results is also discussed in brief.

CHAPTER 3: Attenuation of acidity and inorganic contaminants from acid mine drainage by cryptocrystalline magnesite

This chapter describes the process of optimization of the reaction conditions between simulated acid mine drainage (SAMD) and magnesite. The species of concern were Al, Fe, Mn and SO_4^{2-}. This section also discusses the chemistry of the product residues and the fate of chemical species in AMD before and after the treatment process. It also employs geochemical modelling to complement results obtained from laboratory experiments.

CHAPTER 4: Efficiency of ball milled South African bentonite clay for remediation of acid mine drainage

This chapter pointed out the optimum conditions that were used for treatment of AMD using bentonite clay. The species of concern were Al, Fe, Mn and SO_4^{2-}. The chemistry of the product residues and the fate of chemical species in AMD after the treatment process are elucidated. Mechanisms of neutralization and metals attenuation by bentonite clay composite were also reported in this section.

CHAPTER 5: Synthesis of cryptocrystalline magnesite-bentonite clay composite and its application for neutralization and attenuation of inorganic contaminants in acidic and metalliferous mine drainage

This chapter describes the process of optimization of the reaction conditions between AMD and magnesite-bentonite clay composite. The species of concern were Al, Fe, Mn and SO_4^{2-}. The chemistry of the product residues and the fate of chemical species in AMD after the treatment process are elucidated. Mechanisms of neutralization and metals attenuation by magnesite-bentonite clay composite were also reported in this section.

CHAPTER 6: Conclusions and recommendation

This is the last chapter of the thesis. It presents an executive summary of the findings and discussions of the results of this study. It also makes recommendations for further research.

REFERENCES

Abreu, M. M., Batista, M. J., Magalhães, M. C. F. & Matos, J. X. 2011. Acid mine drainage in the Portuguese Iberian Pyrite Belt. *Mine Drainage and Related Problems.*

Achterberg, E. P., Herzl, V. M. C., Braungardt, C. B. & Millward, G. E. 2003. Metal behaviour in an estuary polluted by acid mine drainage: the role of particulate matter. *Environmental Pollution,* 121**,** 283-292.

Afriyie-Debrah, C., Obiri-Danso, K. & Ephraim, J. H. Acid mine drainage - Effect on creeks or streams in a mining community in Ghana and treatment options. ICEEA 2010 - 2010 International Conference on Environmental Engineering and Applications, Proceedings, 2010. 285-290.

Akcil, A. & Koldas, S. 2006. Acid Mine Drainage (AMD): causes, treatment and case studies. *Journal of Cleaner Production,* 14**,** 1139-1145.

Baker, B. J. & Banfield, J. F. 2003. Microbial communities in acid mine drainage. *FEMS Microbiology Ecology,* 44**,** 139-152.

Bálintová, M. & Singovszká, E. Acid mine drainage as environmental risk for surface water. 11th International Multidisciplinary Scientific Geoconference and EXPO - Modern Management of Mine Producing, Geology and Environmental Protection, SGEM 2011, 2011. 175-182.

Behum, P. T., Kiser, R. & Lewis, L. Investigation of the acid mine drainage at the tabsimco mine, Illinois: Observations and implications for treatment. Joint Mining Reclamation Conf. 2010 - 27th Meeting of the ASMR, 12th Pennsylvania Abandoned Mine Reclamation Conf. and 4th Appalachian Regional Reforestation Initiative Mined Land Reforestation Conf., 2010. 1-5.

Bhattacharyya, K. G. & Gupta, S. S. 2006. Kaolinite, montmorillonite, and their modified derivatives as adsorbents for removal of Cu(II) from aqueous solution. *Separation and Purification Technology,* 50**,** 388-397.

Bhattacharyya, K. G. & Gupta, S. S. 2008a. Adsorption of a few heavy metals on natural and modified kaolinite and montmorillonite: A review. *Advances in Colloid and Interface Science,* 140**,** 114-131.

Bhattacharyya, K. G. & Gupta, S. S. 2008b. Influence of acid activation on adsorption of Ni(II) and Cu(II) on kaolinite and montmorillonite: Kinetic and thermodynamic study. *Chemical Engineering Journal,* 136**,** 1-13.

Bhattacharyya, K. G. & Gupta, S. S. 2011. Removal of Cu(II) by natural and acid-activated clays: An insight of adsorption isotherm, kinetic and thermodynamics. *Desalination,* 272**,** 66-75.

Borrego, J., Carro, B., López-González, N., De La Rosa, J., Grande, J. A., Gómez, T. & De La Torre, M. L. 2012. Effect of acid mine drainage on dissolved rare earth elements geochemistry along a fluvial-estuarine system: The Tinto-Odiel Estuary (S.W. Spain). *Hydrology Research,* 43**,** 262-274.

Bortnikova, S. B., Smolyakov, B. S., Sidenko, N. V., Kolonin, G. R., Bessonova, E. P. & Androsova, N. V. 2001. Geochemical consequences of acid mine drainage into a natural reservoir: Inorganic precipitation and effects on plankton activity. *Journal of Geochemical Exploration,* 74**,** 127-139.

Botz, M. K. & Mason, S. E. 1990. Prevention of acid drainage from gold mining in the western United States and impacts on water quality. *International Journal of Mine Water,* 9**,** 27-41.

Boukhalfa, C. & Chaguer, M. 2012. Characterisation of sediments polluted by acid mine drainage in the northeast of Algeria. *International Journal of Sediment Research,* 27**,** 402-407.

Brenner, F. J. Use of constructed wetlands for acid mine drainage abatement on a watershed basis. Bridging the Gap: Meeting the World's Water and Environmental Resources Challenges - Proceedings of the World Water and Environmental Resources Congress 2001, 2004.

Butler, B. A. 2011. Effect of imposed anaerobic conditions on metals release from acid-mine drainage contaminated streambed sediments. *Water Research,* 45**,** 328-336.

Buzzi, D. C., Viegas, L. S., Rodrigues, M. a. S., Bernardes, A. M. & Tenório, J. a. S. 2013. Water recovery from acid mine drainage by electrodialysis. *Minerals Engineering,* 40**,** 82-89.

Chen, Y. F., Cao, L. X., Lin, H., Dong, Y. B., Cheng, H. & Huo, H. X. 2013. Adsorption of Cu2+ from simulated acid mine drainage by herb-medicine residues and wheat bran. *Zhongguo Youse Jinshu Xuebao/Chinese Journal of Nonferrous Metals,* 23**,** 1775-1782.

Cheng, H., Hu, Y., Luo, J., Xu, B. & Zhao, J. 2009. Geochemical processes controlling fate and transport of arsenic in acid mine drainage (AMD) and natural systems. *Journal of Hazardous Materials,* 165**,** 13-26.

Cormier, J. Acid Mine Drainage as a sustainable solution to eliminate risk and reduce costs. Tailings and Mine Waste'10 - Proceedings of the 14th International Conference on Tailings and Mine Waste, 2011. 439-449.

Da Silveira, F. Z., Defaveri, T. M., Ricken, C., Zocche, J. J. & Pich, C. T. Toxicity and genotoxicity evaluation of acid mine drainage treatment using Artemia sp. and geophagus brasiliensis as bioindicators. 26th Annual Meetings of the American Society of Mining and Reclamation and 11th Billings Land Reclamation Symposium 2009, 2009. 1704-1721.

Demchak, J., Morrow, T. & Skousen, J. 2001. Treatment of acid mine drainage by four vertical flow wetlands in Pennsylvania. *Geochemistry: Exploration, Environment, Analysis,* 1**,** 71-80.

Dong, H., Guan, X., Wang, D., Li, C., Yang, X. & Dou, X. 2011. A novel application of H2O2–Fe(II) process for arsenate removal from synthetic acid mine drainage (AMD) water. *Chemosphere,* 85**,** 1115-1121.

Dsa, J. V., Johnson, K. S., Lopez, D., Kanuckel, C. & Tumlinson, J. 2008. Residual toxicity of acid mine drainage-contaminated sediment to stream macroinvertebrates: Relative contribution of acidity vs. metals. *Water, Air, and Soil Pollution,* 194**,** 185-197.

Dukić, A. B., Kumrić, K. R., Vukelić, N. S., Dimitrijević, M. S., Baščarević, Z. D., Kurko, S. V. & Matović, L. L. 2015. Simultaneous removal of Pb(II), Cu(II), Zn(II) and Cd(II) from highly acidic solutions using mechanochemically synthesized montmorillonite-kaolinite/TiO2 composite. *Applied Clay Science,* 103**,** 20-27.

Ekemen Keskin, T., Toptaş, S. & Ersöz, F. 2013. Acid rock drainage, and trace element pollution in groundwater in surrounding of Kurşunlu mine area. *Jeoloji Muhendisligi Dergisi,* 37**,** 1-25.

Equeenuddin, S. M., Tripathy, S., Sahoo, P. K. & Panigrahi, M. K. 2013. Metal behavior in sediment associated with acid mine drainage stream: Role of pH. *Journal of Geochemical Exploration,* 124**,** 230-237.

Falayi, T. & Ntuli, F. 2014. Removal of heavy metals and neutralisation of acid mine drainage with un-activated attapulgite. *Journal of Industrial and Engineering Chemistry,* 20**,** 1285-1292.

Figueiredo, M. O. & Da Silva, T. P. 2011. The positive environmental contribution of jarosite by retaining lead in acid mine drainage areas. *International Journal of Environmental Research and Public Health,* 8**,** 1575-1582.

Gaikwad, R. W. 2010. Review and research needs of active treatment of acid mine drainage by ion exchange. *Electronic Journal of Environmental, Agricultural and Food Chemistry,* 9**,** 1343-1350.

Ghosh, S., Moitra, M., Woolverton, C. J. & Leff, L. G. 2012. Effects of remediation on the bacterial community of an acid mine drainage impacted stream. *Canadian Journal of Microbiology,* 58**,** 1316-1326.

Gitari, M., Petrik, L., Etchebers, O., Key, D., Iwuoha, E. & Okujeni, C. 2006. Treatment of acid mine drainage with fly ash: Removal of major contaminants and trace elements. *Journal of Environmental Science and Health - Part A Toxic/Hazardous Substances and Environmental Engineering,* 41**,** 1729-1747.

Gitari, W. M. 2014. Attenuation of metal species in acidic solutions using bentonite clay: implications for acid mine drainage remediation. *Toxicological & Environmental Chemistry,* 96**,** 201-217.

Gitari, W. M., Petrik, L. F., Etchebers, O., Key, D. L. & Okujeni, C. 2008. Utilization of fly ash for treatment of coal mines wastewater: Solubility controls on major inorganic contaminants. *Fuel,* 87**,** 2450-2462.

Gitari, W. M., Petrik, L. F., Key, D. L. & Okujeni, C. 2011. Interaction of acid mine drainage with Ordinary Portland Cement blended solid residues generated from active treatment of acid mine drainage with coal fly ash. *Journal of Environmental Science and Health - Part A Toxic/Hazardous Substances and Environmental Engineering,* 46**,** 117-137.

Gitari, W. M., Petrik, L. F., Key, D. L. & Okujeni, C. 2013. Inorganic contaminants attenuation in acid mine drainage by fly ash and its derivatives: Column experiments. *International Journal of Environment and Pollution,* 51**,** 32-56.

Grawunder, A., Merten, D. & Büchel, G. 2014. Origin of middle rare earth element enrichment in acid mine drainage-impacted areas. *Environmental Science and Pollution Research,* 21**,** 6812-6823.

Hallberg, K. B. 2010. New perspectives in acid mine drainage microbiology. *Hydrometallurgy,* 104**,** 448-453.

Hedin, R. S., Stafford, S. L. & Weaver, T. J. 2005. Acid mine drainage flowing from abandoned gas wells. *Mine Water and the Environment,* 24**,** 104-106.

Heviánková, S., Bestová, I. & Kyncl, M. 2014. The application of wood ash as a reagent in acid mine drainage treatment. *Minerals Engineering,* 56**,** 109-111.

Johnson, D. B. & Hallberg, K. B. 2005. Acid mine drainage remediation options: a review. *Science of The Total Environment,* 338**,** 3-14.

Labastida, I., Armienta, M. A., Lara-Castro, R. H., Aguayo, A., Cruz, O. & Ceniceros, N. 2013. Treatment of mining acidic leachates with indigenous limestone, Zimapan Mexico. *Journal of Hazardous Materials,* 262**,** 1187-1195.

Lepoitevin, M., Jaber, M., Guégan, R., Janot, J. M., Dejardin, P., Henn, F. & Balme, S. 2014. BSA and lysozyme adsorption on homoionic montmorillonite: Influence of the interlayer cation. *Applied Clay Science,* 95**,** 396-402.

Luptakova, A., Ubaldini, S., Macingova, E., Fornari, P. & Giuliano, V. 2012. Application of physical–chemical and biological–chemical methods for heavy metals removal from acid mine drainage. *Process Biochemistry,* 47**,** 1633-1639.

Macingova, E. & Luptakova, A. Recovery of metals from acid mine drainage by selective sequential precipitation processes. 11th International Multidisciplinary Scientific Geoconference and EXPO - Modern Management of Mine Producing, Geology and Environmental Protection, SGEM 2011, 2011. 573-578.

Madzivire, G., Gitari, W. M., Vadapalli, V. R. K., Ojumu, T. V. & Petrik, L. F. 2011. Fate of sulphate removed during the treatment of circumneutral mine water and acid mine drainage with coal fly ash: Modelling and experimental approach. *Minerals Engineering*, 24**,** 1467-1477.

Madzivire, G., Maleka, P. P., Vadapalli, V. R. K., Gitari, W. M., Lindsay, R. & Petrik, L. F. 2014. Fate of the naturally occurring radioactive materials during treatment of acid mine drainage with coal fly ash and aluminium hydroxide. *Journal of Environmental Management,* 133**,** 12-17.

Madzivire, G., Petrik, L. F., Gitari, W. M., Ojumu, T. V. & Balfour, G. 2010. Application of coal fly ash to circumneutral mine waters for the removal of sulphates as gypsum and ettringite. *Minerals Engineering,* 23**,** 252-257.

Maree, J. P., De Beer, M., Strydom, W. F., Christie, A. D. M. & Waanders, F. B. 2004. Neutralizing coal mine effluent with limestone to decrease metals and sulphate concentrations. *Mine Water and the Environment,* 23**,** 81-86.

Martí-Calatayud, M. C., Buzzi, D. C., García-Gabaldón, M., Ortega, E., Bernardes, A. M., Tenório, J. a. S. & Pérez-Herranz, V. 2014. Sulfuric acid recovery from acid mine drainage by means of electrodialysis. *Desalination,* 343**,** 120-127.

Masindi, V. & Gitari Mugera, W. 2015. The potential of ball-milled South African bentonite clay for attenuation of heavy metals from acidic wastewaters: Simultaneous sorption of Co(II), Cu(II), Ni(II), Pb(II), and Zn(II) ions. *Journal of Environmental Chemical Engineering*, 3**,** 2416-2425.

Masindi, V., Gitari, M. W., Tutu, H. & De Beer, M. 2014a. Application of magnesite–bentonite clay composite as an alternative technology for removal of arsenic from industrial effluents. *Toxicological & Environmental Chemistry,* 96**,** 1435-1451.

Masindi, V., Gitari, M. W., Tutu, H. & De Beer, M. 2015a. Synthesis of a porous magnesite-bentonite clay composite and its application for neutralisation and attenuation of inorganic contaminants in acidic and metalliferous mine drainage. 69 - 77.

Masindi, V., Gitari, M. W., Tutu, H. & Debeer, M. 2015b. Removal of boron from aqueous solution using magnesite and bentonite clay composite. *Desalination and Water Treatment***,** 1-11.

Masindi, V. & Gitari, W. M. 2015. Simultaneous removal of metal species from acidic aqueous solutions using cryptocrystalline magnesite/bentonite clay composite: An experimental and modelling approach. *Journal of Cleaner Production*.

Masindi, V., Gitari, W. M. & Ngulube, T. 2014b. Defluoridation of drinking water using Al3+-modified bentonite clay: optimization of fluoride adsorption conditions. *Toxicological & Environmental Chemistry,* 96**,** 1294-1309.

Masindi, V., Gitari, W. M. & Pindihama, K. G. 2015c. Synthesis of nanocomposite of cryptocrystalline magnesite-bentonite clay and its application for phosphate removal from municipal effluents. *Environ Technol,* 24**,** 1-27.

Mayo, A. L., Petersen, E. C. & Kravits, C. 2000. Chemical evolution of coal mine drainage in a non-acid producing environment, Wasatch Plateau, Utah, USA. *Journal of Hydrology,* 236**,** 1-16.

Mohan, D. & Chander, S. 2006. Removal and recovery of metal ions from acid mine drainage using lignite—A low cost sorbent. *Journal of Hazardous Materials,* 137**,** 1545-1553.

Morais, C., Rosado, L., Mirão, J., Pinto, A. P., Nogueira, P. & Candeias, A. E. 2008. Impact of acid mine drainage from Tinoca Mine on the Abrilongo dam (southeast Portugal). *Mineralogical Magazine,* 72**,** 467-472.

Motsi, T., Rowson, N. A. & Simmons, M. J. H. 2009. Adsorption of heavy metals from acid mine drainage by natural zeolite. *International Journal of Mineral Processing,* 92**,** 42-48.

Ntuli, F., Falayi, T. & Harmse, L. Immobilisation of Co, Fe, and Mn from acid mine drainage using activated bentonite. WIT Transactions on the Built Environment, 2014. 267-274.

Oberholster, P. J., Genthe, B., Hobbs, P., Cheng, P. H., De Klerk, A. R. & Botha, A. M. 2013. An ecotoxicological screening tool to prioritise acid mine drainage impacted streams for future restoration. *Environmental Pollution,* 176**,** 244-253.

Park, S. M., Yoo, J. C., Ji, S. W., Yang, J. S. & Baek, K. 2013. Selective recovery of Cu, Zn, and Ni from acid mine drainage. *Environmental Geochemistry and Health,* 35**,** 735-743.

Pérez-López, R., Castillo, J., Quispe, D. & Nieto, J. M. 2010. Neutralization of acid mine drainage using the final product from CO2 emissions capture with alkaline paper mill waste. *Journal of Hazardous Materials,* 177**,** 762-772.

Radić, S., Vujčić, V., Cvetković, Ž., Cvjetko, P. & Oreščanin, V. 2014. The efficiency of combined CaO/electrochemical treatment in removal of acid mine drainage induced toxicity and genotoxicity. *Science of The Total Environment,* 466–467**,** 84-89.

Rimstidt, J. D. & Vaughan, D. J. 2014. Acid mine drainage. *Elements,* 10**,** 153-154.

Ruihua, L., Lin, Z., Tao, T. & Bo, L. 2011. Phosphorus removal performance of acid mine drainage from wastewater. *Journal of Hazardous Materials,* 190**,** 669-676.

Sarmiento, A. M., Olías, M., Nieto, J. M., Cánovas, C. R. & Delgado, J. 2009. Natural attenuation processes in two water reservoirs receiving acid mine drainage. *Science of The Total Environment,* 407**,** 2051-2062.

Sheridan, C., Harding, K., Koller, E. & De Pretto, A. 2013. A comparison of charcoal- and slag-based constructed wetlands for acid mine drainage remediation. *Water SA,* 39**,** 369-374.

Simate, G. S. & Ndlovu, S. 2014. Acid mine drainage: Challenges and opportunities. *Journal of Environmental Chemical Engineering,* 2**,** 1785-1803.

Sracek, O., Choquette, M., Gélinas, P., Lefebvre, R. & Nicholson, R. V. 2004. Geochemical characterization of acid mine drainage from a waste rock pile, Mine Doyon, Québec, Canada. *Journal of Contaminant Hydrology,* 69**,** 45-71.

Sun, H., Zhao, F., Zhang, M. & Li, J. 2012. Behavior of rare earth elements in acid coal mine drainage in Shanxi Province, China. *Environmental Earth Sciences,* 67**,** 205-213.

Suponik, T. & Blanco, M. 2014. Removal of heavy metals from groundwater affected by acid mine drainage. *Physicochemical Problems of Mineral Processing,* 50**,** 359-372.

Torres, E. & Auleda, M. 2013. A sequential extraction procedure for sediments affected by acid mine drainage. *Journal of Geochemical Exploration,* 128**,** 35-41.

Tutu, H., Mccarthy, T. S. & Cukrowska, E. 2008. The chemical characteristics of acid mine drainage with particular reference to sources, distribution and remediation: The Witwatersrand Basin, South Africa as a case study. *Applied Geochemistry,* 23**,** 3666-3684.

Valente, T. M. & Leal Gomes, C. 2009. Occurrence, properties and pollution potential of environmental minerals in acid mine drainage. *Science of The Total Environment,* 407**,** 1135-1152.

Van Vuuren, L. 2011. Acid mine drainage: Solutions rearing to go. *Water Wheel,* 10**,** 16-17.

Vazquez, O. Effect of acid mine drainage on aluminum release from clay minerals. Proceedings of World Environmental and Water Resources Congress 2009 - World Environmental and Water Resources Congress 2009: Great Rivers, 2009. 5253-5260.

Wade, C., Dold, B. & Fontboté, L. Geochemistry and mineralogy of the Quiulacocha tailings impoundment from the polymetallic Zn-Pb-(Ag-Bi-Cu) deposit Cerro de Pasco, Peru. 7th International Conference on Acid Rock Drainage 2006, ICARD - Also Serves as the 23rd Annual Meetings of the American Society of Mining and Reclamation, 2006. 2199-2206.

Wang, H. Characteristics of acid mine drainage and its pollution control. 2010 4th International Conference on Bioinformatics and Biomedical Engineering, iCBBE 2010, 2010.

Watten, B. J., Sibrell, P. L. & Schwartz, M. F. 2005. Acid neutralization within limestone sand reactors receiving coal mine drainage. *Environmental Pollution,* 137**,** 295-304.

White, R. A., Freeman, C. & Kang, H. 2011. Plant-derived phenolic compounds impair the remediation of acid mine drainage using treatment wetlands. *Ecological Engineering,* 37**,** 172-175.

Whitehead, P. G. & Prior, H. 2005. Bioremediation of acid mine drainage: An introduction to the Wheal Jane wetlands project. *Science of The Total Environment,* 338**,** 15-21.

Wildeman, T., Vatterrodt, K. & Figueroa, L. A. The generation and treatment of acid rock drainage. Mineral Processing and Extractive Metallurgy: 100 Years of Innovation, 2014. 619-628.

Wisskirchen, C., Dold, B., Friese, K. & Glaesser, W. Element distribution in water and sediments of an acid mine drainage discharge lake (pH ~1) of the Zn-Pb(-Ag-Bi-Cu) deposit, Cerro de Pasco (Peru). 7th International Conference on Acid Rock Drainage

2006, ICARD - Also Serves as the 23rd Annual Meetings of the American Society of Mining and Reclamation, 2006. 2470-2479.

Xu, C., Xia, B. C., Wu, H. N., Lin, X. F. & Qiu, R. L. 2009. Speciation and bioavailability of heavy metals in paddy soil irrigated by acid mine drainage. *Huanjing Kexue/Environmental Science,* 30**,** 900-906.

Xu, G., Jiang, Q., Liang, X. & Yue, M. Research on hydrochemical characteristics of acid mine drainage and its prevention. Water-Rock Interaction - Proceedings of the 12th International Symposium on Water-Rock Interaction, WRI-12, 2007. 1287-1290.

Zhang, C., Wu, P., Tang, C., Tao, X., Han, Z., Sun, J. & Liu, H. 2013. The study of soil acidification of paddy field influenced by acid mine drainage. *Environmental Earth Sciences,* 70**,** 2931-2940.

Zhang, M. 2011. Adsorption study of Pb(II), Cu(II) and Zn(II) from simulated acid mine drainage using dairy manure compost. *Chemical Engineering Journal,* 172**,** 361-368.

Zhao, L., Sun, J., Zhao, Y., Xu, L. & Zhai, M. 2011. Removal of hazardous metal ions from wastewater by radiation synthesized silica-graft-dimethylaminoethyl methacrylate adsorbent. *Chemical Engineering Journal,* 170**,** 162-169.

Zvimba, J. N., Mulopo, J., Bologo, L. T. & Mathye, M. 2012. An evaluation of waste gypsum-based precipitated calcium carbonate for acid mine drainage neutralization. *Water Science and Technology,* 65**,** 1577-1582.

CHAPTER TWO

LITERATURE REVIEW

2.0 Introduction

This chapter presents a thorough literature review on the formation, chemical composition, environmental implications and treatment technologies for acid mine drainage. It will also give detailed discussion on the formation and application of magnesite and bentonite clay for wastewater remediation. Background information on geochemical modelling will also be introduced to highlight its importance as a problem-solving tool.

2.1 Acid mine drainage

Contamination of surface and subsurface water by AMD has raised public concern. It has degraded the quality of terrestrial and aquatic ecosystems and their ability to sustain life (Levings et al., 2005, Macedo-Sousa et al., 2007, Mapanda et al., 2007, Gray and Delaney, 2010, Gray and Vis, 2013, Netto et al., 2013, Simate and Ndlovu, 2014, Torres et al., 2014). Depending on the source of rock, AMD can be formed by weathering of sulphide bearing rocks (Table 2.1) (Sracek et al., 2004, Johnson and Hallberg, 2005b, Frempong and Yanful, 2006, Cheng et al., 2009, Peretyazhko et al., 2009, Sheoran et al., 2011, Zhao et al., 2012, Quispe et al., 2013, Kim, 2015, Nordstrom et al., 2015). The mineral phases that are responsible for the formation of AMD are shown in Table 2.1 (Johnson and Hallberg, 2005b, Peretyazhko et al., 2009, Sheoran et al., 2011, Zhao et al., 2012).

Table 2.1: Acid mine drainage forming minerals

Mineral phase	Composition	Mineral phase	Composition
Pyrite	FeS_2	**Molybdenite**	MoS_2
Marcasite	FeS_2	**Millerite**	NiS
Pyrrhotite	Fe_xS_x	**Galena**	PbS
Chalcocite	Cu_2S	**Sphalerite**	ZnS
Covellite	CuS	**Arsenopyrite**	FeAsS
Chalcopyrite	$CuFeS_2$	**Cinnabar**	HgS

The chemical composition of acid mine drainage depends on the composition of the parent rock and associated geological strata. Depending on the mineral being weathered, AMD is characterized by acidic pH that ranges from 1 - 4 and is enriched with iron, manganese, aluminium, sulphate, and toxic chemical species such as lead, copper, mercury, cadmium and zinc. It is generally regarded as the main environmental problem caused by the mining of sulphide bearing ore deposits (Johnson and Hallberg, 2005b, Peretyazhko et al., 2009, Sheoran et al., 2011). National, regional and international scientific communities have declared AMD an issue of prime environmental concern (Bálintová and Singovszká, 2011). It contains chemical species that are potentially toxic to terrestrial and aquatic organisms on exposure (Sracek et al., 2004). As such, this effluent emanating from mining activities needs to be contained and treated to prevent contamination of receiving aquatic ecosystems. In South Africa, the Witwatersrand basins contain on average 4800 mg/L sulphate, 800 mg/L of Fe(II), 100mg/L of Fe(III), 230 mg/L of Mn, 11 mg/L of Zn, 18 mg/L of Ni, 5 mg/L of Co, 6 mg/L of Al, 150 mg/L of Mg, some radioactive elements and 700 mg/L acidity (as $CaCO_3$) (Tutu et al., 2008). It has been documented that the Western Basin discharges approximately 10 – 60 ML/day. This water is discharged to the adjacent river that passes through the heritage site of the Cradle of Humankind and it has been projected that its impacts may permeate to the Sterkfontein Cave Systems which partially include the Cradle of Humankind, where the earliest known hominid fossils remains were discovered and where paleontological excavation continues (Maree et al., 1989, Maree and Du Plessis, 1993, Maree et al., 2004b, Bologo et al., 2012, Maree et al., 2013). This raises a need for urgent treatment of AMD.

2.2 Generation of acid mine drainage

AMD is formed by a series of geo-chemical and microbial reactions that occur when sulphide minerals are exposed to oxygen and water to form sulphuric acid. This acid leaches out metals in the rock, which can either enter nearby streams and rivers or seep into groundwater. Oxidation of sulphide minerals occurs primarily via oxidation reactions mediated by microorganisms (Hallberg, 2010, Zhao et al., 2012, Candeias et al., 2014, Amos et al., 2015). Iron sulphide containing strata are oxidized to ferric iron and sulphate (Equation 2.1) (Amos et al., 2015).

$$2FeS_{2(s)} + 7O_{2(g)} + 2H_2O \xrightarrow{\text{bacteria}} 2Fe^{2+}_{(aq)} + 4H^{+}_{(aq)} + 4SO^{2-}_{4(aq)} \quad (2.1)$$

2.2.1 Chemistry of acid mine drainage and its generation

The formation of AMD from pyrite can be represented by three basic chemical reactions, pyrite oxidation, ferrous oxidation and iron hydrolysis (Equation 2.2). Pyrite (FeS_2) is the dominant form of sulphur mineral in coal and gold lithology and stratigraphy. During pyrite oxidation sulphur is oxidized to sulphate and ferric iron is released (Equations 2.2 – 2.5). The acidity formed promotes leaching of other minerals (Al, Mn and trace metals) which are associated with the mined strata (Sracek et al., 2004, Zhao et al., 2012, Amos et al., 2015).

2.2.1.1 Chemistry of pyrite in acid mine drainage formation

During the oxidation of pyrite there are two species that can be oxidized: the ferrous iron and the sulphur. When pyrite is exposed to large quantities of oxygenated waters, ferrous iron easily leaches out of the oxidised pyrite but stays in solution (Equation 2.2 – 2.5) (Sracek et al., 2004, Johnson and Hallberg, 2005b, Sheoran and Sheoran, 2006, Peretyazhko et al., 2009, Sheoran et al., 2011, Zhao et al., 2012, Amos et al., 2015, Nordstrom et al., 2015).

$$2FeS_2 + 7O_2 + 2H_2O \rightarrow 2Fe^{2+} + 4SO_4{}^{2-} + 4H^{+} \quad (2.2)$$

$$4Fe^{2+} + O_2 + 4H^{+} \rightarrow 4Fe^{3+} + 2H_2O \quad (2.3)$$

$$4Fe^{3+} + 12H_2O \rightarrow 4Fe(OH)_3 + 12H^{+} \quad (2.4)$$

$$FeS_2 + 14Fe^{3+} + 8H_2O \rightarrow 15Fe^{2+} + 2SO_4{}^{2-} + 16H^{+} \quad (2.5)$$

Equation 2.2: When pyrite is initially exposed to oxygen and water it leads to the formation of ferric iron, sulphate and acidity. However, dissolved ferrous iron ($Fe^{2+}_{(aq)}$) and sulphate ions ($SO_4^{2-}{}_{(aq)}$) are colourless and the water may look crystal clear. Oxidation of pyrite is a particularly fast reaction as compared to formation of rust.

Equation 2.3: Aqueous ferrous (Fe^{2+}) ions react with oxygen and acidic hydrogen ions to form ferric (Fe^{3+}) ions and water. The conversion of ferrous to ferric iron consumes one mole of acidity.

Equation 2.4: This describes the next reaction where the ferric ions hydrolyse in water to form ferric hydroxide. Three moles of acidity are generated. Many metal ions are capable of undergoing hydrolysis. The formation of ferric hydroxide precipitate (solid) is pH dependent. Solids form if the pH is above about 3.5, but below pH 3.5, little or no solids will precipitate.

Equation 2.5: The oxidation of additional pyrite or other metals by ferric iron can take place. The ferric iron is generated in reaction steps 2.1 and 2.2. This is the cyclic and self-propagating part of the overall reaction and takes place very rapidly and continues until either ferric iron or pyrite and other metals are depleted. In this reaction, iron(III) is the oxidizing agent, not oxygen. Fe^{2+}/Fe^{3+} in solution is the source of acidity because the chemical reactions involved lead to the precipitation of iron species releasing acidity (H^+).

2.2.2 Role of bacteria in chemistry of acid mine drainage

All bacterial species have a definite pH growth range and pH growth optimum. Acidophile have their growth optimum between pH 0.1 and pH 5.5. Bacterial death may occur when the internal pH increase > 5.5, because changes in the external pH can alter the ionization of nutrient molecules and therefore lower their availability to the organism. However, there are some microorganisms which can survive extreme acidic environments. These microorganisms frequently change the pH of their own habitat by producing acidic metabolic waste products. The organisms play a pivotal role in accelerating the oxidation of pyrite. Several bacterial species have been documented to play a significant role in mediating the process of AMD formation. The most common species is *Thiobacillus ferrooxidans*, which is an iron and sulphur oxidizing bacterium. Microbiological oxidation of pyrite proceeds by the following stages (Brake et al., 2004, Johnson and Hallberg, 2005c, Johnson and Hallberg, 2005b, Fang et al., 2007, Natarajan, 2008, Hallberg, 2010, Zhou et al., 2010, Sheoran et al., 2011, Simate and Ndlovu, 2014, Nordstrom et al., 2015).

Stage 1

Reaction 2.2 proceeds abiotically and by direct bacterial oxidation (Equation 2.2). Reaction 2.3 proceeds abiotically and slows down as pH increase (Equation 2.3) Thus, the chemistry is: pH almost above 4.5, high sulphate, low Fe, little or no acidity.

Stage 2

Reaction 2.1 proceeds abiotically and by direct bacterial oxidation (Equation 2.1). Reaction 2.3 occurs at a rate determined by the activity of *Thiobacillus ferrooxidans* (Equation 2.3). (Chemistry: pH almost above 4.5, high sulphate, acidity, and Fe increase, low Fe^{3+}/Fe^{2+} ratio.)

Stage 3

Reaction 2.4, proceeds at a rate determined only by the activity of *Thiobacillus ferrooxidans* (Equation 2.4). Reaction 2.5 proceeds at a rate entirely determined by reaction 2.4, (Chemistry: pH below 2.5, high Sulphate, acidity, and Fe, and Fe^{3+}/Fe^{2+} ratio.)

Under many conditions, Equation 2.3 is the rate-limiting step in pyrite oxidation because the conversion of ferrous iron to ferric iron is slow at pH values below 5 under abiotic conditions. However, Fe-oxidizing bacteria, principally *Thiobacillus* spp., greatly accelerate this reaction, so the activities of bacteria are crucial for generation of most AMD, and much work on bactericides has been conducted. In contrast, availability of oxygen may be the rate-limiting step in mine-spoil of low porosity and permeability such as that composed of soft shale, so that oxidation is limited to the upper few metres of spoil. In porous and permeable spoil, composed of coarse sandstone, air convection driven by the heat generated by pyrite oxidation may provide high amounts of oxygen deep into the spoil. The rate of pyrite oxidation depends on numerous variables such as reactive surface area of pyrite, form of pyritic sulphur, oxygen concentration, solution pH, catalytic agents, flushing frequencies, and the presence of *Thiobacillus* spp. bacteria.

Formation of AMD is an intricate process that relies on several factors. These include pH, temperature, oxygen content of the gaseous phase, oxygen content of the aqueous phase, degree of saturation with regard to aqueous phase, chemical activity of Fe^{3+}, surface area of exposed sulphidic mineral phases, chemical activation energy required to initiate acid generation capabilities and bacterial activities. As sequentially enumerated above, formation of AMD follows different stages and the process is catalysed by micro-organisms. Primarily, *Thiobacillus ferrooxidans* catalyse the oxidation of Fe at pH below 3.5, whilst at pH between

3.5 to 4.5 catalysis is via a variety of *Metallogenium* spp., a filamentous bacterium. The species of microorganisms which are involved in oxidation of sulphidic materials are shown in **Table 2.2**.

Table 2.2: Sulphide oxidizing bacteria and their growth conditions (Johnson and Hallberg, 2005b, Fang et al., 2007, Natarajan, 2008, Lacelle and Léveillé, 2010, Sheoran et al., 2011, Zhao et al., 2012)

Bacteria species	pH	Temp, (◦C)	Classification	Nutrition mode
Thiobacillus thioparus	4.5 – 10	10 - 37	Aerobic	Autotrophic
Thiobacillus ferrooxidans	0.5 – 6.1	15 – 25	Aerobic	Autotrophic
Thiobacillus thiooxidans	0.5 – 6.0	10 – 37	Aerobic	Autotrophic
Thiobacillus neapolitanus	3.0 – 8.5	8 – 38	Aerobic	Autotrophic
Thiobacillus denitrificans	4.0 – 9.5	10 – 37	Aerobic	Autotrophic
Thiobacillus novellus	5.0 – 9.2	25 – 35	Aerobic	Autotrophic
Thiobacillus intermedius	1.9 – 7.0	25 – 35	Aerobic	Autotrophic
Thiobacillus perometabolis	2.8 – 6.8	25 – 35	Aerobic	Autotrophic
Sulfolobus acidocalderius	2.0 – 5.0	55 – 85	Aerobic	Autotrophic
Desulfovibrio desulphuricans	5.0 – 9.0	10 - 45	Anaerobic	Heterotrophic

Depending on the local geology and mineral phases being mined, the chemistry of the resultant mine drainage will vary (Sracek et al., 2004, Sheoran and Sheoran, 2006, Natarajan, 2008, Peretyazhko et al., 2009, Sheoran et al., 2011, Zhao et al., 2012, Nordstrom et al., 2015).

2.3 Physical properties of acid mine drainage

The colour of AMD is determined by the dissolution and precipitation of metals in wastewater. The dominant metal present in AMD is iron, which may give water a typically reddish colour, while in streams with a higher pH (pH 5 - 6.5), orange-yellow ferric iron-rich sediments ("yellow boy") are present. The white colour of AMD is determined by the presence of Al which precipitates as $Al(OH)_3$ (Gibbsite). The black colour arises by the presence of Mn which precipitates as $Mn(OH)_2$ (Cheng et al., 2009, Zhao et al., 2012, Amos et al., 2015).

2.4 Deleterious effects of acid mine drainage on terrestrial and aquatic ecosystems

The introduction of effluents from mining activities into receiving streams can severely impact aquatic ecosystems through habitat destruction and impairment of water quality. This will eventually lead to reduction in biodiversity of a given aquatic ecosystem and its ability to sustain life. The severity and extent of damage depends on a variety of factors including the frequency of influx, volume, and chemistry of the drainage, and the buffering capacity of the receiving stream (Šucha et al., 2002, Levings et al., 2005, Peretyazhko et al., 2009, Martins et al., 2011, Mohapatra et al., 2011, Netto et al., 2013, Simate and Ndlovu, 2014, Torres et al., 2014).

2.4.1 Acidity

When metals in AMD are hydrolysed, they lower the pH of the water making it unsuitable for aquatic organisms to thrive (Torres et al., 2014). AMD is highly acidic (pH 2 – 4) and this promotes the dissolution of toxic metals (Tutu et al., 2008). Those toxic species exert hazardous effects on terrestrial and aquatic organisms (Simate and Ndlovu, 2014). Also, if the water is highly acidic only acidophile microorganisms will thrive on such water with the rest of aquatic organisms migrating to other regions which are conducive to their survival. Many streams contaminated by AMD are largely devoid of life for a long way downstream. To some aquatic organisms, if the pH range falls below the tolerance range, probability of death is very high due to respiratory and osmoregulation failure. Acidic conditions are dominated by H^+ which is adsorbed and pumps out Na from the body which is important in regulating body fluids (Mitsch and Wise, 1998, Šucha et al., 2002, Levings et al., 2005, Mahmoud et al., 2005, Mapanda et al., 2007, Gray and Delaney, 2010, Strosnider and Nairn, 2010, Martins et al., 2011, Mohapatra et al., 2011, Gray and Vis, 2013, Simate and Ndlovu, 2014, Torres et al., 2014, Sun et al., 2015).

2.4.2 Toxic chemical species

Exposure of aquatic and terrestrial organisms to potentially toxic metals and metalloids can have devastating impacts to living organisms (Tutu et al., 2008, Rubin et al., 2011, Skoczyńska-Gajda and Labus, 2011). Toxic chemical species present in AMD have been reported to be toxic to aquatic and terrestrial organisms. They are associated with numerous

diseases including cancers. Some of these chemical species may accumulate and be biomagnified in living organisms hence threatening the life of higher trophic organisms such as birds (Jooste and Thirion, 1999). Lead cause blood disorders, kidney damage, miscarriages and reproductive disorders and is linked to various cancers. The exposure of living organisms to toxic chemical species in AMD can also lead to nausea, diarrhea, liver and kidney damage, dermatitis, internal hemorrhage and respiratory problems. Epidemiological studies have shown a significant increase in the risk of lung, bladder, skin, liver and other cancers on exposure to these chemical species. Effects of Al, Fe, Mn, Cu, Mg, and Zn on the health of living organisms are summarized in Table 2.3.

Table 2.3: Effects of selected metals on the health of living organisms

Element	DWA limit	Ecological impacts of AMD
Al	< 0.5 mg/L	Prolonged exposure to aluminium has been implicated in chronic neurological disorders such as *dialysis dementia* and Alzheimer's disease. Severe aesthetic effects (discolouration) occur in the presence of iron or manganese
Fe	< 1 mg/L	Severe aesthetic effects (taste) and effects on plumbing (slimy coatings). Slight iron overload possible in some individuals. Chronic health effects in young children and sensitive individuals in the range 10 - 20 mg/L, and occasional acute effects toward the upper end of this range.
Mn	< 0.2 mg/L	Very severe, aesthetically unacceptable staining. Domestic use unlikely due to adverse aesthetic effects. Some chance of manganese toxicity under unusual conditions.
Cu	< 1 mg/L	Gastrointestinal irritation, nausea and vomiting. Severe taste and staining problems. Severe poisoning with possible fatalities. Severe taste and staining problems
Mg	< 200 mg/L	Water aesthetically unacceptable because of bitter taste users if sulphate present. Increased scaling problems. Diarrhoea in most new consumers
Zn	< 5 mg/L	Bitter taste; milky appearance. Acute toxicity with gastrointestinal, irritation, nausea and vomiting. Severe, acute toxicity with electrolyte disturbances and possible renal damage

2.4.3 Sedimentation

Acid mine drainage receiving water is initially clear but turns a vivid orange colour because of the precipitation of iron oxides and hydroxides (Peretyazhko et al., 2009, Sheoran et al., 2011, Zhao et al., 2012). This precipitate, often called ochre or "yellow boy", is very fine and smothers the river bed with very fine silt. Thus, destroying the habitat and nursery of benthic organism and fish respectively (Lottermoser, 2007). Because these organisms are at the bottom of the aquatic food chain, this has impacts on fish higher up the food chain. In addition to killing bottom-dwelling organisms, this smothering ochre or orange precipitate smothers gravel for fish to lay their eggs on, and hence can affect fish breeding (Netto et al., 2013, Papassiopi et al., 2014, Simate and Ndlovu, 2014). The sediment also contains the toxic elements that co-precipitate with the yellow boys. These are now transported as particulates downstream and, eventually, into the sea. Precipitation of these chemicals in AMD also poses hazards to aquatic life and reduces the habitat of aquatic organisms (Sun et al., 2015).

2.5 Acid mine drainage treatment technologies

Several AMD remediation techniques have been used to treat and reclaim mine wastewater. The fundamental goals of remediating AMD waters are to raise the pH and to remove metal concentrations. Chemical treatment, which is considered expensive and requires frequent plant maintenance, is currently the most common remediation technology in use. An alternative to chemical treatment are passive treatments which include constructed wetlands and limestone channels. They are more widely used because of their economic advantages.

Treatment processes for AMD are usually reactive rather than pro-active, and are generally designed to:

- Raise pH;
- Remove toxic metal concentrations,;
- Remove aqueous sulphate concentrations; and
- Collect, dispose of or isolate the metallic sludge generated followed by metal recovery.

Acid drainage control and treatment techniques can be broadly classified into physical, chemical and biological, and combinations of these processes (Sheoran and Sheoran, 2006, Lefebvre et al., 2012, Luptakova et al., 2012a, Li et al., 2013, Name and Sheridan, 2014,

Wildeman et al., 2014). Within the two major groups, chemical and biological, there are processes that may be described as either active or passive (Sheoran and Sheoran, 2006) as mentioned previously. Biotic and abiotic methods for treatment of AMD are summarized in Figure 2.1.

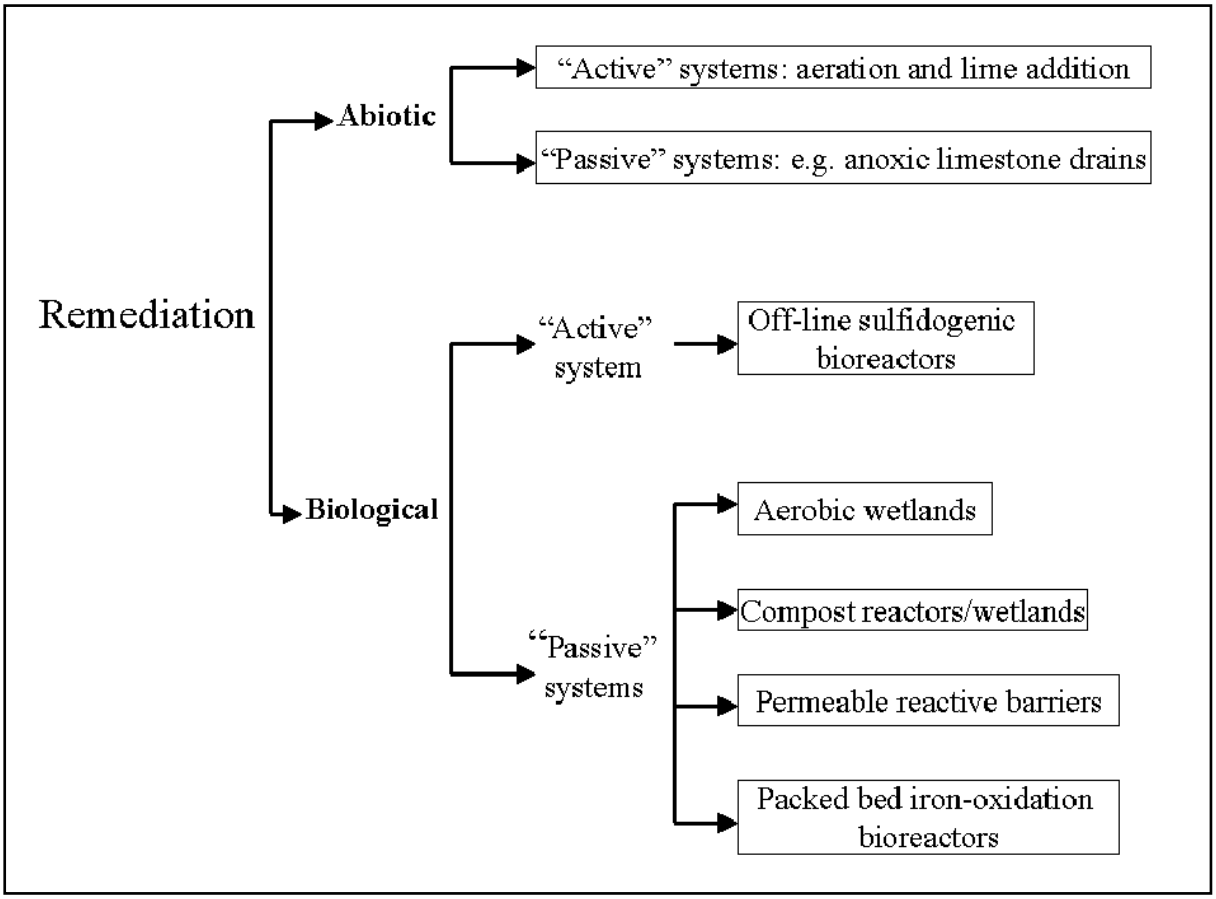

Figure 2.1: Summary of abiotic and biological technologies for remediating AMD (Groudev et al., 2008, Papirio et al., 2013, Shabani et al., 2014).

2.5.1 Active Treatment

2.5.1.1 Chemical treatment technologies

Chemical treatment systems are the standard remediation technique for treatment of AMD. They treat water with additions of highly alkaline chemicals such as $CaCO_3$, NaOH, $Ca(OH)_2$, CaO, Na_2CO_3, and NH_3 (Sheoran and Sheoran, 2006, Zvimba et al., 2012, Simate and Ndlovu, 2014). The mechanism of these systems is to raise the pH of the effluent until metals are precipitated and can settle out in a retention pond. Enough alkalinity is needed to raise the pH of the water and supply hydroxide so as to form insoluble metal hydroxides that settle out. In most instances, the required pH for metals to precipitate ranges from 6 - 9

except for ferric iron which precipitates at pH >3.5., Precipitation of metal hydroxides vary depending on pH (Table 2.4) (Demchak et al., 2001, Johnson and Hallberg, 2005a, Skousen et al., 2006, Yang et al., 2006)

Table 2.4: Precipitation of metals at varying pH gradients

Metal ion	pH	Metal ion	pH
Al^{3+}	4.1	Hg^{2+}	7.3
Fe^{3+}	3.5	Na^{+}	6.7
Mn^{2+}	8.5	Pb^{2+}	6.0
Cr^{3+}	5.3	Zn^{2+}	7.0
Cd^{2+}	6.7	Cu^{2+}	5.3
Fe^{2+}	5.5		

AMD chemical treatment systems consist of an inflow pipe or ditch, a storage tank or bin holding the treatment chemical, a means of controlling chemical application rate, a settling pond to capture precipitated metal hydroxides, and a discharge point. Limestone, pebble quicklime, hydrated lime, soda ash, brucite, caustic soda and ammonia are the commonly used chemicals (Sheoran and Sheoran, 2006, Strosnider et al., 2011a, Zheng et al., 2011, Wang et al., 2012, Wei et al., 2013, Wildeman et al., 2014). The selection of a treatment chemical depends on the characteristics of the effluent, the receiving aquatic ecosystem, and availability of electrical power, proximity of the feedstock, cost of the material, treatment time and quantity of resultant solids. Although chemical treatment is often very efficient in promoting metal removal and neutralizing acidity, the chemicals are mostly expensive or dangerous and when misused can result in discharge of excessively polluted water (Maree and Du Plessis, 1993, Maree et al., 1997, Gitari et al., 2006, Maree et al., 2013).

2.5.1.2 Adsorption

Adsorption is a phenomenon whereby an adsorbate adheres to the surface of an adsorbent. Due to reversibility and desorption capabilities, adsorption has been regarded as one of the best methods for metal removal from aqueous solution . Kuroki et al. (2014) documented the possible use of La(III)-modified bentonite for phosphate removal from aqueous media. The

phosphate retention at room temperature reached > 95%, when initial phosphate concentration in solution was 5 mg L^{-1}. Sen Gupta and Bhattacharyya (2008) documented that kaolinite and montmorillonite clay have the efficiency to remove > 99 % of Pb(II), Cd(II) and Ni(II) ions from aqueous solution. Kubilay et al. (2007) noted that natural bentonite clay has the capabilities to remove Cu(II), Zn(II) and Co(II) from aqueous solution. Al-Shahrani (2014) reported that Saudi bentonite clay has the ability to remove > 99 % of Ni(II), Cd(II), Cu(II) and Pb(II) from aqueous solution. Anna et al. (2014) reported that natural bentonite clay has the ability to remove mono- and multi-metal systems of toxic chemical species such as Cd(II), Cu(II), Ni(II) and Pb(II). Bereket et al. (1997) evaluated the use of bentonite clay for removal of Cd(II), Cu(II), Ni(II) and Pb(II) and reported that it has > 99% removal efficiencies. Gitari (2014) documented that South African bentonite clay has the ability to remove toxic chemical species of Al, Fe and Mn from acid mine drainage altogether with sulphate and trace metals. Van Der Watt and Waanders (2012) reported the possibilities of bentonite clay to be activated by acid while leaching trace metals from its matrices.

2.5.1.3 Ion-exchange

Ion-exchange is the exchange of ions between two or more electrolyte solutions. It can also refer to exchange of ions on a solid substrate to soil solution. In most instances, ion-exchange uptake of metals from aqueous solution is by using ion-exchange surfaces such as high cation-exchange capacity clay and resins. However, it has disadvantages of relying on several parameters such as contact time, concentration of the solution, pH of the supernatants solution and temperature. Also, it is costly and laborious to use on a large scale. The efficiency of ion-exchange methods is limited to a certain concentration of metals. For wastewater treatment and attenuation of metals from aqueous systems, natural and synthetic clays, zeolites and synthetic resins have been used (Gaikwad, 2010, Buzzi et al., 2013).

Pehlivan and Altun (2007) reported that Pb^{2+}, Cu^{2+}, Zn^{2+}, and Ni^{2+} can be exchanged on Lewatit CNP 80 resin. Montmorillonite containing clay was used for removal of Cu^{2+} from aqueous solution (Oubagaranadin and Murthy, 2010). Xu et al. (2012) reported that phosphate modified PS-EDTA resin has the efficiency to remove > 90% of Cu^{2+}, Zn^{2+}, and Cd^{2+} from contaminated water. Inglezakis et al. (2003) noted that natural clinoptilolite has the efficiency to remove Cu^{2+}, Pb^{2+}, Fe^{3+} and Cr^{3+} from contaminated water bodies.

2.5.2 Piloted mine water desalination technologies in South Africa

The increase in environmental concerns to water pollution by mining industries has prompted the South African government and its associate authorities to develop, pilot and implement a number of waste water treatment technologies. Treatment methods that have been piloted in South Africa for treatment of acid mine drainage are summarized in Table 2.5. This table only focused on the cost required for producing a given quantity of water.

Table 2.5: Desalination technologies that have been developed in South Africa

Technology	Process	Cost
Alkali Barium Calcium (CSIR-ABC)	Precipitation and adsorption	R4.04/m^3
Lime treatment	Precipitation and adsorption	R5.50/m^3
Magnesium Barium Alkali (MBA)	Precipitation and adsorption	R2.20/m^3
EARTH	ion-exchange	R12.95/m^3
BioSure	Adsorption	R3.80/m^3
SAVMIN	Precipitation	R11.30/m^3
HiPRO	Reverse Osmosis	R9.12/m^3

The major factors that determine which type of treatment is best suited to a particular application include the levels of salinity and temporary hardness, the presence of colloidal suspended matter, dissolved metal-ions, oxidizing agents, hydrogen sulphide content and temperature of the feed water (Zick, 2011). As such, the development of a new treatment model is governed by the drawbacks of treatment methods that have been or are being used. Moreover, the majority of effluent treatment technologies are costly, generate toxic secondary sludge which is expensive to dispose of and some are inefficient and do not yield treated water compliant with water quality standards. **Table 2.5** summarises mine effluent treatment technologies that have been developed and implemented in South Africa. As shown in **Table 2.5** the MBA process (Bologo et al., 2012) seems to be sustainable as compared to other traditional methods.

2.5.3 Other acid mine drainage treatment technologies

Several laboratory based technologies have been developed for treatment of AMD. Since most of the methods are not sustainable to treat mine water, research is continuing to come up with a sustainable treatment technology. Use of waste materials will reduce the cost of the any treatment process. In the quest to develop low-cost and effective technologies to remediate AMD, Gitari et al. (2006) have used coal combustion fly ash to neutralize and remove metals in AMD. The availability of Ca in a form of lime in elevated concentration enhances the efficiency of coal fly ash to neutralize AMD. Also, the presence of other cations, which include Al, Si, Fe, Na, and K, increase the probability of ion-exchange and adsorption of chemical constituencies from AMD. In their study, the authors noted that co-disposal of coal fly ash and acid mine drainage raises the pH to circumneutral levels, and hence attenuation of metal species.

Madzivire et al. (2014) reported that the application of a jet loop reactor for mine water treatment using fly ash, lime and aluminium hydroxide can lower the sulphate concentration to DWA water quality guidelines acceptability and raise the pH to >10. Bologo et al. (2012) reported that the application of magnesium hydroxide for treatment of AMD can lead to an increase of the pH to 9.6 and lower the TDS from 9242 to 6037 mg/L and remove other metals except for magnesium. In their study, the authors reported that the addition of lime may lead to lowering of the concentrations of magnesium species in aqueous solution, hence increasing the pH further to 12.5. Maree et al. (1997) investigated the use of dolomite to neutralize coal acid mine water. The authors reported that after 15 minutes of interaction, the pH of the solution was observed to increase from 2.5 to 6.5 and the acidity of the solution was reduced from 600 to 50 mg/L (as $CaCO_3$). Leite et al. (2013) claimed that the use of steel slag for neutralization of AMD may result in an increase in pH and reduction in TDS content and metal concentrations.

Maree et al. (2004a) reported that the application of limestone for coal mine effluent treatment can raise the pH from 1.8 to 6.6 with subsequent oxidation of iron if done with exposure to the atmosphere. In their study, the authors also mentioned that the liming process lowers the sulphate concentration from 8342 mg/L to 1969 mg/L. Strosnider et al. (2013) explored the feasibility of co-treating Zn-rich AMD and raw municipal wastewater by mixing the two effluents. They reported that after mixing of Zn-rich AMD and raw municipal

effluents, the pH of the resultant solution was 7 and Al, Fe, Mn and Zn concentrations were reduced by 99.7, 99.9, 4.5 and 33.9% respectively. Madzivire et al. (2011) have successfully employed fly ash to neutralize and remove toxic elements from AMD. Approximately 90% of sulphate was removed when coal fly ash was used while treating low pH, Fe, Al and sulphate rich AMD.

Bone meal was applied as an alternative technology for treatment of acid and metal contaminated AMD. It was reported that after interaction of AMD with bone meal the pH rose from 3.0 to 5.7 within 6 h 30 mins and during the neutralization process 99% removal of Fe, Zn, Al and Cu were observed and Mg removal of 36% was observed by Payus et al. (2014). Heviánková et al. (2014) reported that interaction of wood ash with acid mine drainage led to an increase of pH from 3.5 to 8.3 after 20 mins and 0.5 g L^{-1} of prepared solution. Under optimized condition, wood ash removed close to 100% of Fe, As, Co, Cu, Zn and Al. Coal fly ash, natural clinker and synthetic zeolite were used for the removal of heavy metals from acid mine drainage. It was observed that the pH regimes shifted from 1.96 to 2.66 and 4.20 for coal fly ash, 1.86 and 1.85 for zeolite. Selectivity of faujasite for metal removal was in decreasing order of Fe>As>Pb>Zn>Cu>Ni>Cr (Ríos et al., 2008).

López et al. (2010) investigated the capabilities of using the final products from CO_2 emissions capture with alkaline paper mill waste for neutralization of acid mine drainage. The authors complemented experimental results with PHREEQC geochemical modelling. It was reported that alkaline paper mill waste can raise the pH of acid mine drainage from 3.6 to 8.3. Electrical conductivity was also observed to decrease drastically indicating a possible metal attenuation. Levels of Al, As, Cu and Cr were also removed to below detection limit by similar waste material. Tolonen et al. (2014) found that the by-products from quicklime manufacturing can be used as an alternative material for treatment of AMD. In their study, the authors reported that 30 min of contact time led to an increase of pH from 2.6 to 9.5. A drastic removal of Al, As, Cd, Co, Cu, Fe, Mn, Ni and Zn by 99% and approximately 60% of sulphate concentration, was also observed.

Name and Sheridan (2014) reported that interaction of acid mine drainage for 30 minutes with metallurgical slags may lead to an increase in pH from 2.5 to 12.1 and lowering of Fe and sulphate concentrations by 99.7 and 75%, respectively. Luptakova et al. (2012b) reported that that electro winning can be a physical-chemical and biological method for treatment of

acid mine drainage. The authors reported that electro winning can achieve approximately 97% removal efficiency for Al, Fe, Mn, As in the form of hydroxides and Cu and Zn in the form of metal sulphides. Li et al. (2008) investigated the application of clinoptilolite for treatment of acid rock drainage. The authors reported that clinoptilolite managed to adsorb Cu, Fe, Al and Zn within 30 mins of interaction with AMD. Falayi and Ntuli (2014) investigated the use of un-activated attapulgite for neutralization and attenuation of toxic chemical species from AMD. The authors reported that after 4 hours of contact, 100% removal of Cu and Fe, 93% for Co, 95% for Ni and 66% for Mn removal were achieved using 10% (w/v) attapulgite loading.

2.5.4 Passive Treatment systems

Passive treatment refers to any little or no maintenance treatment of acid mine drainage that does not require continual chemical addition and monitoring. These are dynamically complex systems that integrate both chemical and biological mechanisms in AMD pollution abatement and environmental protection. Selection of appropriate passive system is primarily based on the chemistry of water and efficiency of the treatment system. Wetlands have received particular attention because processes within wetlands can precipitate and remove metals. Limestone drains, wetlands, or a combination of both are the most often used passive treatment system (Sheoran and Sheoran, 2006, Groudev et al., 2008, Lange et al., 2010, Strosnider et al., 2011b, Macías et al., 2012b, Labastida et al., 2013, Hengen et al., 2014). As shown in **Figure 2.2**, ppassive treatments are discussed in detail below.

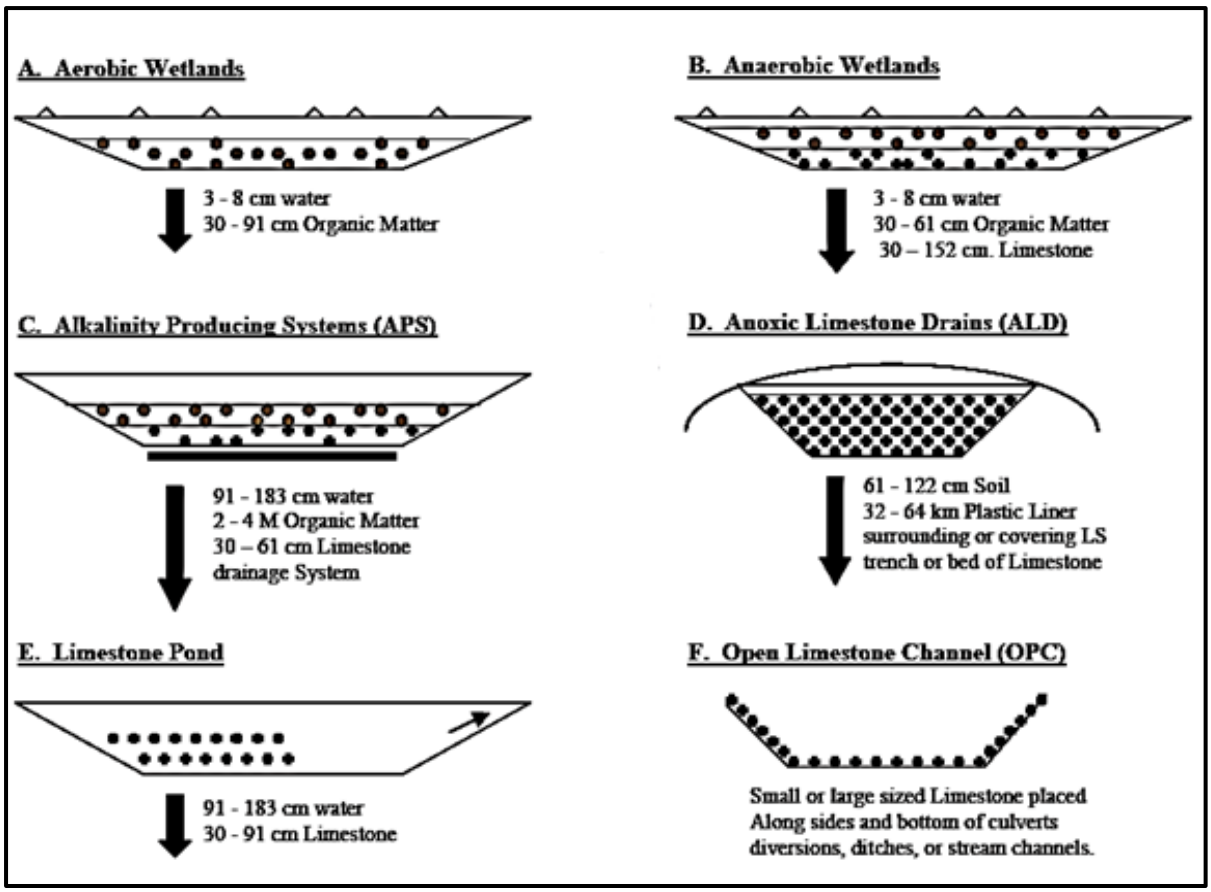

Figure 2.2: Passive systems of treating acid mine drainage.

2.5.4.1 Phytoremediation

Constructed wetlands are man-made and engineered ecosystems that mimic naturally occurring wetland ecosystems. Due to pitfalls and drawbacks of chemical treatment methodologies interest in aerobic wetlands has evolved as an alternative of active treatments. Passive treatment was generated as a result of observations that natural *Sphagnum* peat wetlands that received AMD improved water quality without any obvious adverse ecological effects (Hedin et al., 2005, Hedin et al., 2010). Discharge of polluted waters into natural wetlands, however, is prohibited in the United States, so wetlands are constructed specifically for the purpose of treating AMD. Early efforts to treat AMD with constructed wetlands mimicked the *Sphagnum* peat wetland model. Laboratory experiments have shown promising results (Kleinmann and Chatwin, 2011), but *Sphagnum* proved to be very sensitive to transplanting stress, abrupt changes in growing conditions, and excessive accumulation of iron (Hallberg and Johnson, 2005, Johnson and Hallberg, 2005b, Whitehead and Prior, 2005, Sheoran and Sheoran, 2006, Groudev et al., 2008, White et al., 2011).

The current conventional design of wetlands constructed to treat AMD looks nothing like a *Sphagnum* wetland, although the same processes are used to treat water. Constructed wetlands consist of a series of cells that allow hydrology to be easily controlled to maximize treatment effectiveness. AMD treatment wetlands are planted with *Juncus, Eleocharis, Scirpus,* and *Typha,* although *Typha latifolia* (common cattail) is used most often. Vegetation is planted into an organic substrate such as topsoil, rotten animal manure, spoiled hay, and compost. Water flow is slow, with a depth of 15-45 cm. Wetlands can be constructed at the discharge point of AMD contaminated streams, or AMD contaminated waters can be pumped into a more convenient wetland construction site. The placement of a constructed wetland with respect to mine waste and AMD contaminated stream.

The principal mechanism of metal removal in constructed wetlands formation of metal oxides and hydroxides, formation of sulphides, organic complexation reactions, Cation and anion exchange and phytoremediation. Other methods may entail filtration of suspended solids and adsorption and exchange of metals on algal mat. The way in which a wetland is constructed affects the way in which water is purified. As such, there are two types of engineered artificial ecosystems which include aerobic (vegetation are plated <30cm deep with relative impermeable sediments of soil and clay) and anaerobic (vegetation are plated >30cm deep with relative permeable sediments of soil, peat, sawdust, compost, and hay) wetland. In some cases, constructed wetlands have been documented to successfully remove Fe with Al and Mn removal been variable (Mitsch and Wise, 1998, Gibert et al., 2004, Hallberg and Johnson, 2005, Johnson and Hallberg, 2005c, Johnson and Hallberg, 2005b, Whitehead et al., 2005, Whitehead and Prior, 2005, Batty et al., 2006, Kalin et al., 2006, Sheoran and Sheoran, 2006, Lagos et al., 2011, White et al., 2011, Lizama Allende et al., 2014).

2.5.4.2 Open Limestone Channels

Research studies have documented that limestone is one of the excellent neutralizing agent for acidic water (Maree and Du Plessis, 1993, Maree et al., 2004a). This led to construction of open limestone channels to pre-treat AMD effluent. Open limestone channels raise the pH of effluent by the reaction of calcite with carbonic acid. Complications arise when the Fe^{3+} and Al^{3+} present in AMD are exposed to the atmosphere, forming metal hydroxides and resulting in a surface coating of the limestone channel known as armoring. This coating reduces limestone pore space, decreasing the limestone solubility and acid neutralization

effect (Alcolea et al., 2012b). Due to that, large quantities of limestone are needed to generate the alkalinity to ensure long-term success of open limestone channels, but high flow velocity and turbulence keep precipitates in solution and reduce the armoring effect and the quantities of limestone needed. It has since been suggested that if the channels are constructed correctly, open limestone channels should be maintenance free and provide AMD treatment for decades (Alcolea et al., 2012a). Channels constructed with steep slopes and with flow velocities that keep metal hydroxides in suspension showed that the drains were only 2-45% less effective when armored (Merovich Jr et al., 2007, Stiles and Ziemkiewicz, 2010). Although open limestone channels suggest a promising remediation technique, more research is needed to test the effects of armoring on different characteristics of AMD effluent.

2.5.4.3 Anoxic Limestone Drains

LaBar et al. (2008) reported that if mine wastewater is interacted with limestone in an anoxic environment, armoring would not occur. In their study, the authors revealed that AMD water was channeled through an underground limestone-lined trench, became alkaline, and was discharged into wetlands where the metal contaminants were then precipitated. The rise in pH of Anoxic Limestone Drains (ALD) treated effluent occurs due to the principle bicarbonate-producing process that occurs in open limestone channels, the reaction of calcite with carbonic acid. Although ALDs are documented to have success in raising pH, they have shown large variation in generating alkalinity and removing metals (Whitehead and Prior, 2005, Kleiv and Thornhill, 2008, LaBar et al., 2008, Cui et al., 2012, Genty et al., 2012).

2.5.4.4 Alkalinity Producing Systems

The alkalinity producing systems (APS) operate in a similar manner to the anaerobic wetlands, but require a reduced land area. APS are constructed with a layer of composted organic matter on top of a bed of limestone. A layer of AMD water settles on top of the organic layer, and drains into perforated drainage pipes, placed in the lower part of the limestone layer. The water then flows through the organic layer and limestone. The limestone then gets dissolved by the anaerobic water with the production of hydroxide ions. Once the water is drawn into the drainage pipes and is discharged into the adjacent settling pond, re-oxygenation of the water and precipitation of the metals occurs (Deocampo and Jones, 2014).

2.5.4.5 Limestone Ponds

In Limestone Ponds, limestone is placed at the bottom of the pond and water flows upward through the limestone. If lime is coated by Fe and Al hydroxide, the lime in the pond will be agitated using a stirring material to loosen the limestone and the precipitates. If the limestone is exhausted by dissolution, the fresh limestone will be introduced to the chamber so that neutralization and precipitation of metals can take place (Macías et al., 2012a).

2.6 Magnesite

Magnesite essentially refers to magnesium carbonate ($MgCO_3$). It is characterized by 47.8% of MgO and 52.2% CO_2. It is a white sedimentary rock which is formed as an evaporate from the alteration of Mg – rich igneous and metamorphic rocks. Magnesium can be formed in numerous ways such as the substitution of Fe in siderite ($FeCO_3$) to form $MgCO_3$, carbonation of olivine in the presence of water and carbon dioxide and carbonation of magnesium serpentine to form talc, magnesite and water (Simonov et al., 1979, Zachmann and Johannes, 1989, Pohl, 1990, Mandour and Elmaatty, 2001, Nasedkin et al., 2001, Niemelä, 2001, Prasannakumar and Kumar, 2001, Prasannakumar et al., 2004, Vágvölgyi et al., 2008, Wang et al., 2011, Palinkaš et al., 2012, Sibanda et al., 2013). There are two types of magnesite. i.e. crystalline magnesite and cryptocrystalline magnesite (Nasedkin et al., 2001).

2.7 Magnesite in South Africa

The viable deposit of magnesite in South Africa occurs as a weathering product of rocks with high contents of magnesium. The main magnesite deposits in South Africa are in Mpumalanga and Limpopo Provinces. In Mpumalanga, it is found in the Malelane area, Lydenburg and in the north of Southernburg and Burgersfort. In Limpopo province, it is found in Giyani and Folovhodwe. Magnesite is mined by open cast mineral extraction. Currently South Africa has two operating mines for magnesite: Chamotte Holdings (Pty) Ltd in Mpumalanga and Syferfontein Calcite (Pty) Ltd in Limpopo. Magnesite in South Africa is primarily used for amendments of agricultural soil. The deposits of magnesite in South Africa have been estimated to be 18 Mt in total (Afonin and Maryasev, 2006, Jeleni et al., 2012, Sibanda et al., 2013, Masindi et al., 2014a). The deposits of magnesite in South Africa are shown in **Figure 2.3** below.

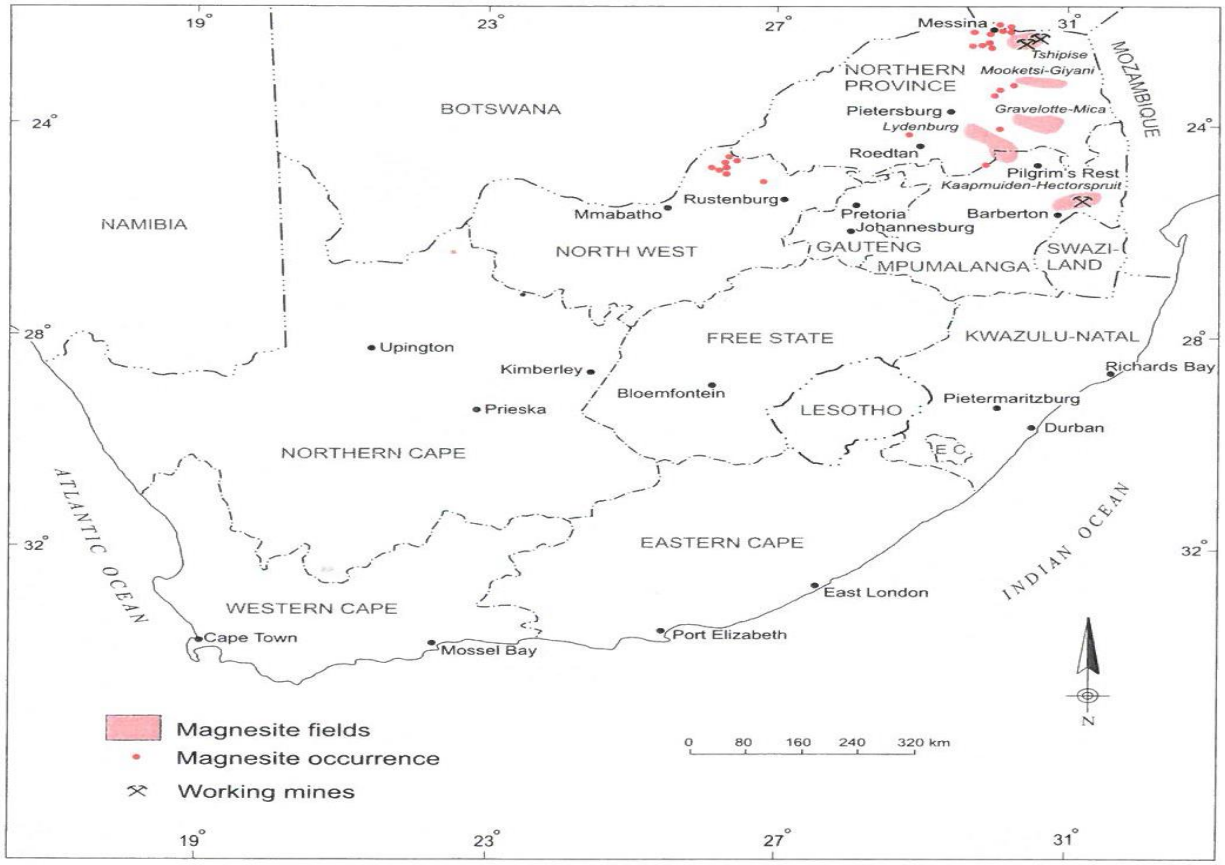

Figure 2.3: Magnesite field of the republic of South Africa

2.8 Genesis of Folovhodwe magnesite

Sibanda et al. (2013) have reported on petrographic and geochemical studies about magnesite genesis. The authors pointed out that, the major rock-forming minerals of basalt are plagioclase and clinopyroxene, and of dolerite are olivine, orthopyroxene, clinopyroxene and plagioclase. Experimental evidence revealed that magnesite mineralisation took place along the joints, cracks and crevices within weathered basalt and dolerite, resulting from the carbonation of forsterite that were altered to amphibole, serpentine and talc in the presence of CO_2 and H_2O to produce magnesite, smectite, palygorskite and sepiolite. Forsterite and enstatite were the primary sources of the Mg^{2+} ion. The high content of olivine and pyroxene in dolerite led to the abundance of the Mg^{2+} ion during alteration, hence, the dominance of magnesite in dolerite (Dabitzias, 1980, Zachmann and Johannes, 1989, Afonin and Maryasev, 2006, Palinkaš et al., 2012). Thus mode of formation and the content of magnesite in Folovhodwe magnesite make it amorphous (Sibanda et al., 2013).

2.9 Beneficial application of magnesite

Crude magnesite is used for Epsom salts manufacture and Mg metal manufacture. It is also used in the manufacture of fertilizers for agricultural soil amendment or neutralization (Kleinevoss et al., 1975, Masindi et al., 2014b). It can be used as a feedstock for the production of magnesium chemicals, pharmaceuticals, and animal feeds. It is also used for rayon manufacture and as a vulcanizing agent in the rubber industry. It can also be used for desulphurization of flue gases in power utilities and water treatment. It is used mainly as sintered grains in ramming mixes, gunning mixes and bricks. It can be used as an insulator for high temperatures and as a desiccant (Bron et al., 1961, Kaibicheva et al., 1962, Bluvshtein and Boricheva, 1963, Bron et al., 1964, Zubakov and Yusupova, 1964, Bugaev et al., 1969, Kaibicheva et al., 1971, Erten and Gokmenoglu, 1994, Aras and Demirhan, 2004, Kawasaki et al., 2006).

2.10 Clay materials and their applications in environmental remediation

Clays are fine grained and hydrous aluminosilicate materials which are mainly composed of colloid fractions of soils, sediments, rocks and water bodies (van Olphen, 1963, Fedorov et al., 2005, Güven, 2009, Sherry, 2013, Stucki, 2013, Zhu and Elzinga, 2014). They are the products of rock weathering and they play an exceptional role in determining the physical and chemical properties of soil. The clay fractions contain particle sizes of less than 2 μm diameter. They are also referred to as inorganic materials with sheet like structures of phylosilicates. The clay minerals are characterized by a two dimensional array of tetrahedral sheets of T_2O_5 composition, usually with polycations of Al^{3+} or Si^{4+} sandwiched to pentagonal oxygen, the octahedral sheet which is mainly characterized by Al^{3+}, Fe^{3+}, Fe^{2+}, or Mg^{2+} coordinated with oxygen or hydroxyl anions. The tetrahedral and octahedral sheets are bonded together via oxygen. Depending on charge valences, if trivalent species such as Al occupies the site arrangement it is called trioctahedral and if the octahedral sheet is dominated by divalent ions such as Mg, it is classified as trioctahedral .

Depending on charge density and valence, species in octahedral or tetrahedral sheets may replace each other through isomorphous substitution. They are the most abundant and widespread natural resources that are readily available on the earth's surface. Depending on

their nature and composition, there are different types of clays and these include smectite, vermiculite, kaolinite, sepiolite, chlorites, and mica. Due to the negatively charged end of the clay fraction, high surface area, and swelling properties, clay minerals have the ability to scavenge positively charged species through adsorption and ion-exchange. Clays can adsorb anions to clay interlayers since they have high cation-exchange capacity. Clays containing montmorillonite as the main mineral are referred to as bentonite clays and are categorized within the smectite family. A number of research studies have recommended bentonite clay as having good physico-chemical properties that result in it being an excellent adsorbent (Ayari et al., 2005, Zulfahmi et al., 2012).

2.10.1 Bentonite clay

The term bentonite is ambiguous. As defined by geologists, it is a crystalline silicate clay rock formed of highly colloidal and plastic clays largely dominated by montmorillonite, a clay mineral of the smectite family. The formation of bentonite predominantly takes place in aqueous environmental conditions during or after deposition. In addition to montmorillonite as the main mineral, bentonite may also contain feldspar, biotite, kaolinite, illite, cristobalite, pyroxene, zircon, and crystalline quartz. This may also depend on the physicochemical properties of the parent material being weathered. Depending on the dominant element, bentonite clay can be classified into K, Na, Ca, Al and Fe bentonite. The chemical properties of bentonite can be modified by introducing highly ionic, stable, and higher density species to bentonite clay interlayer through a process known as ion-exchange and sorption

2.10.2 Physicochemical properties of bentonite clay

2.10.2.1 Physical properties of bentonite clay

Bentonite is white to pale green or blue and, darkens in time to yellow, red, or brown. It feels greasy and soap-like when touched. It has flat and thin sheet crystal morphology which is irregularly shaped and can be up to 1000 μm in dimension. It has a large surface area of about 800 m^2/g that significantly contributes to its high cation-exchange capacity. Nevertheless, bentonite has a high water holding capacity which enables it to swell to 30 times its original size hence allowing it to retain water within its matrices for a long period of time thus

promoting higher chemical reactivity between soil, solution and bentonite clay. This good physical property of bentonite clay enables it to scavenge polar pollutants and firmly hold them on clay fractions through weak Van der Waals forces or chemical bonding

2.10.2.2 Chemical properties of bentonite clay

As mentioned, bentonite clay is mainly dominated by montmorillonite as the principal element. Montmorillonite is a very soft phyllosilicate group of minerals that typically forms microscopic crystals. It is derived from volcanic glass, mica, feldspar, various FeMg silicates or precipitates directly from solution. Bentonite clay may also contain feldspar, biotite, kaolinite, illite, cristobalite, pyroxene, zircon, and crystalline quartz as impurities depending on the weathered parent materials. The basic crystal structure of smectite clay (bentonite) is an octahedral alumina sheet sandwiched between two tetrahedral silica sheets (**Figure 2.4**).

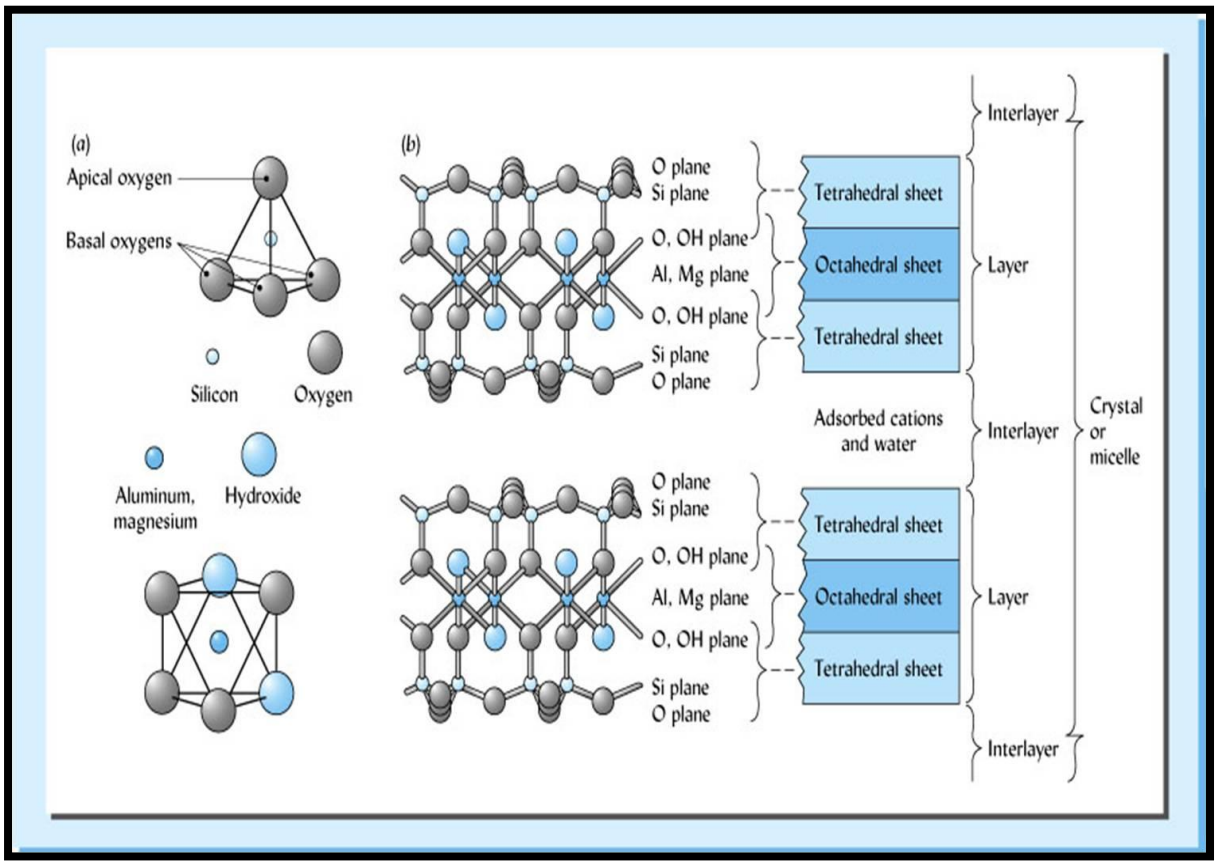

Figure 2.4: Structure of bentonite clay

As such, they are classified within the family of expansible 2:1 phylosilicates clays having permanent charges that can undergo cation- and anion-exchange. Atoms in these sheets common to both layers are oxygen. These three-layer units are stacked one above the other

with oxygen in neighboring layers adjacent to each other. This produces a weak bond, allowing water and other polar molecules to enter between layers and induce an expansion of the mineral structure (swelling). In the tetrahedral coordination, silicon may be substituted by aluminium or iron. In the octahedral coordination, aluminium may be substituted by magnesium, iron, lithium, chromium, zinc, or nickel by the process known as isomorphous substitution. Differences in the substitutions within the lattice in terms of position and elemental composition give rise to the various montmorillonite clay minerals (Velde, 1992, Velde, 1995, Kehew, 2001, Murray, 2006, Mukherjee, 2013). The molecular formula for montmorillonite is usually expressed as:

$(M^{+}_{x}\cdot nH_2O)\ (Al_{2-y}Mg_x)Si_4O_{10}(OH)_2$, where $M^{+} = Na^{+}$, K^{+}, Mg^{2+}, or Ca^{2+} (exchangeable base cations). Ideally, x = 0.33 (Velde, 1977, Velde, 1992).

Due to its favorable physicochemical properties bentonite clay is valued for its versatile uses, sorption properties, catalytic action, bonding power, plasticity, high swelling and water holding capacity, high surface area and ion-interchange capacity (Cation Exchange Capacity (CEC) and Anion Exchange Capacity (AEC)). The addition of water to bentonite causes the platy-particles of the clay to partly swell. The plates of this clay have negative charges on the edges which attract positively charged species on the surface using electrostatic forces or weak Van der Waals forces. Bentonite clay can attract and hold a large number of water molecules, because the charges on the internal and external colloid surfaces attract the oppositely, partially charged end of the polar water molecule. Water adsorbed between the crystal layers can cause the layer to move apart, making the clay more plastic and resulting in swelling. The water in bentonite clay is driven off when the clay is heated in air, and this leads to the platy - layers collapsing, hence causing the clay to have an undefined structure with an overall slightly negative charge (Kehew, 2001, Eby, 2004, Murray, 2006, Thibodeaux and Mackay, 2010, Masindi, 2013, Mukherjee, 2013).

2.10.3 Application of bentonite clay for waste water treatment

Due to its high cation-exchange capacity, surface area and swelling abilities clays have been widely used for wastewater treatment. Of late, bentonite clay has been reported to be the only low-cost material that is widely used in numerous fields of material science and technology and the utilization of this clay material for the treatment of wastewater containing hazardous substances has received great attention. Moreover, bentonite clay can also be modified by

other exogenous species in an attempt to enhance its adsorption capacities (Burgos et al., 2002, Bhattacharyya and Gupta, 2008a, Bineesh and Park, 2011, Anjum et al., 2013, Anadão et al., 2014, Đukić et al., 2015a, Zhuang et al., 2015).

Xu et al. (2008) documented that MX-80 bentonite clay has the ability to adsorb Pb(II) from aqueous solution. Vieira et al. (2010) showed the possibility of removing Ni(II) from aqueous solution using Befo bentonite clay in a porous bed. Vieira et al. (2014) evaluated mechanisms of Cu(II) and Hg(II) adsorption on bentonite clay from EXAFS spectroscopy. Veli and Alyüz (2007) reported the adsorption of Cu(II) and Zn(II) from aqueous solution by using natural clays.

Abollino et al. (2003) reported that Na-montmorillonite has the ability to remove toxic chemical species from aqueous media. Ayari et al. (2007) noted that Pb(II), Zn(II) and Ni(II) can be removed from aqueous solution using Na-activated bentonite clay. Bourliva et al. (2013) reported that Pb(II) can be removed from aqueous solution using Greek bentonite. Manohar et al. (2006) reported that Co(II) can be removed from aqueous solution using Al-pillared bentonite clay. Missana and Garcı´a-Gutiérrez (2007) showed that bivalent species of Ca(II), Sr(II) and Co(II) can be effectively removed from aqueous solution using FEBEX bentonite clay. Gitari (2014) documented that South African bentonite clay can remove Al, Mn and Fe from acid mine drainage.

2.11 Bentonite clay composite

The high adsorption, ion exchange and expansion properties, as well as high surface area, layered structure, abundance and low cost that make clay minerals to be an attractive alternative material widely used for the removal of different inorganic and organic pollutants; in addition, these materials are environmentally friendly (Zhuang et al., 2015). Modification techniques such as intercalation and pillaring, acid activation (Bhattacharyya and Gupta, 2008b, Bhattacharyya and Gupta, 2008a, Bhattacharyya and Gupta, 2011) and mechanochemical activation (Oliker et al., 2008, Ghorai and Pramanik, 2011, Hosseini et al., 2012, Kim et al., 2013, Kumrić et al., 2013, Đukić et al., 2015a) can be used for improving the adsorption properties of the clays. The preparation of organoclays (OC) by grafting and direct synthesis was also reported when pollutants were removed from contaminated water (Li and

Bowman, 2001, Oyanedel-Craver et al., 2007, Stathi et al., 2007, Yapar, 2009, Sarkar et al., 2010, Sarkar et al., 2013, Silva et al., 2014, Şimşek et al., 2014).

Among composite synthesis science, mechanochemical activation has been reported to present best properties that enable it to retain pollutants due to its cost-effective and environmentally friendly technique of modification (Oliker et al., 2008, Ghorai and Pramanik, 2011, Đukić et al., 2015a). Documented literature pointed out that mechanochemical activation improves morphological and microstructural properties of the clay (Dellisanti and Valdré, 2005). Only a limited number of studies investigated the use of mechanical milling on their adsorption properties (Kumrić et al., 2013, Đukić et al., 2015a, Đukić et al., 2015b). Milling can lead to fragmentation, distortion, breakage of crystalline network and particle size reduction followed by an increase of the surface area, exfoliation of particles and amorphization, hence improving the efficiencies of the material to remove contaminants from wastewaters (Dellisanti and Valdré, 2005). Even though removal of metals from aqueous media by clay minerals is primarily reliant on pH of the metals laddened solution, there is a need to enhance its removal potentials since acidic pH has limited the use of clay for removal of pollutants (pH < 4) (Dukić et al., 2015). In an attempt to overcome the limitations in the use of the raw as well as the modified clays as adsorbents, the adsorbents can be prepared in a composite form with some metal oxides and carbonates (Kumrić et al., 2013, Đukić et al., 2015b).

2.12 Application of composite for wastewater amelioration

Although there are numerous methods for fabricating modified clays and clay composites (Dellisanti and Valdré, 2005), very little studies have investigated the use of mechanochemically modified clay composite for remediation of wastewaters. Dukić et al. (2015) investigated the use of mechanochemical synthesised montmorillonite-kaolinite/TiO_2 composite for simultaneous removal of Pb^{2+}, Cu^{2+}, Zn^{2+} and Cd^{2+} from highly acidic solutions. The authors revealed that mechanochemical modification is the effective way of modifying clay and evaluate its ability to sorb metal species from aqueous system. In their study, it was observed that 60 mins of shaking, 200 rpm shaking speed and 50 ppm multicomponent solution was removed from highly acidic water using the mechanochemical synthesised montmorillonite-kaolinite/TiO_2 composite. Kumrić et al. (2013) evaluated the use of mechanochemical treated interstratified montmorillonite/kaolinite clay for simultaneous

removal of Pb^{2+}, Cu^{2+}, Zn^{2+} and Cd^{2+} from aqueous solutions. The authors disclosed that 60 mins of equilibration, 50 ppm multi-component solution, 200 rpm shaking speed and 2: 100 S/L ratios were optimum for removal of divalent species from contaminated water bodies.

2.12 Legal requirements of water quality

The National Environmental Management Act (NEMA) 108 of 1998, stipulates that everyone has right to live in an environment which is safe and unlikely to pose any deleterious effects to their health. The legislative requirements for industrial effluents are primarily governed by the DWA Water Quality Guidelines (Kidd, 2011). These require that any person who uses water for industrial purposes shall purify or otherwise treat such water in accordance with requirements of DWA (Africa et al., 2010, Kidd, 2011, Vicente et al., 2013, Biswas et al., 2014). The relevant criteria for discharge of acidic and sulphate-rich water are given in Table 2.6.

Table 2.6: The relevant criteria for discharge of acidic and sulphate-rich water as compared to DWS water quality guidelines

Parameter	Gold AMD*	Coal AMD**	Neutral drainage†	DWS Industrial	DWS Irrigation
pH	2.3	2.5	6.5	5.0-10.0	6.5-8.4
EC	22713	13980	500	0-250	>540
Na	248.4	70.5	20.1	-	430-460
K	21.6	34.2	29.1	-	-
Mg	2.3	398.9	861.8	-	-
Ca	710.8	598.7	537.5	-	-
Al	134.4	473.9	0.01	-	5.0-20
Fe	1243	8158.2	0.07	0.0-10	5.0-20
Mn	91.5	88.2	25.0	0.0-10.0	0.02-10.0
Cu	7.8	-	-	-	0.2-5.0
Zn	7.9	8.36	0.16	-	1.0-5.0
Pb	6.3	-	-	-	0.2-2.0
Co	41.3	1.89	0.29	-	0.05-5.0
Ni	16.6	2.97	0.21	-	0.2-2.0
SO_4^{2-}	4635	42862	4603	0-500	-

Note: *) Gold mining AMD (Tutu et al., 2008), **), Coalmining AMD and †), Neutral drainage water (Gitari et al., 2006, Gitari et al., 2008, Madzivire et al., 2010, Madzivire et al., 2011, Madzivire et al., 2013, Madzivire et al., 2014, Masindi et al., 2014c).

As shown in Table 2.6, mine effluents in South Africa are dominated by dissolved Fe, Al, Mn, Ca, Na, Mg and traces of Cu, Co, Zn, Pb and Ni. These concentrations are far above the legal requirements.

2.12 Geochemical modelling

Modelling and computer simulation is a valuable tool that can be used to gain insight into geochemical processes both to interpret laboratory experiments and field data as well as to make predictions of long-term behaviour of chemical components in a system under study.

A growing awareness of potential environmental hazards caused by activities such as mining, disposal of wastes, and chemical spillage, have sparred an interest in the ability to anticipate pollution scenarios and design management strategies for the minimisation of environmental impact. Owing to issues of complexity and the time-scales involved, it is often not possible to conduct sufficiently realistic laboratory experiments to observe the long-term behaviour of most environmental systems. Geochemical models can be used to both interpret and predict processes that may take place over time-scales that are not achievable in experiments as such modelling becomes the most important tool that is indispensable from long term experiments.

From a design viewpoint, geochemical modelling can be applied to optimise remediation efforts, identify parameters of importance in environmental systems, and to help design effective techniques to prevent the release of environmentally hazardous substances. Although by no means a substitute for experimental work, modelling is a valuable predictive tool that can be used to bridge the gap between laboratory experiments, field observations, and the long-term behaviour of geochemical systems (Parkhurst, 1995, Parkhurst and Appelo, 1999, Halim et al., 2005, Zhang and Luo, 2007, Martens et al., 2008, Tiruta-Barna, 2008, Wissmeier and Barry, 2010, Charlton and Parkhurst, 2011, Van Den Akker and Ahn, 2011, Chidambaram et al., 2012, Van Pham et al., 2012, Zhao et al., 2012). In this work, PHREEQC Geochemical Modelling Code will be used to model the processes involving the interaction of magnesite/bentonite clay and the contaminant-containing solutions. The processes will include adsorption, desorption, neutralization and speciation, amongst others.

2.13 Conclusions

From the literature survey, the undermentioned areas of concern in relation to the theme of the present study were identified. Traditional AMD treatment technologies have been developed but cost factors, handling procedures and generation of secondary sludge which is toxic and harmful and requires special disposal facilities which are costly to maintain. This has raised numerous legislative concerns and strictness of environmental regulations. Magnesium based materials have been successfully used for remediation of AMD but the manufacturing costs in case of brucite becomes a limiting factor when is being applied in the CSIR-MBA process since cost is a concern factor in all the treatment technologies. Crystalline magnesite has been employed for remediation of AMD but it raises the pH of acid

mine drainage to 5 which is less than the legal guideline value. It was also reported to remove metals from acid and metalliferous drainages but the resulting treated water is far from compliant with environmental regulations. Cryptocrystalline magnesite has never been employed for AMD remediation as such there is a need to evaluate the efficiency of amorphous magnesite to remediate AMD.

Bentonite clay has been employed for remediation of industrial effluents but it has the limitation of poor adsorption from solutions with high concentrations of metals. Combinations of bentonite clay with limestone have been employed for neutralization and removal of metals from AMD but it has shown poor inorganic contaminants attenuation potential. It has also been demonstrated that interaction of bentonite clay with high density cations such as Al and Fe leads to the replacement of base cations through isomorphous substitution. In an attempt to overcome the over exploitation of resources and to limit the use of the virgin and raw materials as well as the modified clays as adsorbents, the adsorbents can be prepared in a composite form with some metal oxides and carbonates.

To respond to the challenges that are been presented by current technologies, government, mining houses, and scientific communities are seeking for innovative and locally available technologies for remediating AMD. The present study was designed to address those challenges by synthesizing the composite with high adsorption and neutralisation capabilities. Magnesite in Folovhodwe is cryptocrystalline and has never been used for wastewater treatment; rather it is used for agricultural soil amendment. It has tri-lithological properties (brucite, periclase and magnesite properties) due to the formation conditions. This makes it an outstanding material for wastewater remediation since it is a combination of various magnesium-based materials. This literature review revealed a need to use magnesite individually and magnesite-bentonite blends for treatment of acidic and metalliferous mine drainage. Mechanochemical synthesized composites have never been used for acid mine drainage remediation. They have been successfully used for removal of toxic chemical species from wastewater. This will be the first study to explore the potential application of cryptocrystalline magnesite-bentonite clay composite for neutralisation and attenuation of inorganic contaminants from metalliferous and acidic mine effluents.

REFERENCES

Abollino, O., Aceto, M., Malandrino, M., Sarzanini, C. & Mentasti, E. 2003. Adsorption of heavy metals on Na-montmorillonite. Effect of pH and organic substances. *Water Research,* 37**,** 1619-1627.

Afonin, Y. A. & Maryasev, I. G. 2006. Cryptocrystalline magnesite in weathering crust of ultrabasic rocks. *Refractories and Industrial Ceramics,* 47**,** 269-274.

Africa, S., Van Der Linde, M. & Feris, L. 2010. *Compendium of South African Environmental Legislation*, Pretoria University Law Press.

Al-Shahrani, S. S. 2014. Treatment of wastewater contaminated with cobalt using Saudi activated bentonite. *Alexandria Engineering Journal,* 53**,** 205-211.

Alcolea, A., Vázquez, M., Caparrós, A., Ibarra, I., García, C., Linares, R. & Rodríguez, R. 2012a. Heavy metal removal of intermittent acid mine drainage with an open limestone channel. *Minerals Engineering,* 26**,** 86-98.

Alcolea, A., Vázquez, M., Caparrós, A., Ibarra, I., García, C., Linares, R. & Rodríguez, R. 2012b. Heavy metal removal of intermittent acid mine drainage with an open limestone channel. *Minerals Engineering,* 26**,** 86-98.

Amos, R. T., Blowes, D. W., Bailey, B. L., Sego, D. C., Smith, L. & Ritchie, A. I. M. 2015. Waste-rock hydrogeology and geochemistry. *Applied Geochemistry,* 57**,** 140-156.

Anadão, P., Pajolli, I. L. R., Hildebrando, E. A. & Wiebeck, H. 2014. Preparation and characterization of carbon/montmorillonite composites and nanocomposites from waste bleaching sodium montmorillonite clay. *Advanced Powder Technology,* 25**,** 926-932.

Anjum, A., Seth, C. K. & Datta, M. 2013. Removal of As3+ using chitosan-montmorillonite composite: Sorptive equilibrium and kinetics. *Adsorption Science and Technology,* 31**,** 303-323.

Anna, B., Kleopas, M., Constantine, S., Anestis, F. & Maria, B. 2014. Adsorption of Cd(II), Cu(II), Ni(II) and Pb(II) onto natural bentonite: study in mono- and multi-metal systems. *Environmental Earth Sciences,* 73**,** 5435-5444.

Aras, A. & Demirhan, H. 2004. Firing behavior of alkaline earth flux in ceramic bodies: The effect of magnesite on firing mineralogy and physical properties. *Key Engineering Materials,* 264**,** 1523-1526.

Ayari, F., Srasra, E. & Trabelsi-Ayadi, M. 2005. Characterization of bentonitic clays and their use as adsorbent. *Desalination,* 185**,** 391-397.

Ayari, F., Srasra, E. & Trabelsi-Ayadi, M. 2007. Removal of lead, zinc and nickel using sodium bentonite activated clay. *Asian Journal of Chemistry,* 19**,** 3325-3339.

Bálintová, M. & Singovszká, E. Acid mine drainage as environmental risk for surface water. 11th International Multidisciplinary Scientific Geoconference and EXPO - Modern Management of Mine Producing, Geology and Environmental Protection, SGEM 2011, 2011. 175-182.

Batty, L. C., Baker, A. J. M. & Wheeler, B. D. 2006. The effect of vegetation on porewater composition in a natural wetland receiving acid mine drainage. *Wetlands,* 26**,** 40-48.

Bereket, G., Aroğuz, A. Z. & Özel, M. Z. 1997. Removal of Pb(II), Cd(II), Cu(II), and Zn(II) from aqueous solutions by adsorption on bentonite. *Journal of Colloid and Interface Science,* 187**,** 338-343.

Bhattacharyya, K. G. & Gupta, S. S. 2008a. Adsorption of a few heavy metals on natural and modified kaolinite and montmorillonite: A review. *Advances in Colloid and Interface Science,* 140**,** 114-131.

Bhattacharyya, K. G. & Gupta, S. S. 2008b. Adsorption of Fe(III), Co(II) and Ni(II) on ZrO-kaolinite and ZrO-montmorillonite surfaces in aqueous medium. *Colloids and Surfaces A: Physicochemical and Engineering Aspects,* 317**,** 71-79.

Bhattacharyya, K. G. & Gupta, S. S. 2011. Removal of Cu(II) by natural and acid-activated clays: An insight of adsorption isotherm, kinetic and thermodynamics. *Desalination,* 272**,** 66-75.

Bineesh, K. V. & Park, D. W. 2011. Structural modification of montmorillonite clay by pillaring process: Its characterization and applications. *Clay: Types, Properties and Uses.* 371-390.

Biswas, A. K., Tortajada, C. & Izquierdo, R. 2014. *Water Quality Management: Present Situations, Challenges and Future Perspectives*, Taylor & Francis.

Bluvshtein, M. N. & Boricheva, V. N. 1963. Zonal change in the properties of magnesite brick after service in the roof of an open-hearth furnace. *Refractories,* 4**,** 445-450.

Bologo, V., Maree, J. P. & Carlsson, F. 2012. Application of magnesium hydroxide and barium hydroxide for the removal of metals and sulphate from mine water. *Water SA,* 38**,** 23-28.

Bourliva, A., Michailidis, K., Sikalidis, C., Filippidis, A. & Betsiou, M. 2013. Lead removal from aqueous solutions by natural Greek bentonites. *Clay Minerals,* 48**,** 771-787.

Brake, S. S., Hasiotis, S. T. & Dannelly, H. K. 2004. Diatoms in acid mine drainage and their role in the formation of iron-rich stromatolites. *Geomicrobiology Journal,* 21**,** 331-340.

Bron, V. A., Diesperova, M. I. & Krotova, G. S. 1964. The effect of additives, fineness and firing temperature on the sintering of caustic magnesite. *Refractories,* 5**,** 225-230.

Bron, V. A., Zamotayev, S. P., Medyakova, M. V., Semavina, K. P. & Khorashavin, L. B. 1961. Production and service testing of magnesite-chrome concrete. *Refractories,* 2**,** 90-96.

Bugaev, N. F., Simonov, K. V., Osipova, L. Y. A., Lyubimov, V. N., Pchelkin, M. S. & Barmotin, I. P. 1969. Porous magnesite plugs for degassing of steel through the ladle bottom. *Ogneupory i Tekhnicheskaya Keramika***,** 4-9.

Burgos, W. D., Pisutpaisal, N., Mazzarese, M. C. & Chorover, J. 2002. Adsorption of quinoline to kaolinite and montmorillonite. *Environmental Engineering Science,* 19**,** 59-68.

Buzzi, D. C., Viegas, L. S., Rodrigues, M. a. S., Bernardes, A. M. & Tenório, J. a. S. 2013. Water recovery from acid mine drainage by electrodialysis. *Minerals Engineering,* 40**,** 82-89.

Candeias, C., Ávila, P. F., Ferreira Da Silva, E., Ferreira, A., Salgueiro, A. R. & Teixeira, J. P. 2014. Acid mine drainage from the Panasqueira mine and its influence on Zêzere river (Central Portugal). *Journal of African Earth Sciences,* 99, Part 2**,** 705-712.

Charlton, S. R. & Parkhurst, D. L. 2011. Modules based on the geochemical model PHREEQC for use in scripting and programming languages. *Computers and Geosciences,* 37**,** 1653-1663.

Cheng, H., Hu, Y., Luo, J., Xu, B. & Zhao, J. 2009. Geochemical processes controlling fate and transport of arsenic in acid mine drainage (AMD) and natural systems. *Journal of Hazardous Materials,* 165**,** 13-26.

Chidambaram, S., Anandhan, P., Prasanna, M. V., Ramanathan, A. L., Srinivasamoorthy, K. & Kumar, G. S. 2012. Hydrogeochemical Modelling for Groundwater in Neyveli Aquifer, Tamil Nadu, India, Using PHREEQC: A Case Study. *Natural Resources Research,* 21**,** 311-324.

Cui, M., Jang, M., Cho, S.-H., Khim, J. & Cannon, F. S. 2012. A continuous pilot-scale system using coal-mine drainage sludge to treat acid mine drainage contaminated with high concentrations of Pb, Zn, and other heavy metals. *Journal of Hazardous Materials,* 215–216**,** 122-128.

Dabitzias, S. G. 1980. Petrology and genesis of the vavdos cryptocrystalline magnesite deposits, chalkidiki peninsula, Northern Greece. *Economic Geology,* 75**,** 1138-1151.

Dellisanti, F. & Valdré, G. 2005. Study of structural properties of ion treated and mechanically deformed commercial bentonite. *Applied Clay Science,* 28**,** 233-244.

Demchak, J., Morrow, T. & Skousen, J. 2001. Treatment of acid mine drainage by four vertical flow wetlands in Pennsylvania. *Geochemistry: Exploration, Environment, Analysis,* 1**,** 71-80.

Deocampo, D. M. & Jones, B. F. 2014. 7.13 - Geochemistry of Saline Lakes. *In:* TUREKIAN, H. D. H. K. (ed.) *Treatise on Geochemistry (Second Edition).* Oxford: Elsevier**,** 437-469.

Dukić, A. B., Kumrić, K. R., Vukelić, N. S., Dimitrijević, M. S., Baščarević, Z. D., Kurko, S. V. & Matović, L. L. 2015. Simultaneous removal of Pb2+, Cu2+, Zn2+ and Cd2+ from highly acidic solutions using mechanochemically synthesized montmorillonite-kaolinite/TiO2 composite. *Applied Clay Science,* 103**,** 20-27.

Đukić, A. B., Kumrić, K. R., Vukelić, N. S., Dimitrijević, M. S., Baščarević, Z. D., Kurko, S. V. & Matović, L. L. 2015a. Simultaneous removal of Pb(II), Cu(II), Zn(II) and Cd(II) from highly acidic solutions using mechanochemically synthesized montmorillonite–kaolinite/TiO2 composite. *Applied Clay Science,* 103**,** 20-27.

Đukić, A. B., Kumrić, K. R., Vukelić, N. S., Stojanović, Z. S., Stojmenović, M. D., Milošević, S. S. & Matović, L. L. 2015b. Influence of ageing of milled clay and its composite with TiO2 on the heavy metal adsorption characteristics. *Ceramics International,* 41**,** 5129-5137.

Eby, G. N. 2004. *Principles of Environmental Geochemistry*, Thomson-Brooks/Cole.

Erten, H. N. & Gokmenoglu, Z. 1994. Sorption behavior of Co(II), Zn(II) and Ba(II) ions on alumina, kaolinite and magnesite. *Journal of Radioanalytical and Nuclear Chemistry Articles,* 182**,** 375-384.

Falayi, T. & Ntuli, F. 2014. Removal of heavy metals and neutralisation of acid mine drainage with un-activated attapulgite. *Journal of Industrial and Engineering Chemistry,* 20**,** 1285-1292.

Fang, J., Hasiotis, S. T., Gupta, S. D., Brake, S. S. & Bazylinski, D. A. 2007. Microbial biomass and community structure of a stromatolite from an acid mine drainage system as determined by lipid analysis. *Chemical Geology,* 243**,** 191-204.

Fedorov, N. N., Doroshenko, S. P. & Koroid, V. N. 2005. Physical-and-mechanical activation of bentonite clays. *Litejnoe Proizvodstvo***,** 17-19.

Frempong, E. M. & Yanful, E. K. 2006. Chemical and mineralogical transformations in three tropical soils due to permeation with acid mine drainage. *Bulletin of Engineering Geology and the Environment,* 65**,** 253-271.

Gaikwad, R. W. 2010. Review and research needs of active treatment of acid mine drainage by ion exchange. *Electronic Journal of Environmental, Agricultural and Food Chemistry,* 9**,** 1343-1350.

Genty, T., Bussière, B., Potvin, R., Benzaazoua, M. & Zagury, G. J. 2012. Dissolution of calcitic marble and dolomitic rock in high iron concentrated acid mine drainage: Application to anoxic limestone drains. *Environmental Earth Sciences,* 66**,** 2387-2401.

Ghorai, T. K. & Pramanik, P. Mechanochemical synthesis, characterization and photocatalytic properties of m2o3/tio2 (m = Fe, mn) nano-composite under visible light. Frontiers in Mechanochemistry and Mechanical Alloying, 2011. 97-103.

Gibert, O., De Pablo, J., Luis Cortina, J. & Ayora, C. 2004. Chemical characterisation of natural organic substrates for biological mitigation of acid mine drainage. *Water Research,* 38**,** 4186-4196.

Gitari, M., Petrik, L., Etchebers, O., Key, D., Iwuoha, E. & Okujeni, C. 2006. Treatment of acid mine drainage with fly ash: Removal of major contaminants and trace elements. *Journal of Environmental Science and Health - Part A Toxic/Hazardous Substances and Environmental Engineering,* 41**,** 1729-1747.

Gitari, W. M. 2014. Attenuation of metal species in acidic solutions using bentonite clay: implications for acid mine drainage remediation. *Toxicological and Environmental Chemistry*.

Gitari, W. M., Petrik, L. F., Etchebers, O., Key, D. L., Iwuoha, E. & Okujeni, C. 2008. Passive neutralisation of acid mine drainage by fly ash and its derivatives: A column leaching study. *Fuel,* 87**,** 1637-1650.

Gray, J. B. & Vis, M. L. 2013. Reference diatom assemblage response to restoration of an acid mine drainage stream. *Ecological Indicators,* 29**,** 234-245.

Gray, N. F. & Delaney, E. 2010. Measuring community response of bentic macroinvertebrates in an erosional river impacted by acid mine drainage by use of a simple model. *Ecological Indicators,* 10**,** 668-675.

Groudev, S., Georgiev, P., Spasova, I. & Nicolova, M. 2008. Bioremediation of acid mine drainage in a uranium deposit. *Hydrometallurgy,* 94**,** 93-99.

Güven, N. 2009. Bentonites - Clays for molecular engineering. *Elements,* 5**,** 89-92.

Halim, C. E., Short, S. A., Scott, J. A., Amal, R. & Low, G. 2005. Modelling the leaching of Pb, Cd, As, and Cr from cementitious waste using PHREEQC. *Journal of Hazardous Materials,* 125**,** 45-61.

Hallberg, K. B. 2010. New perspectives in acid mine drainage microbiology. *Hydrometallurgy,* 104**,** 448-453.

Hallberg, K. B. & Johnson, D. B. 2005. Biological manganese removal from acid mine drainage in constructed wetlands and prototype bioreactors. *Science of The Total Environment,* 338**,** 115-124.

Hedin, R., Weaver, T., Wolfe, N. & Weaver, K. 2010. Passive Treatment of Acidic Coal Mine Drainage: The Anna S Mine Passive Treatment Complex. *Mine Water and the Environment,* 29**,** 165-175.

Hedin, R. S., Stafford, S. L. & Weaver, T. J. 2005. Acid mine drainage flowing from abandoned gas wells. *Mine Water and the Environment,* 24**,** 104-106.

Hengen, T. J., Squillace, M. K., O'sullivan, A. D. & Stone, J. J. 2014. Life cycle assessment analysis of active and passive acid mine drainage treatment technologies. *Resources, Conservation and Recycling,* 86**,** 160-167.

Heviánková, S., Bestová, I. & Kyncl, M. 2014. The application of wood ash as a reagent in acid mine drainage treatment. *Minerals Engineering,* 56**,** 109-111.

Hosseini, S. N., Karimzadeh, F. & Enayati, M. H. 2012. Mechanochemical synthesis of Al 2O 3/Co nanocomposite by aluminothermic reaction. *Advanced Powder Technology,* 23**,** 334-337.

Inglezakis, V. J., Loizidou, M. D. & Grigoropoulou, H. P. 2003. Ion exchange of Pb2+, Cu2+, Fe3+, and Cr3+ on natural clinoptilolite: Selectivity determination and influence of acidity on metal uptake. *Journal of Colloid and Interface Science,* 261**,** 49-54.

Jeleni, M. N., Gumbo, J. R., Muzerengi, C. & Dacosta, F. A. 2012. An assessment of toxic metals in soda mine tailings and a native grass: A case study of an abandoned Nyala Magnesite mine, Limpopo, South Africa. *WIT Transactions on Ecology and the Environment,* 164**,** 415-426.

Johnson, D. B. & Hallberg, K. B. 2005a. Acid mine drainage remediation options: A review. *Science of the Total Environment,* 338**,** 3-14.

Johnson, D. B. & Hallberg, K. B. 2005b. Acid mine drainage remediation options: a review. *Science of The Total Environment,* 338**,** 3-14.

Johnson, D. B. & Hallberg, K. B. 2005c. Biogeochemistry of the compost bioreactor components of a composite acid mine drainage passive remediation system. *Science of The Total Environment,* 338**,** 81-93.

Jooste, S. & Thirion, C. 1999. An ecological risk assessment for a South African acid mine drainage. *Water Science and Technology,* 39**,** 297-303.

Kaibicheva, M. N., Mar'evich, N. I., Tulin, N. A., Smakotin, I. V., Lande, P. A. & Terekhina, P. Y. 1962. The use of unburned metal-encased chrome-magnesite bricks in electric furnace walls. *Metallurgist,* 6**,** 362-363.

Kaibicheva, M. N., Panov, G. A. & Rozhdestvenskaya, G. Y. 1971. Developing magnesite bodies for lining vacuum induction furnaces. *Refractories,* 12**,** 791-795.

Kalin, M., Fyson, A. & Wheeler, W. N. 2006. The chemistry of conventional and alternative treatment systems for the neutralization of acid mine drainage. *Science of The Total Environment,* 366**,** 395-408.

Kawasaki, S., Shinoda, M., Iwai, Y., Ogawa, M., Hara, T., Hattori, Y. & Kubota, T. 2006. Mechanism of single-walled carbon nanotube growth on natural magnesite. *Solid State Communications,* 138**,** 382-385.

Kehew, A. E. 2001. *Applied Chemical Hydrogeology*, Prentice Hall. Page 1 - 180

Kidd, M. 2011. *Environmental Law*, Juta, page 1 - 300

Kim, W., Kim, K., Lee, H., Shin, M. & Kim, S. 2013. Mechanochemical activation on the preparation of β-eucryptite from powder mixture of pyrophyllite, gibbsite and lithium carbonate. *Materials Transactions,* 54**,** 380-383.

Kim, Y. 2015. Mineral phases and mobility of trace metals in white aluminum precipitates found in acid mine drainage. *Chemosphere,* 119**,** 803-811.

Kleinevoss, A., Kuennecke, M., Haefe, H. & Wieland, K. 1975. Causes of Wear of Magnesite Linings in the Firing Zones of Rotary Cement Kilns. *Ber Dtsch Keram Ges,* 52**,** 130-135.

Kleinmann, R. L. & Chatwin, T. The GARD Guide and its general applicability to mine water issues. 28th Annual Meeting of the American Society of Mining and Reclamation 2011, 2011. 317-325.

Kleiv, R. A. & Thornhill, M. 2008. Predicting the neutralisation of acid mine drainage in anoxic olivine drains. *Minerals Engineering,* 21**,** 279-287.

Kubilay, Ş., Gürkan, R., Savran, A. & Şahan, T. 2007. Removal of Cu(II), Zn(II) and Co(II) ions from aqueous solutions by adsorption onto natural bentonite. *Adsorption,* 13**,** 41-51.

Kumrić, K. R., Crossed D Signukić, A. D. S. B., Trtić-Petrović, T. M., Vukelić, N. S., Stojanović, Z., Grbović Novaković, J. D. & Matović, L. L. 2013. Simultaneous removal of divalent heavy metals from aqueous solutions using raw and mechanochemically treated interstratified montmorillonite/kaolinite clay. *Industrial and Engineering Chemistry Research,* 52**,** 7930-7939.

Kuroki, V., Bosco, G. E., Fadini, P. S., Mozeto, A. A., Cestari, A. R. & Carvalho, W. A. 2014. Use of a La(III)-modified bentonite for effective phosphate removal from aqueous media. *Journal of Hazardous Materials,* 274**,** 124-131.

Labar, J. A., Nairn, R. W. & Canty, G. A. Generation of 400-500 MG/L alkalinity in a vertical anoxic limestone drain. 25th Annual Meetings of the American Society of Mining and Reclamation and 10th Meeting of IALR 2008, 2008. 553-565.

Labastida, I., Armienta, M. A., Lara-Castro, R. H., Aguayo, A., Cruz, O. & Ceniceros, N. 2013. Treatment of mining acidic leachates with indigenous limestone, Zimapan Mexico. *Journal of Hazardous Materials,* 262**,** 1187-1195.

Lacelle, D. & Léveillé, R. 2010. Acid drainage generation and associated Ca-Fe-SO4 minerals in a periglacial environment, Eagle Plains, Northern Yukon, Canada: A potential analogue for low-temperature sulfate formation on Mars. *Planetary and Space Science,* 58**,** 509-521.

Lagos, G. I., M.Sc & Geo, P. 2011. The Use of Bench-scale Treatability Studies in the Design of Engineered Wetlands for the Remediation of Acid Mine Drainage (AMD) and Leachate in the Vicinity of Coal MinesA Case Study in Ohio, United States. *Procedia Earth and Planetary Science,* 3**,** 11-16.

Lange, K., Rowe, R. K. & Jamieson, H. 2010. The potential role of geosynthetic clay liners in mine water treatment systems. *Geotextiles and Geomembranes,* 28**,** 199-205.

Lefebvre, O., Neculita, C. M., Yue, X. & Ng, H. Y. 2012. Bioelectrochemical treatment of acid mine drainage dominated with iron. *Journal of Hazardous Materials,* 241–242**,** 411-417.

Leite, C. M. C., Cardoso, L. P. & De Mello, J. W. V. 2013. Use of steel slag to neutralize acid mine drainage (AMD) in sulfidic material from a uranium mine. *Revista Brasileira de Ciencia do Solo,* 37**,** 804-811.

Levings, C. D., Varela, D. E., Mehlenbacher, N. M., Barry, K. L., Piercey, G. E., Guo, M. & Harrison, P. J. 2005. Effect of an acid mine drainage effluent on phytoplankton biomass and primary production at Britannia Beach, Howe Sound, British Columbia. *Marine Pollution Bulletin,* 50**,** 1585-1594.

Li, L. Y., Tazaki, K., Lai, R., Shiraki, K., Asada, R., Watanabe, H. & Chen, M. 2008. Treatment of acid rock drainage by clinoptilolite - Adsorptivity and structural stability for different pH environments. *Applied Clay Science,* 39**,** 1-9.

Li, X., Dai, H. X. & Yang, X. L. 2013. The generation and treatment of acid mine drainage. *Advanced Materials Research.*

Li, Z. & Bowman, R. S. 2001. Retention of inorganic oxyanions by organo-kaolinite. *Water Research,* 35**,** 3771-3776.

Lizama Allende, K., Mccarthy, D. T. & Fletcher, T. D. 2014. The influence of media type on removal of arsenic, iron and boron from acidic wastewater in horizontal flow wetland microcosms planted with Phragmites australis. *Chemical Engineering Journal,* 246**,** 217-228.

López, D. L., Gierlowski-Kordesch, E. & Hollenkamp, C. 2010. Geochemical mobility and bioavailability of heavy metals in a lake affected by acid mine drainage: Lake Hope, Vinton County, Ohio. *Water, Air, and Soil Pollution,* 213**,** 27-45.

Lottermoser, B. 2007. *Mine Wastes: Characterization, Treatment and Environmental Impacts*, Springer Berlin Heidelberg.

Luptakova, A., Ubaldini, S., Fornari, P. & Macingova, E. 2012a. Physical-chemical and biological-chemical methods for treatment of acid mine drainage. *Chemical Engineering Transactions.*

Luptakova, A., Ubaldini, S., Macingova, E., Fornari, P. & Giuliano, V. 2012b. Application of physical-chemical and biological-chemical methods for heavy metals removal from acid mine drainage. *Process Biochemistry,* 47**,** 1633-1639.

Macedo-Sousa, J. A., Pestana, J. L. T., Gerhardt, A., Nogueira, A. J. A. & Soares, A. M. V. M. 2007. Behavioural and feeding responses of Echinogammarus meridionalis (Crustacea, Amphipoda) to acid mine drainage. *Chemosphere,* 67**,** 1663-1670.

Macías, F., Caraballo, M. A., Nieto, J. M., Rötting, T. S. & Ayora, C. 2012a. Natural pretreatment and passive remediation of highly polluted acid mine drainage. *Journal of Environmental Management,* 104**,** 93-100.

Macías, F., Caraballo, M. A., Nieto, J. M., Rötting, T. S. & Ayora, C. 2012b. Natural pretreatment and passive remediation of highly polluted acid mine drainage. *Journal of Environmental Management,* 104**,** 93-100.

Madzivire, G., Gitari, W. M., Vadapalli, V. R. K., Ojumu, T. V. & Petrik, L. F. 2011. Fate of sulphate removed during the treatment of circumneutral mine water and acid mine

drainage with coal fly ash: Modelling and experimental approach. *Minerals Engineering*, 24**,** 1467-1477.

Madzivire, G., Maleka, P., Lindsay, R. & Petrik, L. F. 2013. Radioactivity of mine water from a gold mine in South Africa. *WIT Transactions on Ecology and the Environment,* 178**,** 147-158.

Madzivire, G., Maleka, P. P., Vadapalli, V. R. K., Gitari, W. M., Lindsay, R. & Petrik, L. F. 2014. Fate of the naturally occurring radioactive materials during treatment of acid mine drainage with coal fly ash and aluminium hydroxide. *Journal of Environmental Management,* 133**,** 12-17.

Madzivire, G., Petrik, L. F., Gitari, W. M., Ojumu, T. V. & Balfour, G. 2010. Application of coal fly ash to circumneutral mine waters for the removal of sulphates as gypsum and ettringite. *Minerals Engineering,* 23**,** 252-257.

Mahmoud, K. K., Leduc, L. G. & Ferroni, G. D. 2005. Detection of Acidithiobacillus ferrooxidans in acid mine drainage environments using fluorescent in situ hybridization (FISH). *Journal of Microbiological Methods,* 61**,** 33-45.

Mandour, M. A. & Elmaatty, M. A. 2001. Egyptian magnesite and talc deposits: A brief review. *Mineralia Slovaca,* 33**,** 587-590.

Manohar, D. M., Noeline, B. F. & Anirudhan, T. S. 2006. Adsorption performance of Al-pillared bentonite clay for the removal of cobalt(II) from aqueous phase. *Applied Clay Science,* 31**,** 194-206.

Mapanda, F., Nyamadzawo, G., Nyamangara, J. & Wuta, M. 2007. Effects of discharging acid-mine drainage into evaporation ponds lined with clay on chemical quality of the surrounding soil and water. *Physics and Chemistry of the Earth, Parts A/B/C,* 32**,** 1366-1375.

Maree, J. P., Bosman, D. J. & Jenkins, G. R. 1989. Chemical removal of sulphate, calcium and heavy metals from mining and power station effluents. *Water Sewage Effluent,* 9**,** 10-25.

Maree, J. P., De Beer, M., Strydom, W. F., Christie, A. D. M. & Waanders, F. B. 2004a. Neutralizing coal mine effluent with limestone to decrease metals and sulphate concentrations. *Mine Water and the Environment,* 23**,** 81-86.

Maree, J. P. & Du Plessis, P. 1993. Neutralization of acid mine water calcium carbonate. *Proc. IAWQ Conference on Pre-treatment of IndustrialWastewaters, Athens*.

Maree, J. P., Mujuru, M., Bologo, V., Daniels, N. & Mpholoane, D. 2013. Neutralisation treatment of AMD at affordable cost. *Water SA,* 39**,** 245-250.

Maree, J. P., Streydom, W. F., Adlem, C. J. L., De Beer, M., Van Tonder, G. J. & Van Dijk, B. J. 2004b. Neutralization of acid mine water and sludge disposal. *WRC Report No. 1057/1/04, Water Research Commission*.

Maree, J. P., Van Tonder, G. J., Adlem, C., Millard, P., De Beer, M. & Strydom, W. F. 1997. Pilot Plant Studies on Limestone Neutralization and Gypsum Crystallization of Acidic Colliery Ef fluent. *Confidential CSIR Report*.

Martens, E., Jacques, D., Van Gerven, T., Wang, L. & Mallants, D. PHREEQC modelling of leaching of major elements and heavy metals from cementitious waste forms. Materials Research Society Symposium Proceedings, 2008. 475-482.

Martins, M., Santos, E. S., Faleiro, M. L., Chaves, S., Tenreiro, R., Barros, R. J., Barreiros, A. & Costa, M. C. 2011. Performance and bacterial community shifts during bioremediation of acid mine drainage from two Portuguese mines. *International Biodeterioration & Biodegradation,* 65**,** 972-981.

Masindi, V. 2013. *Adsorption of Oxyanions of As, B, Cr, Mo and Se from Coal Fly Ash Leachates Using AI3+/Fe3+ Modified Benonite Clay*, South Africa, University of Venda.

Masindi, V., Gitari, M. W., Tutu, H. & De Beer, M. 2014a. Application of magnesite–bentonite clay composite as an alternative technology for removal of arsenic from industrial effluents. *Toxicological & Environmental Chemistry***,** 1-17.

Masindi, V., Gitari, M. W., Tutu, H. & De Beer, M. Neutralization and Attenuation of Metal Species in Acid Mine Drainage and Mine Leachates Using Magnesite: a Batch Experimental Approach. An Interdisciplinary Response to Mine Water Challenges - Sui, Sun & Wang (eds), 2014b. China University of Mining and Technology Press, Xuzhou, 640 - 644.

Masindi, V., Gitari, W. M. & Ngulube, T. 2014c. Defluoridation of drinking water using Al3+-modified bentonite clay: optimization of fluoride adsorption conditions. *Toxicological & Environmental Chemistry***,** 1-16.

Merovich Jr, G. T., Stiles, J. M., Petty, J. T., Ziemkiewicz, P. F. & Fulton, J. B. 2007. Water chemistry-based classification of streams and implications for restoring mined Appalachian watersheds. *Environmental Toxicology and Chemistry,* 26**,** 1361-1369.

Missana, T. & Garcı´a-Gutiérrez, M. 2007. Adsorption of bivalent ions (Ca(II), Sr(II) and Co(II)) onto FEBEX bentonite. *Physics and Chemistry of the Earth, Parts A/B/C,* 32**,** 559-567.

Mitsch, W. J. & Wise, K. M. 1998. Water quality, fate of metals, and predictive model validation of a constructed wetland treating acid mine drainage. *Water Research,* 32**,** 1888-1900.

Mohapatra, B. R., Douglas Gould, W., Dinardo, O. & Koren, D. W. 2011. Tracking the prokaryotic diversity in acid mine drainage-contaminated environments: A review of molecular methods. *Minerals Engineering,* 24**,** 709-718.

Mukherjee, S. 2013. *The Science of Clays: Applications in Industry, Engineering, and Environment,* Springer.

Murray, H. H. 2006. *Applied Clay Mineralogy: Occurrences, Processing and Applications of Kaolins, Bentonites, Palygorskitesepiolite, and Common Clays*, Elsevier Science.

Name, T. & Sheridan, C. 2014. Remediation of acid mine drainage using metallurgical slags. *Minerals Engineering,* 64**,** 15-22.

Nasedkin, V. V., Krupenin, M. T., Safonov, Y. G., Boeva, N. M., Efremova, S. V. & Shevelev, A. I. 2001. The comparison of amorphous (cryptocrystalline) and crystalline magnesites. *Mineralia Slovaca,* 33**,** 567-574.

Natarajan, K. A. 2008. Microbial aspects of acid mine drainage and its bioremediation. *Transactions of Nonferrous Metals Society of China,* 18**,** 1352-1360.

Netto, E., Madeira, R. A., Silveira, F. Z., Fiori, M. A., Angioleto, E., Pich, C. T. & Geremias, R. 2013. Evaluation of the toxic and genotoxic potential of acid mine drainage using physicochemical parameters and bioassays. *Environmental Toxicology and Pharmacology*, 35**,** 511-516.

Niemelä, M. 2001. Talc-magnesite deposits in Finland. *Mineralia Slovaca,* 33**,** 561-566.

Nordstrom, D. K., Blowes, D. W. & Ptacek, C. J. 2015. Hydrogeochemistry and microbiology of mine drainage: An update. *Applied Geochemistry,* 57**,** 3-16.

Oliker, V. E., Sirovatka, V. L., Gridasova, T. Y., Timofeeva, I. I. & Bykov, A. I. 2008. Mechanochemical synthesis and structure of Ti-Al-B-based alloys. *Powder Metallurgy and Metal Ceramics,* 47**,** 546-556.

Oubagaranadin, J. U. K. & Murthy, Z. V. P. 2010. Isotherm modeling and batch adsorber design for the adsorption of Cu(II) on a clay containing montmorillonite. *Applied Clay Science,* 50**,** 409-413.

Oyanedel-Craver, V. A., Fuller, M. & Smith, J. A. 2007. Simultaneous sorption of benzene and heavy metals onto two organoclays. *Journal of Colloid and Interface Science,* 309**,** 485-492.

Palinkaš, L. A., Jurković, I., Garašić, V. & Palinkaš, S. S. 2012. Genesis of vein-stockwork cryptocrystalline magnesite from the dinaride ophiolites. *Ofioliti,* 37**,** 13-26.

Papassiopi, N., Zaharia, C., Xenidis, A., Adam, K., Liakopoulos, A. & Romaidis, I. 2014. Assessment of contaminants transport in a watershed affected by acid mine drainage, by coupling hydrological and geochemical modeling tools. *Minerals Engineering,* 64**,** 78-91.

Papirio, S., Villa-Gomez, D. K., Esposito, G., Pirozzi, F. & Lens, P. N. L. 2013. Acid mine drainage treatment in fluidized-bed bioreactors by sulfate-reducing bacteria: A critical review. *Critical Reviews in Environmental Science and Technology,* 43**,** 2545-2580.

Parkhurst, D. L. 1995. User's guide to PHREEQC - A computer program for speciation, reaction-path, advective-transport, and inverse geochemical calculations. *User's Guide to PHREEQC (Version 2) - A Computer Program for Speciation, Batch-Reaction, One-Dimensional Transport, and Inverse Geochemical Calculations*.

Parkhurst, D. L. & Appelo, C. a. J. 1999. Users guide to Phreeqc (Version 2) - A computer program for speciation, batch-reactions, one-dimensional transport and inverse geochemical calculations. *Water-Resources Investigations Report 99-4259*.

Payus, C., David, O. & Yan, M. P. 2014. Bone meal as alternative treatment for acidic and metal contaminated acid mine drainage water effluent: Lab scale. *American Journal of Environmental Sciences,* 10**,** 61-73.

Pehlivan, E. & Altun, T. 2007. Ion-exchange of Pb(II), Cu(II), Zn(II), Cd(II), and Ni(II) ions from aqueous solution by Lewatit CNP 80. *Journal of Hazardous Materials,* 140**,** 299-307.

Peretyazhko, T., Zachara, J. M., Boily, J. F., Xia, Y., Gassman, P. L., Arey, B. W. & Burgos, W. D. 2009. Mineralogical transformations controlling acid mine drainage chemistry. *Chemical Geology,* 262**,** 169-178.

Pohl, W. 1990. Genesis of magnesite deposits - models and trends. *Geologische Rundschau,* 79**,** 291-299.

Prasannakumar, V., Krupenin, M. T., Gulyaeva, T. Y. & Petrischeva, V. G. 2004. Geological and geochemical comparison of Southern Urals and South Indian cryptocrystalline magnesite. *Acta Petrologica Sinica,* 20**,** 821-828.

Prasannakumar, V. & Kumar, S. N. 2001. Magnesite and talc- The Indian scenario. *Mineralia Slovaca,* 33**,** 599-602.

Quispe, D., Pérez-López, R., Acero, P., Ayora, C., Nieto, J. M. & Tucoulou, R. 2013. Formation of a hardpan in the co-disposal of fly ash and sulfide mine tailings and its influence on the generation of acid mine drainage. *Chemical Geology,* 355**,** 45-55.

Ríos, C. A., Williams, C. D. & Roberts, C. L. 2008. Removal of heavy metals from acid mine drainage (AMD) using coal fly ash, natural clinker and synthetic zeolites. *Journal of Hazardous Materials,* 156**,** 23-35.

Rubin, H., Rubin, K., Siodlak, A. & Skuza, P. 2011. Assessment of contamination of the bottom sediments of the stola river with selected metals and metalloids within the urban-industrial area of tarnowskie góry. *Biuletyn - Panstwowego Instytutu Geologicznego***,** 615-624.

Sarkar, B., Naidu, R. & Megharaj, M. 2013. Simultaneous adsorption of tri- and hexavalent chromium by organoclay mixtures topical collection on remediation of site contamination. *Water, Air, and Soil Pollution,* 224.

Sarkar, B., Xi, Y., Megharaj, M., Krishnamurti, G. S. R., Rajarathnam, D. & Naidu, R. 2010. Remediation of hexavalent chromium through adsorption by bentonite based Arquad® 2HT-75 organoclays. *Journal of Hazardous Materials,* 183**,** 87-97.

Sen Gupta, S. & Bhattacharyya, K. G. 2008. Immobilization of Pb(II), Cd(II) and Ni(II) ions on kaolinite and montmorillonite surfaces from aqueous medium. *Journal of Environmental Management,* 87**,** 46-58.

Shabani, K. S., Ardejani, F. D., Badii, K. & Olya, M. E. 2014. Acid mine drainage treatment by perlite nanomineral, batch and continuous systems. *Archives of Mining Sciences,* 59**,** 107-122.

Sheoran, A. S. & Sheoran, V. 2006. Heavy metal removal mechanism of acid mine drainage in wetlands: A critical review. *Minerals Engineering,* 19**,** 105-116.

Sheoran, V., Sheoran, A. S. & Choudhary, R. P. 2011. Biogeochemistry of acid mine drainage formation: A review. *Mine Drainage and Related Problems.* 119-154.

Sherry, C. 2013. Quantifying clays. *Mining Magazine***,** 22-23.

Sibanda, Z., Amponsah-Dacosta, F. & Mhlongo, S. E. 2013. Characterization and evaluation of magnesite tailings for their potential utilization: A case study of nyala magnesite mine, Limpopo province of South Africa. *ARPN Journal of Engineering and Applied Sciences,* 8**,** 606-613.

Silva, I. A., Sousa, F. K. A., Menezes, R. R., Neves, G. A., Santana, L. N. L. & Ferreira, H. C. 2014. Modification of bentonites with nonionic surfactants for use in organic-based drilling fluids. *Applied Clay Science,* 95**,** 371-377.

Simate, G. S. & Ndlovu, S. 2014. Acid mine drainage: Challenges and opportunities. *Journal of Environmental Chemical Engineering,* 2**,** 1785-1803.

Simonov, K. V., Bocharov, L. D. & Ust'yantsev, V. M. 1979. Formation of alkali and alkaline earth sulfates and magnesium fluoride when magnesite is roasted in rotary furnaces, and their deposition in the electrostatic precipitators. *Refractories,* 20**,** 218-223.

Şimşek, S., Baybaş, D., Koçyiğit, M. C. & Yildirim, H. 2014. Organoclay modified with lignin as a new adsorbent for removal of Pb(II) and UO_2(II). *Journal of Radioanalytical and Nuclear Chemistry,* 299**,** 283-292.

Skoczyńska-Gajda, S. & Labus, K. 2011. Acid mine drainage within the abandoned lignite mining area-muskau arch. *Biuletyn - Panstwowego Instytutu Geologicznego***,** 643-650.

Skousen, J., Mcdonald, L., Mack, B. & Demchak, J. Water quality from above-drainage underground mines over a 35-year period. 7th International Conference on Acid Rock Drainage 2006, ICARD - Also Serves as the 23rd Annual Meetings of the American Society of Mining and Reclamation, 2006. 2044-2054.

Sracek, O., Choquette, M., Gélinas, P., Lefebvre, R. & Nicholson, R. V. 2004. Geochemical characterization of acid mine drainage from a waste rock pile, Mine Doyon, Québec, Canada. *Journal of Contaminant Hydrology,* 69**,** 45-71.

Stathi, P., Litina, K., Gournis, D., Giannopoulos, T. S. & Deligiannakis, Y. 2007. Physicochemical study of novel organoclays as heavy metal ion adsorbents for environmental remediation. *Journal of Colloid and Interface Science,* 316**,** 298-309.

Stiles, J. M. & Ziemkiewicz, P. F. Evaluating options for large-scale watershed remediation. Joint Mining Reclamation Conf. 2010 - 27th Meeting of the ASMR, 12th Pennsylvania Abandoned Mine Reclamation Conf. and 4th Appalachian Regional Reforestation Initiative Mined Land Reforestation Conf., 2010. 1199-1235B.

Strosnider, W. H. & Nairn, R. W. 2010. Effective passive treatment of high-strength acid mine drainage and raw municipal wastewater in Potosí, Bolivia using simple mutual incubations and limestone. *Journal of Geochemical Exploration,* 105**,** 34-42.

Strosnider, W. H., Winfrey, B. K. & Nairn, R. W. 2011a. Alkalinity Generation in a Novel Multi-stage High-strength Acid Mine Drainage and Municipal Wastewater Passive Co-treatment System. *Mine Water and the Environment,* 30**,** 47-53.

Strosnider, W. H. J., Nairn, R. W., Peer, R. a. M. & Winfrey, B. K. 2013. Passive co-treatment of Zn-rich acid mine drainage and raw municipal wastewater. *Journal of Geochemical Exploration,* 125**,** 110-116.

Strosnider, W. H. J., Winfrey, B. K. & Nairn, R. W. 2011b. Novel passive Co-treatment of acid mine drainage and municipal wastewater. *Journal of Environmental Quality,* 40**,** 206-213.

Stucki, J. W. 2013. Chapter 11 - Properties and Behaviour of Iron in Clay Minerals. *In:* FAÏZA, B. & GERHARD, L. (eds.) *Developments in Clay Science.* Elsevier**,** 559-611.

Šucha, V., Dubiková, M., Cambier, P., Elsass, F. & Pernes, M. 2002. Effect of acid mine drainage on the mineralogy of a dystric cambisol. *Geoderma,* 110**,** 151-167.

Sun, M., Ru, X.-R. & Zhai, L.-F. 2015. In-situ fabrication of supported iron oxides from synthetic acid mine drainage: High catalytic activities and good stabilities towards electro-Fenton reaction. *Applied Catalysis B: Environmental,* 165**,** 103-110.

Thibodeaux, L. J. & Mackay, D. 2010. *Handbook of Chemical Mass Transport in the Environment,* Taylor & Francis.

Tiruta-Barna, L. 2008. Using PHREEQC for modelling and simulation of dynamic leaching tests and scenarios. *Journal of Hazardous Materials,* 157**,** 525-533.

Tolonen, E.-T., Sarpola, A., Hu, T., Rämö, J. & Lassi, U. 2014. Acid mine drainage treatment using by-products from quicklime manufacturing as neutralization chemicals. *Chemosphere,* 117**,** 419-424.

Torres, E., Ayora, C., Jiménez-Arias, J. L., García-Robledo, E., Papaspyrou, S. & Corzo, A. 2014. Benthic metal fluxes and sediment diagenesis in a water reservoir affected by acid mine drainage: A laboratory experiment and reactive transport modeling. *Geochimica et Cosmochimica Acta,* 139**,** 344-361.

Tutu, H., Mccarthy, T. S. & Cukrowska, E. 2008. The chemical characteristics of acid mine drainage with particular reference to sources, distribution and remediation: The Witwatersrand Basin, South Africa as a case study. *Applied Geochemistry,* 23**,** 3666-3684.

Vágvölgyi, V., Frost, R. L., Hales, M., Locke, A., Kristóf, J. & Horváth, E. 2008. Controlled rate thermal analysis of hydromagnesite. *Journal of Thermal Analysis and Calorimetry,* 92**,** 893-897.

Van Den Akker, B. P. & Ahn, J. Solubilities of radionuclides released from graphite waste calculated using PHREEQC. 13th International High-Level Radioactive Waste Management Conference 2011, IHLRWMC 2011, 2011. 369-377.

Van Der Watt, J. G. & Waanders, F. B. 2012. Leaching of rare earth elements from bentonite clay. *Journal of the Southern African Institute of Mining and Metallurgy,* 112**,** 281-285.

Van Olphen, H. 1963. An Introduction to Clay Colloid Chemistry. *App. I: Preparation of Clay Suspensions, Interscience Publishers***,** 239-243.

Van Pham, T. H., Aagaard, P. & Hellevang, H. 2012. On the potential for CO2 mineral storage in continental flood basalts - PHREEQC batch- and 1D diffusion-reaction simulations. *Geochemical Transactions***,** 5.

Velde, B. 1977. *Clays and clay minerals in natural and synthetic systems*, Elsevier Science.

Velde, B. 1992. *Introduction to clay minerals: chemistry, origins, uses, and environmental significance*, Chapman & Hall.

Velde, B. 1995. *Origin and Mineralogy of Clays: Clays and the Environment*, Springer Berlin Heidelberg.

Veli, S. & Alyüz, B. 2007. Adsorption of copper and zinc from aqueous solutions by using natural clay. *Journal of Hazardous Materials,* 149**,** 226-233.

Vicente, M. A., Gil, A. & Bergaya, F. 2013. Chapter 10.5 - Pillared Clays and Clay Minerals. *In:* FAÏZA, B. & GERHARD, L. (eds.) *Developments in Clay Science.* Elsevier**,** 523-557.

Vieira, M. G. A., De Almeida Neto, A. F. & Da Silva, M. G. C. 2014. Mechanisms of copper and mercury adsorption on bentonite clays from EXAFS Spectroscopy. *Chemical Engineering Transactions,* 39**,** 661-666.

Vieira, M. G. A., Neto, A. F. A., Gimenes, M. L. & Da Silva, M. G. C. 2010. Removal of nickel on Bofe bentonite calcined clay in porous bed. *Journal of Hazardous Materials,* 176**,** 109-118.

Wang, N., Chen, M., Li, Y. Y. & Ni, H. W. 2011. Preparation of MgO whisker from magnesite tailings and its application. *Transactions of Nonferrous Metals Society of China (English Edition),* 21**,** 2061-2065.

Wang, S., Zhao, G., Wang, Z., Zhang, Q. & Zhong, H. 2012. Treatment of copper-containing acid mine drainage by neutralization- adsorption process using calcite as neutralizer and polyhydroxamic acid resin as adsorbent. *Applied Mechanics and Materials.*

Wei, T. T., Yu, Y., Hu, Z. Q., Cao, Y. B., Gao, Y., Yang, Y. Q., Wang, X. J. & Wang, P. J. 2013. Research progress of acid mine drainage treatment technology in China. *Applied Mechanics and Materials.*

White, R. A., Freeman, C. & Kang, H. 2011. Plant-derived phenolic compounds impair the remediation of acid mine drainage using treatment wetlands. *Ecological Engineering,* 37**,** 172-175.

Whitehead, P. G., Cosby, B. J. & Prior, H. 2005. The Wheal Jane wetlands model for bioremediation of acid mine drainage. *Science of The Total Environment,* 338**,** 125-135.

Whitehead, P. G. & Prior, H. 2005. Bioremediation of acid mine drainage: An introduction to the Wheal Jane wetlands project. *Science of The Total Environment,* 338**,** 15-21.

Wildeman, T., Vatterrodt, K. & Figueroa, L. A. The generation and treatment of acid rock drainage. Mineral Processing and Extractive Metallurgy: 100 Years of Innovation, 2014. 619-628.

Wissmeier, L. & Barry, D. A. 2010. Implementation of variably saturated flow into PHREEQC for the simulation of biogeochemical reactions in the vadose zone. *Environmental Modelling and Software,* 25**,** 526-538.

Xu, D., Tan, X. L., Chen, C. L. & Wang, X. K. 2008. Adsorption of Pb(II) from aqueous solution to MX-80 bentonite: Effect of pH, ionic strength, foreign ions and temperature. *Applied Clay Science,* 41**,** 37-46.

Xu, X., Li, Q., Cui, H., Pang, J., An, H., Wang, W. & Zhai, J. 2012. Column-mode fluoride removal from aqueous solution by magnesia-loaded fly ash cenospheres. *Environmental Technology (United Kingdom),* 33**,** 1409-1415.

Yang, J. E., Skousen, J. G., Ok, Y. S., Yoo, K. Y. & Kim, H. J. 2006. Reclamation of abandoned coal mine waste in Korea using lime cake by-products. *Mine Water and the Environment,* 25**,** 227-232.

Yapar, S. 2009. Physicochemical study of microwave-synthesized organoclays. *Colloids and Surfaces A: Physicochemical and Engineering Aspects,* 345**,** 75-81.

Zachmann, D. W. & Johannes, W. 1989. Cryptocrystalline magnesite. *Magnesite: Geology, Mineralogy, Geochemistry, Formation of Mg-Carbonates,* 28**,** 15-28.

Zhang, H. & Luo, S. 2007. Modeling the leaching behavior of simulated HLW-glass using PHREEQC. *Nuclear Science and Techniques/Hewuli,* 18**,** 150-153.

Zhao, H., Xia, B., Qin, J. & Zhang, J. 2012. Hydrogeochemical and mineralogical characteristics related to heavy metal attenuation in a stream polluted by acid mine drainage: A case study in Dabaoshan Mine, China. *Journal of Environmental Sciences,* 24**,** 979-989.

Zheng, Y. J., Peng, Y. L. & Li, C. H. 2011. Treatment of acid mine drainage by two-step neutralization. *Zhongnan Daxue Xuebao (Ziran Kexue Ban)/Journal of Central South University (Science and Technology),* 42**,** 1215-1219.

Zhou, Z.-J., Yin, H.-Q., Liu, Y., Xie, M., Qiu, G.-Z. & Liu, X.-D. 2010. Diversity of microbial community at acid mine drainages from Dachang metals-rich mine, China. *Transactions of Nonferrous Metals Society of China,* 20**,** 1097-1103.

Zhu, Y. & Elzinga, E. J. 2014. Formation of layered Fe(II)-hydroxides during Fe(II) sorption onto clay and metal-oxide substrates. *Environmental Science and Technology,* 48**,** 4937-4945.

Zhuang, G., Zhang, Z., Guo, J., Liao, L. & Zhao, J. 2015. A new ball milling method to produce organo-montmorillonite from anionic and nonionic surfactants. *Applied Clay Science,* 104**,** 18-26.

Zick, R. 2011. High density sludge process reduces AMD volume, operating costs at pennsylvania coal mine site. *Coal Age,* 116**,** 64-67.

Zubakov, S. M. & Yusupova, E. M. 1964. The phase composition of chrome-magnesite refractories. *Refractories,* 5**,** 28-33.

Zulfahmi, A. R., Wan Zuhairi, W. Y., Raihan, M. T., Sahibin, A. R., Wan Mohd Razi, I., Tukimat, L., Siti Nur Syakireen, Z. & Noorulakma, A. 2012. Influence of Amang (Tin Tailing) on Geotechnical Properties of clay soil. *Sains Malaysiana,* 41**,** 303-312.

Zvimba, J. N., Mulopo, J., Bologo, L. T. & Mathye, M. 2012. An evaluation of waste gypsum-based precipitated calcium carbonate for acid mine drainage neutralization. *Water Science and Technology,* 65**,** 1577-1582.

CHAPTER THREE

Paper 1:

This paper addresses the Attenuation of acidity and inorganic contaminants from acid mine drainage by cryptocrystalline magnesite

This chapter is devoted to answer the undermentioned objectives which are:

- Evaluation of the treatment of AMD using cryptocrystalline magnesite in batch tests, and exploration of the interaction chemistry thereof, and the processed water quality;
- Investigation of the mineralogical transformation and chemical characterization of resultant solid residues and geochemical modelling of process water.

CHAPTER THREE

Attenuation of acidity and inorganic contaminants from acid mine drainage by cryptocrystalline magnesite

[*]Masindi Vhahangwele[1,3], Gitari W.Mugera[1], Tutu Hlanganani[2], Debeer Marinda[4]

[1]Environmental Remediation and Water Pollution Chemistry Research Group, Department of Ecology and Resources Management, School of Environmental Science, University of Venda, P/bag X5050, Thohoyandou, 0950, South Africa, Tel: +2712 841 4107, VMasindi@csir.co.za
[2]Molecular Sciences Institute, School of Chemistry, University of the Witwatersrand, P/Bag X4, WITS, 2050, Johannesburg, South Africa,
[3]CSIR (Council of Scientific and Industrial Research), Built Environment, Building Science and Technology (BST), P.O Box 395, Pretoria, 0001, South Africa,
[4]DST/CSIR National Centre for Nano-Structured Materials, Council for Scientific and Industrial Research, P.O Box 395, Pretoria, 0001, South Africa

Abstract

Effluents emanating from mining activities are usually acidic and often contain high concentrations of Fe, Mn, Al and SO_4^{2-} in addition to traces of Pb, Co, Ni, Cu, Zn, Mg, Ca and Na. These effluents impact surface and subsurface water resources negatively and have to be treated before release to receiving aquatic systems. To this end, mining companies are in constant search for cheaper, more effective and efficient mine water treatment technologies. This study assessed the potential of applying cryptocrystalline magnesite as an initial remediation step in an integrated acid mine drainage (AMD) management system. To accomplish this, neutralization and metal attenuation were evaluated using laboratory batch experiments and complemented with simulations using geochemical modelling. Mineral phase formation and changes during the reaction of magnesite and AMD were also evaluated. The geochemical computer code PHREEQC and WATEQ4 database were used for geochemical modelling of the process water. The resulting solid residues were analyzed by X-ray fluorescence (XRF), X-ray Diffraction (XRD), Fourier Transforms Infrared Spectroscopy (FTIR), scanning electron microscopy (SEM) coupled with energy dispersive X-ray spectroscopy (EDS) (SEM-EDS), and transmission electron microscopy (TEM) coupled with energy dispersive X-ray spectroscopy (EDS) (TEM-EDS) in an attempt to

detect the minerals phases controlling the inorganic contaminants concentration in solution. Carbon and sulphur were also monitored using ELTRA technique. Interaction of AMD with magnesite at an optimum solid: liquid ratio of 1:100 and contact time of 60 min led to an increase in pH, reaching a maximum pH of 10, resulting in significant precipitation of most metal species. Increase of pH in solution with contact time caused the removal of the metal ions mainly by precipitation, co-precipitation and adsorption. Sulphate concentration was lowered from 4640 to 1910 mg/L. Fe was mainly removed as $Fe(OH)_3$, goethite, and jarosite, Al as basaluminite, boehmite and jurbanite, $Al(OH)_3$ and as gibbsite and diaspore. Al and Fe precipitated as iron (oxy)-hydroxides and aluminium (oxy)-hydroxides. Mn precipitated as rhodochrosite and manganite. Ca was removed as gypsum, sulphate was removed as gypsum, and Fe, Al hydroxyl sulphate minerals and Mg was removed as brucite and dolomite. These would explain the decrease in the metal species and sulphate concentration in the product water. Cryptocrystalline magnesite effectively neutralized AMD and attenuated concentration of inorganic species to within Department of Water and Sanitation (DWS) water quality guidelines for 2013. Though > 60% sulphate removal was achieved, a polishing technology will be required to remove alkali and alkaline earth metal species and remaining sulphate from the aqueous system.

Keywords: Acid mine drainage; magnesite; metals; sulphate; neutralization; Geochemical modelling

3.1 Introduction

Mining contributes significantly to the gross domestic product and, consequently, to the economy of South Africa. However, it has been reported to impair the quality of terrestrial and aquatic ecosystems and their integrities to foster life due to generation of acid mine drainage (AMD). AMD is a common legacy in most gold and coal mines and results from the oxidation of pyrite (FeS_2) in the host rock (Jooste and Thirion, 1999, Johnson et al., 2002, Tutu et al., 2008, Ramontja et al., 2011, Van Deventer and Cho, 2014). AMD is formed when sulphide minerals such as pyrite are exposed to oxygen and water leading to the formation of iron hydroxide, sulphate and acid as indicated in Equation 3.1.

$$4FeS_2 + 15O_2 + 14H_2O \xrightarrow{\text{bacteria}} 4Fe(OH)_3 + 8SO_4^{2-} + 16H^+ \quad (3.1)$$

This acid promotes weathering and leaching of toxic elements such as Al, Fe, As, B, Ba, Co, Cr, Cu, Mo, Ni, Sr, Zn and Mn contained in the host rock (Jooste and Thirion, 1999, Johnson et al., 2002, Pinetown et al., 2007, Tutu et al., 2008, Ramontja et al., 2011, Funke et al., 2012, Henri et al., 2014, Van Deventer and Cho, 2014). In the Witwatersrand basin gold mines in South Africa, close to 70 minerals have been identified in the host rock including gold, pyrite, uraninite (U_3O_8), sphalerite (ZnS), galena (PbS) and various silicates (Jooste and Thirion, 1999, Tutu et al., 2008, Ramontja et al., 2011, Henri et al., 2014).

In the last decades, AMD has received great attention due to the devastating impacts that it can impose onto aquatic and terrestrial ecosystems. Currently, a total volume of 360 ML/d is generated by gold mines in Johannesburg which is discharging to adjacent aquatic ecosystem and accelerating the degradation of waterbodies downstream. Out of that, 20 ML/d of contaminated water flows into the Tweelopies Spruit near Randfontein (Western Basin). It has been predicted that, by 2013, a further 60 ML/d will decant near Boksburg (Central Basin) and a further 120 ML/day by 2014 near Springs (Eastern Basin) (Bologo *et al*., 2012). The mines near Westonaria and Carletonville produce 160 ML/d of AMD. Mine effluent contains approximately 10 000 mg/L total dissolved solids, with many mine waters being acidic and sulphate rich and therefore unsuitable for utilization. Stringent regulatory frameworks recommends that mine water must be treated before discharge into the receiving environment (Maree et al., 1998; Maree and Du Plessis, 1993; Maree et al., 2013).

Worldwide, a number of treatment methods, both passive and active, have been proposed and used for abating AMD (Akcil and Koldas, 2006, Kalin et al., 2006, Sheoran and Sheoran, 2006, Zipper and Skousen, 2010). Among these, the common ones include ion-exchange (Gaikwad, 2010, Buzzi et al., 2013, Torres and Auleda, 2013), adsorption (Mohan and Chander, 2006, Gitari et al., 2008, Motsi et al., 2009, Zhang, 2011, Chen et al., 2013a, Falayi and Ntuli, 2014), biosorption (Groudev et al., 2008, Freitas et al., 2011, Ramírez-Paredes et al., 2011, Çabuk et al., 2013, Chen et al., 2013b), neutralisation (Kalin et al., 2006, Kumar Vadapalli et al., 2008, Romero et al., 2011, Zheng et al., 2011, Zvimba et al., 2012, Alakangas et al., 2013, Zvimba et al., 2013), coagulation and precipitation (Lee et al., 2002, Kleiv and Thornhill, 2008, Macingova and Luptakova, 2011, Zammit et al., 2011, Macías et al., 2012, Zhao et al., 2012). The extent of application of most of these methods has largely been limited by factors such as cost and generation of excessive secondary sludge (Johnson and Hallberg, 2005b,

Sheoran and Sheoran, 2006, Gaikwad, 2010, Sheoran et al., 2011, Papirio et al., 2013, Sahoo et al., 2013, Pozo-Antonio et al., 2014, Simate and Ndlovu, 2014).

Deterioration of water quality due to AMD has been reported in a number of studies hence indicating a need for water reclamation (Jooste and Thirion, 1999, Johnson et al., 2002, Tutu et al., 2008, Oberholster et al., 2010, Ramontja et al., 2011, Funke et al., 2012, Henri et al., 2014, Van Deventer and Cho, 2014). In South Africa, limestone is the main agent for treatment of AMD. However, it has a limitation of raising the pH to less than 7 which is unsuitable for removal of metals. Bologo et al. (2012) have attempted to integrate limestone treatment with lime which raises the pH to > 12. However the cost of the lime is a limitation for this technology. Synthetic magnesium hydroxide has been used for AMD treatment. Although effective, its production cost might be a limiting factor in this treatment technology (Maree et al., 1989, Maree et al., 1998, Maree et al., 2004, Bologo et al., 2012, Mulopo et al., 2012, Maree et al., 2013).

This study proposes an AMD treatment approach using cryptocrystalline magnesite. The most common method for removing metals from AMD is by precipitating the metals as hydroxides. Typically for the present study, this will be achieved almost exclusively by the application of cryptocrystalline magnesite to the wastewater until the pH reaches the minimum solubility of the metals, (Equation 3.2 – 3.4 for Fe):

$$2Fe^{2+} + \frac{1}{2}O_2 + 2H^+ \rightarrow 2Fe^{3+} + H_2O \quad (3.2)$$

$$2Fe^{3+} + 6H_2O \rightarrow 2Fe(OH)_3 + 6H^+ \quad (3.3)$$

$$2Fe^{2+} + 2O_2 + 2H^+ + 3MgCO_3 \rightarrow 2Fe(OH)_3 + 3Mg^{2+} + H_2O + 3CO_2 \quad (3.4)$$

When this pH is reached, small particles of the metal hydroxide are formed as shown below:

$$M^{n+} + nOH^- \rightarrow M(OH)_n \downarrow \quad (3.5)$$

Magnesium will form a complex with sulphate in AMD solution. Due to the high solubility of $MgSO_4$ (K_{sp} = 5.9 x 10^{-3}) compared to $CaSO_4$ (K_{sp} = 4.93 x 10^{-5}), it should be possible to keep sulphate in solution while precipitating metals as hydroxides or co-precipitating metals with sulphate (Bologo et al., 2012). Moreover, the availability of sufficient deposits of magnesite in South Africa and its low cost makes it an attractive option (Toulkeridis et al.,

2010, Jeleni et al., 2012, Sibanda et al., 2013). This study evaluates, for the first time, changes in solution chemistry, quality of product water, solid residues and chemical speciation during the reaction of magnesite with AMD.

3.2 Materials and methods

3.2.1 Sampling

Raw magnesite rock was collected from the Folovhodwe Magnesite Mine in Limpopo Province, South Africa (22°35”47.0”S and 30°25”33”E), prior to any processing at the mine. Field AMD samples were collected from a discharging point in a disused mine shaft in Krugersdorp, Gauteng Province, South Africa.

3.2.2 Synthetic acid mine drainage

Synthetic acid mine drainage (SAMD) was used for the batch optimization experiments as real acid drainage is unstable over long periods of time due to oxidation and hydrolysis which changes its chemistry. A simplified solution containing the major ions found in acid mine waters was prepared with reference to the study by Tutu et al. (2008) (**Table 3.1**).

Table 3.1: Synthetic acid mine drainage used in this study

Salt dissolved	Species	Concentration (mg/L)
$Al_2(SO_4)_3.18H_2O$	Al^{3+}	200
$Fe_2(SO_4)_3.H_2O$	Fe^{3+}	2000
$MnCl_2$	Mn^{2+}	100
H_2SO_4 and Al and Fe salts	SO_4^{2-}	6000

Synthetic AMD solution was simulated by dissolving the following quantities of salts (7.48 g $Fe_2(SO_4)_3.H_2O$, 2.46 g $Al_2(SO_4)_3 \cdot 18H_2O$, and 0.48 g $MnCl_2$ from Merck, 99% purity) in 1000 mL of Merck Millipore Milli-Q 18.2 MΩ.cm water to give a solution of 2000 mg/L Fe^{3+}, 200 mg/L Al^{3+} and 200 mg/L Mn^{2+}. 5 mL of 0.05 M H_2SO_4 was added to make up SO_4^{2-} concentration to 6000 mg/L and ensure pH below 3 and in order to prevent immediate precipitation of ferric hydroxide.

3.2.3 Preparation of magnesite

Magnesite samples were milled to a fine powder for 15 minutes at 800 rpm using a Retsch RS 200 vibratory ball mill and passed through a 32 µm particle size sieve. The samples were kept in a zip-lock plastic bag until utilization for AMD treatment.

3.2.4 Characterisation of aqueous samples

pH, Total Dissolved Solids (TDS) and Electrical Conductivity (EC) were monitored using CRISON MM40 portable pH/EC/TDS/Temperature multimeter probe. Aqueous samples were analysed using ICP-MS (7500ce, Agilent, Alpharetta, GA, USA) for metal cations and sulphate was analysed using IC (850 professional IC Metrohm, Herisau, Switzerland). The accuracy of the analysis was monitored by analysis of National Institute of Standards and Technology (NIST) water standards. Three replicate measurements were made on each sample and results are reported as mean of the three samples.

3.2.5 Batch Experiments

To establish the optimum condition for AMD treatment, several operational parameters were optimized and these include: time, dosage of magnesite, species concentration and particle size.

3.2.5.1 Effect of time

Aliquots of 100 mL SAMD were pipetted into 250 mL flasks into which 1 g of magnesite samples were added. The mixtures were then equilibrated for 1, 10, 20, 60, 120, 180, 240, 300 and 400 minutes at 250 rpm using the Stuart reciprocating shaker. After shaking, the mixtures were filtered through a 0.45 µm pore nitrate cellulose filter membrane. After filtration each sample was divided into two for anion and cation analysis. For cations, the filtrates were preserved by adding two drops of concentrated HNO_3 acid to prevent aging and precipitation of Al, Fe and Mn and refrigerated at 4ºC prior to analysis by an ELAN 6000 inductively coupled plasma mass spectrometer (ICP-MS) (7500ce, Agilent, Alpharetta, GA, USA). For anion analysis the samples were stored in a refrigerator until analysis by Professional Ion Chromatography Metrohm model 850 (Switzerland). The pH before and after agitation was measured using the CRISON multimeter probe (model MM40).

3.2.5.2 Effect of dosage

Aliquots of 100 mL each of multicomponent SAMD were pipetted into 250 mL flasks and varying masses (0.1 g, 0.5 g, 1 g, 2 g, 3 g, 4 g, 5 g, and 8 g) of magnesite added into each flask. The mixtures were agitated using a shaker for 60 min at 250 rpm using a Stuart reciprocating shaker. The pH and metal content were measured as described in the preceding section.

3.2.5.3 Effect of chemical species concentration

To investigate the effects of adsorbate concentration on reaction kinetics, several dilutions were made from the stock solution. The pH of the simulated AMD was not adjusted. The capacity of the adsorbent to neutralize and attenuate metals from aqueous solutions was then assessed by increasing metal concentrations. Each 100 mL solution of SAMD was prepared in triplicate and 1 g of magnesite added to each sample container. The initial pH of the working solutions was maintained at pH < 3.

3.2.5.4 Effect of particle size

Aliquots of 100 mL each of SAMD were pipetted into 250 mL flasks and 1g of varying particle sizes (1, 32, 125, 250, 500 and 2000 µm) of magnesite added into each flask. The mixtures were agitated using a reciprocating shaker for an optimum time of 60 min at 250 rpm.

3.2.5.5 Treatment of field AMD at optimized conditions

Field AMD samples were treated at established optimized conditions in order to assess the effectiveness of magnesite. pH, EC and TDS were measured using CRISON MM40 multimeter probe. The resultant solid residue after treatment of field AMD was characterized in an attempt to gain an insight as to the fate of chemical species.

3.2.6 Chemical and microstructural characterization

Mineralogical composition of composite and resulting solid residues were determined using XRD, Analyses were performed using a Philip PW 1710 diffractometer equipped with graphite secondary monochromatic. Elemental composition was determined using XRF, the Thermo Fisher ARL-9400 XP+ Sequential XRF with WinXRF software. XRF and XRD

were done at University of Pretoria, South Africa. Functional groups were determined using Perkin-Elmer Spectrum 100 Fourier Transform Infrared Spectrometer (FTIR) equipped with a Perkin-Elmer Precisely Universal Attenuated Total Reflectance (ATR) sampling accessory equipped with a diamond crystal. Morphology was determined using SEM-EDS (JOEL JSM – 840, Hitachi, Tokyo, Japan). Crystallography and micrographs of cryptocrystalline magnesite were also ascertained using TEM (JEM – 2100 electron microscope, Angus Crescent, Netherland). Carbon and Sulphur were determined using ELTRA CS – 800 carbons and sulphur analyser (ELTRA GmbH, Retsch – Allee 1 – 542781, Haan, Germany).

3.2.7 Geochemical modelling

To complement chemical solution and physicochemical characterization results, the ion association model PHREEQC was used to calculate ion activities and saturation indices of mineral phases based on the pH and solution concentrations of major ions in supernatants that were analysed after the optimized conditions. Mineral phases that were likely to form during treatment of AMD were predicted using the PHREEQC geochemical modelling code using the WATEQ4F database (Parkhurst and Appelo, 1999). Species which were more likely to precipitate were determined using saturation index (SI). In this case, SI < 1 = under saturated solution, SI = 1 = saturated solution and SI > 1= Supersaturated solution.

3.3 Results and discussion

3.3.1 Optimization of interaction parameters

3.3.1.1 Effects of equilibration time

The results for neutralization and metal removal efficiency as a function of contact time are presented in **Figure 3.1**.

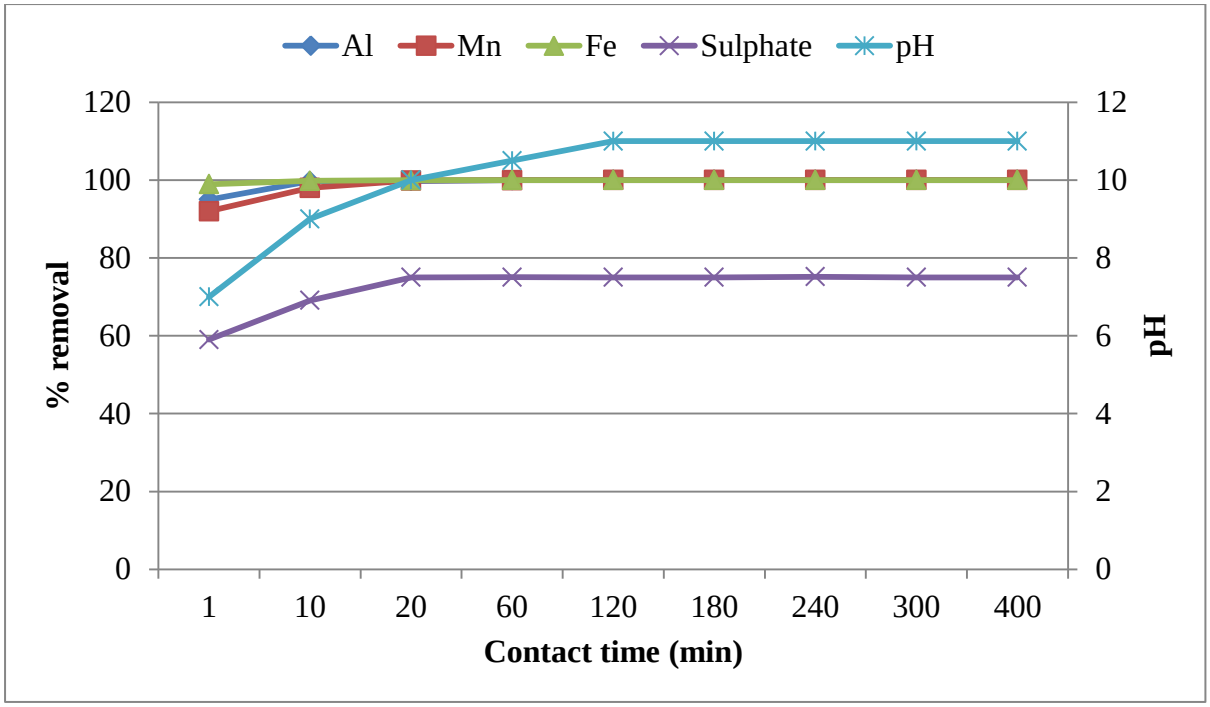

Figure 3.1, Appendix B, Table B 1: Variation of Al, Fe, Mn and SO_4^{2-} with time and pH (Conditions: pH < 3, 2000 mg/L Fe^{3+}, 200 mg/L Al^{3+}, 100 mg/L Mn^{2+}, 6000 mg/L SO_4^{2-} , 1 g magnesite, 32 µm, 250 rpm and 26 ºC).

The results for neutralization and metal removal efficiency function revealed that there was an increase in pH with increasing contact time. The pH increased significantly from 3 (initial pH of AMD) to > 10.5, approaching a steady state at 60 min. An increase in pH may have been due to the consumption of H^+ from sulphuric acid by magnesite, contributing to the elevation of pH as shown in Equations 3.9 and 3.10. Moreover, there was elevated removal of Al (93 - 100%), Fe (95 – 100%) and Mn (98 – 100%) after 20 min, suggesting precipitation, adsorption and/or co-precipitation. This was attributed to an increase in the pH of the solution, resulting in Fe precipitating at pH >3, Al at pH > 4 and Mn at pH > 9 (Johnson and Hallberg, 2005a, Sheoran and Sheoran, 2006, Skousen et al., 2006, Somerset et al., 2011, Zvimba et al., 2012, Pozo-Antonio et al., 2014). Sulphate achieved > 60% removal efficiency in less than 20 min. This indicates that there is direct relationship between metals precipitation and sulphate removal.

3.3.1.2 Effect of dosage

The results for neutralization and metal removal efficiency as a function of magnesite dosage are presented in **Figure 3.2**.

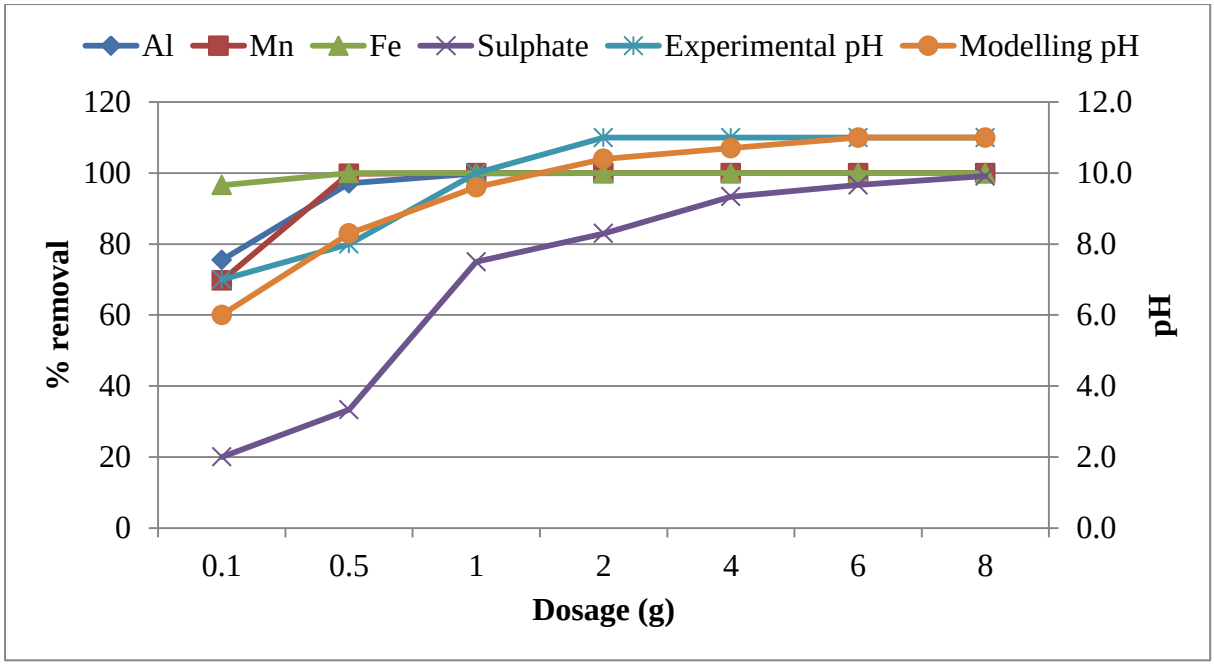

Figure 3.2, Appendix B, Table B 2: Variation of pH, Al, Fe, Mn and sulphate concentrations in AMD with magnesite dosage (Conditions: pH < 3, 2000 mg/L Fe^{3+}, 200 mg/L Al^{3+}, 100 mg/L Mn^{2+}, 6000 mg/L SO_4^{2-}, 250 rpm, 60 min reaction time, < 32 µm particles size and 26ºC)

The experimental results showed that there was an increase in pH with increase in magnesite dosage. The modelling results from PHREEQC showed an increase in alkalinity from -3.648 x 10^{-15} to 3.497 (eq/kg) and an increase in pH results from dissolution and hydrolysis of components such as MgO, $Mg(OH)_2$ and $MgCO_3$ (Equation 3.15 – 3.17).

$$MgO + H_2O \rightarrow Mg^{2+} + 2OH^- \quad (3.15)$$

$$MgCO_3 + H_2O \rightarrow Mg^{2+} + 2OH^- + CO_2 \uparrow \quad (3.16)$$

$$Mg(OH)_2 + H_2O \rightarrow MgOH^+ + H_2O + OH^- \quad (3.17)$$

Modelling predicted that as pH increases, Fe^{3+} species precipitate at pH > 6, Al^{3+} bearing species at pH > 6, Fe^{2+} species at pH > 8 and Mn^{2+} bearing species at pH > 10 (Table 5). The trend showed a smaller % removal of sulphate compared to that of metals. This was attributed to association of Mg and SO_4 and partly, $CaSO_4$ that remain in solution until saturation is attained leading to precipitation at elevated dosages. This is substantiated by the higher solubility of $MgSO_4$ (K_{sp} =5.9 x 10^{-3}) compared to that of $CaSO_4$ (K_{sp} = 4.93 x 10^{-5}), suggesting that more magnesium would be required to be in solution to precipitate $MgSO_4$ than $CaSO_4$. Metal complexes were predicted to precipitate as hydroxide, oxyhydroxides and

oxyhydroxysulphates. From the dosage experiments, it was concluded that optimum neutralization and metal attenuation conditions were 1:100 solid/liquid ratios.

3.3.1.3 Effect of particle size

The results for neutralization and metal removal by magnesite, as a function of particle size, are presented in **Figure 3.3**.

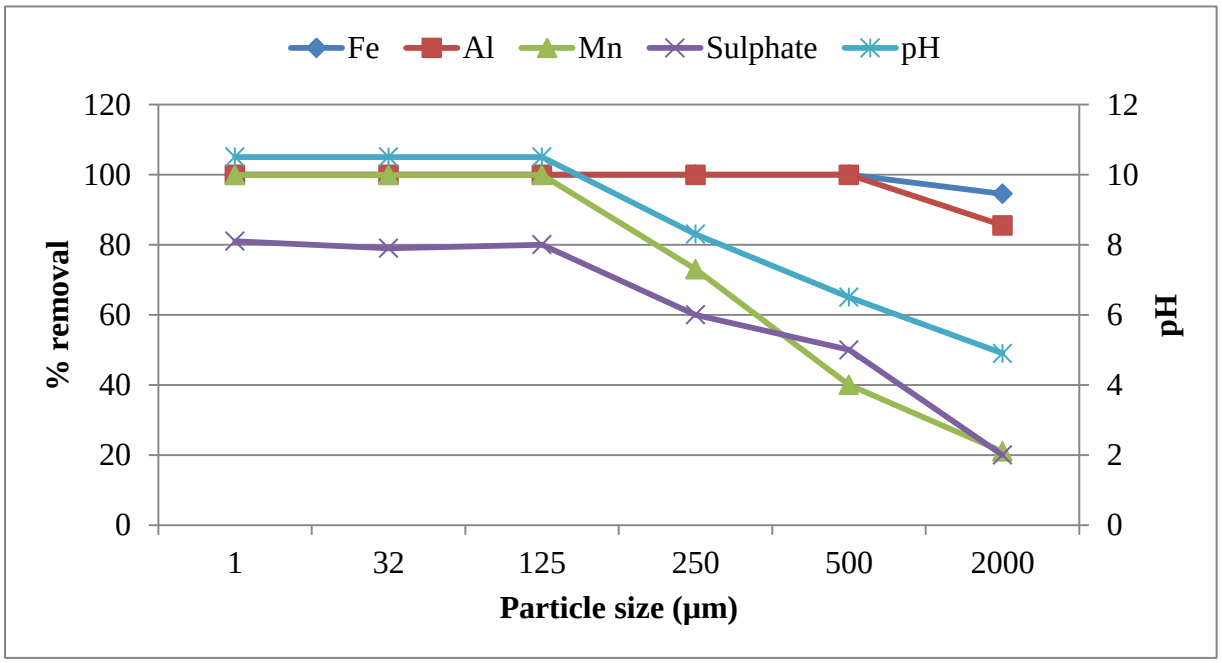

Figure 3.3, Appendix B, Table B 3: Variation of Al, Fe, Mn, SO_4^{2-} and pH as a function of magnesite particle size (Conditions: pH < 3, 2000 mg/L Fe^{3+}, 200 mg/L Al^{3+}, 100 mg/L Mn^{2+}, 6000 mg/L SO_4^{2-}, 1 g magnesite, 100 mL solution, 250 rpm and 26ºC).

Particle size is an important parameter in neutralization and metal attenuation processes. The smaller the particle size, the larger the surface area provided for reaction and the faster the rate of neutralization and metal attenuation. As shown in **Figure 3.3**, the rate of neutralization and metal attenuation decreased with increasing particle size. At particle sizes < 125 µm, Al, Mn, Fe and sulphate were completely removed. Particles with size > 125 µm were observed to increase the pH of the aqueous solution from 4 to 10.5. This study is comparable to those for calcium-based materials Maree et al., 1998) For instance, with limestone, pH values of 6 and higher were achieved with particle sizes of 300 µm and smaller (Maree et al., 1998), whereas particle sizes of 500 µm and smaller for magnesite were used to achieve pH >6. Thus, the efficiency of magnesite was found to be better than limestone.

3.3.1.4 Effect of chemical species concentration

The results for neutralization and metal removal efficiency of magnesite as a function of metal concentration are presented in **Figure 3.4**.

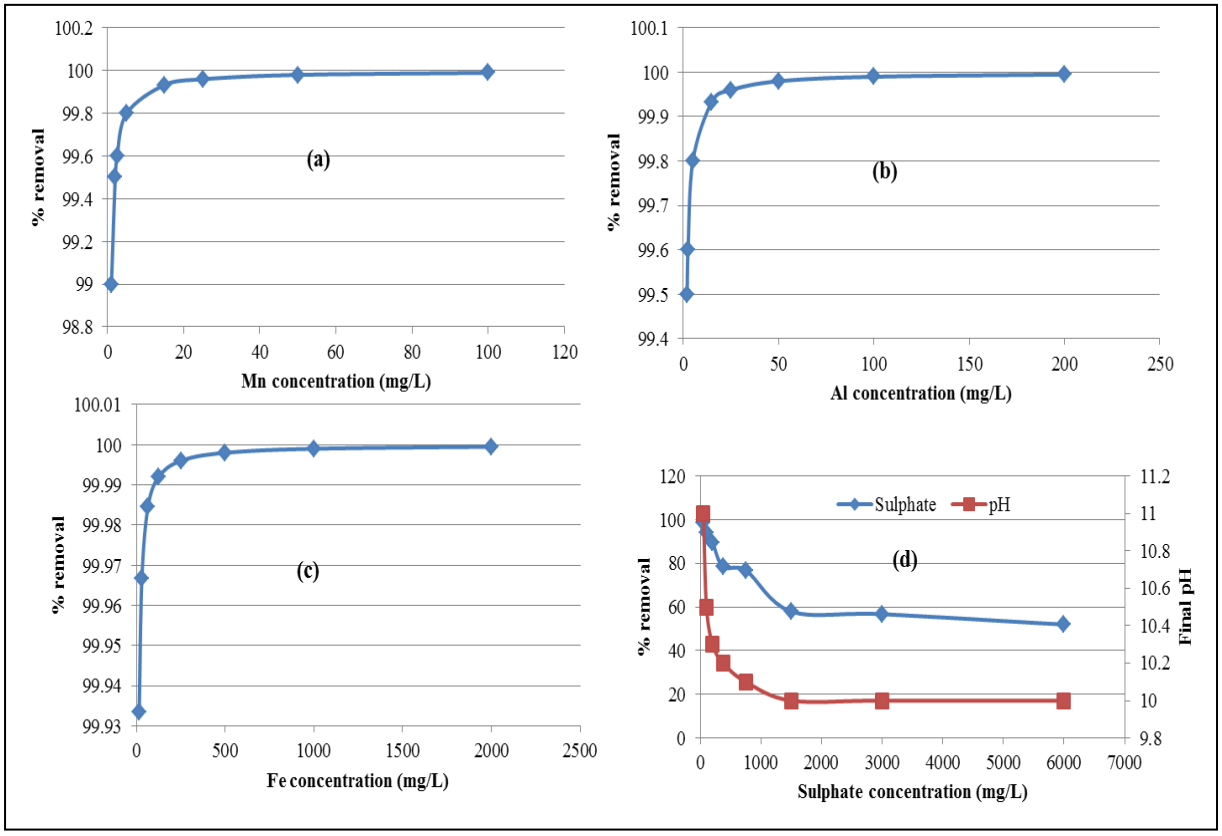

Figure 3.4, Appendix B, Table B 4: (a) Variation in % removal of Mn^{2+} as a function of species concentration. (b) variation in % removal of Al^{3+} as a function of ion concentration, (c) variation in % removal of Fe^{3+} as a function of ion concentration and (d) variation in % removal of SO_4^{2-} as a function of concentration (Conditions: pH < 3, 60 min, 1 gram, 1:100 S/L ratios, 32 µm, 250 rpm and 26 ºC).

Removal of Mn^{2+} and Al^{3+} is independent of Mn^{2+} and Al^{3+} concentrations for the range tested because the pH was high enough to precipitate all the metals. From **Figure 3.4** (c), the removal of Fe from SAMD is gradually increasing with an increase in Fe concentration because the pH was high enough to precipitate all the metals. From **Figure 3.4** (d), the removal of sulphate was observed to gradually decrease with an increase in sulphate concentration. As sulphate concentration increased, the pH of the solution decreased. As shown in Figure 3.11, drastic increases in pH were observed at varying Fe^{3+} ion concentrations. An increase in pH was attributed to dissolution of calcite, periclase, brucite and dolomite as shown by XRD.

3.3.1.5 Variation of pH with an increase in Fe3+ concentration

The decrease in pH with an increase in chemical species concentration is due to hydrolysis of metal species cations leading to release of H^+. The hydrolysis of Fe^{3+} and Al^{3+} releases protons and offsets the pH of the solution (Equation 3.18 and 3.19 and **Figure 3.5**).

$$Fe^{3+} + 3H_2O \rightarrow Fe(OH)_{3(s)} + 3H^+ \quad (3.18)$$

$$Al^{3+} + 3H_2O \rightarrow Al(OH)_{3(s)} + 3H^+ \quad (3.19)$$

The variation of pH profile with varying concentration of Fe^{3+} as representative of the inorganic contaminants in the SAMD is shown in **Figure 3.5.**

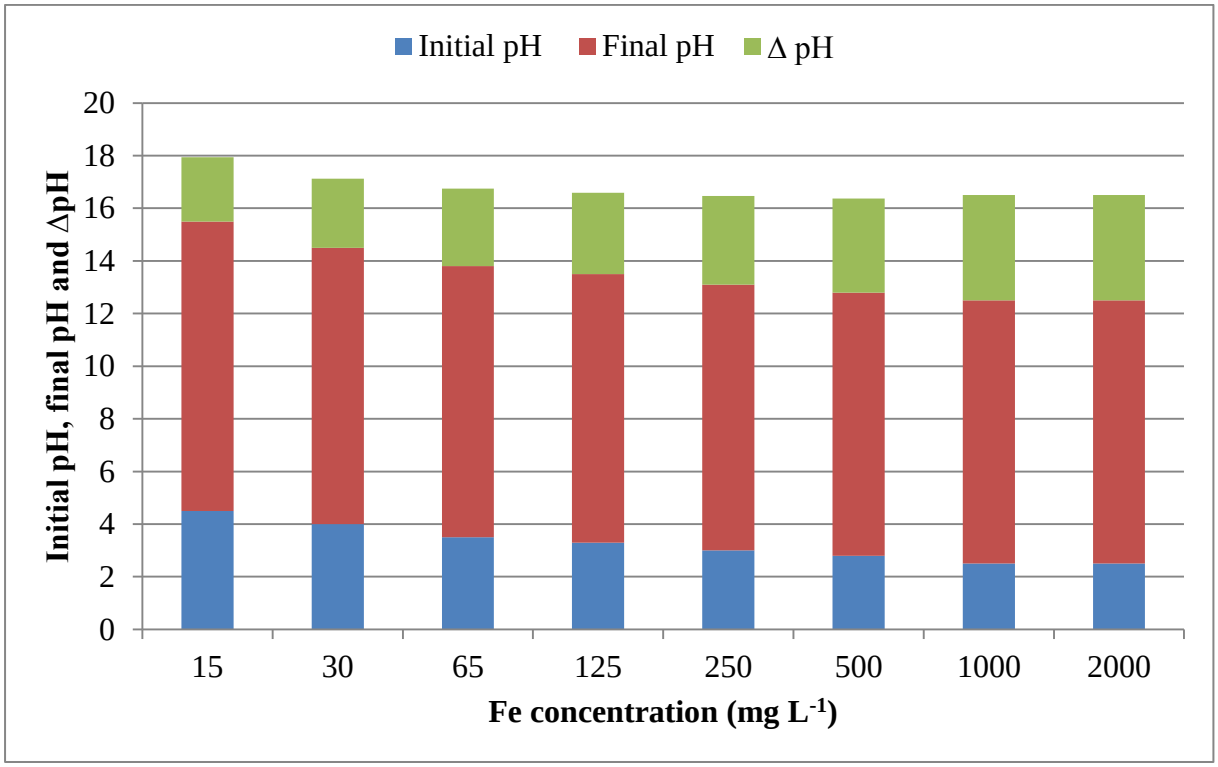

Figure 3.5: Variation of pH gradient with varying Fe concentrations.

3.3.1.5 Treatment of field acid mine drainage samples

Chemical compositions of AMD before and after contacting magnesite are shown in **Table 3.2**.

Table 3.2: Chemical compositions of AMD before and after contacting magnesite (Units: concentration is mg/L and EC is µS/cm).

Parameter	Feed AMD water	DWS Guidelines	Magnesite treated AMD
Alkalinity	< 5	N/A	120
pH	2	6 - 10	10
TDS	10240	0 - 1200	4345
EC	22710	0 - 700	4636
Na	170	0 - 50	165
K	18	NA	20
Mg	180	0 - 30	400
Ca	760	0 - 32	300
Al	190	0 – 0.9	< 0.03
Fe	260	0 – 0.1	<0.02
Mn	40	0 – 0.05	0.04
Cu	7.8	0 – 1	< 0.05
Zn	7.9	0 – 0.5	0.1
Pb	6.3	0 – 0.01	0.2
Co	41.3	N/A	0.2
Ni	17	0 - 0.07	0.5
As	20	0.001	<0.01
B	5	0.01	<0.01
Cr	20	0.01	<0.01
Mo	16	0.01	<0.01
Se	17	0.02	<0.01
Si	1.5	NA	6
SO_4^{2-}	4600	0 - 500	1910

The pH of the AMD used in this study was 2. Acidity was quantified to be 200 mg/L as $CaCO_3$. Total dissolved solids (TDS) and electrical conductivity (EC) were 240 mg/L and 403 µS/cm respectively. This is attributed to large quantity of dissolved metal species and sulphates. The sulphate recorded in this sample was 4600 mg/L making this anion dominant. Major cations included Na, Ca, Mg, Al, Mn and Fe. The predominance of Fe and SO_4^{2-}

indicated that this mine water was subjected to pyrite dissolution. Dissolution of silicate minerals such as feldspar, kaolinite, and chlorite accounts for most or all of the dissolved K, Na, Mg, Al and Ca (Langmuir 1997). Traces of gold associated minerals such as Cu, Pb, Zn, Co, Ni, As, B, Cr, Mo and Se were also observed to be present. Post treatment, only Ca, Na, Mg and sulphate remained at elevated concentrations. Saturation indices from geochemical simulations suggested that Mg was below precipitation levels. Mg species form relatively high solubility salts hence are expected to remain largely in solution. Ca was reduced significantly and it was predicted to precipitate as gypsum, calcite and dolomite. The simulations showed that in the feed water, Fe existed mainly as Fe^{2+} and Fe^{3+} while the rest of the metals, except for Na and K, were in their divalent states at acidic solution. A large proportion of Mg existed as aqueous $MgSO_4$. From these results, the treated water is suitable for agricultural use, especially in acidic soils owing to its elevated pH. Most of the water quality parameters of the treated water fell within those stipulated by the South African Department of Water and Sanitation (DWS) Water Quality Guidelines for irrigation (**Table 3.2**).

3.3.2 Mineralogy, elemental and microstructural characterization

3.3.2.1 X-ray diffraction analysis

The mineralogical compositions by X-ray diffraction (XRD), for raw and reacted magnesite, with field AMD, are presented in **Figure 3.6**.

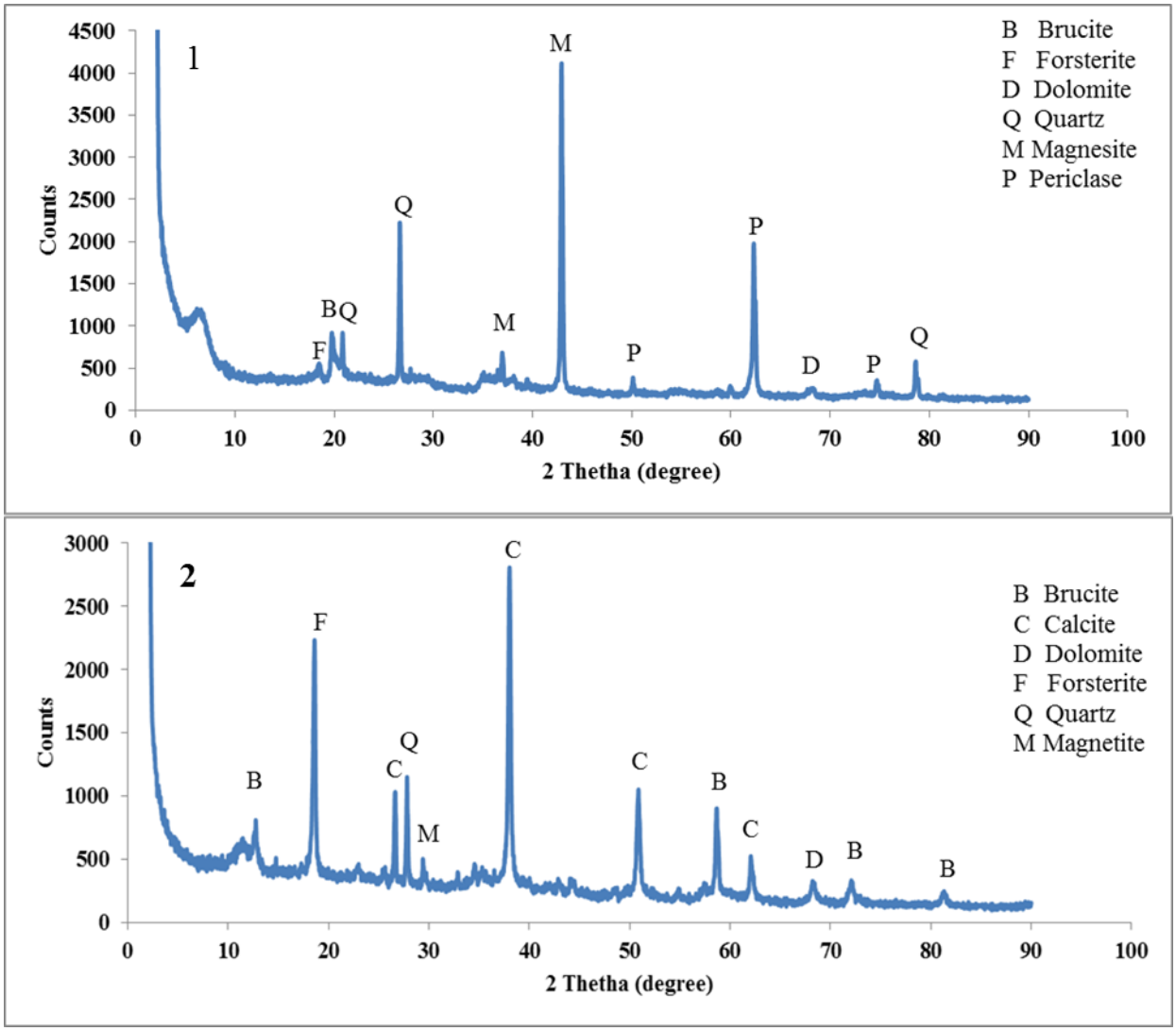

Figure 3.6: XRD patterns of raw (1) and reacted magnesite (2)

The results revealed that raw magnesite contain magnesite, periclase, brucite, dolomite, forsterite and quartz as the crystalline phases. After treatment of field AMD, the following minerals were detected in the reacted magnesite: brucite, calcite, and magnetite. Calcite, dolomite, brucite and magnetite were observed to be present hence indicating that the conditions were suitable for precipitation of Ca, Mg and Fe bearing species (pH > 10). The peak of periclase was observed to be absent in the secondary residues hence indicating the dissolution of MgO. The precipitation of calcite and brucite from AMD can be represented by the following equations:

$$Mg^{2+} + H_2O + CO_3^{2-} \rightarrow Mg(OH)_2 + CO_2 \uparrow \quad (3.6)$$

$$MgCO_3 + 2H_2O \rightarrow Mg(OH)_2 + H_2CO_3 \quad (3.7)$$

$$Ca^{2+} + 2HCO_3^- \rightarrow CaCO_3 \downarrow + H_2CO_3 \quad (3.8)$$

Magnesium will react with water and carbonate in AMD to precipitate as brucite at pH > 10 (Equation 3.6 and 3.7). Ca^{2+} in AMD will react with carbonic acid in water to form calcium carbonate (Equation 3.7). Magnesite will react with sulphuric acid in AMD to form magnesium sulphate, water and carbon dioxide as shown in the Equation 3.9:

$$MgCO_3 + H_2SO_4 \rightarrow MgSO_{4(aq)} + H_2O + CO_2 \uparrow \quad (3.9)$$

Periclase will react with acidity in AMD to give magnesium ions and hydroxyl ions

$$MgO + H^+ \rightarrow Mg^{2+} + OH^- \quad (3.10)$$

Brucite will react with acidity in AMD to form magnesium ions and water

$$MgOH^+ + H^+ \rightarrow Mg^{2+} + H_2O \quad (3.11)$$

Silicate will react with acid in AMD through ion exchange and lead to pH increase

$$\equiv SiOH \leftrightarrow SiO^- + H^+ \quad (3.12)$$

$$\equiv SiOH + Ca^{2+} \leftrightarrow = SiOCa + H^+ \quad (3.13)$$

$$\equiv SiOCa + M^{2+} + HOH \rightarrow = SiOM + Ca^{2+} + HOH \quad (3.14)$$

3.3.2.2 Carbon and Sulphur determination by ELTRA

ELTRA analytical technique revealed that magnesite contains 6% of carbon on cryptocrystalline magnesite and 8% elemental composition post interaction with AMD. This shows that the material understudy is a carbonate. An increase in carbon may be attributed to precipitation of carbonate from the atmosphere at pH > 10. Sulphur content was recorded to be 0.002% on raw magnesite and 0.97% on reacted magnesite hence confirming that magnesite is a sinks of sulphate from AMD. This has corroborated XRF, FTIR, SEM-EDS results and PHREEQC geochemical modelling.

3.3.2.3 X-ray fluorescence analysis

The elemental composition of magnesite before and after interaction with field AMD is shown in **Table 3.3**.

Table 3.3: Elemental composition of magnesite before and after treatment

Sample (wt %)	Magnesite	AMD-magnesite
SiO_2	6.09	5.25
Al_2O_3	0.71	0.63
Fe_2O_3 (t)	0.54	2.47
MnO	0.01	0.45
MgO	82.09	60
CaO	2.39	4.91
Na_2O	0.13	0.11
K_2O	0.06	0.05
SO_3	0.2	10
LOI	7.34	19.05
Total	99.56	100
H_2O-	1.62	2
mg/L		
As	<4	9
Ba	<5	8.9
Br	2.5	<2
Co	<1	6.2
Cr	3.9	16
Cu	6.2	11.3
Ga	1.1	1.9
Hf	8.8	10.3
Nb	158	225
Ni	11	137
Pb	4	21
Se	11	21
Sr	5.4	84
Ta	4.3	22
Y	2	32
Zn	1	39
Zr	<2	5.5

After the reaction, Zn, Cu, Co, Nb, Ni, Pb, SO_3, Sr, Y, Zr, Cr and Ba were found to be present in the resultant solid residues. The results obtained for the raw magnesite corroborated results from the study by (Nasedkin et al., 2001). In their study, they reported that cryptocrystalline magnesite was characterised by 90 – 92 wt % of MgO and very few other impurities. The levels of Fe, Ca, Mn and S were observed to increase in the resultant solid residues indicating formation of new phases whereas Al, Si and Mg decrease hence indicating possible dissolution. The X-ray fluorescence (XRF) results are confirming the XRD (**Figure 3.6**), Scanning electron microscopy (SEM) – electron dispersion spectrometry (EDS) (SEM-EDS) (**Figure 3.8**) and flourier transform infrared spectroscopy (FTIR) (**Figure 3.7**) results as reported above.

3.3.2.4 Fourier transform infrared spectroscopy analysis

The spectra for raw and AMD-reacted magnesite are shown in **Figure 3.7**.

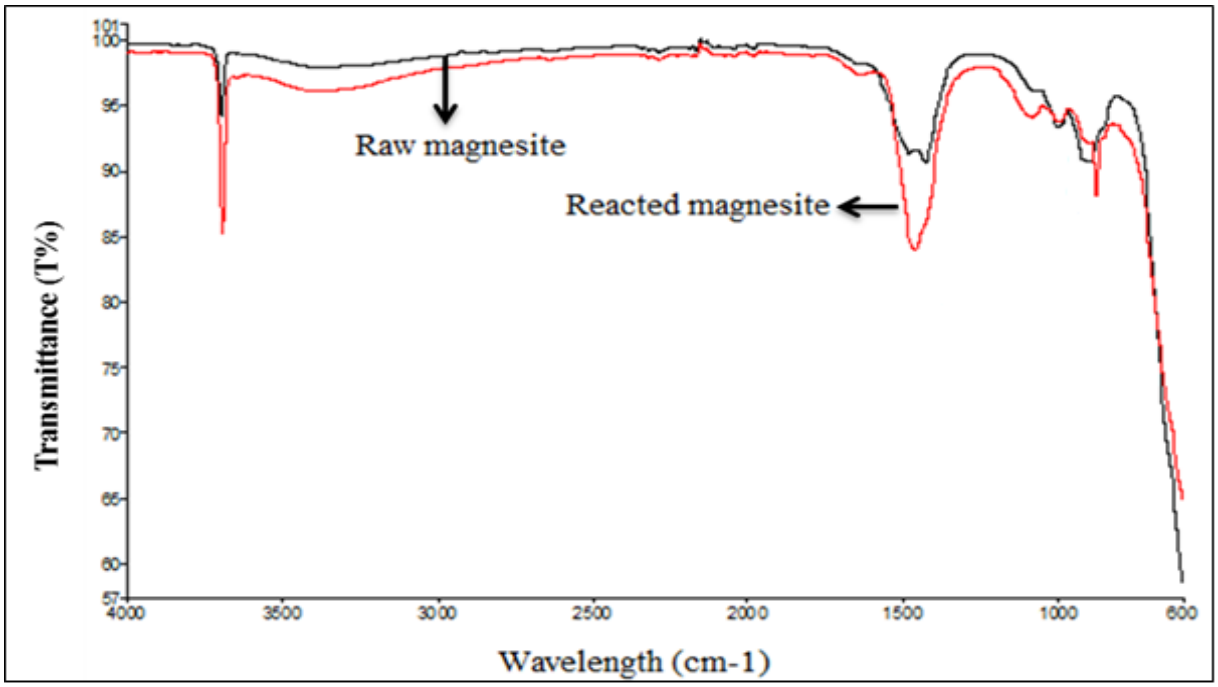

Figure 3.7: Functional groups for unreacted and reacted magnesite

Spectroscopic studies confirm the results of XRD studies. The system of bands in raw magnesite is characteristic of brucite bending vibration corresponding to band 3702 cm^{-1}, periclase stretching vibration corresponding to band 1500 and 950 cm^{-1} and magnesite stretching vibration corresponding to bands 1680, 1450, 850 cm^{-1}. The doublet at 1490, 1419 cm^{-1} corresponds to asymmetric stretching vibrations of carbonate. The reason for the split of

this peak into a doublet could be due to the formation of new carbonates such as $CaCO_3$ and $MgCO_3$. The band at 1117 cm^{-1} correspond to symmetric stretching of carbonate, and those at 886, 795 cm^{-1} are assigned to in plane and out-of-plane bending vibrations of carbonate ion. The presence of carbonates in raw magnesite suggests the presence of magnesite and calcite. The presence of carbonates in reacted magnesite suggests the precipitation of rhodochrosite, siderite, calcite and dolomite. The system of bands for reacted magnesite is characterised of brucite stretches corresponding to band 3702 cm^{-1}, bands at 3600 – 3700 cm^{-1} are associated with OH groups adsorbed water and new bands corresponding to calcite stretches at band 630 cm^{-1} and magnetite at band 880 cm^{-1}. FTIR results provide evidence that magnesite is acting as a sink of inorganic contaminants from aqueous solution. These results corroborate with results obtained using XRD (**Figure 3.7**) and XRF (**Table 3.2**).

3.3.2.5 Scanning electron microscope-electron dispersion spectrometry analysis

In order to better understand the mode of interaction of AMD with magnesite and the formation of mineral phases SEM was utilized to assess the change in morphology of the resulting solid residues as compared with unreacted magnesite while SEM-EDS was utilized to semi-quantitatively identify the mineral phases resulting from the neutralization reactions.

Figure 3.8 (A, C and E) shows the raw magnesite before contacting AMD**. Figures 3.8 (B, D and F)** shows the morphological changes taking place after interaction of cryptocrystalline magnesite with AMD. Before contacting AMD, the morphology of cryptocrystalline magnesite was shown to contain spherical, leafy like, rod shaped structures and lumps which are grape shaped hence indicating that the material is heterogeneous (**Figure 3.8** - A, C and E). After contacting with AMD, the uneven rough platelet mixed with spherical and rod-like structures were observed to be present hence providing evidence of mineral phases/precipitates coating the surfaces or removal of soluble salts that covered the magnesite surface. The small spheres are seen to be aggregating and filling in the spaces between the large spheres forming a dense mass (**Figure 3.8 - B, D and F**). Bulky solution precipitation could be responsible for the formation of mineral phases which are deposited in-between the secondary residues to form fibre-like, rod shaped and grape structured lumps of tetrahedral folding appearances, thereby acting as a binding link between the micro-particles hence the dense packing observed in the SEM micrographs. Three main features are observed in the solid residues by SEM technique.

- Appearance of spherical, rod and fibre-like and aggregated lump-like structures indicates formation of new mineral phases in the solid residues.

- Rods-like structures of varying length and thickness/some are flat shaped and are observed over the whole solid residue samples. Lumps with aggregated substances that are grape shaped.

- Aggregation of the small particles forming lumps and rod and grape shaped structures with varying sizes of tetrahedral folding hence confirming the deposition of new mineral phases.

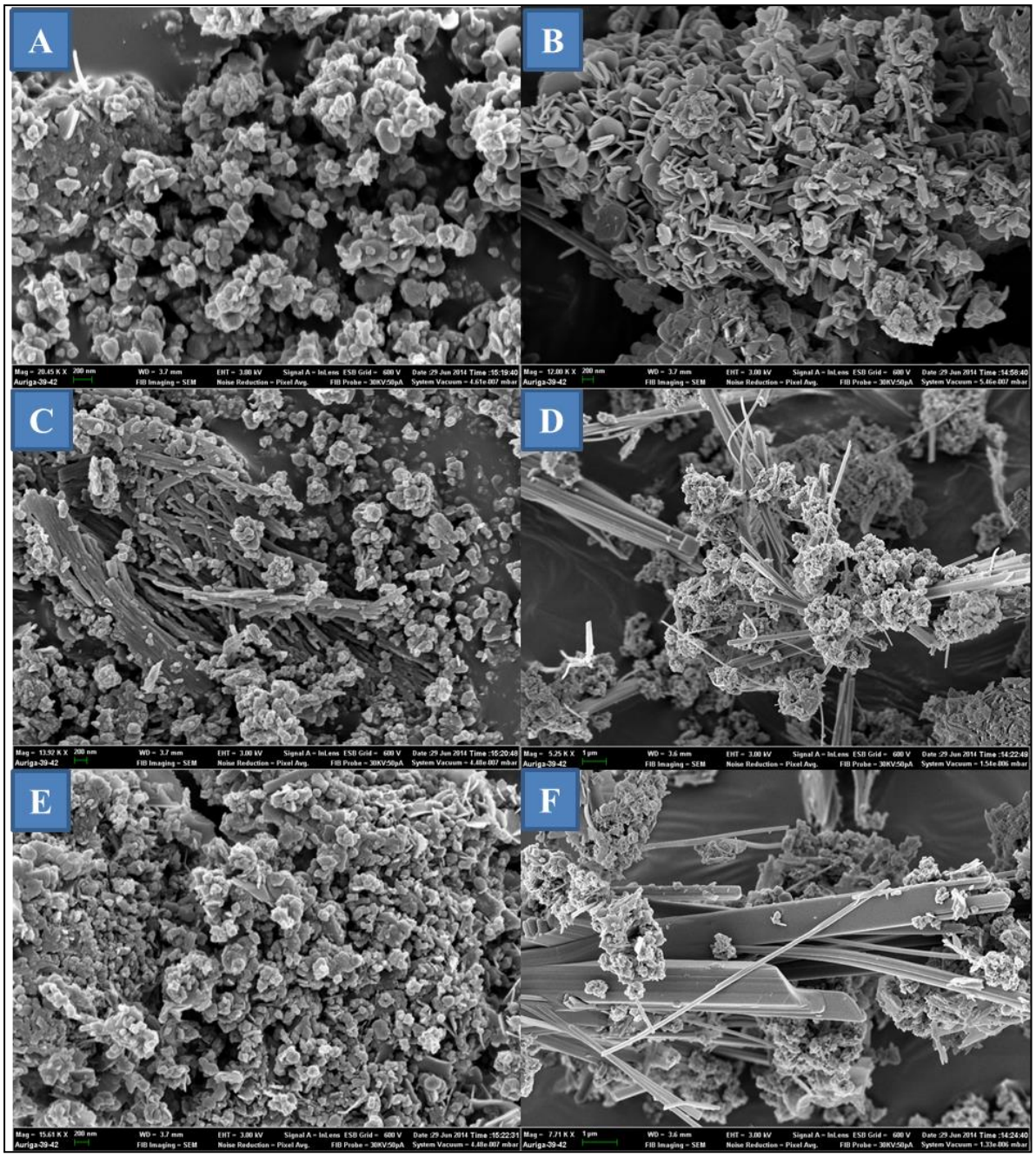

Figure 3.8: SEM images of raw magnesite (A, C and E) and AMD-reacted magnesite (B, D and F).

The SEM-EDS spot elemental analysis of the raw magnesite expressed as weight % are presented in **Table 3.4**.

Table 3.4: SEM-EDS spot % elemental analysis of raw magnesite

Magnesite	C	O	Mg	Si	Ca	Fe
Point 1	8.5	30.9	59.9	-	0.7	-
Point 2	16.9	34.9	27.9	16.6	2.4	1.4
Point 3	-	27.9	67.4	2.3	2.5	-
Average	8.5	31.2	51.7	6.3	1.9	0.5

The spot elemental composition and morphology of magnesite is shown in **Figure 3.9**.

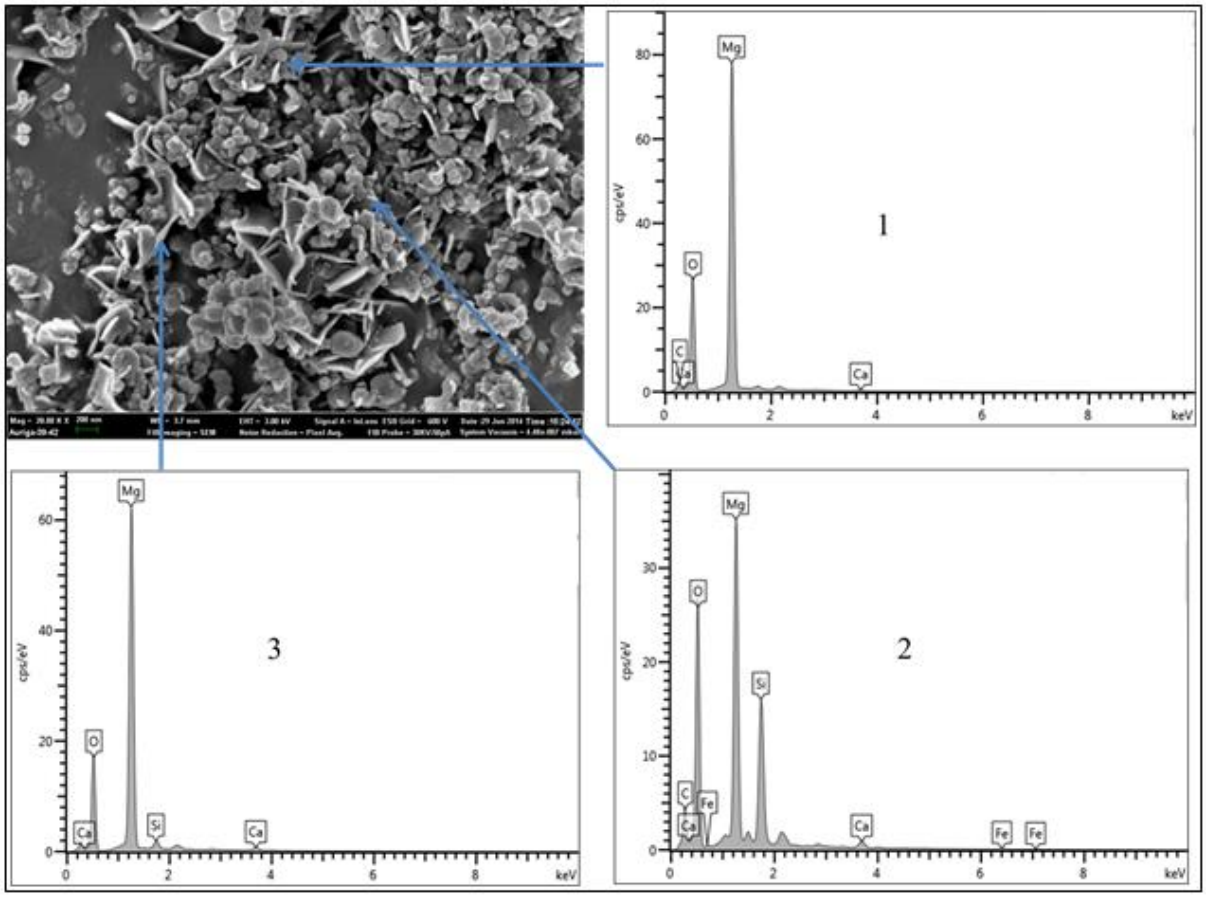

Figure 3.9: Micro image and elemental composition of raw magnesite

As shown in **Table 3.4**, the elemental compositions of magnesite were determined using EDS at 3 spots. The analysis showed that the mineral is composed of C, O and Mg with percentage

composition of 8.5, 31.2, and 51.7 wt% respectively. There were impurities of Si, Fe and Ca. Again, the results correspond to arithmetic averages of 3 data points obtained from randomly selected locations on the surface of magnesite.

Point 1 (Figure 3.9): The morphology of cryptocrystalline magnesite was shown to contain spherical, leafy like and rod shaped structures hence indicating that the material is heterogeneous. EDS revealed high levels of C, O, Mg and Ca were on the heterogeneous structures hence indicating that the material is magnesite with impurities of calcium.

Point 2 (Figure 3.9): The morphology of cryptocrystalline magnesite was shown to contain spherical, leafy like and rod shaped structures hence indicating that the material is heterogeneous. EDS revealed high levels of C, O, Mg and Ca on the heterogeneous structures hence indicating that the material is magnesite with impurities of silicon, calcium and iron.

Point 3 (Figure 3.9): The morphology of cryptocrystalline magnesite was shown to contain sheet and leafy structures. EDS revealed high levels of O, Mg, Si and Ca on the magnesite structures. This proves the presence of periclase as indicated by XRD. The accompanying SEM-EDS spot elemental analysis of the reacted magnesite is shown in **Table 3.5** and **Figure 3.10** respectively.

Table 3.5: SEM-EDS spot % elemental analysis of solid residue collected at pH > 10.

Magnesite	**C**	**O**	**Mg**	**Al**	**Si**	**S**	**Ca**	**Mn**	**Fe**
Point 1	6.54	47.29	36.24	0.05	1.13	0.41	6.55	0.48	1.36
Point 2	19.06	45.84	28.32	-	0.93	0.71	3.71	0.33	1.11
Point 3	7.01	45.87	33.99	-	1.39	0.50	5.88	0.87	4.49
Average	10.9	46.3	32.9	0.01	1.2	0.5	5.4	0.6	2.3

The spot elemental composition and morphology of magnesite is shown in **Figure 3.10**.

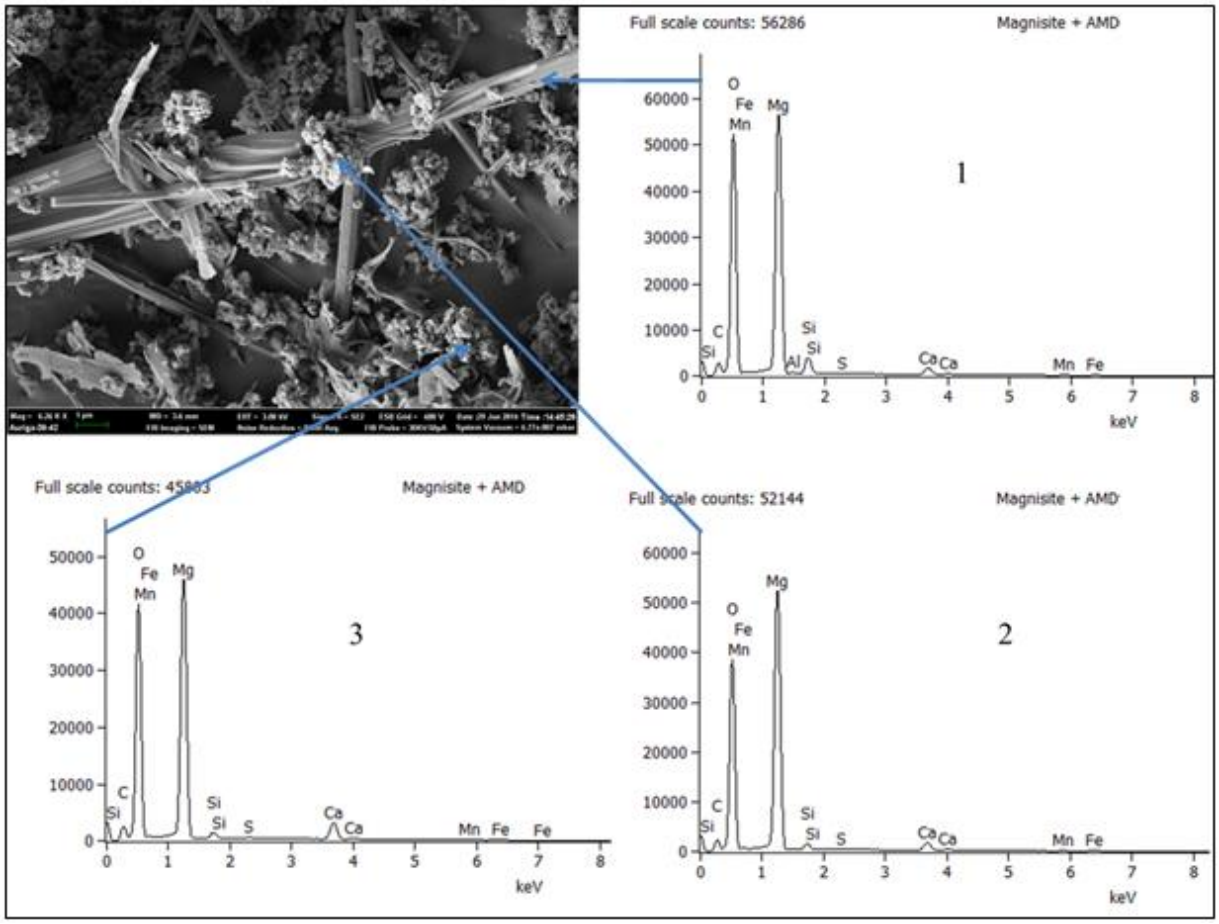

Figure 3.10: Micro image and elemental composition of reacted magnesite

The leafy like, spherical and sheet structures have disappeared after reaction of magnesite with AMD indicating dissolution of magnesite on contact with AMD. Appearance of rod like structures and aggregated lump-like structures indicates formation of new mineral phases in the solid residues.

Point 1 (Figure 3.10): The morphology of reacted magnesite is showing the presence of rod shaped structures that are folding in a bundle like formation. EDS indicated an increase in Ca, Fe, Mn and Si levels. Mg and C were also observed to be present. An introduction of Fe, Mn and S was also observed in the secondary residues hence indicating formation of mineral phases incorporating these metal species. This would explain the decrease in the metal species and sulphate concentration in the product water. The presence of Si could suggest the precipitation of Si bearing amorphous phases. The presence of Fe could indicate the precipitation of ferrihydrite-like phases and schwertmannite. This was also indicated by the yellowish colour on the secondary residue. The presence of Mn suggests the formation of rhodochrosite. The presence of Al is indicating availability of Al hydroxysulphates minerals such as hydrobasaluminite and basaluminite. The increase in Fe, Al, and S would probably

suggest some kind of Fe, Al hydroxysulphates. The presence of Mg and Ca is indicating the presence of brucite and calcite respectively. To be particular, the presence of Mn, Fe, Al, Ca, Mg, C and O suggest minerals such as Mn, Fe, Al oxide, metals hydroxides, Mn and Fe carbonate, gypsum, Al and Fe oxyhydrosulphates. The PHREEQC simulation also predicted precipitation of mineral phases bearing these metal species.

Point 2 (Figure 3.10): The morphology of reacted magnesite is showing that it contains flowery tetrahedral folding and grape shaped structures. EDS indicated an increase in Ca, Fe, Mn and Si levels. Mg and C were also observed to be present. An increase in Ca is indicating the formation of gypsum. An increase in Mg is indicating the formation of brucite. The presence of Fe could indicate the precipitation of ferrihydrite-like phases and schwertmannite. This was also verified by the yellowish colour on the secondary residue. Carbonates were observed to precipitate as rhodochrosite, calcite and dolomite from Mn, Mg and Ca respectively. The presence of Mn, Fe, Ca, Mg, C and O suggest minerals such as Mn, Fe oxide, metals hydroxides, Mn and Fe carbonate, gypsum, Fe oxyhydrosulphates.

Point 3 (Figure 3.10): The SEM micro image of AMD reacted magnesite is showing the presence of a flowery tetrahedral folding and grape shaped structures. This spot shows a significant increase in Fe, Mn, Ca and C strongly suggesting that phase constituted by those elements are being formed. An increase in Ca would suggest a Ca and S rich precipitate is being formed probably $CaSO_4$ or gypsum. The presence of Si could suggest the precipitation of Si bearing amorphous phases. An increase in Mg is indicating the formation of brucite. An increase in Fe is presenting the precipitation of Fe bearing minerals. The presence of Mn, Fe, Ca, Mg, C and O suggest minerals such as Mn, Fe oxide, metals hydroxides, Mn and Fe carbonate, gypsum, Fe oxyhydrosulphates**.** The PHREEQC simulation also predicted precipitation of mineral phases bearing these metal species.

3.3.2.6 Transmission electron microscopy analysis

The transmission electron microscopy (TEM) diffraction pattern of the area (**A**) and micrographs (**B**) of raw magnesite are shown in **Figure 3.11**.

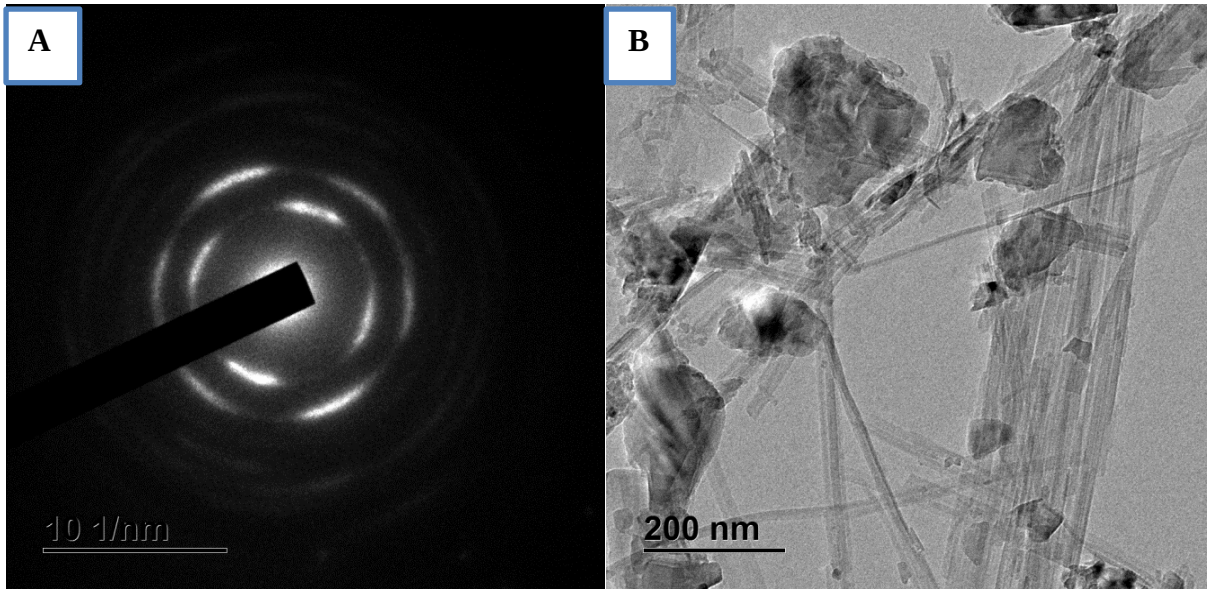

Figure 3.11: TEM diffraction pattern of the area (**A**) and micrographs (**B**) of magnesite

From the TEM diffraction pattern it can be observed that the material is polycrystalline (cryptocrystalline). This was determined by the breakages and inconsistencies on the crystalline phases. This result corroborates with results obtained by Nasedkin et al (2001). The micrograph indicated the presence of nanotubes on the matrices of magnesite with the bundle like arrangement. This is corresponding to SEM-EDS results.

3.4 Calculation of Saturation Indices for various mineral phases

The results for calculation of mineral precipitation at various pH values during treatment of simulated AMD with magnesite are presented in **Table 3.6**.

Table 3.6: Calculation of SI for selected mineral phases at various pH

Mineral phase	pH and saturation indices (SI)					
	3	4	6	8	10	11
Alkalinity (eq/kg)	$-3.6x10^{-2}$	$1.5x10^{-2}$	$6.4x10^{-2}$	$3x10^{-1}$	$-3x10^{-1}$	3.5
$Al(OH)_3$	-0.9	3.5	2.9	1.2	-0.1	-1.5
Boehmite (AlOOH)	-0.5	7	5	3.4	2.1	0.7
Basaluminite $Al_4(OH)_{10}SO_4$	-0.8	23	17.4	6	-1.4	-10.2
Brucite $Mg(OH)_2$	-11	-9	-6.6	-2	0.6	3.6
Calcite	-11	-2.3	-1.5	1.8	3.4	4
Aragonite	-8.6	-2.5	-0.2	1.7	3.7	3.8
Diaspore (AlOOH)	-0.9	8.3	6.8	5.1	3.1	2
Dolomite $CaMg(CO_3)_2$	-6	-2.5	-1.3	4.9	6.9	8
Epsomite	-7	-4	-2	-1.8	-1.8	-1.8
$Fe(OH)_3$	5	4.4	3.7	4.6	3.2	3.1
Gibbsite $Al(OH)_3$	0.3	6.7	5.5	3.7	1.8	0.8
Geothite (FeOOH)	6	8	9.7	10.5	9.1	9
Gypsum ($CaSO_4.H_2O$)	-0.1	-0.2	-0.2	4	5	8
Jarosite H $(H_3O)Fe_3(SO_4)_2(OH)_6$	5	3.2	2.9	-3.7	-16	-20
Jurbanite ($AlOHSO_4$)	1	5	2.5	-3.6	-9.8	-12.8
Rhodochrosite ($MnCO_3$)	-8.75	-0.9	-0.4	0	0	0
Manganite MnOOH	-8.1	-5.3	-2.9	4	6	8
Pyrochroite $Mn(OH)_2$	-8	-7.1	-6.4	0.2	0.9	2.2

Most of the Al and Fe could precipitate as hydroxides at pH > 6. Mn could precipitates as manganese hydroxide at pH > 10 and rhodochrosite at pH > 8. Sulphate-bearing minerals could precipitates at pH 6 – 8 (basaluminite), pH > 8 (gypsum), pH 6 (jarosite and jurbanite). Generally, mineral phases were predicted to precipitate as metal hydroxides, hydroxysulphates and oxyhydroxysulphates. Epsomite ($MgSO_4$) was observed to be near precipitation but it did not precipitate and may be attributed to the high solubility of epsomite (K_{sp} =5.9 x 10^{-3}) (Bologo et al., 2012). However, sulphates were removed from solution together with Al, Fe and Ca. This corroborate the SEM-EDS and XRF detected Al, Fe, Mn and S rich mineral phases were deposited to solid residues. This indicates that the Al, Fe, Mn

and S rich mineral phases were too amorphous to be detected by XRD or the concentration was below the detection limits.

3.5 Conclusions

This study has shown that magnesite can be used to remediate AMD. Contact of AMD with magnesite led to an increase in pH and a notable reduction in metal and sulphate concentrations. Removal of Al, Mn, Fe and other metals was maximized after 60 min of agitation for a S: L ratio of 1 g: 100 mL and particle size ranging from 0.1 – 125 µm. Under these conditions, the pH achieved was >10, an ideal regime for metal removal. Using geochemical modelling, it was shown that most metals e.g. Fe, Al, Mn, and Ca formed sulphate-bearing minerals. From modelling simulations, the formation of these phases follow a selective precipitation sequence with Fe^{3+} at pH > 6, Al^{3+} at pH > 6, Fe^{2+} at pH > 8, Mn^{2+}, Ca^{2+} and Mg^{2+} at pH >10. This sequence implied that it would be possible to separate precipitates of various metals, making this technology viable for instances where the commercial value of the recovered metals are being pursued. This study has pointed to the efficiency of magnesite in neutralizing and attenuating metals from AMD and metalliferous industrial effluents. A disadvantage of this technology is that most of the alkali and alkaline earth metals remain in solution which means a post treatment processes such as ion exchange or reverse osmosis might be required for polishing the product water.

REFERENCES

Akcil, A. & Koldas, S. 2006. Acid Mine Drainage (AMD): causes, treatment and case studies. *Journal of Cleaner Production,* 14**,** 1139-1145.

Alakangas, L., Andersson, E. & Mueller, S. 2013. Neutralization/prevention of acid rock drainage using mixtures of alkaline by-products and sulfidic mine wastes. *Environmental Science and Pollution Research,* 20**,** 7907-7916.

Bologo, V., Maree, J. P. & Carlsson, F. 2012. Application of magnesium hydroxide and barium hydroxide for the removal of metals and sulphate from mine water. *Water SA,* 38**,** 23-28.

Buzzi, D. C., Viegas, L. S., Rodrigues, M. a. S., Bernardes, A. M. & Tenório, J. a. S. 2013. Water recovery from acid mine drainage by electrodialysis. *Minerals Engineering,* 40**,** 82-89.

Çabuk, A., Aytar, P., Gedikli, S., Özel, Y. K. & Kocabiyik, E. 2013. Biosorption of acidic textile dyestuffs from aqueous solution by Paecilomyces sp. isolated from acidic mine drainage. *Environmental Science and Pollution Research,* 20**,** 4540-4550.

Chen, Y., Gao, K., Lin, H., Dong, Y., Wang, H., Li, Y., Huo, H. & Cao, L. 2013a. Adsorption properties of microbe resistant to lead and zinc on Zn2+ and Pb2+ in acid mine drainage (AMD). *Zhongnan Daxue Xuebao (Ziran Kexue Ban)/Journal of Central South University (Science and Technology),* 44**,** 1741-1746.

Chen, Y. F., Cao, L. X., Lin, H., Dong, Y. B., Cheng, H. & Huo, H. X. 2013b. Adsorption of Cu2+ from simulated acid mine drainage by herb-medicine residues and wheat bran. *Zhongguo Youse Jinshu Xuebao/Chinese Journal of Nonferrous Metals,* 23**,** 1775-1782.

Falayi, T. & Ntuli, F. 2014. Removal of heavy metals and neutralisation of acid mine drainage with un-activated attapulgite. *Journal of Industrial and Engineering Chemistry,* 20**,** 1285-1292.

Freitas, A. P. P., Schneider, I. a. H. & Schwartzbold, A. 2011. Biosorption of heavy metals by algal communities in water streams affected by the acid mine drainage in the coal-mining region of Santa Catarina state, Brazil. *Minerals Engineering,* 24**,** 1215-1218.

Funke, N., Nienaber, S. & Gioia, C. 2012. An interest group at work: Environmental activism and the case of acid mine drainage on Johannesburg's West Rand. *Public Opinion and Interest Group Politics: South Africa's Missing Links?* **,** 193-214.

Gaikwad, R. W. 2010. Review and research needs of active treatment of acid mine drainage by ion exchange. *Electronic Journal of Environmental, Agricultural and Food Chemistry,* 9**,** 1343-1350.

Gitari, W. M., Petrik, L. F., Etchebers, O., Key, D. L. & Okujeni, C. 2008. Utilization of fly ash for treatment of coal mines wastewater: Solubility controls on major inorganic contaminants. *Fuel,* 87**,** 2450-2462.

Groudev, S., Georgiev, P., Spasova, I. & Nicolova, M. 2008. Bioremediation of acid mine drainage in a uranium deposit. *Hydrometallurgy,* 94**,** 93-99.

Henri, A. J., Wepener, V., Ferreira, M., Malherbe, W. & Van Vuren, J. H. J. 2014. The effect of acid mine drainage on the hatching success of branchiopod egg banks from endorheic wetlands in South Africa. *Hydrobiologia,* 738**,** 35-48.

Jeleni, M. N., Gumbo, J. R., Muzerengi, C. & Dacosta, F. A. 2012. An assessment of toxic metals in soda mine tailings and a native grass: A case study of an abandoned Nyala Magnesite mine, Limpopo, South Africa. *WIT Transactions on Ecology and the Environment,* 164**,** 415-426.

Johnson, D. B., Dziurla, M. A., Kolmert, Å. & Hallberg, K. B. 2002. The microbiology of acid mine drainage: Genesis and biotreatment. *South African Journal of Science,* 98**,** 249-255.

Johnson, D. B. & Hallberg, K. B. 2005a. Acid mine drainage remediation options: A review. *Science of the Total Environment,* 338**,** 3-14.

Johnson, D. B. & Hallberg, K. B. 2005b. Acid mine drainage remediation options: a review. *Science of The Total Environment,* 338**,** 3-14.

Jooste, S. & Thirion, C. 1999. An ecological risk assessment for a South African acid mine drainage. *Water Science and Technology,* 39**,** 297-303.

Kalin, M., Fyson, A. & Wheeler, W. N. 2006. The chemistry of conventional and alternative treatment systems for the neutralization of acid mine drainage. *Science of the Total Environment,* 366**,** 395-408.

Kleiv, R. A. & Thornhill, M. 2008. Predicting the neutralisation of acid mine drainage in anoxic olivine drains. *Minerals Engineering,* 21**,** 279-287.

Kumar Vadapalli, V. R., Klink, M. J., Etchebers, O., Petrik, L. F., Gitari, W., White, R. A., Key, D. & Iwuoha, E. 2008. Neutralization of acid mine drainage using fly ash, and strength development of the resulting solid residues. *South African Journal of Science,* 104**,** 317-322.

Lee, G., Bigham, J. M. & Faure, G. 2002. Removal of trace metals by coprecipitation with Fe, Al and Mn from natural waters contaminated with acid mine drainage in the Ducktown Mining District, Tennessee. *Applied Geochemistry,* 17**,** 569-581.

Macías, F., Caraballo, M. A., Rötting, T. S., Pérez-López, R., Nieto, J. M. & Ayora, C. 2012. From highly polluted Zn-rich acid mine drainage to non-metallic waters: Implementation of a multi-step alkaline passive treatment system to remediate metal pollution. *Science of The Total Environment,* 433**,** 323-330.

Macingova, E. & Luptakova, A. Recovery of metals from acid mine drainage by selective sequential precipitation processes. 11th International Multidisciplinary Scientific Geoconference and EXPO - Modern Management of Mine Producing, Geology and Environmental Protection, SGEM 2011, 2011. 573-578.

Maree, J. P., Bosman, D. J. & Jenkins, G. R. 1989. Chemical removal of sulphate, calcium and heavy metals from mining and power station effluents. *Water Sewage Effluent,* 9**,** 10-25.

Maree, J. P., De Beer, M., Strydom, W. F., Christie, A. D. M. & Waanders, F. B. 2004. Neutralizing coal mine effluent with limestone to decrease metals and sulphate concentrations. *Mine Water and the Environment,* 23**,** 81-86.

Maree, J. P., Dingemans, D., Van Tonder, G. J. & Mtimkulu, S. 1998. Biological iron(II) oxidation as pre-treatment to limestone neutralisation of acid water. *Water Science and Technology,* 38**,** 331-337.

Maree, J. P., Mujuru, M., Bologo, V., Daniels, N. & Mpholoane, D. 2013. Neutralisation treatment of AMD at affordable cost. *Water SA,* 39**,** 245-250.

Mohan, D. & Chander, S. 2006. Removal and recovery of metal ions from acid mine drainage using lignite—A low cost sorbent. *Journal of Hazardous Materials,* 137**,** 1545-1553.

Motsi, T., Rowson, N. A. & Simmons, M. J. H. 2009. Adsorption of heavy metals from acid mine drainage by natural zeolite. *International Journal of Mineral Processing,* 92**,** 42-48.

Mulopo, J., Zvimba, J. N., Swanepoel, H., Bologo, L. T. & Maree, J. 2012. Regeneration of barium carbonate from barium sulphide in a pilot-scale bubbling column reactor and utilization for acid mine drainage. *Water Science and Technology,* 65**,** 324-331.

Nasedkin, V. V., Krupenin, M. T., Safonov, Y. G., Boeva, N. M., Efremova, S. V. & Shevelev, A. I. 2001. The comparison of amorphous (cryptocrystalline) and crystalline magnesites. *Mineralia Slovaca,* 33**,** 567-574.

Oberholster, P. J., Myburgh, J. G., Ashton, P. J. & Botha, A. M. 2010. Responses of phytoplankton upon exposure to a mixture of acid mine drainage and high levels of nutrient pollution in Lake Loskop, South Africa. *Ecotoxicology and Environmental Safety,* 73**,** 326-335.

Papirio, S., Villa-Gomez, D. K., Esposito, G., Pirozzi, F. & Lens, P. N. L. 2013. Acid mine drainage treatment in fluidized-bed bioreactors by sulfate-reducing bacteria: A critical review. *Critical Reviews in Environmental Science and Technology,* 43**,** 2545-2580.

Pinetown, K. L., Ward, C. R. & Van Der Westhuizen, W. A. 2007. Quantitative evaluation of minerals in coal deposits in the Witbank and Highveld Coalfields, and the potential impact on acid mine drainage. *International Journal of Coal Geology,* 70**,** 166-183.

Pozo-Antonio, S., Puente-Luna, I., Lagüela-López, S. & Veiga-Ríos, M. 2014. Techniques to correct and prevent acid mine drainage: A review. *DYNA (Colombia),* 81**,** 73-80.

Ramírez-Paredes, F. I., Manzano-Muñoz, T., Garcia-Prieto, J. C., Zhadan, G. G., Shnyrov, V. L., Kennedy, J. F. & Roig, M. G. 2011. Biosorption of heavy metals from acid mine drainage onto biopolymers (chitin and α (1,3) β-D-glucan) from industrial biowaste exhausted brewer's yeasts (Saccharomyces cerevisiae L.). *Biotechnology and Bioprocess Engineering,* 16**,** 1262-1272.

Ramontja, T., Eberle, D., Coetzee, H., Schwarz, R. & Juch, A. Critical challenges of acid mine drainage in South Africa's Witwatersrand gold mines and mpumalanga coal fields and possible research areas for collaboration between South African and German researchers and expert teams. The New Uranium Mining Boom: Challenge and Lessons Learned, 2011. 389-400.

Romero, F. M., Núñez, L., Gutiérrez, M. E., Armienta, M. A. & Ceniceros-Gómez, A. E. 2011. Evaluation of the potential of indigenous calcareous shale for neutralization and removal of arsenic and heavy metals from acid mine drainage in the Taxco mining area, Mexico. *Archives of Environmental Contamination and Toxicology,* 60**,** 191-203.

Sahoo, P. K., Kim, K., Equeenuddin, S. M. & Powell, M. A. 2013. Current approaches for mitigating acid mine drainage. *Reviews of environmental contamination and toxicology,* 226**,** 1-32.

Sheoran, A. S. & Sheoran, V. 2006. Heavy metal removal mechanism of acid mine drainage in wetlands: A critical review. *Minerals Engineering,* 19**,** 105-116.

Sheoran, V., Sheoran, A. S. & Choudhary, R. P. 2011. Biogeochemistry of acid mine drainage formation: A review. *Mine Drainage and Related Problems.* 119-154.

Sibanda, Z., Amponsah-Dacosta, F. & Mhlongo, S. E. 2013. Characterization and evaluation of magnesite tailings for their potential utilization: A case study of nyala magnesite mine, Limpopo province of South Africa. *ARPN Journal of Engineering and Applied Sciences,* 8**,** 606-613.

Simate, G. S. & Ndlovu, S. 2014. Acid mine drainage: Challenges and opportunities. *Journal of Environmental Chemical Engineering,* 2**,** 1785-1803.

Skousen, J., Mcdonald, L., Mack, B. & Demchak, J. Water quality from above-drainage underground mines over a 35-year period. 7th International Conference on Acid Rock Drainage 2006, ICARD - Also Serves as the 23rd Annual Meetings of the American Society of Mining and Reclamation, 2006. 2044-2054.

Somerset, V., Klink, M., Petrik, L. & Iwuoha, E. 2011. Neutralisation of acid mine drainage with fly ash in South Africa. *Mine Drainage and Related Problems.* 211-226.

Torres, E. & Auleda, M. 2013. A sequential extraction procedure for sediments affected by acid mine drainage. *Journal of Geochemical Exploration,* 128**,** 35-41.

Toulkeridis, T., Peucker-Ehrenbrink, B., Clauer, N., Kröner, A., Schidlowski, M. & Todt, W. 2010. Pb-Pb age, stable isotope and chemical composition of Archaean magnesite, Barberton Greenstone Belt, South Africa. *Journal of the Geological Society,* 167**,** 943-952.

Tutu, H., Mccarthy, T. S. & Cukrowska, E. 2008. The chemical characteristics of acid mine drainage with particular reference to sources, distribution and remediation: The Witwatersrand Basin, South Africa as a case study. *Applied Geochemistry,* 23**,** 3666-3684.

Van Deventer, H. & Cho, M. A. 2014. Assessing leaf spectral properties of phragmites australis impacted by acid mine drainage. *South African Journal of Science,* 110.

Zammit, C. M., Mutch, L. A., Watling, H. R. & Watkin, E. L. J. 2011. The recovery of nucleic acid from biomining and acid mine drainage microorganisms. *Hydrometallurgy,* 108**,** 87-92.

Zhang, M. 2011. Adsorption study of Pb(II), Cu(II) and Zn(II) from simulated acid mine drainage using dairy manure compost. *Chemical Engineering Journal,* 172**,** 361-368.

Zhao, H., Xia, B., Qin, J. & Zhang, J. 2012. Hydrogeochemical and mineralogical characteristics related to heavy metal attenuation in a stream polluted by acid mine drainage: A case study in Dabaoshan Mine, China. *Journal of Environmental Sciences,* 24**,** 979-989.

Zheng, Y. J., Peng, Y. L. & Li, C. H. 2011. Treatment of acid mine drainage by two-step neutralization. *Zhongnan Daxue Xuebao (Ziran Kexue Ban)/Journal of Central South University (Science and Technology),* 42**,** 1215-1219.

Zipper, C. E. & Skousen, J. G. 2010. Influent water quality affects performance of passive treatment systems for acid mine drainage. *Mine Water and the Environment,* 29**,** 135-143.

Zvimba, J. N., Mathye, M., Vadapalli, V. R. K., Swanepoel, H. & Bologo, L. 2013. Fe(II) oxidation during acid mine drainage neutralization in a pilot-scale sequencing batch reactor. *Water Science and Technology,* 68**,** 1406-1411.

Zvimba, J. N., Mulopo, J., Bologo, L. T. & Mathye, M. 2012. An evaluation of waste gypsum-based precipitated calcium carbonate for acid mine drainage neutralization. *Water Science and Technology,* 65**,** 1577-1582.

CHAPTER FOUR

Paper 2:

This paper addresses the efficiency of ball milled South African bentonite clay for remediation of acid mine drainage

This chapter is devoted to achieve the undermentioned objective which is:

- Evaluation of the treatment of AMD using vibratory ball milled bentonite clay in batch tests, and exploration of the interaction chemistry thereof, and the processed water quality

CHAPTER FOUR

Efficiency of ball milled South African bentonite clay for remediation of acid mine drainage

[*]Masindi Vhahangwele[1,3], Gitari W.Mugera[1], Tutu Hlanganani[2], Debeer Marinda[4]

[1]Environmental Remediation and Water Pollution Chemistry Research Group, Department of Ecology and Resources Management, School of Environmental Science, University of Venda, P/bag X5050, Thohoyandou, 0950, South Africa, Tel: +2712 841 4107, VMasindi@csir.co.za
[2]Molecular Sciences Institute, School of Chemistry, University of the Witwatersrand, P/Bag X4, WITS, 2050, Johannesburg, South Africa,
[3]CSIR (Council of Scientific and Industrial Research), Built Environment, Building Science and Technology (BST), P.O Box 395, Pretoria, 0001, South Africa,
[4]DST/CSIR National Centre for Nano-Structured Materials, Council for Scientific and Industrial Research, P.O Box 395, Pretoria, 0001, South Africa

Abstract

The feasibility of using vibratory ball milled South African bentonite clay for neutralisation and attenuation of inorganic contaminants from acidic and metalliferous mine effluents has been evaluated. Treatment of acid mine drainage (AMD) with bentonite clay was done using batch laboratory assays. Parameters optimised included contact time, adsorbent dosage and adsorbate concentration. Ball milled bentonite clay was mixed with simulated AMD at specific solid: liquid (S/L) ratios and equilibrated on a table shaker. Contact of AMD with bentonite clay led to an increase in pH and a significant reduction in concentrations of metal species. At constant agitation time of 30 mins, the pH increased with the increase in dosage of bentonite clay. Removal of Mn^{2+}, Al^{3+}, and Fe^{3+} was greatest after 30 min of agitation. The adsorption and precipitation affinity obeyed the sequence: Fe > Al > Mn > SO_4^{2-}. The pH of reacted AMD was greater than 6. Bentonite clay showed high adsorption capacities for Al and Fe at concentration less than 500 mg L^{-1}, while the capacity for Mn was lower. Adsorption efficiency for sulphate was > 50%. Adsorption kinetics revealed that the suitable kinetic model describing data was pseudo-second-order hence confirming chemisorption. Adsorption isotherms indicated that removal of metals fitted the Langmuir adsorption isotherm for Fe and SO_4^{2-} and the Freundlich adsorption isotherm for Al and Mn, respectively. Gibbs free energy model predicted that the reaction is not spontaneous in nature for Al, Fe and Mn except for SO_4^{2-}. Ball-milled bentonite clay showed an excellent capacity

in neutralising acidity and lowering the levels of inorganic contaminants in acidic mine effluents.

Keywords: acid mine drainage; bentonite clay; ball-milling; neutralization; heavy metals; adsorption

4.1 Introduction

Exposure of sulphide bearing minerals to water and oxygen during and following mining activities accelerates the formation of acid mine drainage (AMD) which is very acidic and metalliferous. The acidity in AMD promotes the leaching of toxic chemical species from the surrounding geology. Due to its acidic nature and high loads of toxic chemical species, AMD has high electrical conductivity (EC) and total dissolved solids (TDS) concentration which are considerably above the recommended limits for effluents to be discharged into rivers. Thus mine effluent needs to be contained and managed prior to release to the environment as an initial step in preventing environmental degradation (Hince and Robbins, 2003, Johnson and Hallberg, 2005, Akcil and Koldas, 2006).

Discharge of AMD to the environment can reduce the ability of any ecosystem to support life. It lowers water quality rendering it unfit for defined uses such as for domestic and agricultural purposes. It also leads to iron sedimentation in aquatic ecosystems due to precipitation of iron hydroxide (yellow boy sludge). The suspended flocs also lead to reduced hunting abilities of fish due to poor visibility in water bodies (Simate and Ndlovu, 2014). Toxic chemical species in AMD pose hazards to terrestrial and aquatic organisms (Netto et al., 2013). Acidity in water leads to the migration of certain species less tolerant to acidic conditions affecting the integrity of the ecosystem to support life due to reduced biodiversity (Bortnikova et al., 2001, DeNicola and Stapleton, 2002, Achterberg et al., 2003, Dale Marsden et al., 2003, Mapanda et al., 2007, Mohapatra et al., 2011, Anawar, 2013, Yesilnacar and Kadiragagil, 2013, Park et al., 2014, Simate and Ndlovu, 2014). This has emphasised the need to develop pragmatic solutions to treat AMD by neutralizing the acidity and removing heavy loads of dissolved metals and sulphate.

Due to their high surface areas, cation-exchange capacity (CEC), swelling ability, low cost, abundance and versatility, clays have received much attention for treatment of contaminated waters (Sen Gupta and Bhattacharyya, 2012). High surface area enables bentonite clay to efficiently scavenge chemical species from wastewater (Sen Gupta and Bhattacharyya, 2014).

High cation-exchange capacity enables the clay to remove low-density chemical species such as Na, K, Ca and Mg from clay matrices through isomorphous substitution by high density poly-cationic species. High swelling ability promotes high retention of polluted water within clay interlayers leading to high exchange capacities (Bethke et al., 1986, Konta, 1995, Potgieter et al., 2006, Bedelean et al., 2010, Wu et al., 2011, Zhang et al., 2011, Vicente et al., 2013, Zhou and Keeling, 2013).

South Africa has large deposits of bentonite clay that is projected for extraction in the next 60 years, if the demand does not increase (Gitari, 2014). Gitari (2014) has evaluated the ability of pestle-and-mortar milled bentonite clay for the attenuation of metal species concentrations in synthetic AMD and gold-mine tailings leachates. Low surface area, poor adsorption efficiencies and insignificant increases in pH were observed. Consequently, mortar-and-pestle milling was shown to be an inefficient milling procedure for clay minerals (Dellisanti and Valdré, 2005, Dukić et al., 2015). Literature reports show that ball-milling of clays leads to fragmentation, distortion, breakage of crystalline networks and cobwebs, and particle size reduction followed by an increase of the surface area, exfoliation of particles and amorphization. Thus enhancing the contaminants removal abilities of ball milled bentonite clay (Kumrić et al., 2013, Dukić et al., 2015, Đukić et al., 2015a, Đukić et al., 2015b, Zhuang et al., 2015). The present study was designed to demonstrate the ability of ball-milled bentonite clay to neutralize and attenuate toxic chemical species concentrations in AMD. It also compared the efficiencies of the ball-milled clay to mortar-milled clay for surface area enhancement and metal species removal efficiency. Following a study conducted by Gitari (2014), the author recommended the testing of bentonite clay using AMD from different sources since the author had used gold-mine tailings leachates and synthetic AMD. The present study also investigated some physicochemical properties of ball-milled clay before and after contact with gold-mine AMD.

4.2 Materials and methods

4.2.1 Sampling

Bentonite clay was supplied by ECCA Holdings (Pty) Ltd, Cape Bentonite mine (Cape Town, South Africa). Raw AMD was collected from a disused gold-mine shaft near Krugersdorp, Gauteng Province, South Africa.

4.2.2 Preparation of bentonite clay

The raw bentonite was washed by soaking in ultra-pure water and draining after 10 minutes. The ultrapure water used was such that it covered the entire sample in the beaker and was allowed to overflow. The procedure was repeated four times. The washed bentonite was dried at 105°C for 24 h. The dried samples were milled into a fine powder (Retsch RS 200 ball-mill, Fritsch, Germany) and sieved (< 32 µm particle size). The ball-mill was cleaned with uncontaminated quartz after milling each sample to avoid cross-contamination.

4.2.3 Synthetic acid mine drainage

Synthetic acid mine drainage (SAMD) was used for experimentation as real AMD is extremely difficult to work with in optimization due to oxidation and hydrolysis on exposure to the open leading rapid changes in chemistry. A simplified solution containing the major ions found in AMD was prepared as described by Tutu et al. (2008) as shown in Table 4.1.

Table 4.1: Synthetic acid mine drainage used in this study

Salt dissolved	Species	Concentration (mg L^{-1})
$Al_2(SO_4)_3.18H_2O$	Al^{3+}	200
$Fe_2(SO_4)_3.H_2O$	Fe^{3+}	2000
$MnCl_2$	Mn^{2+}	100
H_2SO_4 and Al and Fe salts	SO_4^{2-}	6000

AMD was simulated by dissolving the following quantities of salts in 1000 mL of Milli-Q ultra-pure water (18MΩ), 7.48 g $Fe_2(SO_4)_3.H_2O$, 2.46 g $Al_2(SO_4)_3 \cdot 18H_2O$, and 0.48 g $MnCl_2$ to give a solution of 2000 mg L^{-1} Fe^{3+}, 200 mg L^{-1} Al^{3+} and 200 mg L^{-1} Mn^{2+}.and 5 mL of 0.05 M H_2SO_4 was added to make up the SO_4^{2-} concentration to 6000 mg/L. The salts were dissolved in 1000 mL volumetric flasks. Prior to the addition of ferric sulphate, 5 mL of 0.05 M of H_2SO_4 was added to ensure a pH < 3, in order to prevent immediate precipitation of ferric hydroxide. For the batch experiments, the working solutions were prepared from these stock solutions by appropriate dilutions

4.2.4 Characterization of aqueous solution

Total Dissolved Solids (TDS), pH, and Electrical Conductivity (EC) were monitored using a CRISON MM40 portable pH/EC/TDS/Temperature multimeter probe. Aqueous samples were analysed using ICP-MS (7500ce, Agilent, Alpharetta, GA, USA) for metal cations and sulphate concentration was determined using ion-chromatography (IC; 850 Professional IC, Metrohm, Herisau, Switzerland). The accuracy of the analysis was checked by simultaneous analysis of water standards [National Institute of Standards and Technology, (NIST)].

4.2.5 Mineralogical, chemical and microstructural characterisation

Mineralogical composition of bentonite clay and resulting solid residues was determined using XRD (Philips PW 1710 Diffractometer; graphite secondary monochromatic source). Elemental composition was determined using XRF (Thermo Fisher ARL-9400 XP+ Sequential XRF equipped with WinXRF software). Morphology was determined using SEM-EDS (JOEL JSM – 840, Hitachi, Tokyo, Japan). Functional groups were determined using Perkin-Elmer Spectrum 100 Fourier Transform Infrared Spectrometer (FTIR) equipped with a Perkin-Elmer Precisely Universal Attenuated Total Reflectance (ATR) sampling accessory equipped with a diamond crystal. Surface area and porosity were determined using BET analysis (Micromeritics Tristar II, Norcross, GA, USA). The cation-exchange capacity of bentonite clay and AMD-bentonite clay complex was determined using the ammonium acetate method (Gitari, 2014).

4.2.6 Experimental procedures

To determine the optimum conditions for AMD treatment with milled bentonite, the following operational parameters were optimized: shaking time, adsorbent dosage and adsorbate concentration. All experiments were performed in triplicate and the data averaged.

4.2.6.1 Effect of time

Portions (100 mL) each of simulated AMD were pipetted into 250 mL flasks into which 1 g portions of bentonite clay were added. The mixtures were equilibrated for 1, 5, 10, 20, 30, 60, 180, and 360 minutes (Stuart reciprocating shaker, 250 rpm). After shaking, the mixtures were filtered (0.45 µm pore nitrocellulose filter membrane). The filtrates were preserved by

adding two drops of concentrated HNO_3 to prevent aging and immediate precipitation of Al, Fe and Mn, and refrigerated at 4ºC prior to analysis by ICP-MS. The respective pHs of samples before and after agitation were recorded. A separate set was left un-acidified for sulphate analysis.

4.2.6.2 Effect of dosage

Portions of 100 mL each of simulated AMD were pipetted into 250 mL flasks and varying masses (0.1 - 8 g) of bentonite clay were added to each flask, respectively. The mixtures were agitated on a shaker for 30 min at 250 rpm. After shaking, the pH, metal and sulphate contents were determined as described in the preceding section.

4.2.6.3 Effect of adsorbate concentration

To investigate the effects of adsorbate concentration on reaction kinetics, several dilutions were made from the simulated AMD stock solution. The pHs of the simulated AMD were not adjusted. The capacity of the adsorbent to neutralize and attenuate metal concentrations from aqueous solution was then assessed by increasing metal concentrations. Solutions of 100 mL each containing 100-2000 mg/L Fe^{3+}; 10-200 mg/L Al^{3+}; 5-100 mg/L Mn^{2+} and 300 - 6000 mg/L SO_4^{2-} were prepared in triplicate and 2 g of bentonite clay was added to each sample container. The mixtures were equilibrated by shaking for 30 minutes. The initial pH of the working solutions was < 3. The pH, metal and sulphate contents were determined as described in the preceding section.

4.2.6.4 Treatment of field acid mine drainage at optimized conditions

Field AMD samples were treated at established optimized conditions in order to assess the effectiveness of bentonite clay treatment. The pH and metal contents were determined as described previously while a separate set of samples was left un-acidified for SO_4^{2-} analysis. Metals were assayed using ICP-MS. The pH, EC and TDS of samples were measured. The resultant solid residue, after contact with AMD, was characterized in order to gain an insight into the fates of chemical species after bentonite treatment.

4.2.7 Calculation of extent of metal species and sulphate removal and adsorption capacity

Computation of % removal and adsorption capacity was done using equations (4.1) and (4.2).

Percentage removal (%) $= \left(\frac{C_i - Ce}{C_i}\right) \times 100$ (4.1)

Adsorption capacity $(q_e) = \frac{(C_i - C_e)V}{m}$ (4.2)

Where: C_i = initial concentration (mg/L); Ce = equilibrium ion concentration (mg/L), V = volume of solution (L); m = mass of bentonite clay (g).

4.2.8 Adsorption Kinetics

Adsorption kinetics was done using pseudo-first-order, second order kinetics and Intraparticle diffusion model (Falayi and Ntuli, 2014).

4.2.9 Adsorption isotherms

Adsorption isotherms were plotted using the equations for Langmuir and Freundlich adsorption models (Falayi and Ntuli, 2014).

An error analysis is required to evaluate the fit of the adsorption isotherms to experimental data. In the present study, the linear coefficient of determination (R^2) was employed for the error analysis. The linear coefficient of determination was calculated by using the equation 4.3:

$$r = \frac{n\sum xy - (\sum x)(\sum y)}{\sqrt{n(\sum x^2) - (\sum x)^2} - \sqrt{(\sum y^2) - (\sum y)^2}} \quad (4.3)$$

Theoretically, the R^2 value varies from 0 to 1. The R^2 value shows the variation of experimental data as explained by the regression equation. In most studies, the coefficient of determination, R^2, was applied to determine the fitness of the model to predict the adsorption behavior and mechanisms.

4.3 Results and discussion

4.3.1 Optimization of chemical species removal conditions

4.3.1.1 Effect of contact time

Variation of Al^{3+}, Fe^{3+}, Mn^{2+}, SO_4^{2-} concentrations and pH levels with an increase in equilibration time is shown in **Figure 4.1**.

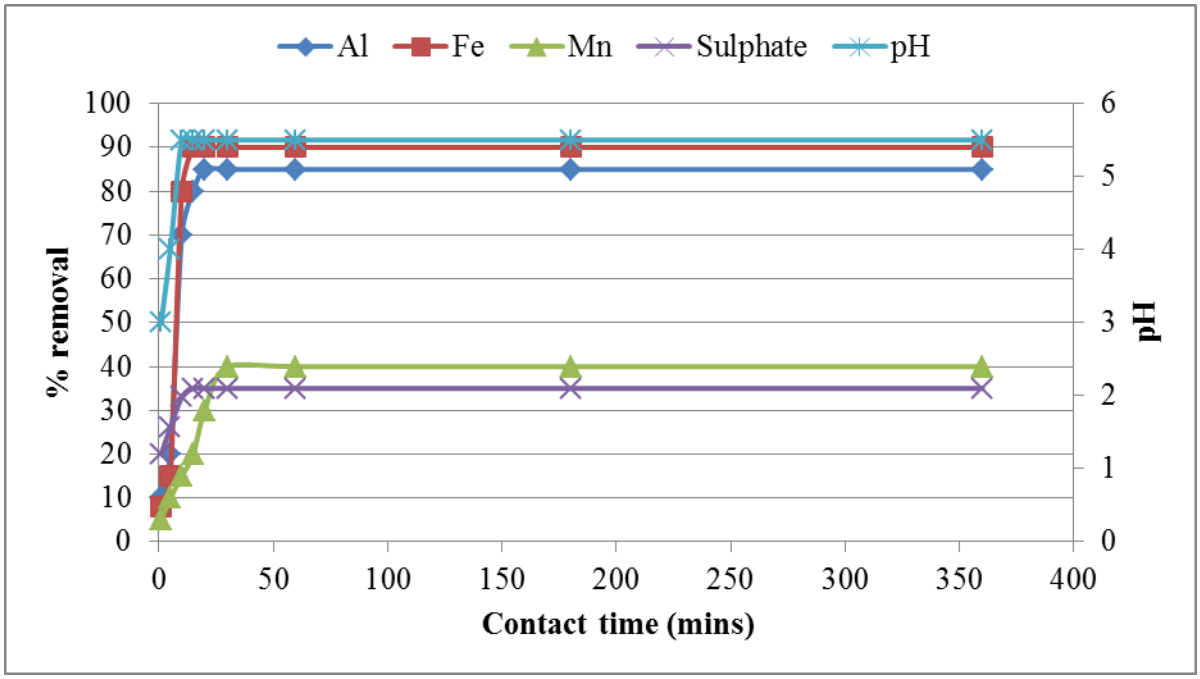

Figure 4.1, Appendix B, Table B 5: Effect of equilibration time on neutralization and removal of Al^{3+}, Fe^{3+}, Mn^{2+}, and SO_4 (Conditions: pH < 3, 2000 mg/L Fe^{3+}, 200 mg/L Al^{3+}, 100 mg/L Mn^{2+}, 6000 mg/L SO_4^{2-} , 1 g bentonite clay (32 µm), 100 mL solution, 1:100 S/L ratios, 250 rpm shaking, 26ºC).

As shown in **Figure 4.1**, there was an increase in pH with an increase in contact time. From 1 – 30 mins, the pH of the solution increased from 3 to > 5.5. This pH is adequate for precipitation of Al and Fe from aqueous systems. Thereafter, no significant change in pH was observed. Fe^{3+} was observed to decrease with an increase in reaction time. After 30 min, > 90% of Fe was removed from the aqueous system. Removal of Fe may be attributed to an increase in pH that promotes the precipitation of $Fe(OH)_3$. Al removal was also observed to decrease with an increase in agitation time. Greater than 80% was removed before 30 min of shaking. Thereafter, no significant removal in Al was observed. Mn removal increased with increase in contact time. Approximately 50% and 30% of Mn and sulphate respectively were removed with an increase in contact time. From 1 – 30 min, the removal rate was very rapid. After 30 min no further significant removal was observed indicating that the reaction had reached a steady state or the clay surfaces were saturated with pollutants from the SAMD. Though removal efficiencies of Al, Fe, Mn and sulphate varied with time, the optimum adsorption time was observed to be 30 min. This was rapid removal compared to the 60 min exhibited by mortar-and-pestle milled bentonite clay (Gitari, 2014). Thus, 30 mins was the optimum time under these laboratory conditions and was applied in subsequent batch

experiments. The adsorption affinity varied as follow: Fe>Al> sulphate> Mn. Though, adsorption was the principal mechanisms, from the results, it can be concluded that both adsorption and precipitation may be governing the removal of toxic chemical species in aqueous system.

4.3.1.2 Adsorption kinetics

The effect of contact time on removal of chemical species from aqueous solution was evaluated using different kinetic models to reveal the nature of the adsorption process and rate limiting processes. A Lagergren pseudo first order kinetic model is a well-known model that is used to describe mechanisms of metal species adsorption by an adsorbent. It can be written as follow (Albadarin et al., 2012, Iakovleva et al., 2015):

$$ln(q_e - q_t) = ln\, q_e - k_1 t \quad (4.5)$$

Where k_1 (min^{-1}) is the pseudo-first-order adsorption rate coefficient and q_e and q_t are the values of the amount adsorbed per unit mass at equilibrium and at time t, respectively. The experimental data was fitted by using the pseudo-first-order kinetic model by plotting $\ln(q_e - q_t)$ vs. t, and the results are shown in **Table 4.5.** The pseudo-first-order was applied and it was found to poorly converge with the experimental data, and the correlation coefficients were less than 0.33. Moreover, the calculated amounts of Mn, Al, Fe and sulphate ions adsorbed by ball milled bentonite clay [qe, calc (mgg-1)] were less than the experimental values [$q_{e,\,exp}$ (mgg^{-1})] (**Table 4.5**). The finding indicated that the Lagergren pseudo-first-order kinetic model is inappropriate to describe the adsorption of Mn, Al, Fe and sulphate ions from aqueous system by ball milled bentonite clay.

The pseudo-second-order kinetic model is another kinetic model that is widely used to describe the adsorption process from an aqueous solution. The linearized form of the pseudo-second-order rate equation is given as follow:

$$\frac{t}{q_r} = \frac{1}{k_2 q_e^2} + \frac{t}{q_e} \quad (4.6)$$

Where k_2 [g(mg min^{-1})] is the pseudo-second-order adsorption rate constant and q_e and q_t are the values of the amount adsorbed per unit mass at equilibrium and at time t, respectively. An application of the pseudo-second-order rate equation for adsorption of chemical species to bentonite clay matrices portrayed a good fit $\boldsymbol{R^2}$ value with experimental data (**Figure 4.1 and**

Table 4.2). The results obtained confirms that pseudo-second-order model is the more suitable kinetic model to describe adsorption of Mn, Al, Fe and sulphate by ball milled bentonite clay from aqueous system. Moreover, this also confirms that the mechanism of metals species removal from aqueous solution is chemisorption. Different kinetic model parameters for adsorption of Mn, Al, Fe and sulphate on ball milled bentonite clay are shown in **Table 4.2**. Note the theoretical adsorption capacity is close to the experimental adsorption capacity further confirming that this model describes the adsorption data. The overall kinetics of the adsorption from solutions may be governed by the diffusional processes as well as by the kinetics of the surface chemical reaction. In diffusion studies, the rate is often expressed in terms of the square root time

$$q_t = k_{id} t^{1/2} + C_i \qquad (4.7)$$

Where k_{id} (mgg^{-1} $min^{-1/2}$) is the Intraparticle diffusion coefficient (slope of the plot of q_t vs. $t^{1/2}$) and C_i is the Intraparticle diffusion rate constant. The results also showed that the Intraparticle diffusion model by Webber and Morris 1963 was not applicable for the present process due to lower correlation coefficients. The R^2 showed the good fit however, it did not suffice the pseudo-second-order kinetics. Different kinetic model parameters for adsorption of Mn, Al, Fe and sulphate on ball milled bentonite clay are shown in **Table 4.2**.

Table 4.2: Different kinetic model parameters for adsorption of Mn, Al, Fe and sulphate on ball milled bentonite clay.

Pseudo first order kinetic model				
Element	**$q_{e,\ exp}$ (mgg^{-1})**	**$q_{e,\ calc}$ (mgg^{-1})**	**K_1 ($mgg^{-1}\ min^{-1}$)**	**R^2**
Mn	4	-10.9	0.2	0.89
Al	17	-12.9	0.2	0.76
Fe	180	-21.5	0.2	0.78
Sulphate	210	-21.6	0.2	0.78
Pseudo second order kinetic model				
Element	**$q_{e,\ exp}$ (mgg^{-1})**	**$q_{e,\ calc}$ (mgg^{-1})**	**K_2 ($mgg^{-1}\ min^{-1}$)**	**R^2**
Mn	4	4.14	0.32	0.997
Al	17	17.27	0.48	0.998
Fe	180	185.19	0.41	0.995
Sulphate	210	208.33	1.44	1
Intraparticle diffusion model				
Element	**$q_{e,\ exp}$ (mgg^{-1})**	**C_i (mgg^{-1})**	**K_{id} ($mgg^{-1}\ min^{-1/2}$)**	**R^2**
Mn	4	0.389	0.85	0.98
Al	17	-3.87	4.9	0.91
Fe	180	-52.2	56.1	0.86
Sulphate	210	96.01	28.07	0.94

The coefficient of determination and regression analysis for adsorption of Mn, Al, Fe and sulphate on ball milled bentonite clay using pseudo-first-order, pseudo-second-order and Intraparticle diffusion models are shown in **Figure 4.2, 4.3 and 4.4** respectively.

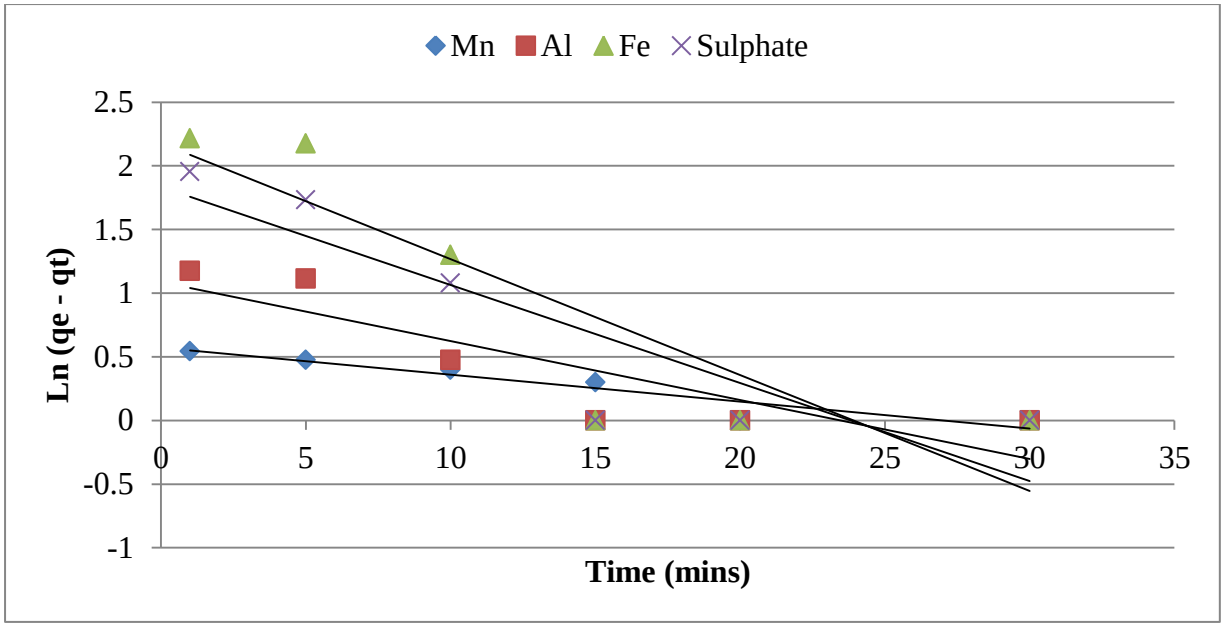

Figure 4.2: Pseudo-first-order plots of Mn, Al, Fe and sulphate ions adsorbed on ball milled bentonite clay

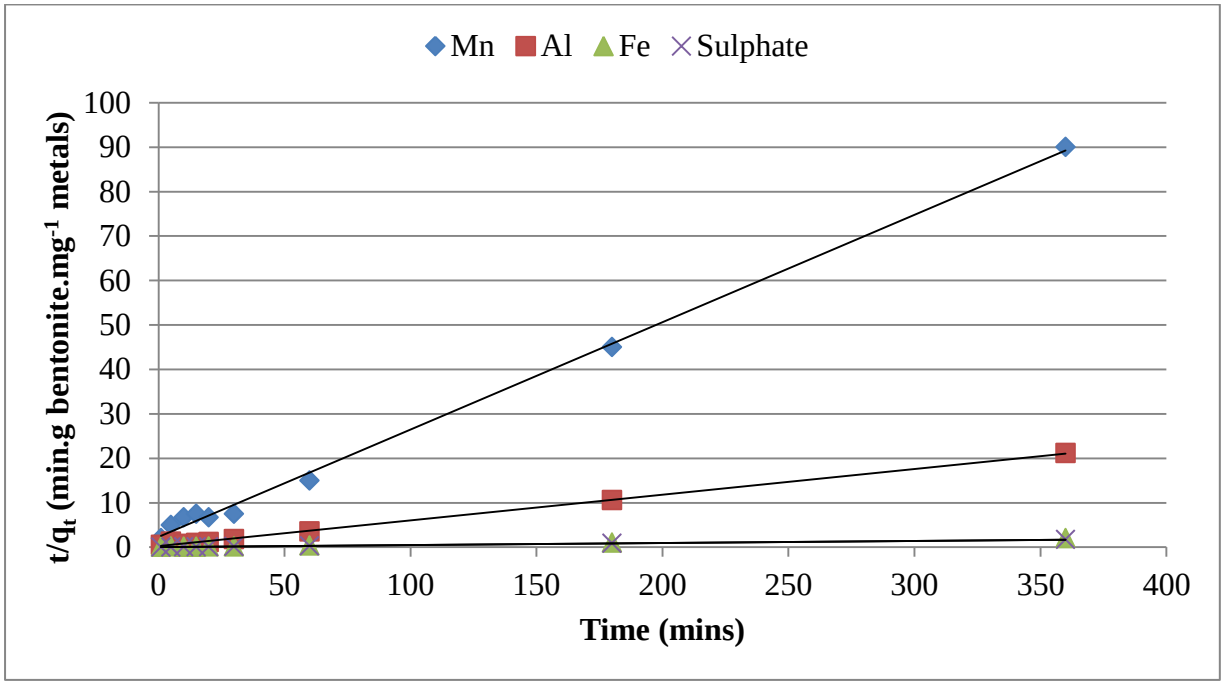

Figure 4.3: Pseudo-second-order plots of Mn, Al, Fe and sulphate ions adsorbed on ball milled bentonite clay

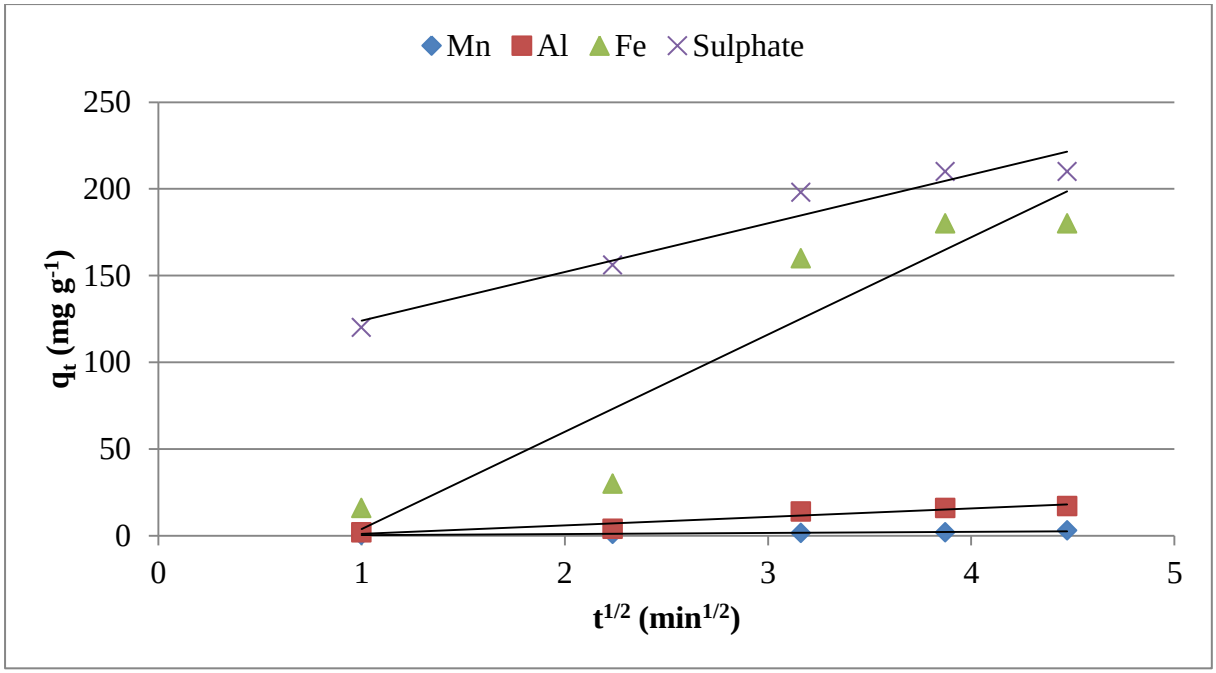

Figure 4.4: Intraparticle diffusion plots of Mn, Al, Fe and sulphate ions adsorbed on ball milled bentonite clay

4.3.1.3 Effect of bentonite dosage

Variation of Al^{3+}, Fe^{3+}, Mn^{2+}, SO_4^{2-} and pH levels with increases in adsorbent dosage are shown in **Figure 4.5**.

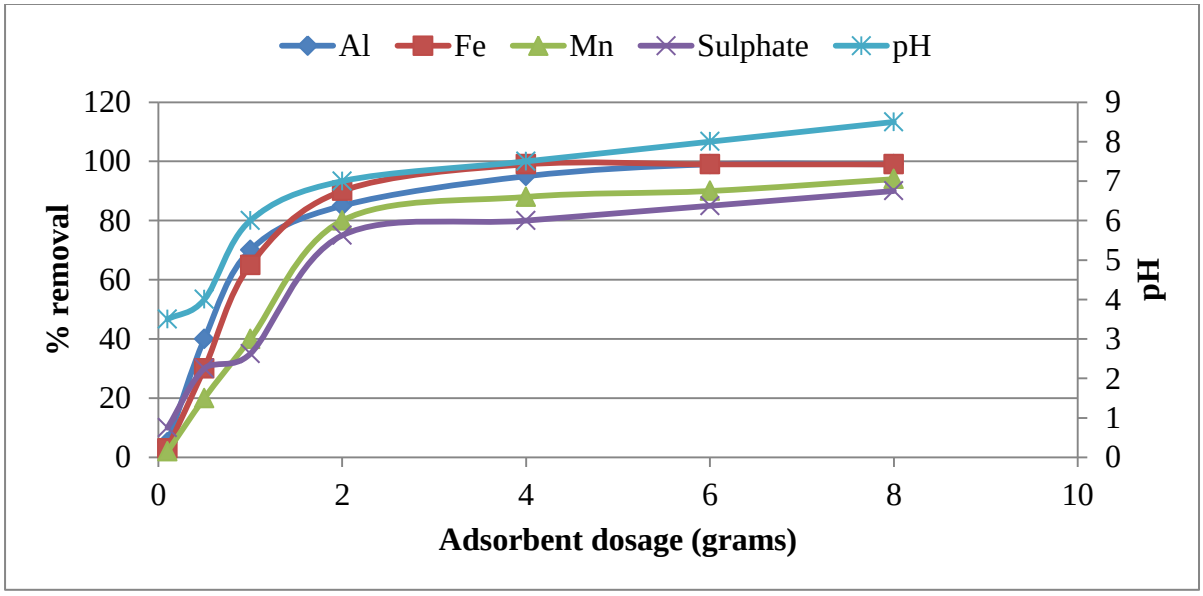

Figure 4.5, Appendix B, Table B 6: Effect of adsorbent dosage on neutralization and removal of Al^{3+}, Fe^{3+}, Mn^{2+} and sulphate (Conditions: pH < 3, 100 mL multicomponent

solution, 2000 mg/L Fe^{3+}, 200 mg/L Al^{3+}, 100 mg/L Mn^{2+}, 6000 mg/L SO_4^{2-} , 30 min, 32 µm, 250 rpm shaking, 26ºC).

The effect of adsorbent dosage for removal of inorganic contaminants in AMD using ball-milled bentonite clay was evaluated at 30 min of equilibration. As shown in **Figure 4.5**, the pH of the solution increased with increase in bentonite clay dosage. The pH increased from 3 to 8.5 making it suitable for removal of the majority of contaminants in synthetic mine effluent. The increase in pH was attributed to the dissolution of alkali and alkaline earth metals species from bentonite clay matrices as shown by XRF. The release of basic alkaline earth metals due to ion exchange by polymeric species of Al^{3+} and Fe^{3+} may also contribute to an increase in pH of the supernatants. Removal efficiencies of metal species also increased with increases in bentonite clay dosage. The adsorption and precipitation affinity at 2 g followed this trend: Fe > Al > Mn > SO_4^{2-}. The overall removal efficiency was > 80% for all the chemical species. High removal efficiencies for metal species was also attributed to the precipitation of Fe (pH > 4) and Al (> 5), ion-exchange with base cations as shown by XRF (**Table 4.3**), co-precipitation with metals during precipitation and adsorption on bentonite clay matrices. An increase in pH may be due to dissolution of traces of calcite and silicates (**Equation 4.4**) and attenuation of sulphate concentration as shown by XRD and ion exchange of Mg, Ca, K and Na as revealed by XRF and EDS may also contribute to an increase in pH of the product water. Silicate will react with acidity in AMD through ion exchange and lead to an increase in pH.

$$\equiv \mathrm{SiOH} \leftrightarrow \mathrm{SiO^-} + \mathrm{H^+} \quad (4.8)$$

$$\equiv \mathrm{SiOH} + \mathrm{Ca^{2+}} \leftrightarrow = \mathrm{SiOCa} + \mathrm{H^+} \quad (4.9)$$

$$\equiv \mathrm{SiOCa} + \mathrm{M^{e+}} + 2\mathrm{HOH} \rightarrow = \mathrm{SiOM} + \mathrm{Ca^{2+}} + 2\mathrm{OH^-} \quad (4.10)$$

Therefore, 2 g was taken as the optimum dosage for removal of contaminants in SAMD, under these laboratory conditions and was applied in subsequent experiments. The optimum dosage (20g L^{-1}) recorded in this study is comparable to dosage that were used by conventional technologies for remediation of AMD such as cryptocrystalline magnesite (10 g L^{-1}) (Masindi et al., 2014), crystalline magnesite (10 g L^{-1}) (Bernier, 2005), pestle and mortar milled bentonite clay (10 g L^{-1}) (Gitari, 2014), limestone (10 g L^{-1}) , dolomite (40 g L^{-1}) (Potgieter-Vermaak et al., 2006) and fly ash (500g L^{-1}) (Gitari et al., 2008). This signifies that the present technology can be employed as a polishing technology post the use of pre-treatment technology for remediation of AMD.

4.3.1.4 Adsorbate concentration

Variation of Al^{3+}, Fe^{3+}, Mn^{2+}, SO_4^{2-} and adsorption capacity (q) with an increase in initial species concentration are shown in **Figure 4.6**.

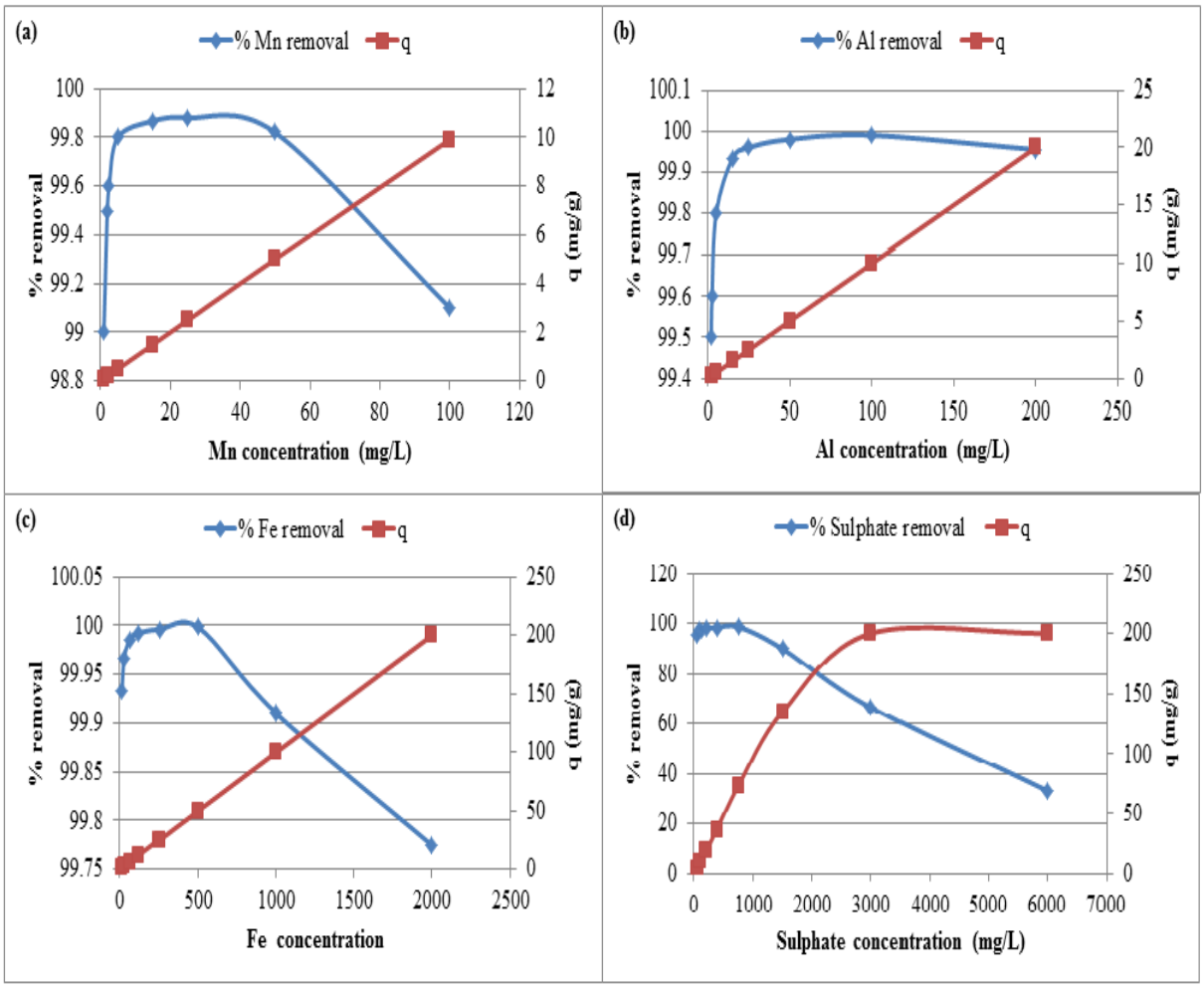

Figure 4.6, Appendix B, Table B 7: Effect of initial species concentration and adsorption capacity with increasing species concentration removal of Al^{3+}, Fe^{3+}, Mn^{2+}, and Sulphate (Conditions: pH <3, 30 min, 2 g of bentonite clay, 2: 100 S/L ratios, 100 mL multicomponent solution, 32 µm particle size, 250 rpm shaking, 26º C).

As shown in **Figure 4.6**, as the chemical species concentrations increased, the removal efficiency of contaminants decreased and the adsorption capacity increased. When the concentration is low, more surfaces are available to scavenge all the contaminants that are present and when the concentration is high, the adsorption surfaces become fewer for pollutants to be adsorbed. At high adsorbate concentration the adsorption sites becomes the limiting factor. At low pollutant concentrations, bentonite clay showed good adsorption of

Mn^{2+}, Al^{3+}, Fe^{3+} and SO_4^{2-} from aqueous solution. For Mn^{2+}, bentonite clay showed that > 99% removal efficiency can be achieved for concentrations ranging up to 100 mg/L. For Al^{3+}, > 99% removal efficiency can be achieved for concentrations up to 200 mg/L. For Fe^{3+}, > 99% removal efficiency can be achieved for concentrations ranging up to 2000 mg/L. For SO_4^{2-}, > 60% removal efficiency is possible for concentrations ranging up to 3000 mg/L. Removal of Mn, Al and Fe occurs by precipitation and formation of various metal bearing phases due to an increase in pH, co-precipitation with metals to form hydrocomplexes and ion-exchange with a release of Na, K, Mg and Ca ions to solution. Removal of sulphate takes place by adsorption, formation of hydrocomplexes, precipitation and co-precipitation as oxyhydrosulphates as shown by SEM-EDS. The variation of pH profile with varying concentration of iron is shown in **Figure 4.7.**

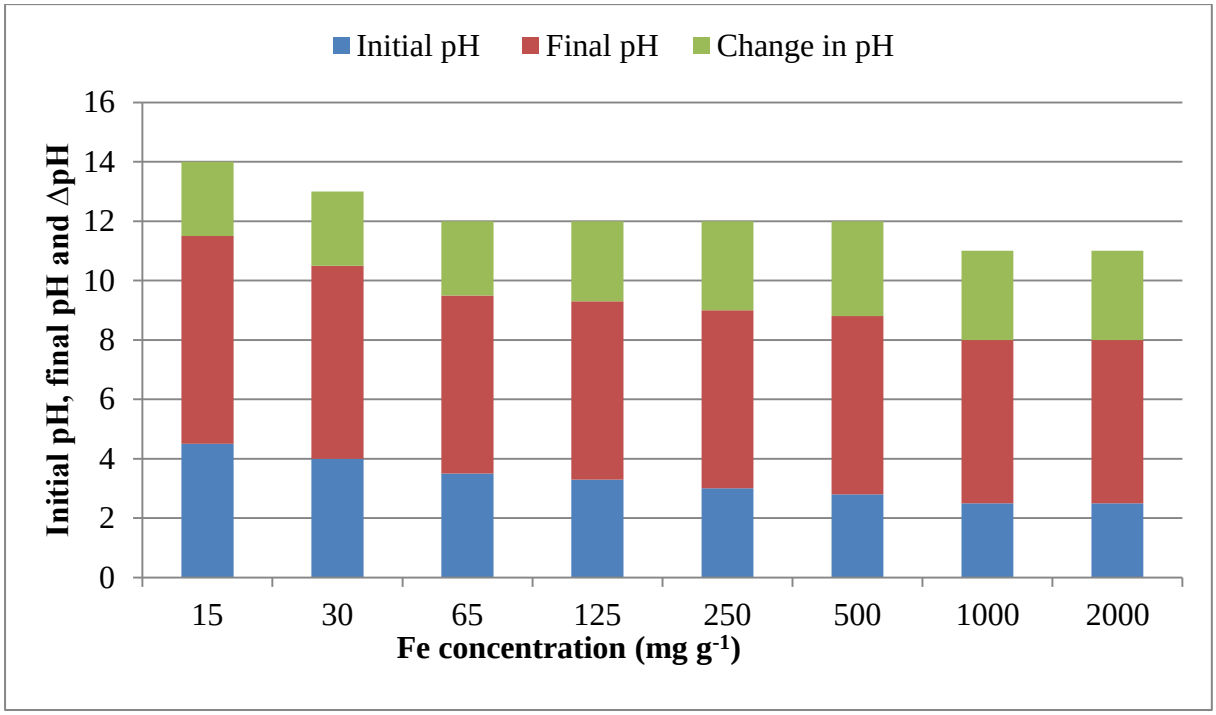

Figure 4.7: Variation of pH gradient with varying sulphate concentrations.

As shown in **Figure 4.7**, a drastic increase in pH was observed at varying Fe concentrations. An increase in pH was attributed to the possible dissolution of calcite as shown by XRD and base cations as shown by XRF from bentonite clay matrices. The decrease in pH with an increase in adsorbate concentration is due to hydrolysis of metal species cations leading to release of H^+. The hydrolysis of $Fe^{3+,}$ $Al^{3+,}$ Fe^{2+} and Mn^{2+} releases protons and offsets the pH of the solution (Equation 4.5 and 4.6).

$$Fe^{3+} + 3H_2O \rightarrow Fe(OH)_{3(s)} + 3H^+ \quad (4.11)$$

$$Al^{3+} + 3H_2O \rightarrow Al(OH)_{3(s)} + 3H^+ \quad (4.12)$$

4.3.1.5 Adsorption isotherms and thermodynamics

The relationship between the amounts of ions adsorbed and the ion concentration remaining in solution is described by an isotherm. The two most common isotherm models for describing this type of system are the Langmuir and Freundlich adsorption isotherms (Iakovleva et al., 2015). These models describe adsorption processes on a homogenous (monolayer) or heterogeneous (multilayer) surface, respectively. The most important model of monolayer adsorption came from Langmuir . This isotherm is given as follows:

$$q_e = \frac{Q_0 b C_e}{1 + b C_e} \quad (4.13)$$

The constant Q_0 and b are characteristics of the Langmuir equation and can be determined from a linearized form of Equation 6. The Langmuir isotherm is valid for monolayer adsorption onto a surface with a finite number of identical sites and can be expressed in the following linear form:

$$\frac{Ce}{Q_e} = \frac{1}{Q_m b} + \frac{Ce}{Q_m} \quad (4.14)$$

Where, Ce = Equilibrium concentration (mg L^{-1}), Qe = Amount adsorbed at equilibrium (mg g^{-1}), Qm = Langmuir constant related to adsorption capacity (mg g^{-1}) and b = Langmuir constant related to energy of adsorption (L mg^{-1}).

The essential characteristics of the Langmuir isotherm is expressed in terms of a dimensionless constant separation factor or equilibrium parameter, R_L , which is defined as:

$$R_L = \frac{1}{1 + b C_o} \quad (4.15)$$

Where C_0 = in initial concentration

A plot of Ce versus Ce/Qe should be linear if the data conform to the Langmuir isotherm. The value of Qm is determined from the slope and the intercept of the plot. It is used to

derive the maximum adsorption capacity and b is determined from the original equation and represents the degree of adsorption.

The Freundlich adsorption isotherm describes the heterogeneous surface energy by multilayer adsorption and is expressed as follows:

$$q_e = kCe^{1/n} \quad (4.16)$$

The equation may be linearized by taking the logarithm of both sides of the equation and can be expressed in linear form as follows:

$$log\, q_e = \frac{1}{n} log\, C_e + log\, K \quad (4.17)$$

Where Ce = Equilibrium concentration (mg L^{-1}), q_e = Amount adsorbed at equilibrium (mg g^{-1}), K = Partition Coefficient (mg g^{-1}) and n = degree of adsorption.

A linear plot of log Ce versus log q_e indicates whether the data conforms to the Freundlich isotherm. The value of K implies that the energy of adsorption on a homogeneous surface is independent of surface coverage and n is an adsorption constant which reveals the rate at which adsorption takes place. These two constants are determined from the slope and intercept of the plot of each isotherm.

In order to fully understand the nature of adsorption the thermodynamic parameters such as free energy change (ΔG) could be calculated. It was possible to estimate these thermodynamic parameters for adsorption reaction by considering the equilibrium constant under the experimental conditions. The Gibbs free energy change of adsorption was calculated using the following equation:

$$\Delta G = -RT\, ln\, K_c \quad (4.18)$$

Where, R is gas constant (8.314 J mg^{-1} K^{-1}), T is temperature and Kc is the equilibrium constant ($K_c = q_e/c_e$). The positive ΔG value indicates that the sorption process is spontaneous in nature and also feasible whereas the negative value indicates that the reaction is not spontaneous and feasible. The parameters of Langmuir and Freundlich adsorption isotherms are shown in **Table 4.3.**

Table 4.3: Parameters of Langmuir and Freundlich adsorption isotherms

	Langmuir isotherm					Freundlich isotherm		
Parameters	**R^2**	**b**	**Q_m**	**R_L**	**$\Delta G/1000$ (kJ/mg)**	**R^2**	**K_F**	**n**
Mn	0.265	1.66	17.09	0.0060	-2479.77	0.75	0.031	1.98
Al	0.059	-8.5	-6.05	-0.0005	-112671	0.33	0.011	3.81
Fe	0.905	1.92	217.4	0.0003	-15786.1	0.58	0.002	0.90
Sulphate	0.999	0.02	204.1	0.0080	30.22	0.78	0.031	0.55

The Langmuir adsorption isotherm experimental data showed that the best correlation coefficient of sulphate and Fe were 0.99 and 0.905, respectively. Q_{max} and b were determined from the slopes and intercepts of the plots and were found to be 204.1 and 217.4 mg/g, respectively. R_L values between 0 and 1 indicate favourable adsorption. The R_L parameters were found to range from 0.0003 to 0.008 showing that adsorption was favourable.

Freundlich adsorption isotherm experimental data showed the best correlation coefficients for Al and Mn. The regression ranged from 0.3 to 0.78, respectively. For sulphate and Fe the adsorption data showed a better fit to the Langmuir rather than the Freundlich adsorption isotherm, confirming predominance of homogenous adsorption. Al and Mn data showed a better fit to the Freundlich adsorption isotherm, showing predominance of heterogeneous adsorption on bentonite clay surfaces. K_f and n were calculated from the intercept and slopes of the Freundlich plots respectively. The constants were found to range from 0.01 to 0.03, and n from 1.98 to 3.81, respectively. According to Langmuir (1997), n values between 1 and 10 represent beneficial adsorption. This showed that the adsorptions of Al and Mn were favourable and conformed to Langmuir adsorption. Gibbs free energy model predicted that the reaction is not spontaneous in nature for Al, Fe and Mn except for sulphates hence indicating that sulphate has being the species that is adsorbed more than any other species.

4.3.1.6 Mechanisms of metal removal

Ion exchange (release of Na, Mg, Ca and K ions), precipitation and formation of various metal bearing phases due to an increase in pH, co-precipitation to Fe oxides, hydroxides and oxyhydroxides through complexation and adsorption of metals and sulphate on the bentonite clay surfaces are the chief mechanisms governing the process of metals reduction. The rapid removal of the chemical species from aqueous system indicates surface bound through chemisorption, ion exchange of base metals from bentonite clay matrices with subsequent

precipitation of metals. The fitting of the adsorption data could further point to chemical adsorption and precipitation probably due to interaction with the chemical species in the interlayers and hydroxyl groups on the clay surfaces. For example, sulphate could interact with $[Al(H_2O)_3(OH)_3]$ and $[Fe(H_2O)_3(OH)_3]$ to form sulphate complexes (Equation 4.19 and 4.20).

$$Al(H_2O)_3(OH)_3 + SO_4^{2-} \rightarrow Al(H_2O)_3(OH)(SO_4) + 2OH^- \quad (4.19)$$

$$Fe(H_2O)_3(OH)_3 + SO_4^{2-} \rightarrow Fe(H_2O)_3(OH)(SO_4) + 2OH^- \quad (4.20)$$

Adsorption of most of the chemical species was observed to be governed by both physiosorption and chemisorption interaction which occurred on matrices. Chemical interaction could have occurred through monodentate or multidentate ligands with the surface hydroxyl groups. Both inner and outer sphere complexation were facilitating chemical species attenuation since the data fitted well to Langmuir and Freundlich adsorption isotherms. The interlayer of clay matrices could also chemically interact with the chemical species through the OH- groups on hydrolysis hence releasing the hydroxyl group which will eventually increase the pH. Silicate will react with acidity in AMD through ion exchange and lead to pH increase

$$\equiv SiOH \leftrightarrow SiO^- + H^+ \quad (3.21)$$

$$\equiv SiOH + Ca^{2+} \leftrightarrow = SiOCa^+ + H^+ \quad (3.22)$$

$$\equiv SiOH + Mg^{2+} \leftrightarrow = SiOMg^+ + H^+ \quad (3.23)$$

$$\equiv SiOCa + M^{e+} + 2HOH \rightarrow = SiOM + Ca^{2+} + 2OH^- \quad (3.24)$$

$$\equiv SiOMg + M^{e+} + 2HOH \rightarrow = SiOM + Mg^{2+} + 2OH^- \quad (3.25)$$

Solubilization of alkaline oxides and calcites from bentonite which is a natural geological material will also contribute to an increase in pH. The removal of metals from aqueous solution is strongly influenced by pH. An explanation for such behaviour should consider both the hydration of metallic ions in solution and formation of equilibrium hydrocomplexes. In the pH range 1- 4, different hydrochemical species of metals are present in solution, namely: $[Me(OH)]^+$, $[Me_2(OH)]^{3+}$ and $[Me_2(OH)_2]^{2+}$ with the first species having the highest concentration.

A basic aqueous medium favours the formation of some anionic hydrocomplex forms (e.g. hydroxysulphates) that do not influence the adsorption process. Furthermore, adsorption can be governed by the following reaction equilibrium:

$$[Me(H_2O)_x]^{2+} + H_2O \leftrightarrow [Me(H_2O)_{x-1}(OH)]^{+} + H_3O^{+} \quad (4.26)$$

Under low acidity (pH = 4), the equilibrium is moved to the left and generates a decrease of the hydrocomplex form. Due to the net negative charge on clay surfaces, those hydrocomplexes will be adsorbed onto the clay surface. Other equilibria that describe the interaction between heavy metals ions and clay are:

$$yFe^{2+}_{(s)} + 2M^{y+}_{(c)} \rightarrow yFe^{2+}_{(c)} + 2M^{y+}_{(s)} \quad (4.27)$$

$$yMn^{2+}_{(s)} + 2M^{y+}_{(c)} \rightarrow yMn^{2+}_{(c)} + 2M^{y+}_{(s)} \quad (4.28)$$

$$yFe^{3+}_{(s)} + 2M^{y+}_{(c)} \rightarrow yFe^{3+}_{(c)} + 2M^{y+}_{(s)} \quad (4.29)$$

$$yAl^{3+}_{(s)} + 2M^{y+}_{(c)} \rightarrow yAl^{3+}_{(c)} + 2M^{y+}_{(s)} \quad (4.30)$$

Where y is valence of the exchangeable cation M (= Na, K, Ca, Mg) and subscripts s and c denote solution and clay phases, respectively.

4.3.1.7 Treatment of field acid mine drainage at optimised conditions

The concentration of chemical species for untreated and bentonite-treated acid mine drainage is shown in **Table 4.4**.

Table 4.4: Concentrations of chemical species for untreated and AMD treated with bentonite clay (all units in mg/L except pH and EC)

Parameter (mg/L)	Feed water	DWAS Guidelines	Bentonite treated AMD
pH	2.3	6 - 10	6
TDS	10237	0 - 1200	9872
EC	22713	0 - 700	16425
Na	171	0 - 50	316
K	18	NA	17
Mg	183	0 - 30	192
Ca	762	0 - 32	566
Al	190	0 – 0.9	1.1
Fe	259	0 – 0.1	15
Mn	40	0 – 0.05	35
Cu	7.80	0 – 1	0.1
Zn	7.90	0 – 0.5	6.3
Pb	6.30	0 – 0.01	0.1
Co	41.30	NA	44.7
Ni	16.60	0 - 0.07	24.4
As	20	0.001	0.05
B	5	0.01	0.2
Cr	20	0.01	0.1
Mo	16	0.01	0.6
Se	17	0.02	0.9
Si	1.49	NA	5.29
SO_4^{2-}	4000	0 - 500	3454

From **Table 4.4**, the results revealed that, as expected, AMD is very acidic at pH 3 and has high loads of TDS and a high EC. This is attributed to high levels of Fe, Al, Mn, Na, Ca, Mg and sulphates. Traces of Cu, Zn, Pb, Co, Ni, B, Cr, Mo, Se, As, K and Si are also present. After treatment of AMD under optimised conditions, levels of Fe, Al, Mn and sulphates decreased significantly. Base cations at elevated concentrations were also detected in solution indicating that as the metal species are adsorbed and precipitated onto the clay surfaces, base cations were substituted and released through cation-exchange. Ca concentration decreased

after the bentonite treatment indicating the possible precipitation of calcite (**Figure 4.1 and Table 4.4**). The pH was also notice to have increased from 2.3 to 6 hence showing a significant improvement on the physiochemical properties of clay as compared to pestle and mortar clay that had raised the pH from 2.24 to 2.28 from SAMD and 2.56 to 3.72 for gold tailings leachates. Trace amounts of Cu, Co, Pb, and Zn were also observed to have markedly decreased except for Co and Zn which were increasing hence showing possible exchange for Al and Fe. Ni increase slightly hence indicating that it is exchanged in polyvalent species. This was due to the exchange of low density cations from clay matrices by these chemical species. Concentrations of chemical species such as As, B, Cr, Mo and Se were also observed to have been reduced significantly. Even though the majority of DWAS water quality requirements had been met, further "polishing" of the treated water is required to ensure compliance with DWAS regulations governing water quality.

4.4 Characterisation of materials

4.4.1 X-ray diffraction analysis

The mineralogical compositions of raw (1) and reacted (2) bentonite clay by XRD are shown in **Figure 4.8**.

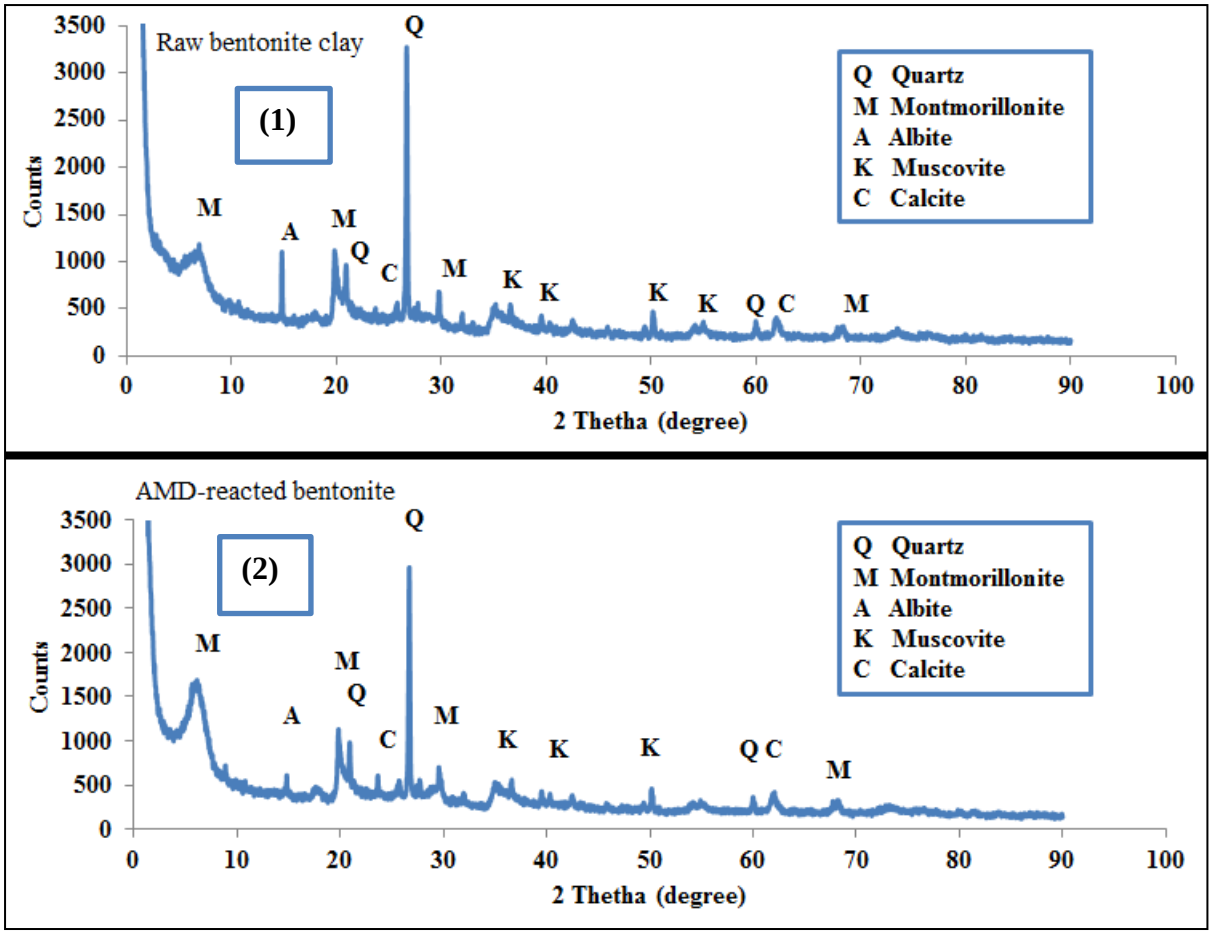

Figure 4.8: Mineralogical composition of raw (1) and reacted (2) bentonite clay by XRD

Montmorillonite, quartz, muscovite, calcite, and albite were observed to be the mineral phases which are present in bentonite clay matrices [**Figure 4.8(1)**]. Mineralogical composition of AMD-reacted bentonite clay is shown in [**Figure 4.8(2)]**. The AMD-reacted bentonite clay contained montmorillonite, quartz, muscovite, calcite, and albite. This indicates that the chemical properties of bentonite clay were not altered after contacting highly acidic wastewaters.

4.4.2 X-ray fluorescence analysis

The elemental compositions by XRF of raw bentonite clay and bentonite clay after contact with AMD (AMD-bentonite clay) are shown in **Table 4.5** (major) **and 4.6** (trace)**.**

Table 4.5: Major elemental composition of bentonite clay and AMD-bentonite clay

Elements (wt %)	Bentonite	Bent-AMD
SiO_2	65.95	64.45
TiO_2	0.46	0.30
Al_2O_3	15.27	16.10
Fe_2O_3	3.63	3.90
MnO	0.05	0.09
MgO	3.11	3.30
CaO	1.08	1.48
Na_2O	2.70	0.58
K_2O	1.09	0.78
P_2O_5	0.07	0.05
Cr_2O_3	0.01	0.01
SO_3	**0.6**	**2.6**
LOI	5.11	4.9
Total	99.13	98.55
H_2O-	9.47	7.68

The raw bentonite clay is mainly composed of Al and Si hence the name alumino-silicate. The relatively high concentration of Fe_2O_3, MgO, CaO, Na_2O and K_2O are an indication that these are the main exchangeable cations in the bentonite clay matrices. This correlates with the CEC results for (Mg, Ca, Na and K) (**Table 4.5**). Insignificant levels of P, Cr and S were observed as major component. Bentonite clay also contains significant trace amounts of other metals that could be released during the interaction of bentonite clay and AMD. The release of base cations from bentonite clay matrices during ion exchange can neutralise acidity in AMD and lead to precipitation of metals simultaneously. This will accelerate the precipitation of Al and Fe from aqueous solution.

$$M^{n+} + nOH^- \rightarrow M(OH)_n \qquad (4.4)$$

The chemical composition of AMD-reacted bentonite clay showed an increase in the contents of Al, Fe, Mn, Ca and SO_3 indicating the adsorption and retention of inorganic contaminants from AMD. A decrease in Na and K indicated that those chemical species were exchanged by Al, Fe and Mn polycations through isomorphous substitution. Trace elements (**Table 4.6**)

were also observed to be present at notable levels in the secondary residues hence validating the composition of the product water.

Table 4.6: Trace elemental composition of bentonite clay and AMD-bentonite clay

Elements (ppm)	Bentonite clay	Bent-AMD
Ba	6.4	200
Br	32	<2
Ce	<10	54
Co	2.6	8.4
Cr	13	<3
Cs	46	<5
Cu	10	15
Ga	19	18
Hf	6.7	<3
La	<10	18
Mo	31	<2
Nb	183	20
Nd	27	22
Ni	168	42
Pb	19	30
Rb	<2	12
Sc	<3	7.4
Se	994	<1
Sm	33	<10
Sr	71	52
Ta	35	<2
Th	5.4	21
Tl	6.7	<3
U	<2	4
V	<3	6.4
Y	21	17
Zn	18	39

4.4.3 Fourier transforms infrared spectroscopy analysis

The functional groups in raw and AMD-reacted bentonite clay are shown in **Figure 4.9**.

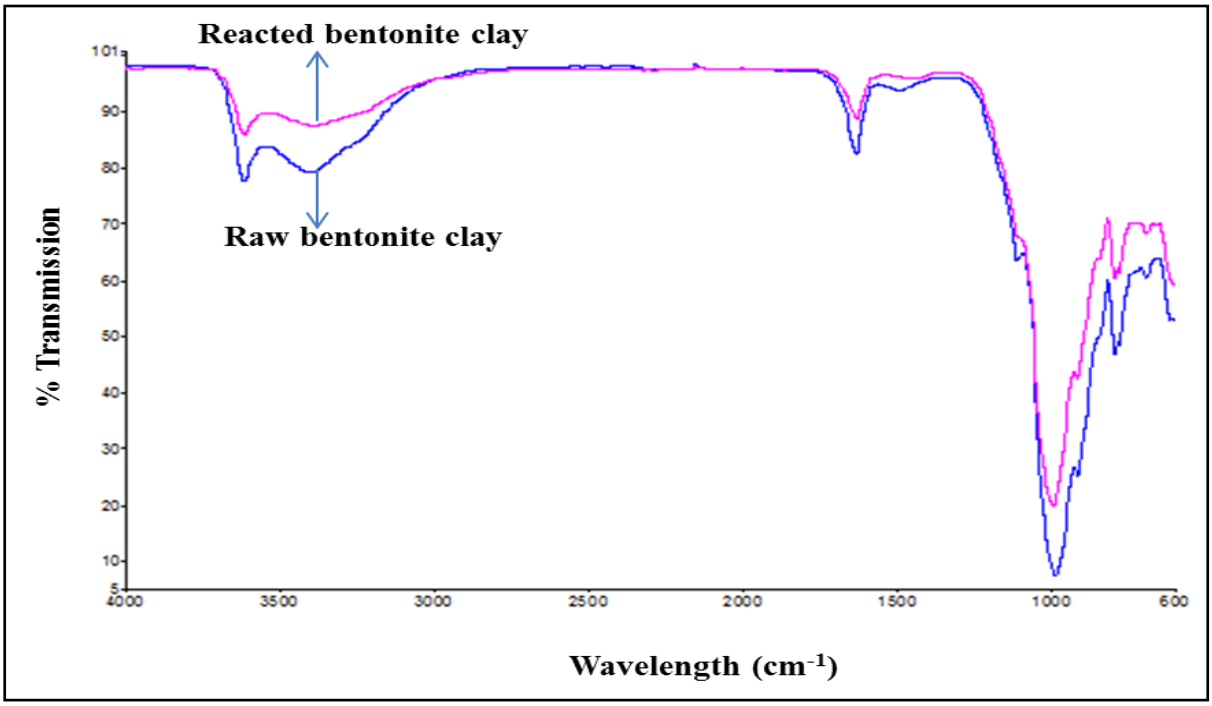

Figure 4.9: Spectra for raw and reacted bentonite clay

Sharp peak at 3616 cm^{-1} was assigned to the asymmetric stretching of Al-OH-Al in the aluminosilicate sheets of pristine montmorillonite (Figure 5.2). Sharp peak at 1039 and 600 cm^{-1} belonged to the stretching of Si-O-Si bond in montmorillonite tetrahedral sheet. Peak at 3698 cm^{-1} was due to vibration of –OH in Mg-OH, while the vibration and bending of water molecule appeared at 3450 and 1654 cm^{-1} respectively. This provides evidence that the clay used in the present study is montmorillonite. This indicates the presence of quartz and aluminium as determined by XRD and XRF respectively. OH stretching at region 3628 – 3260 cm^{-1} shows the presence of hydroxyl groups on bentonite clay matrices. This will also contribute to an increase in pH during ion exchange and adsorption processes. Moreover, the OH band at 3623 cm^{-1} indicates the coordination of Al^{3+} with OH group. The peak at 3623 cm^{-1} indicates the potential of isomorphous substitution of Al^{3+} by Fe^{2+} and Mg^{2+} cations. Bands in 875 cm^{-1} and 836 cm^{-1} correspond to $Fe^{2+/3+}$ and Mg^{2+}. The stretching at 1399 cm^{-1} corresponds to CO_3 stretching for calcite. After contacting raw bentonite clay with AMD, the CO_3 stretches were observed to have disappeared hence indicating the dissolution of calcite. This will also account to an increase in pH of the product water (**Table 4.10**).

4.4.4 Scanning electron microscopy-electron dispersion spectrometry

In order to better understand the mode of interaction of AMD and bentonite clay and the formation of mineral phases, SEM was utilized to appreciate the change in morphology of the secondary solid residues as compared with bentonite clay while SEM-EDX was utilized to semi-quantitatively identify the mineral phases resulting from the neutralization reactions. Spot analysis was done on selected solid residue samples. SEM images of bentonite clay (**Figure 4.10 - A, C and E**) and AMD-reacted bentonite clay (**Figure 4.10 - B, D and F).**

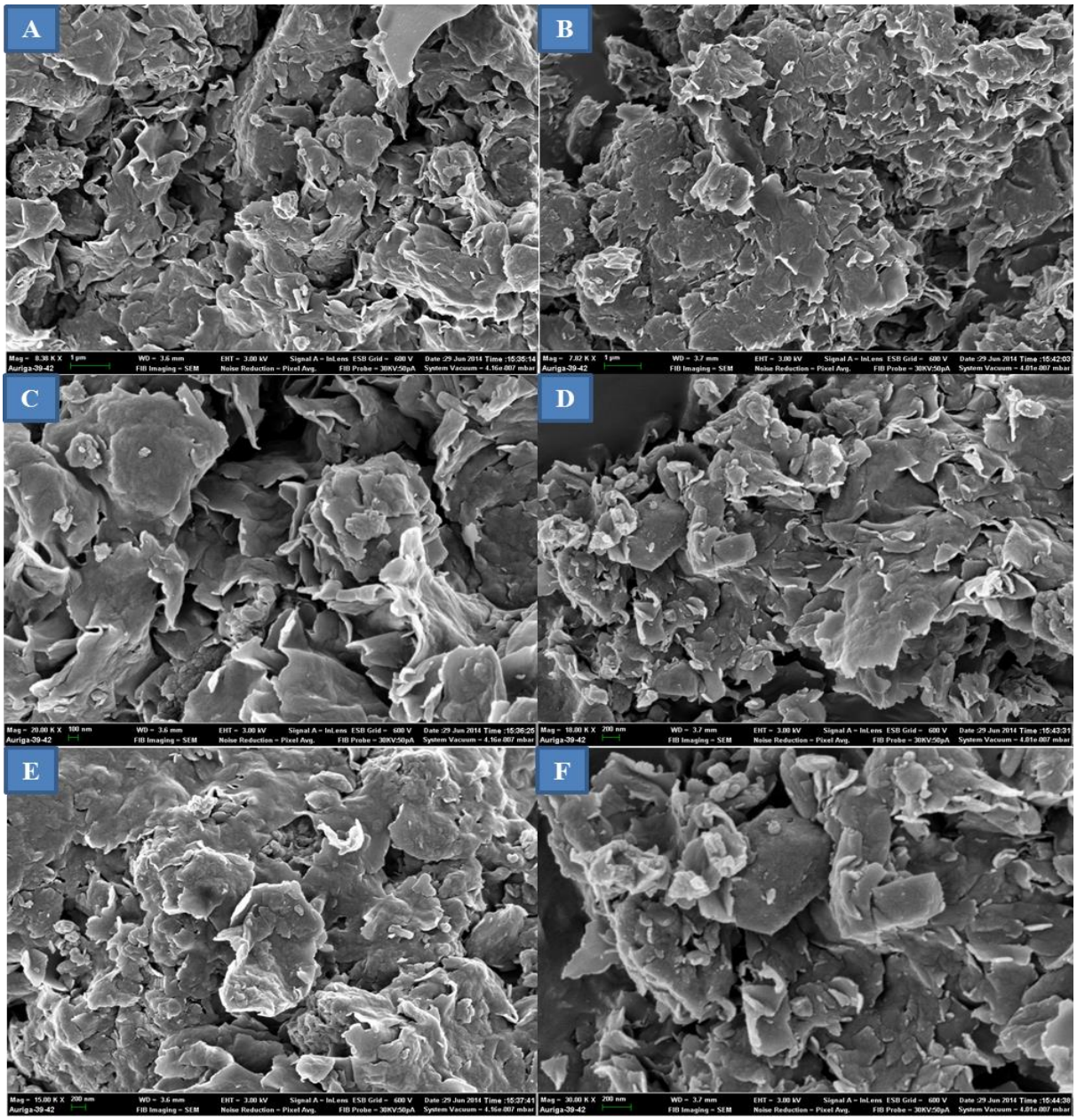

Figure 4.10: SEM images of raw bentonite clay (A, C and E) and AMD-reacted bentonite clay (B, D and F).

Figures 4.10 shows that there were few notable changes that were observed after interaction of bentonite clay with AMD. Raw bentonite clay was observed to contain leafy like structures which are lamella like and very porous. After contacting the AMD the leafy and thin, plate-like structural properties were preserved hence indicating that the mechanical structure of bentonite clay was preserved post the interaction. However, the surface of raw bentonite clay was less dense than the surface of AMD-reacted bentonite clay hence indicating possible deposition of materials on bentonite surfaces after contacting AMD.

The SEM and SEM-EDX spot analysis were done on raw and AMD-reacted bentonite clay. The data trends are then used to tentatively identify the mineral phases that could be forming in the treatment process. The spots and areas analyzed are shown in Figure 4.3 and 4.4 below. The accompanying SEM-EDX analyses are results expressed as weight %. The point elemental analysis by SEM-EDS of raw bentonite clay is shown in **Figure 4.11.**

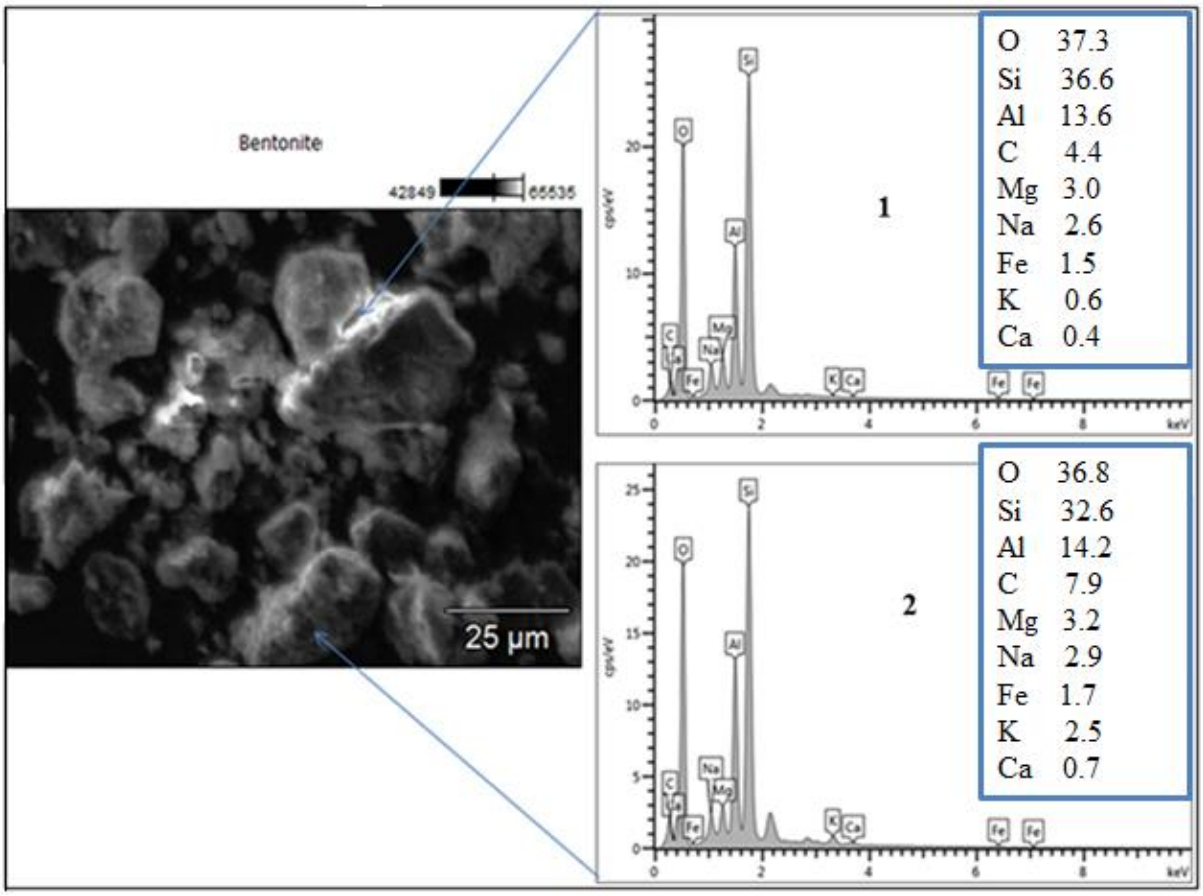

Figure 4.11: SEM-EDS elemental composition of raw bentonite clay

The SEM micrographs (25 µm) showed the presence of spherical agglomerates on the bentonite clay matrices.

Point 1 (Figure 4.11): Al and Si are the main elements since the material under study is an aluminosilicate. High levels of base cations (Mg, Ca, Na and K) were also present. C and O were also present on the clay matrices and may have been introduced into the clay surfaces from the atmosphere, by hydrolysis or decomposition of organic compounds. This result agrees with the XRF results.

Point 2 (Figure 4.11): Al and Si are the main elements since the material under study is an aluminosilicate. High levels of base cations (Mg, Ca, Na and K) were present indicating that these are the charge balancing ions in the interlayers and will be readily available as exchangeable cations. The data showed uniform chemical composition at different points on the clay surfaces. The point elemental analysis by SEM-EDS of AMD - reacted bentonite clay is shown in **Figure 4.12**.

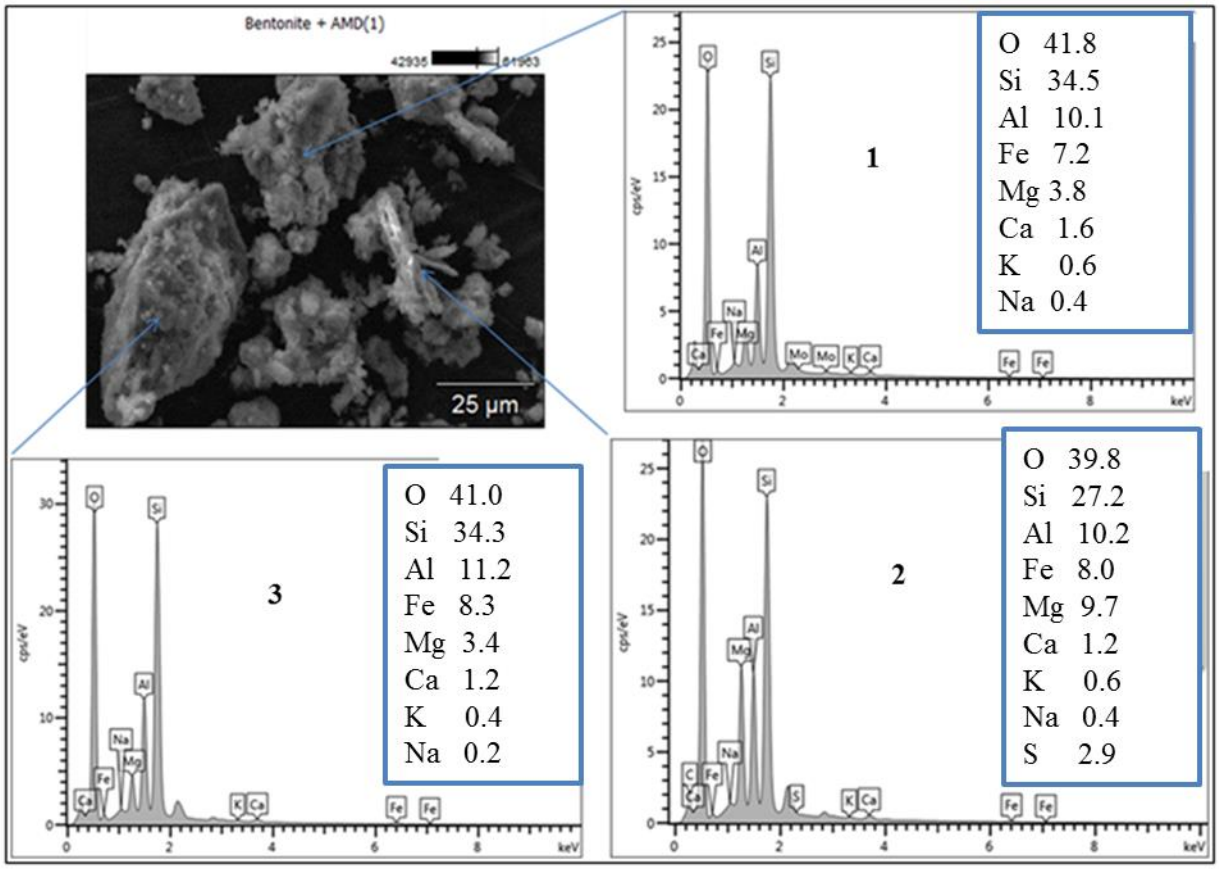

Figure 4.12: SEM-EDS elemental composition of AMD-reacted bentonite clay

The SEM micrographs showed a slight alteration in the morphology of bentonite clay since the spherical agglomerates were still intact indicating that the mechanical structure of bentonite clay was not affected by the reaction of bentonite clay and AMD.

Point 1 (Figure 4.12): The secondary residues were mainly Si and Al. The prevalence of oxygen indicated that the elements from the AMD were precipitated as metal oxides. Fe was also present at notable levels possibly due to ion-exchange on the clay surface and precipitation due to an increase in pH. This indicated that bentonite is a sink for Fe. This was also shown by a significant reduction in levels of Fe in the product water, showing that it had been adsorbed by the bentonite. There was a notable decrease in Na on the AMD reacted bentonite (**Figure 4.12**) and an increase in concentration in the product water (**Table 4.7**) demonstrating that it is a highly exchangeable cation. The Ca content of the AMD- reacted bentonite increased confirming the XRD results which showed the presence of calcite in the AMD-reacted bentonite. Molybdenum was also observed to be present. This indicated that bentonite also removed molybdenum from AMD.

Point 2 (Figure 4.12): The spot elemental analysis at Point 2 indicated that the reacted bentonite clay contained O, Si and Al as the major components. Fe was also present at elevated concentration and this could be attributed to ion-exchange of base cations on clay interlayers and precipitation due to an increase in pH. This again indicated that bentonite clay is a sink for Fe; this was borne out by a significant reduction in levels of Fe in the product water showing that it had been adsorbed by the bentonite clay and ion exchange (release of Na, Mg, Ca and K ions) or precipitation during the dissolution of alkaline and earth alkali metals. There was a large decrease in Na on the AMD-bentonite (**Figure 4.12**) and an increase in Na concentration in the product water (**Table 4.7**) demonstrating that it is a highly exchanged cation. Ca was observed to increase, confirming the XRD results which showed the presence of calcite in the AMD-bentonite. This indicated that calcite was being formed as AMD reacted with bentonite clay. Sulphur was also present in the AMD-bentonite complex indicating that bentonite clay is also a sink for sulphate from AMD, mainly as oxyhydroxysulphates or gypsum on the clay micro-surfaces.

Point 3 (Figure 4.12): Spot analysis revealed that the elemental composition of the secondary residues is dominated by Si, O and Al. Fe was also present, possibly due to ion-exchange and precipitation as the pH increased. This indicated that bentonite clay is a sink for Fe, also shown by a significant reduction in levels of Fe in the product water (**Table 4.7)**, showing that it had been adsorbed by the bentonite clay. There was a large decrease in Na on the AMD bentonite (**Figure 4.12**) and an increase in Na concentration in the product water (**Table 4.7**) again demonstrating that it is a highly exchanged cation. Ca was observed to increase, confirming the XRD results which showed the presence of calcite in the AMD-

bentonite complex. The data from all three spot points were similar, indicating that bentonite clay is capable of scavenging pollutants from AMD.

4.4.5 Brunauer-Emmett-Teller analysis

The results for surface area determination of bentonite clay and AMD-reacted bentonite clay, by BET analysis, are shown in **Table 4.7.**

Table 4.7: Surface areas of two particle sizes of bentonite clay and AMD-reacted bentonite clay by Brunauer-Emmett-Teller (BET) analysis

	Ball-milled clay		**Pestle-and-mortar milled clay (Gitari, 2014)**	
Parameters	**Bentonite clay**	**AMD-reacted**	**Bentonite clay**	**AMD-reacted**
BET surface area (m^2/g)	37.1	70	16	29.4
Single point area (m^2/g)	37	69.1	11	19.6
Pore volume (m^2/g)	0.1	0.9	0.03	0.07
Micropore area (m^2/g)	20.3	43.9	4.9	9.7

Clay minerals have received much attention for the treatment of polluted water due to their high surface areas that enable them to scavenge pollutants. Surface area is the sum of pore volume and singe point area. An increase in surface area has been observed for AMD-reacted bentonite clay as compared to unreacted bentonite clay. This can be attributed to the uptake of high density chemical species into the matrices of bentonite clay leading to the expansion of clay platelets and resulting in increases in surface area, this could also be a results of deposition of metal hydroxides/oxyhydroxysulphates precipitating from the reaction mixture (Bhattacharyya and Gupta, 2011). The surface area of ball-milled, South African bentonite clay corresponds with the surface area of 46.6 m^2/g for Pakistani bentonite clay (Tahir and Naseem, 2007). As a result of the particle-size reduction due to milling, the increase in single point and overall surface area from 11 to 37 m^2/g and 16 to 37.1 m^2/g, respectively, were observed. The lower surface area of the bentonite clay used by Gitari (2014) was attributed to the less efficient mode of milling (pestle-and-mortar). From **Table 4.7**, vibratory ball-milling doubled the surface area of pestle-and-mortar milled bentonite clay leading to better efficiency in water treatment since more surface area is made available for pollutants to be adsorbed. The poorer adsorption on the bentonite clay used by Gitari (2014) was due to the less efficient milling method.

4.4.6 Cation-exchange capacity

The results for the determination of cation-exchange capacity (CEC) of raw and AMD-reacted bentonite clay are shown in **Table 4.8.**

Table 4.8: Concentrations of main exchangeable cations on bentonite clay and AMD-reacted bentonite clay determined using the ammonium acetate method

	pH 7		**pH 5**	
Parameter	**Bentonite**	**Bentonite-AMD**	**Bentonite**	**Bentonite-AMD**
Na (mg L^{-1})	130.4	3.5	128.7	8.7
K (mg L^{-1})	3.9	0.5	4.1	1
Ca (mg L^{-1})	58	69	58	70
Mg (mg L^{-1})	88.5	100	86.9	98.4
CEC (meq /100g)	280.8	173	277.7	178.1

Analysis of CEC by the ammonium acetate method revealed that the main exchangeable cations in the supernatant were Mg^{2+}, Ca^{2+}, Na^{+} and K^{+}. Due to expansion of the inter-lamellar spaces, broken bonds, decrease of particle size, agglomeration and change in CEC, ball-milled bentonite clay has a high adsorption capacity compared to mortar-milled clay. From the supernatant, it was also observed that Na^{+} was the dominant cation for raw bentonite clay, confirming that the clay under study was Na-bentonite. After reacting AMD with bentonite clay, the CEC was observed to decrease indicating that ion-exchange is the chief process governing the removal of contaminants. Moreover, the levels of K and Na were observed to have decreased significantly, showing that these ions were exchanged for the polycations, Al and Fe. This also corroborated result obtained from XRF, XRD and ICP-MS.

4.5 Conclusions

The use of vibratory, ball-milled bentonite clay for neutralisation of acidity and removal of toxic chemical species from acidic and metalliferous mine effluents has delivered good results in treating AMD on a laboratory-scale. Characterisation revealed that ball-milled bentonite clay had double the surface area compared to pestle-and-mortar milled bentonite clay, indicating that more sites are available for adsorption, precipitation and ion-exchange of inorganic contaminants from wastewaters. XRD revealed that the clay used in the present study is montmorillonite that belongs to smectite family. XRF showed the predominance of

Al and Si hence the classification as an aluminosilicate. SEM micrography showed no alteration in the morphology of bentonite clay post-reaction with AMD. Contact of AMD with ball milled bentonite clay led to an increase in pH and large decreases in major metal concentrations. EC and TDS were observed to decrease following treatment of AMD with bentonite clay, indicating that there was attenuation of metal species concentration from aqueous system. Optimum conditions of using bentonite clay for AMD treatment under laboratory conditions were determined to be 2 g of adsorbent to 250 mL of AMD with 30 min of equilibration with shaking. Even though major cations were removed from AMD there is a need to further "polish" treated AMD to lower the residual concentration of sulphate and alkali and alkali earth metal cations. However, ball-milled bentonite clay treatment resulted in water that met some of the water quality guidelines requirements as compared to the poorer performance of mortar-and-pestle milled bentonite.

REFERENCES

Achterberg, E. P., Herzl, V. M. C., Braungardt, C. B. & Millward, G. E. 2003. Metal behaviour in an estuary polluted by acid mine drainage: the role of particulate matter. *Environmental Pollution,* 121**,** 283-292.

Akcil, A. & Koldas, S. 2006. Acid Mine Drainage (AMD): causes, treatment and case studies. *Journal of Cleaner Production,* 14**,** 1139-1145.

Albadarin, A. B., Mangwandi, C., Al-Muhtaseb, A. H., Walker, G. M., Allen, S. J. & Ahmad, M. N. M. 2012. Kinetic and thermodynamics of chromium ions adsorption onto low-cost dolomite adsorbent. *Chemical Engineering Journal,* 179**,** 193-202.

Anawar, H. M. 2013. Impact of climate change on acid mine drainage generation and contaminant transport in water ecosystems of semi-arid and arid mining areas. *Physics and Chemistry of the Earth, Parts A/B/C,* 58–60**,** 13-21.

Bedelean, H., Măicăneanu, A., Burcă, S. & Stanca, M. 2010. Removal of heavy metal ions from wastewaters using natural clays. *Clay Minerals,* 44**,** 487-495.

Bernier, L. R. 2005. The potential use of serpentinite in the passive treatment of acid mine drainage: Batch experiments. *Environmental Geology,* 47**,** 670-684.

Bethke, C. M., Vergo, N. & Altaner, S. P. 1986. Pathways of smectite illitization. *Clays & Clay Minerals,* 34**,** 125-135.

Bhattacharyya, K. G. & Gupta, S. S. 2011. Removal of Cu(II) by natural and acid-activated clays: An insight of adsorption isotherm, kinetic and thermodynamics. *Desalination,* 272**,** 66-75.

Bortnikova, S. B., Smolyakov, B. S., Sidenko, N. V., Kolonin, G. R., Bessonova, E. P. & Androsova, N. V. 2001. Geochemical consequences of acid mine drainage into a natural reservoir: Inorganic precipitation and effects on plankton activity. *Journal of Geochemical Exploration,* 74**,** 127-139.

Dale Marsden, A., Dewreede, R. E. & Levings, C. D. 2003. Survivorship and growth of Fucus gardneri after transplant to an acid mine drainage-polluted area. *Marine Pollution Bulletin,* 46**,** 65-73.

Dellisanti, F. & Valdré, G. 2005. Study of structural properties of ion treated and mechanically deformed commercial bentonite. *Applied Clay Science,* 28**,** 233-244.

Denicola, D. M. & Stapleton, M. G. 2002. Impact of acid mine drainage on benthic communities in streams: The relative roles of substratum vs. aqueous effects. *Environmental Pollution,* 119**,** 303-315.

Dukić, A. B., Kumrić, K. R., Vukelić, N. S., Dimitrijević, M. S., Baščarević, Z. D., Kurko, S. V. & Matović, L. L. 2015. Simultaneous removal of Pb2+, Cu2+, Zn2+ and Cd2+ from highly acidic solutions using mechanochemically synthesized montmorillonite-kaolinite/TiO2 composite. *Applied Clay Science,* 103**,** 20-27.

Đukić, A. B., Kumrić, K. R., Vukelić, N. S., Dimitrijević, M. S., Baščarević, Z. D., Kurko, S. V. & Matović, L. L. 2015a. Simultaneous removal of Pb(II), Cu2(II), Zn(II) and Cd(II) from highly acidic solutions using mechanochemically synthesized montmorillonite–kaolinite/TiO2 composite. *Applied Clay Science,* 103**,** 20-27.

Đukić, A. B., Kumrić, K. R., Vukelić, N. S., Stojanović, Z. S., Stojmenović, M. D., Milošević, S. S. & Matović, L. L. 2015b. Influence of ageing of milled clay and its composite with TiO2 on the heavy metal adsorption characteristics. *Ceramics International,* 41**,** 5129-5137.

Falayi, T. & Ntuli, F. 2014. Removal of heavy metals and neutralisation of acid mine drainage with un-activated attapulgite. *Journal of Industrial and Engineering Chemistry,* 20**,** 1285-1292.

Gitari, W. M. 2014. Attenuation of metal species in acidic solutions using bentonite clay: implications for acid mine drainage remediation. *Toxicological and Environmental Chemistry*.

Gitari, W. M., Petrik, L. F., Etchebers, O., Key, D. L. & Okujeni, C. 2008. Utilization of fly ash for treatment of coal mines wastewater: Solubility controls on major inorganic contaminants. *Fuel,* 87**,** 2450-2462.

Hince, E. C. & Robbins, E. I. 2003. Probing an underground acid-mine drainage ecosystem. *Geotimes,* 48**,** 26-28.

Iakovleva, E., Mäkilä, E., Salonen, J., Sitarz, M., Wang, S. & Sillanpää, M. 2015. Acid mine drainage (AMD) treatment: Neutralization and toxic elements removal with unmodified and modified limestone. *Ecological Engineering,* 81**,** 30-40.

Johnson, D. B. & Hallberg, K. B. 2005. Acid mine drainage remediation options: a review. *Science of The Total Environment,* 338**,** 3-14.

Konta, J. I. 1995. Clay and man: clay raw materials in the service of man. *Applied Clay Science,* 10**,** 275-335.

Kumrić, K. R., Crossed D Signukić, A. D. S. B., Trtić-Petrović, T. M., Vukelić, N. S., Stojanović, Z., Grbović Novaković, J. D. & Matović, L. L. 2013. Simultaneous removal of divalent heavy metals from aqueous solutions using raw and mechanochemically treated interstratified montmorillonite/kaolinite clay. *Industrial and Engineering Chemistry Research,* 52**,** 7930-7939.

Mapanda, F., Nyamadzawo, G., Nyamangara, J. & Wuta, M. 2007. Effects of discharging acid-mine drainage into evaporation ponds lined with clay on chemical quality of the surrounding soil and water. *Physics and Chemistry of the Earth, Parts A/B/C,* 32**,** 1366-1375.

Masindi, V., Gitari, M. W., Tutu, H. & De Beer, M. Neutralization and Attenuation of Metal Species in Acid Mine Drainage and Mine Leachates Using Magnesite: a Batch Experimental Approach. An Interdisciplinary Response to Mine Water Challenges - Sui, Sun & Wang (eds), 2014. China University of Mining and Technology Press, Xuzhou, 640 - 644.

Mohapatra, B. R., Douglas Gould, W., Dinardo, O. & Koren, D. W. 2011. Tracking the prokaryotic diversity in acid mine drainage-contaminated environments: A review of molecular methods. *Minerals Engineering,* 24**,** 709-718.

Netto, E., Madeira, R. A., Silveira, F. Z., Fiori, M. A., Angioleto, E., Pich, C. T. & Geremias, R. 2013. Evaluation of the toxic and genotoxic potential of acid mine drainage using physicochemical parameters and bioassays. *Environmental Toxicology and Pharmacology,* 35**,** 511-516.

Park, J. H., Edraki, M., Mulligan, D. & Jang, H. S. 2014. The application of coal combustion by-products in mine site rehabilitation. *Journal of Cleaner Production,* 84**,** 761-772.

Potgieter-Vermaak, S. S., Potgieter, J. H., Monama, P. & Van Grieken, R. 2006. Comparison of limestone, dolomite and fly ash as pre-treatment agents for acid mine drainage. *Minerals Engineering,* 19**,** 454-462.

Potgieter, J. H., Potgieter-Vermaak, S. S. & Kalibantonga, P. D. 2006. Heavy metals removal from solution by palygorskite clay. *Minerals Engineering,* 19**,** 463-470.

Sen Gupta, S. & Bhattacharyya, K. G. 2012. Adsorption of heavy metals on kaolinite and montmorillonite: A review. *Physical Chemistry Chemical Physics,* 14**,** 6698-6723.

Sen Gupta, S. & Bhattacharyya, K. G. 2014. Adsorption of metal ions by clays and inorganic solids. *RSC Advances,* 4**,** 28537-28586.

Simate, G. S. & Ndlovu, S. 2014. Acid mine drainage: Challenges and opportunities. *Journal of Environmental Chemical Engineering,* 2**,** 1785-1803.

Tahir, S. S. & Naseem, R. 2007. Removal of Cr(III) from tannery wastewater by adsorption onto bentonite clay. *Separation and Purification Technology,* 53**,** 312-321.

Tutu, H., Mccarthy, T. S. & Cukrowska, E. 2008. The chemical characteristics of acid mine drainage with particular reference to sources, distribution and remediation: The Witwatersrand Basin, South Africa as a case study. *Applied Geochemistry,* 23**,** 3666-3684.

Vicente, M. A., Gil, A. & Bergaya, F. 2013. Chapter 10.5 - Pillared Clays and Clay Minerals. *In:* FAÏZA, B. & GERHARD, L. (eds.) *Developments in Clay Science.* Elsevier**,** 523-557.

Wu, D. J., Wang, J. S., Teng, Y. G. & Zhang, K. N. 2011. Mechanism of tritium persistence in porous media like clay minerals. *Huanjing Kexue/Environmental Science,* 32**,** 742-748.

Yesilnacar, M. I. & Kadiragagil, Z. 2013. Effects of acid mine drainage on groundwater quality: A case study from an open-pit copper mine in eastern Turkey. *Bulletin of Engineering Geology and the Environment,* 72**,** 485-493.

Zhang, W., Zhuang, L., Yuan, Y., Tong, L. & Tsang, D. C. W. 2011. Enhancement of phenanthrene adsorption on a clayey soil and clay minerals by coexisting lead or cadmium. *Chemosphere,* 83**,** 302-310.

Zhou, C. H. & Keeling, J. 2013. Fundamental and applied research on clay minerals: From climate and environment to nanotechnology. *Applied Clay Science,* 74**,** 3-9.

Zhuang, G., Zhang, Z., Guo, J., Liao, L. & Zhao, J. 2015. A new ball milling method to produce organo-montmorillonite from anionic and nonionic surfactants. *Applied Clay Science,* 104**,** 18-26.

CHAPTER FIVE

Paper 3: This paper addresses the synthesis of cryptocrystalline magnesite-bentonite clay composite and its application for neutralization and attenuation of inorganic contaminants in acidic and metalliferous mine drainage

This chapter is devoted to achieve the undermentioned objective which is:

- Evaluation of the treatment of AMD using mechanochemical synthesised magnesite-bentonite clay composite in batch tests, and exploring the interaction chemistry thereof and that of the processed water chemistry, mineralogical transformation and chemical characterization of resultant solid residues.

CHAPTER FIVE

Synthesis of cryptocrystalline magnesite-bentonite clay composite and its application for neutralization and attenuation of inorganic contaminants in acidic and metalliferous mine drainage

[*]Masindi Vhahangwele[1,3], Gitari W.Mugera[1], Tutu Hlanganani[2], Debeer Marinda[4]

[1]Environmental Remediation and Water Pollution Chemistry Research Group, Department of Ecology and Resources Management, School of Environmental Science, University of Venda, P/bag X5050, Thohoyandou, 0950, South Africa, Tel: +2712 841 4107, VMasindi@csir.co.za
[2]Molecular Sciences Institute, School of Chemistry, University of the Witwatersrand, P/Bag X4, WITS, 2050, Johannesburg, South Africa,
[3]CSIR (Council of Scientific and Industrial Research), Built Environment, Building Science and Technology (BST), P.O Box 395, Pretoria, 0001, South Africa,
[4]DST/CSIR National Centre for Nano-Structured Materials, Council for Scientific and Industrial Research, P.O Box 395, Pretoria, 0001, South Africa

Abstract

The primary aim of this study was to synthesize cryptocrystalline magnesite-bentonite clay composite by mechanochemical activation and evaluate its usability as low cost adsorbent for neutralization and attenuation of inorganic contaminants in acidic and metalliferous mine drainage. The composite was synthesized at 1:1 weight to weight ratio of magnesite and bentonite clay respectively. The composite was mixed with simulated AMD at specific solid–liquid (S/L) ratios, equilibrated and its capacity to neutralize and remove the concentrations of selected and potentially toxic chemical species from synthetic and field AMD evaluated at optimized conditions. The geochemical computer code PH Redox Equilibrium (in C language) (PHREEQC) and WATEQ4 database was used for geochemical modelling of the process water. The resulting solid residues were analyzed by X-ray fluorescence (XRF), X-ray Diffraction, scanning electron microscopy (SEM) and scanning electron microscopy-energy dispersive X-ray spectroscopy (SEM-EDS), and Fourier Transforms Infrared Spectroscopy (FTIR) in an attempt to detect the minerals phases controlling the inorganic contaminants concentration in solution. Interaction of the composite with AMD led to an increase in pH (pH >11) and lowering of metal concentrations. The removal of Al^{3+}, $Fe^{3+/2+}$, Mn^{2+} and SO_4^{2-} was optimum at 20 min of equilibration and 1g of adsorbent dosage per 100 mL of solution (1:100 S/L ratio). The composite removed ≈99% (Al^{3+}, Fe^{3+}, and Mn^{2+}) and ≈90% (SO_4^{2-}) from raw mine effluent. Minor elements such as Co, Cu, Zn, Ni and Pb were

also removed significantly. The synthesized composite showed a significantly better toxic chemical species and SO_4^{2-} removal ability of from highly acidic solutions as compared to that obtained by cryptocrystalline magnesite and bentonite clay when used individually. Adsorption data fitted better to pseudo-second-order kinetic than pseudo-first-order kinetic hence confirming chemisorption. Adsorption data fitted better to Freundlich adsorption isotherm than Langmuir hence confirming multisite adsorption. Gibbs free energy model predicted that the reaction is spontaneous in nature for Al, Fe and sulphate except for Mn. Geochemical model indicated that Fe was removed as $Fe(OH)_3$, goethite, and jarosite, Al as basaluminite, boehmite and jurbanite, $Al(OH)_3$ and as gibbsite and diaspore. Al and Fe precipitated as iron (oxy)-hydroxides and aluminium (oxy)-hydroxides. Mn precipitated as rhodochrosite and manganite. Ca was removed as gypsum. Sulphate was removed as gypsum, and Fe, Al hydroxyl sulphate minerals. Mg was removed as brucite and dolomite. This would explain the decrease in the metal species and sulphate concentration in the product water. The composite removed the contaminants to below South African legal requirements for water use. It was concluded that the composite has the potential to neutralize acidity and attenuate potentially toxic chemical species from acidic and metalliferous mine drainage.

Keywords: Acid mine drainage; neutralization; magnesite-bentonite clay; composite; mechanochemical; inorganic contaminants, adsorption modelling

5.1 Introduction

Acidic and metalliferous drainage originating from metal mining activities can cause serious environmental pollution (Bortnikova et al., 2001, DeNicola and Stapleton, 2002, Atekwana and Fonyuy, 2009, Couceiro and Schettini, 2010, Anawar, 2013, Netto et al., 2013, Yesilnacar and Kadiragagil, 2013, Simate and Ndlovu, 2014). On release to receiving aquatic ecosystems, acid mine drainage (AMD) can cause major ecological impacts which have the capability to compromise the integrity of terrestrial and aquatic ecosystems to sustain life (Druschel et al., 2004, España et al., 2005, Gammons et al., 2006, Zhao et al., 2007, Zhao et al., 2012).

AMD is generated by oxidation of sulphide bearing minerals such as FeAsS, Fe_xS_x, CuS, Cu_2S, $CuFeS_2$, MoS_2, NiS, ZnS and PbS in the presence of air and water. More prevalently, pyrite associated with coal and gold seams and many ores including copper, silver, uranium and zinc is the main source of AMD (Tutu et al., 2008). During mining processes, sulphide-

rich rocks are exposed to water and oxygen and this promotes the formation of AMD . During rainfall on tailings dumps and rising groundwater in disused mineshafts, water and oxygen interacts with sulphidic minerals leading to the formation of acidic effluent. The resultant acidic water accelerates leaching of metals from surrounding rock strata or tailings (Druschel et al., 2004, Courtin-Nomade et al., 2005, España et al., 2005, Ferreira da Silva et al., 2009, Hallberg, 2010, Blowes et al., 2014, Candeias et al., 2014).

The release of metals to effluent waters makes the water metalliferous. In most instances, the formation of AMD can be represented by the following chemical equations (Gitari, 2014), using pyrite as an example:

$$2FeS_{2(s)} + 7O_{2(g)} + 2H_2O \xrightarrow{\text{bacteria}} 2Fe^{2+}_{(aq)} + 4H^{+}_{(aq)} + 4SO^{2-}_{4(aq)} \quad (5.1)$$

$$4Fe^{2+}_{(aq)} + O_{2(g)} + 4H^{+}_{(aq)} \rightarrow 4Fe^{3+}_{(aq)} + 2H_2O_l \quad (5.2)$$

$$FeS_{2(s)} + 14Fe^{3+} + 8H_2O \rightarrow 15Fe^{2+} + 2SO^{2-}_{4(l)} + 16H^{+} \quad (5.3)$$

$$Fe^{3+}_{(aq)} + 3H_2O_l \rightarrow Fe(OH)_{3(s)} + 3H^{+}_{(aq)} \quad (5.4)$$

These reactions are also mediated by bacteria (Equation 5.1) (Baker and Banfield, 2003, Hallberg, 2010). Acidic and metalliferous drainage is a prime issue of environmental concern since it causes a reduction in biodiversity and loss of authentic value of pristine ecosystems (Bortnikova et al., 2001, Grout and Levings, 2001, Achterberg et al., 2003, Levings et al., 2005, Mapanda et al., 2007, Macedo-Sousa et al., 2008, Martins et al., 2009, Couceiro and Schettini, 2010, Gray and Delaney, 2010, Anawar, 2013, Yesilnacar and Kadiragagil, 2013, Simate and Ndlovu, 2014). Acid mine drainage is characterised by high acidity and elevated concentrations of Al, Fe, Mn and SO_4^{2-}. In addition, it also contains trace amounts of As, B, Cr, Cu, Co, Mo, Ni, Pb, Se, and Zn (Zänker et al., 2002, Sracek et al., 2004, Wade et al., 2006, Tutu et al., 2008, Zhao et al., 2012).

This mine effluent needs to be contained and treated before discharge to natural water bodies (Galan et al., 1999, Macedo-Sousa et al., 2008, Martins et al., 2009, Ghosh et al., 2012, Yesilnacar and Kadiragagil, 2013, Simate and Ndlovu, 2014). Several technologies have been developed for treatment of AMD and these include ion-exchange (Gaikwad, 2010), adsorption (Motsi et al., 2009, Zhang, 2011), precipitation , and phytoremediation (Johnson and Hallberg, 2005, Sheoran and Sheoran, 2006, Groudev et al., 2008, Ramírez-Paredes et al., 2011). Maree et al. (2004) have evaluated the use of limestone for treatment of acid mine

drainage. Biological agents were also used for removal of sulphates from acid mine drainage as a polishing step (Pagnanelli et al., 2008, Chockalingam and Subramanian, 2009, Cruz Viggi et al., 2010). Due to cost implications, inefficient treatment, selective treatment and generation of toxic sludge, the existing technologies have limitation and companies are in constant search for sustainable AMD treatment and management technologies (Zipper and Skousen, 2010). To date, limestone has been used for AMD treatment but has limitations of raising the pH to a maximum of 7 which is not sufficient to remove all metal pollutants in AMD, and additional liming is necessary, thus making it unsustainable (Maree et al., 1989, Maree et al., 1998, Maree et al., 2004, Hlabela et al., 2007, Agboola et al., 2012, Bologo et al., 2012, Maree et al., 2013, Masukume et al., 2014). Moreover limestone treatment leads to generation of huge amounts of sludge that has to be managed. South African bentonite clay has been evaluated for AMD treatment in a recent study by Gitari (2014) but was observed to have low metal removal efficiency especially at high concentrations and could only increase the pH of the reaction mixture to ≈ 4 which is not sufficient for precipitation of metal species.

Clay have excellent physicochemical properties such as high adsorption capacities, ion exchange capacities, swelling properties, surface area, leafy or lamella structure, abundance and low cost. Clay minerals have also received great attention as alternative material for decontamination of polluted waterbodies. In addition, these materials are environmentally friendly, abundant, versatile and readily available making their application economically sustainable (Zhao et al., 2011). Techniques such as intercalation and pillaring (Gupta and Bhattacharyya, 2006, Masindi et al., 2014c), acid activation (Bhattacharyya and Sen Gupta, 2006, Bhattacharyya and Gupta, 2011, Đukić et al., 2015, Zhao et al., 2015) and mechanochemical activation (Narayanan and Lueking, 2007, Sankaranarayanan et al., 2011, Mitrović and Zdujić, 2014, Zhuravleva et al., 2014, Zhuang et al., 2015) can be employed in an attempt to improving the adsorption and inorganic contaminants removal properties of the clays. The preparation of organoclays by grafting and direct synthesis has also been used for metals retention (Sarkar et al., 2010, Yuan et al., 2013, Şimşek et al., 2014, Zhuang et al., 2015).

Amongst all clay modifications and composite synthesis science, mechanochemical activation was reported to present good responses because it is cheap, economically viable and, environmentally friendly technique of modification. Documented literatures have meticulously described the influence of mechanochemical activation on the morphological

and microstructural alterations and improvements of the clay (Kim et al., 2013, Đukić et al., 2015), but only a limited number of research studies have investigated the use of mechanical milling on their adsorption and reactivity properties (Đukić et al., 2015). Moreover, a study by Gitari (2014) observed that bentonite clay being a geological material possessed free alkaline materials that can be released on mechanochemical activation and be available to increase the pH of the reaction mixture. Fragmentation, distortion, breakage of crystalline networks and cobwebs, and particle size reduction followed by an increase of the surface area, exfoliation of particles and amorphization, can lead to the increase of the removal efficiencies of the pollutants on fabricated composites (Paik et al., 2010, Djukić et al., 2013, Hamzaoui et al., 2015, Zhuang et al., 2015).

Clay has been widely used for removal of inorganic and organic contaminants from aqueous systems (Bhattacharyya and Gupta, 2008). The main mode of metals attenuation by clay is adsorption (Gupta and Bhattacharyya, 2011). Adsorption of inorganic chemical species on clay minerals is highly pH dependent, thus, limiting their application in wastewater amelioration (pH < 4) (Đukić et al., 2015). In an attempt to counter for the limitations in the use of the raw and modified clays as adsorbents, the adsorbents can be prepared in a composite form with some metal oxides (Đukić et al., 2015) and carbonates (Masindi et al., 2014b). To respond to the challenges that are being presented by current technologies, government, mining houses, and scientific communities are seeking innovative and locally available technologies for remediating AMD.

To the authors' knowledge, the investigation of mechanochemically synthesized bentonite clay-cryptocrystalline magnesite composite as adsorbent for simultaneous neutralization and attenuation of metal species and sulphate has never been reported before. The purpose of this study was to synthesize a magnesite-bentonite clay composite adsorbent and evaluate its ability to neutralize acidity and remove metal species and sulphate from metalliferous mine drainage in a single process step.

5.2 Materials and methods

5.2.1 Sampling

Raw magnesite rocks from the Folovhodwe Magnesite Mine in Limpopo Province, South Africa, were collected without any prior processing. Bentonite clay was supplied by ECCA

(Pty) Ltd (Cape Town, South Africa). Raw AMD samples were collected from a disused mine shaft near Krugersdorp, Gauteng Province, South Africa.

5.2.2 Preparation of cryptocrystalline magnesite and bentonite clay

Magnesite rock samples were milled to a fine powder (Retsch RS 200 mill) and sieved (32 µm particle sizes). The raw bentonite was washed by soaking in ultra-pure water and draining after 10 minutes. The ultrapure water used was such that it covered the entire sample in the beaker and was allowed to overflow. The procedure was repeated four times. The washed bentonite was dried for 24 h at 105°C. The dried samples were milled into a fine powder (Retsch RS 200 mill) and sieved (32 µm particle size sieves).

5.2.3 Composite preparation

Mechanochemical synthesis was used as a method for the preparation of the clay composite. A vibratory ball-mill was used for making the porous magnesite-bentonite clay composite. Powdered bentonite (500g) and magnesite (500g) were mixed on a 1:1 wt% mass ratio. The mixture was crushed and homogenised by pulverizing into a fine powder (Retsch RS 200 mill) for 30 minutes at 1600 rpm. After sieving to <32 µm particle size, the material was kept in sealed plastic bags (Zip-lock). The parameters for milling were previously determined as optimal milling parameters for mechanochemical modification of bentonite clay-cryptocrystalline magnesite composite by Masindi et al. (2014b).

5.2.4 Synthetic acid mine drainage

Synthetic acid mine drainage (SAMD) was used for experimentation as real AMD is extremely difficult to work with in optimization due to oxidation and hydrolysis on exposure to the open leading to rapid changes in chemistry. A simplified solution containing the major ions found in AMD was prepared as described by (Tutu et al., 2008).

Table 5.1: Simulated acid mine drainage used in this study

Salt dissolved	Species	Concentration
$Al_2(SO_4)_3.18H_2O$	Al^{3+}	200 mg/L
$Fe_2(SO_4)_3.H_2O$	Fe^{3+}	2000 mg/L
$MnCl_2$	Mn^{2+}	100 mg/L
H_2SO_4 and Al and Fe salts	SO_4^{2-}	6000 mg/L

The composition of SAMD used in this study is shown in **Table 5.1**. AMD was simulated by dissolving the following quantities of salts in 1000 mL of Milli-Q ultra-pure water (18MΩ), 7.48 g $Fe_2(SO_4)_3.H_2O$, 2.46 g $Al_2(SO_4)_3 \cdot 18H_2O$, and 0.48 g $MnCl_2$ to give a solution of 2000 mg/L Fe^{3+}, 200 mg/L Al^{3+} and 200 mg/L Mn^{2+}. An aliquot of 5 mL of 0.05 M H_2SO_4 was added to make up the SO_4^{2-} concentration to 6000 mg/L. The salts were dissolved in 1000 mL volumetric flasks. Prior to the addition of ferric sulphate, 5 mL of 0.05 M of H_2SO_4 was added to ensure a pH < 3, in order to prevent immediate precipitation of ferric hydroxide. For the batch experiments, the working solutions were prepared from these stock solutions by appropriate dilutions

5.2.5 Characterization of aqueous solution

pH, Total Dissolved Solids (TDS) and Electrical Conductivity (EC) were monitored using CRISON MM40 portable pH/EC/TDS/Temperature multimeter probe. Aqueous samples were analysed using ICP-MS (7500ce, Agilent, Alpharetta, GA, USA) for metal cations while sulphate was analysed using IC (850 professional IC Metrohm, Herisau, Switzerland). The accuracy of the analysis was monitored by analysis of National Institute of Standards and Technology (NIST) water standards.

5.2.6 Mineralogical, chemical and microstructural characterisation

Mineralogical composition of composite and resulting solid residues was determined using XRD, Analyses were performed by using a Philip PW 1710 diffractometer equipped with graphite secondary monochromatic. Elemental composition was determined using XRF, the Thermo Fisher ARL-9400 XP+ Sequential XRF with WinXRF software. XRF and XRD were done at the University of Pretoria, South Africa. Morphology was determined using SEM-EDS (JOEL JSM – 840, Hitachi, Tokyo, Japan), Surface area and porosity were determined using BET (Micromeritics Tristar II, Norcross, GA, USA). pH_{PZC} was determined using solid addition method (Gitari, 2014).

5.2.7 Experimental procedures

To determine the optimum condition for AMD treatment, several operational parameters were optimized and they include: effect of solid to liquid ratios, shaking time, composite dosage, and species concentrations. All experiments were performed in triplicate and the data averaged.

5.2.7.1 Effect of cryptocrystalline magnesite: bentonite clay ratios

The effect of cryptocrystalline magnesite contents on neutralization and attenuation of metal species and sulphate was assessed. Portions of 100 mL solutions of SAMD were pipetted into 250 mL flasks into which 1 g of the composite samples were added. The magnesite to bentonite clay (wt%) was varied as follow: 0.1:1, 0.2:1, 1:1, 2:1, 3:1, 4:1. The mixture was equilibrated for 60 minutes on a reciprocating shaker. The initial pH of the working solutions was < 3. After shaking, the mixture was filtered through a 0.45 µm pore nitrate cellulose filter membrane. The filtrates were preserved by adding two drops of concentrated HNO_3 acid to prevent aging and immediate precipitation of Al, Fe and Mn and refrigerated at 4 ºC prior to analysis by an inductively coupled plasma mass spectrometer (ICP-MS) (7500ce, Agilent, Alpheretta, GA, USA). The pH before and after agitation was measured using the CRISON multimeter probe (model MM40). A separate set was left un-acidified for sulphate analysis by Ion Chromatograph (850 professional IC Metrohm, Herisau, Switzerland).

5.2.7.2 Effect of time

Portions (100 mL) each of SAMD were pipetted into 250 mL flasks into which 1 g of the composite samples were added. The mixtures were then equilibrated for 1, 10, 20, 60, 120, 180, 240, 300 and 360 minutes at 250 rpm using the Stuart reciprocating shaker. The pH, metal species and sulphate contents were determined as described in the preceding section.

5.2.7.3 Effect of dosage

Portions (100 mL) each of SAMD were pipetted into 250 mL flasks and varying masses (0.1 - 8 g) of the composite were added into each flask, respectively. The mixtures were agitated using a shaker for an optimum time of 30 mins at 250 rpm. The pH, metal species and sulphate contents were determined as described in the preceding section.

5.2.7.4 Effect of species concentration

To investigate the effects of adsorbate concentration on reaction kinetics, several dilutions were made from the simulated AMD stock solution. The pHs of the simulated AMD were not adjusted. The capacity of the adsorbent to neutralize and attenuate metal concentrations from aqueous solution was then assessed by increasing metal concentrations. Solutions of 100 mL each containing 100-2000 mg/L Fe^{3+}; 10-200 mg/L Al^{3+}; 5-100 mg/L Mn^{2+} and 300 - 6000 mg/L SO_4^{2-} were prepared in triplicate and 1 g of the composite was added to each sample container. The mixtures were equilibrated by shaking for 30 minutes. The initial pH of the

working solutions was < 3. The pH, metal and sulphate contents were determined as described in the preceding section.

5.2.7.5 Treatment of field acid mine drainage at optimized conditions

Field AMD samples were treated at established optimized conditions in order to assess the effectiveness of magnesite-bentonite clay composite treatment. The pH and metal species contents were determined as described previously while a separate set of samples was left un-acidified for SO_4^{2-} analysis. Metal species were assayed using ICP-MS, pH, EC and TDS were measured as described previously. The resultant solid residue, after contact with AMD, was characterized in order to gain an insight into the fates of chemical species after magnesite-bentonite clay composite treatment.

5.2.8 Calculation of metal species, sulphate removal and adsorption capacity

Computation of % removal and adsorption capacity were evaluated using Equations (5.5) and (5.6).

$$\text{Percentage removal (\%)} = \left(\frac{Ci - Ce}{Ci}\right) \times 100 \quad (5.5)$$

$$\text{Adsorption capacity } (q_e) = \frac{(C_i - C_e)V}{m} \quad (5.6)$$

Where: Ci = initial concentration (mg/L), Ce = equilibrium ion concentration (mg/L), V = volume of solution (L); m = mass of bentonite clay (g).

5.2.9 Adsorption Kinetics

Adsorption kinetics were evaluated using pseudo-first-order, second order kinetics and Intraparticle diffusion model (Falayi and Ntuli, 2014).

5.2.10 Adsorption isotherms and thermodynamics

Adsorption isotherms were evaluated using Langmuir and Freundlich adsorption models (Falayi and Ntuli, 2014). Thermodynamics evaluations were done using Gibbs free energy model (Rusmin et al., 2015, Shou et al., 2015).

An error analysis was required to evaluate the fit of the adsorption isotherms to experimental data. In the present study, the linear coefficient of determination (R^2) was employed for the error analysis. The linear coefficient of determination was calculated by using the equation 5.3:

$$r = \frac{n\sum xy - (\sum x)(\sum y)}{\sqrt{n(\sum x^2) - (\sum x)^2} - \sqrt{(\sum y^2) - (\sum y)^2}} \quad (5.7)$$

Theoretically, the R^2 value varies from 0 to 1. The R^2 value shows the variation of experimental data as explained by the regression equation. In most studies, the coefficient of determination, R^2, was applied to determine the relationship between the experimental data and the kinetics or isotherms.

5.2.11 Geochemical modelling

To complement chemical solution and physicochemical characterization results, the ion association model PHREEQC was used to calculate ion activities and saturation indices of mineral phases based on the pH and solution concentrations of major ions in supernatants that were analysed after the optimized conditions. Mineral phases that were likely to form during treatment of AMD with magnesite-bentonite clay composite were predicted using the PHREEQC geochemical modelling code using the WATEQ4F database (Parkhurst and Appelo, 1999). Species which are more likely to precipitation was determined using saturation index (SI). SI < 1 = under saturated solution, Si = 1 = saturated solution and SI > 1= Supersaturated solution.

5.3 Results and discussion

5.3.1 Inorganic contaminants removal: Batch experiments

5.3.1.1 Effects of magnesite to bentonite ratios

The results for inorganic contaminants attenuation as a function of magnesite to bentonite clay ratios are shown in **Figure 5.1.**

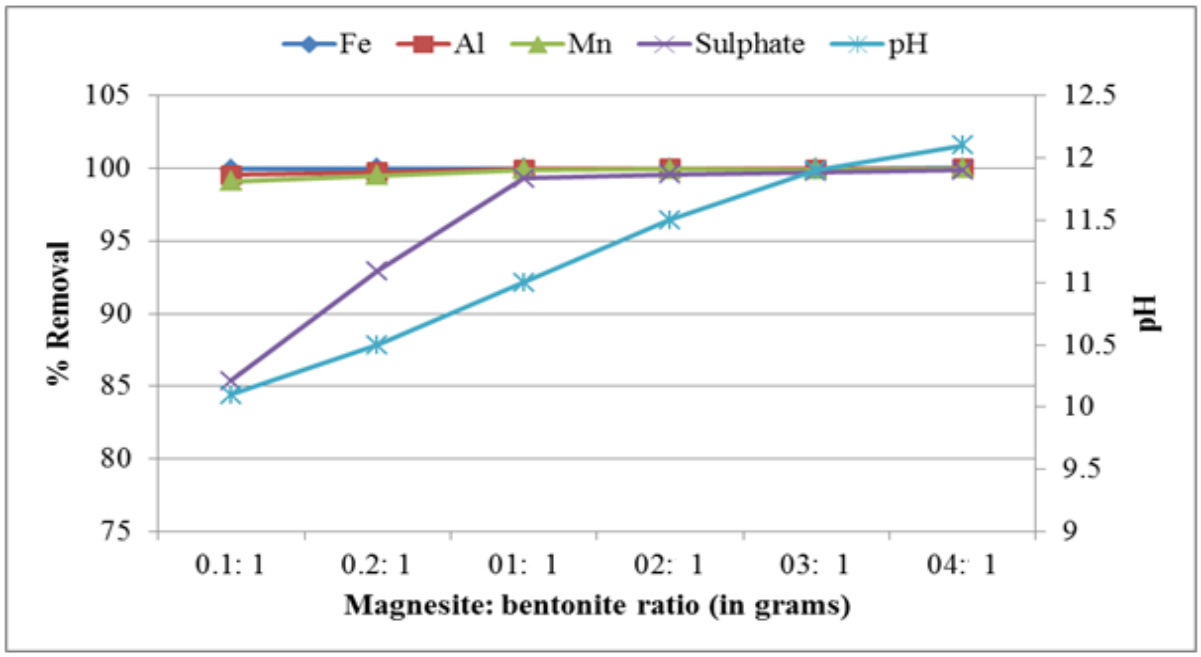

Figure 5.1, Appendix B, Table B 10: Variation in % removal of Fe^{3+}, Al^{3+}, Mn^{2+} and sulphate as a function of solid to solid ratios (Conditions: pH < 3, 2000 mg/L Fe^{3+}, 200 mg/L Al^{3+}, 100 mg/L Mn^{2+}, 6000 mg/L SO_4^{2-} , 60 mins shaking time, 100 mL SAMD solution, 32 µm particle size, 250 rpm shaking speed, 26 ºC temperature).

Variation of the removal efficiencies in neutralization and removal of metals species and sulphate by the composite with different contents of cryptocrystalline magnesite are shown in **Figure 5.1.** It is clear that wt% of cryptocrystalline magnesite, in the composite is an important factor affecting the neutralization and removal of metals and sulphate ions from aqueous solution, especially in highly acidic environment. **Figure 5.1** shows that as the ratio of magnesite to bentonite increases, there was a proportional increase in pH. The pH was observed to increase from ≈ 10.2 to ≈ 12.3. This was attributed to the dissolution of magnesite and partly to the release of base cations from the bentonite clay matrices as shown in the reactions below.

$$MgO + H_2O \rightarrow Mg^{2+} + 2OH^- \quad (5.8)$$

$$CaO + H_2O \rightarrow Ca^{2+} + 2OH^- \quad (5.9)$$

$$Na_2O + H_2O \rightarrow 2Na^+ + 2OH^- \quad (5.10)$$

$$K_2O + H_2O \rightarrow 2K^+ + 2OH^- \quad (5.11)$$

Removal of sulphate was observed to increase with an increase in the magnesite to bentonite ratio. Attenuation of the major metal species concentrations, Al, Mn and Al remained above 99 % since the pH was highly alkaline for their precipitation. At 1:1 magnesite to bentonite all the chemical species removal was above 98 % and the higher ratios seemed to have no significant difference in the removal capacity. Hence a 1:1 ratio was taken as the optimum for the fabrication of the composite.

5.3.1.2 Effect of equilibration time

Results of metals species and sulphate removal in SAMD as a function of contact time are shown in **Figure 5.2.**

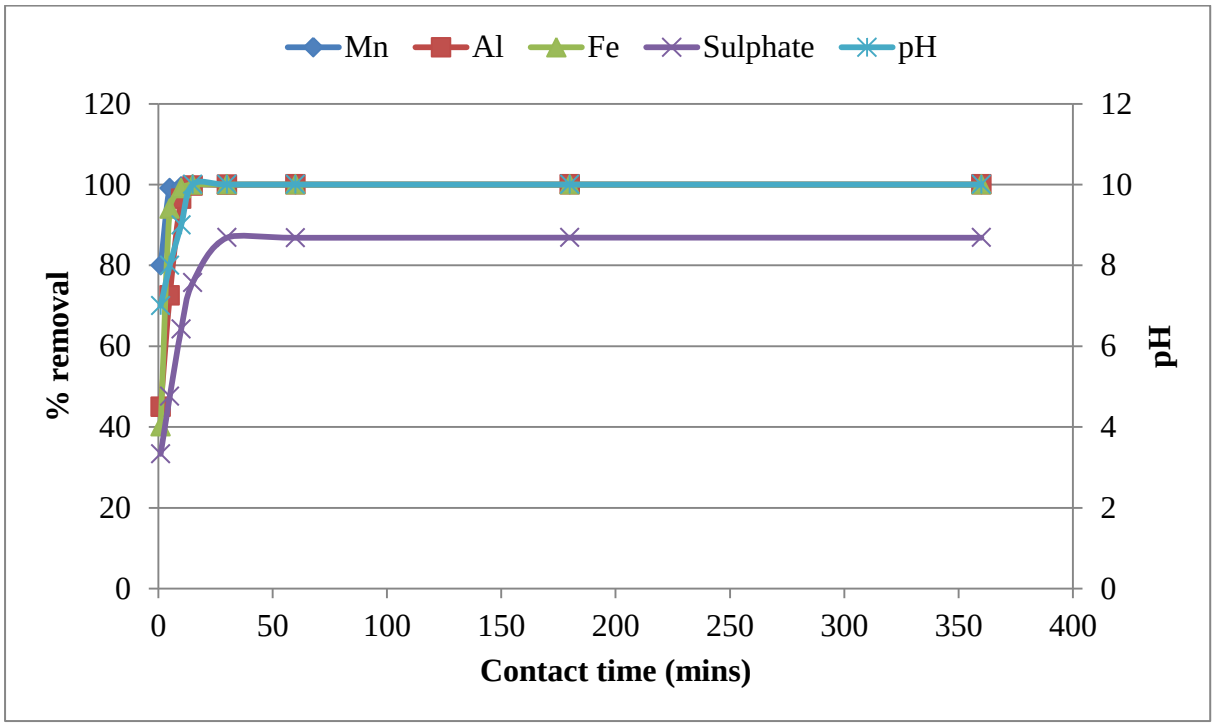

Figure 5.2, Appendix B, Table B 8: Variation of Al, Fe, Mn and SO_4^{2-} with agitation time and variation of pH with agitation time (Conditions: pH < 3, 2000 mg/L Fe^{3+}, 200 mg/L Al^{3+}, 100 mg/L Mn^{2+}, 6000 mg/L SO_4^{2-} , 1 g composite, 100 mL SAMD solution, 1; 100 S/L ratios, 32 µm particle size, 250 rpm shaking speed, 26 ºC ambient temperature).

An increase in pH was observed with increases in contact time. Metal removal also increased with increased contact time. An increase in pH from 6 – 10 and metal concentration attenuations were observed to be high within the first 20 minutes of interaction but stabilizes thereafter. An increase in pH was attributed to dissolution of magnesite, alkali and alkaline earth metal oxides from the composite during the interaction with AMD leading to an increase in alkalinity. An increase in pH also leads to precipitation of metal species from AMD. On precipitation the metal hydroxides incorporate sulphate to form various oxyhydroxysulphates and also adsorb sulphate. The composite also exchanged Al^{3+}, Fe^{3+}, and Mn^{2+} with cations such as Na^{+}, Mg^{2+} and Ca^{2+} in their matrices, the exchanged highly charged cations could also adsorb sulphates as the counter ions. The composite showed good efficiencies in the treatment of AMD since it removed chemical species from contaminated water in a single step as compared to two-step traditional treatment methods. This study also showed good removal efficiencies of chemical species (≈100% Al^{3+}, Fe^{3+}, and Mn^{2+} and > 50 % SO_4^{2-}) as compared to a study conducted by Nkonyane et al. (2012) who reported that 120 min of contact time is efficient in raising the pH to 7.5 and remove metals except for Mn when using a combination of bentonite clay and limestone. The present study achieved maximum removal within the short contact time of 20 min and raised the pH to >10 which is suitable for removal of all metal species. Therefore, 30 min was taken as the optimum agitation time and it will be used as optimum time and applied in subsequent experiments.

5.3.1.3 Adsorption kinetics and mechanism

The effect of contact time on removal of chemical species from aqueous solution was evaluated using different kinetic models to reveal the nature of the adsorption process and rate limiting processes. Different kinetic model parameters for adsorption of Mn, Al, Fe and sulphate on the composite are shown in **Table 5.2**

A Lagergren pseudo first order kinetic model is a well-known model that is used to describe mechanisms of metal species adsorption by an adsorbent. It can be written as follow (Shou et al., 2015):

$$ln(q_e - q_t) = ln\, q_{e-} k_1 t \qquad (5.12)$$

Where k_1 (min^{-1}) is the pseudo-first-order adsorption rate coefficient and q_e and q_t are the values of the amount of adsorbate adsorbed per unit mass at equilibrium and at time t, respectively. The experimental data was fitted by using the pseudo-first-order kinetic model

by plotting $\ln(q_e - q_t)$ vs. t, and the results are shown in **Table 5.2 and Figure 5.2.** The pseudo-first-order was applied and it was found to fairly converge with the experimental data. Moreover, the calculated amounts of Mn, Al, Fe and sulphate ions adsorbed by the composite [$q_{e,\ calc}$ (mgg^{-1})] were less than the experimental values [$q_{e,\ exp}$ (mgg^{-1})] (**Table 5.2**). The finding indicated that the Lagergren pseudo-first-order kinetic model is inappropriate to describe the adsorption of Mn, Al, Fe and sulphate ions from aqueous system by the composite.

The pseudo-second-order kinetic model is another kinetic model that is widely used to describe the adsorption process from an aqueous solution. The linearized form of the pseudo-second-order rate equation is given as follow:

$$\frac{t}{qr} = \frac{1}{k_2 q_e^2} + \frac{t}{q_e} \qquad (5.13)$$

Where k_2 [g(mg min^{-1})] is the pseudo-second-order adsorption rate coefficient and q_e and q_t are the values of the amount adsorbed per unit mass at equilibrium and at time t, respectively. An application of the pseudo-second-order rate equation for adsorption of chemical species to the composite matrices portrayed a good fit with experimental data (**Figure 5.3 - 6 and Table 5.2**). The obtained results confirm that pseudo-second-order model is the most suitable kinetic model to describe adsorption of Mn, Al, Fe and sulphate by the composite from aqueous system. Moreover, this also confirms that the adsorption mechanism of the metals species from aqueous solution is chemisorption.

Note the theoretical adsorption capacity is close to the experimental adsorption capacity further confirming that this model describes the adsorption data (**Table 5.2 and Figure 5.4**). The overall kinetics of the adsorption from solutions may be governed by the diffusional processes as well as by the kinetics of the surface chemical reaction. In diffusion studies, the rate is often expressed in terms of the square root time

$$q_t = k_{id} t^{1/2} + C_i \qquad (5.14)$$

Where k_{id} (mgg^{-1} $min^{-1/2}$) is the Intraparticle diffusion coefficient (slope of the plot of q_t vs. $t^{1/2}$) (**Figure 5.5**) and C_i is the Intraparticle diffusion rate constant. Parameters were calculated to determine whether film diffusion or Intraparticle diffusion is the rate limiting step. The model suggested that if the sorption mechanism is via Intraparticle diffusion then a plot of qt versus $t^{1/2}$ will be linear; and Intraparticle diffusion is the sole rate-limiting step

when such a plot passes through the origin. When the sorption process is controlled by more than one mechanism, then a plot of qt versus $t^{1/2}$ will be multi-linear. Given the multi-linear nature of the plot for metal species sorption on the composite, it is proposed that sorption occurred in three phases. The initial steep phase represented surface diffusion, the second less steep phase represented a gradual sorption of metal species where intra-particle diffusion within the pores is rate-limiting, and the third phase where equilibrium had been achieved. Since the plot did not pass through the origin, intra-particle diffusion was not the only rate-limiting step. There were three processes controlling metals species sorption rate but only one predominates at any particular time phase. The C (mg g^{1}) values indicate the thickness of the boundary layer which was observed to be very small for these soils; and these low C values suggested that surface diffusion plays less role as the rate-limiting step in the overall sorption process. The results also showed that the Intraparticle diffusion model by Webber Morris was not applicable for the present process due to lower correlation coefficients.

Table 5.2: Different kinetic model parameters for adsorption of Mn, Al, Fe and sulphate on the composite

Pseudo-first-order kinetic model				
Element	**$q_{e,\,exp}$ (mgg^{-1})**	**$q_{e,\,calc}$ (mgg^{-1})**	**K_1**	**R^2**
Mn	9.99	-11.12	0.177	0.94
Al	19.99	-4.77	0.309	0.99
Fe	199.9	-8.94	0.331	0.91
Sulphate	521.1	-6.99	1.519	0.90
Pseudo-second-order kinetic model				
Element	**$q_{e,\,exp}$ (mgg^{-1})**	**$q_{e,\,calc}$ (mgg^{-1})**	**K_2**	**R^2**
Mn	9.99	10.01	3.67	1
Al	19.99	20.04	1.24	1
Fe	199.9	200	1.67	1
Sulphate	521.1	526.3	0.69	0.999
Intraparticle diffusion model				
Element	**$q_{e,\,exp}$ (mgg^{-1})**	**C_i (mgg^{-1})**	**K_{id} ($mgg^{-1}\,min^{-1/2}$)**	**R^2**
Mn	9.99	2.85	13.93	0.48
Al	19.99	2.20	2.89	0.18
Fe	199.9	1.02	0.35	0.29
Sulphate	521.1	-0.06	0.05	0.17

The plot for adsorption of Mn, Al, Fe and sulphate on the composite using pseudo-first-order, pseudo-second-order and Intraparticle diffusion models are shown in **Figure 5.3, 5.4 and 5.5**.

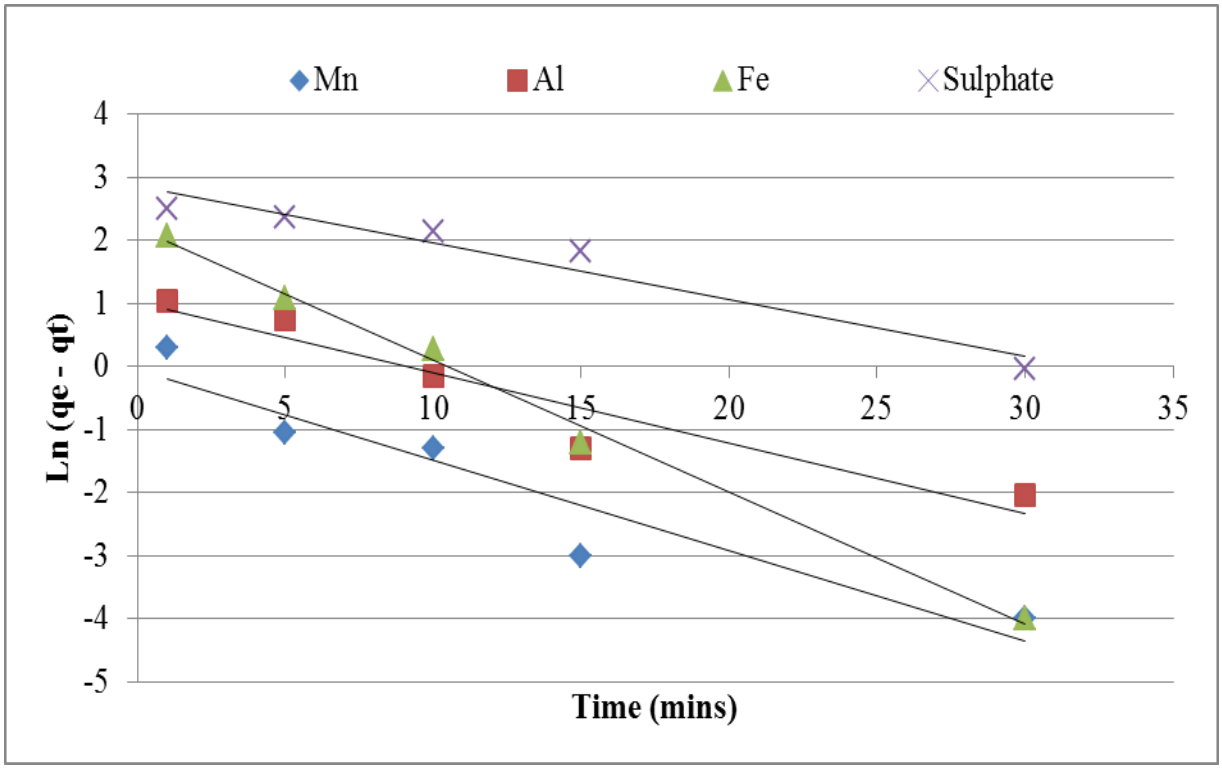

Figure 5.3: Pseudo-first-order plots of Mn, Al, Fe and sulphate ions adsorbed on the composite

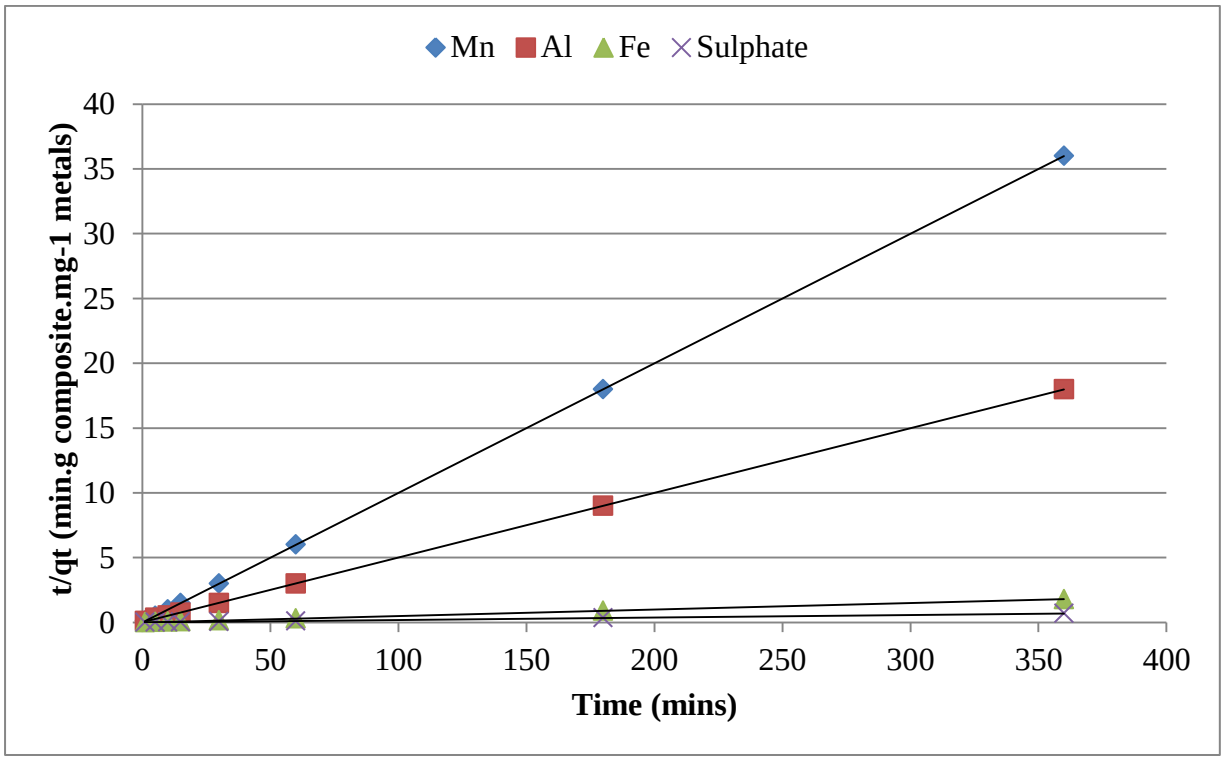

Figure 5.4: Pseudo-second-order plots of Mn, Al, Fe and sulphate ions adsorbed on the composite

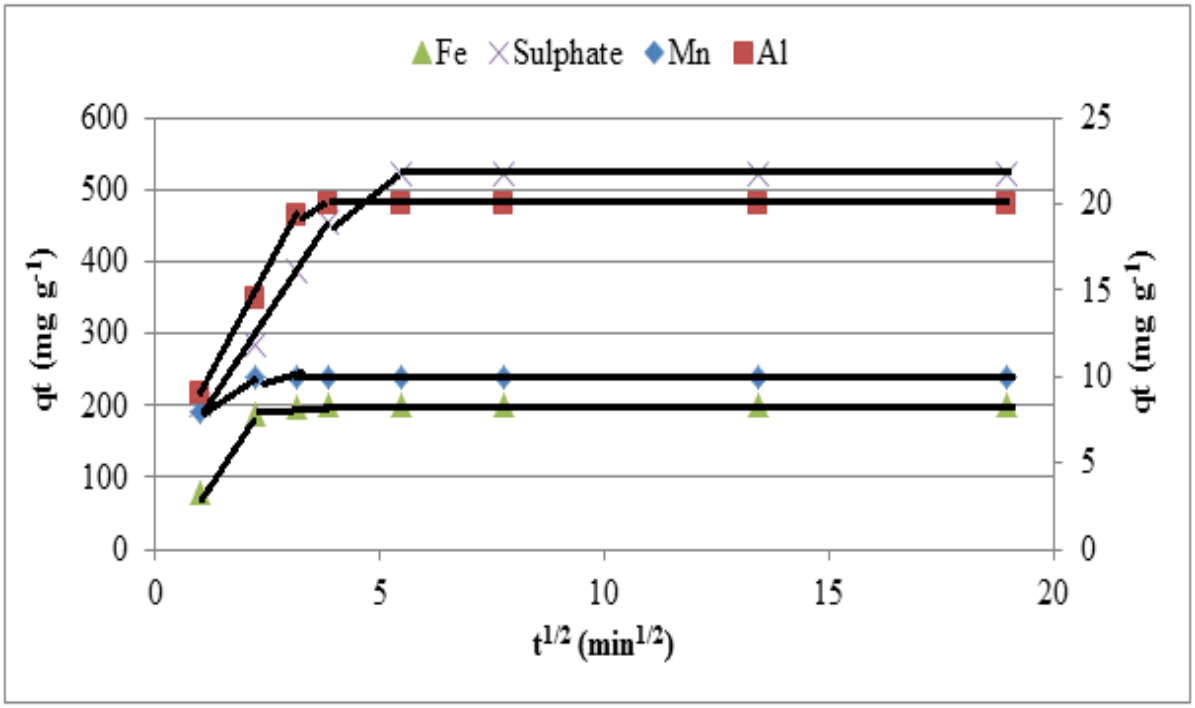

Figure 5.5: Intraparticle diffusion plots of Mn, Al, Fe and sulphate ions adsorbed on the composite

5.3.1.4 Effects of composite dosage

The results of neutralization and attenuation of inorganic contaminants from synthetic AMD as a function of the composite dosage are shown in **Figure 5.6**.

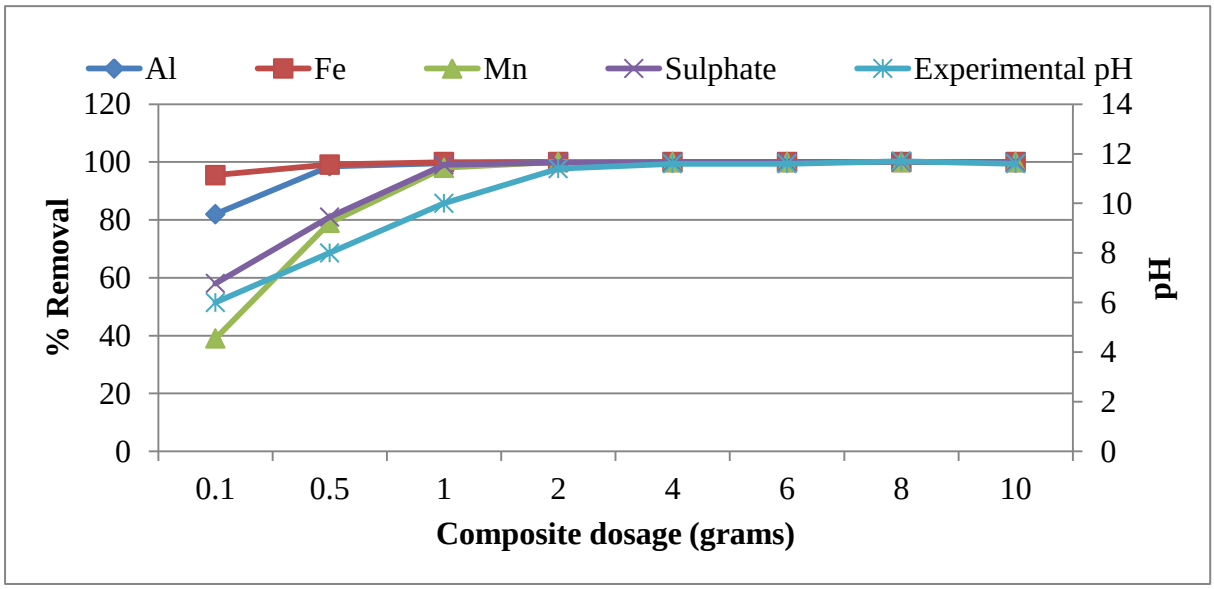

Figure 5.6, Appendix B, Table B 9: Variation of pH, Al, Fe, Mn and sulphate concentration with adsorbent dosage (Conditions: pH < 3, 2000 mg/L Fe^{3+}, 200 mg/L Al^{3+}, 100 mg/L Mn^{2+},

6000 mg/L SO_4^{2-}, 100 mL solution, 250 rpm shaking speed, <32 µm particle size, 30 min reaction, 26 ºC temperature).

Figure 5.6 shows that there was an increase in pH with an increase in composite dosage. Cations and anions in the supernatant solution were also observed to decrease with an increase in dosage. The increase in pH was attributed to dissolution of magnesite, alkali and alkaline earth metal oxides from the composite during the interaction with AMD, hence leading to an increase in pH. The XRF and XRD results also indicated the presence of these oxides and carbonates in the matrices of the feedstock. An increase in pH also led to precipitation of metal species from AMD. On precipitation the metal hydroxides incorporate sulphates to form various oxyhydroxysulphates and also adsorb sulphates. The adsorption data could further point to chemical adsorption probably due to interaction with the $[Al(H_2O)_6]^{3+}$ and $[Fe(H_2O)_6]^{3+}$ incorporated to the interlayers and hydroxyl groups on the clay surfaces. When this pH is reached, small particles of the metal hydroxide are formed (Equation 5.15). For example sulphate could interact with those species as follows [Equation (5.16 – 5.17)].

$$M^{n+} + nOH^- \rightarrow M(OH)_n \downarrow \quad (5.15)$$

$$Al(H_2O)_3(OH)_3 + SO_4^{2-} \rightarrow Al(H_2O)_3(OH)(SO_4) + 2OH^- \quad (5.16)$$

$$Fe(H_2O)_3(OH)_3 + SO_4^{2-} \rightarrow Fe(H_2O)_3(OH)(SO_4) + 2OH^- \quad (5.17)$$

The composite may also exchange Al^{3+}, Fe^{3+}, and Mn^{2+} with cations such as Na^+, Mg^{2+} and Ca^{2+} in their matrices (**Table 5.3**). The exchanged high charge cations could also adsorb sulphates as the counter ions. As composite dosage increased, the pH increased. Moreover, the composite presented more sites for ion-exchange and adsorption of chemical species in aqueous solution. As the dosage increased, more surface sites for exchange of low density cations with high density cations from AMD become available. The composite is effective for AMD treatment since it combines ion-exchange of (Mg, Ca, Na and K), adsorption, co-precipitation and precipitation of metal species from AMD as the pH increase due to dissolution of alkaline materials hence leading to much cleaner effluents. At 1g adsorbent dosage the attenuation capacity of the major metal species concentrations was > 95%. Consequently, 1 g was taken as the optimum dosage for subsequent experiments under these conditions. The optimum dosage (10 g/L) indicated by this work compares favourably with other remediation agents such as limestone (10 g/L), dolomite (40 g/L), limestone bentonite

blend (10 g/L) and fly ash (500g/L) (Maree et al., 1989, Maree et al., 1998, Gitari et al., 2006, Nkonyane et al., 2012, Maree et al., 2013). Moreover, the treatment efficiency of this technology is high as compared to the other technologies since it can neutralize and remove metals and sulphate to within DWAS drinking water quality guidelines. South Africa has large reserves of both bentonite (Gitari, 2014) and magnesite (Masindi et al., 2014b), and thus, the economic viability of this technology is high.

5.3.1.5 Effects of chemical species concentration

The results for chemical species attenuation as a function of concentration are shown in **Figure 5.7.**

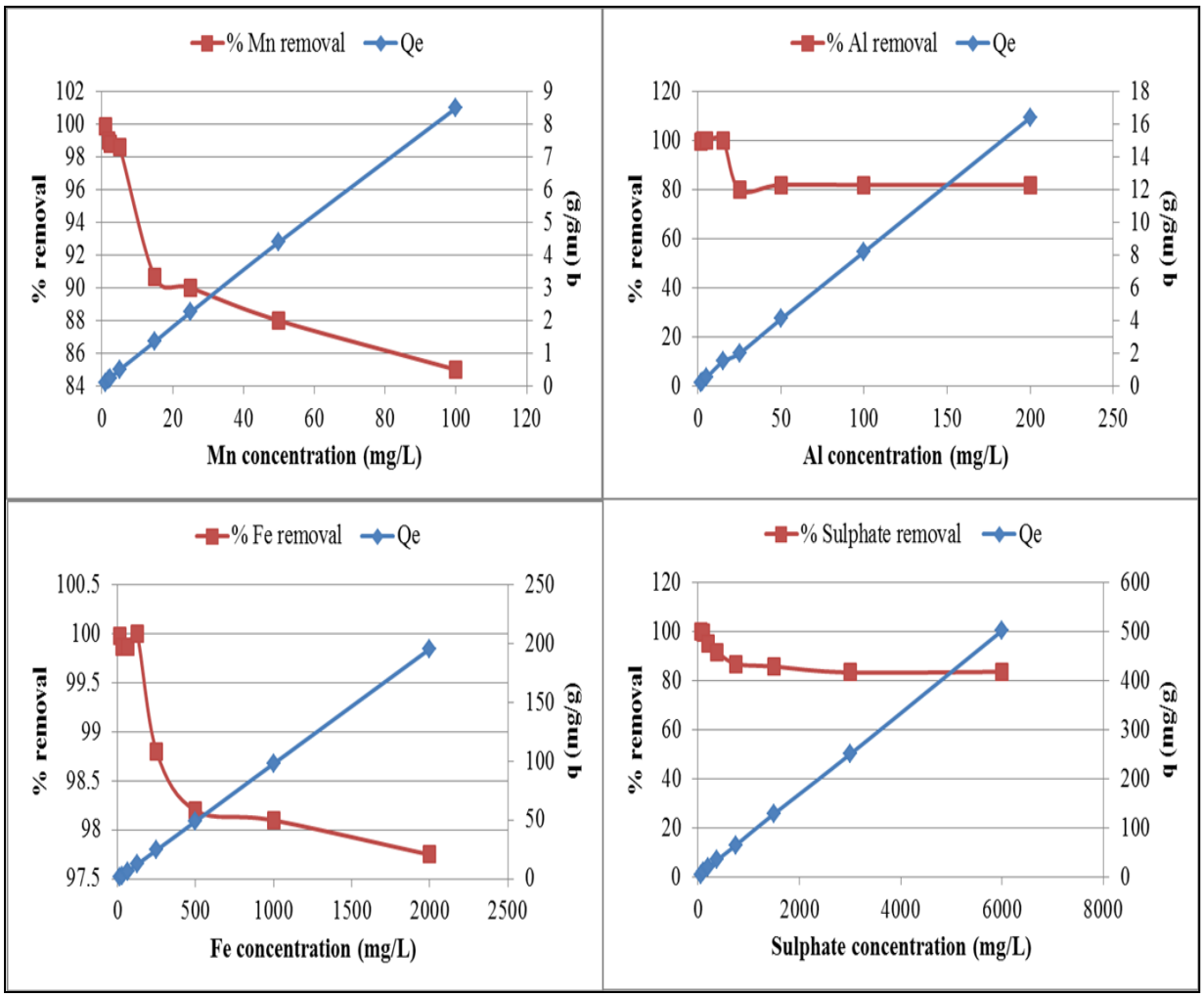

Figure 5.7, Appendix B, Table B 11: Variation in % removal and adsorption capacity of Al^{3+}, Mn^{2+} and $Fe^{3+/2+}$ as a function of ion concentration (pH < 3, 30 mins of shaking, < 32 µm particle size, 1 g composite, 100 mL, 1:100 S/L ratios, 250 rpm shaking speed, and 26 ° C ambient temperature)

At the initial concentration evaluated the composite exhibited ≈ 80 – 100 for Al, ≈ 97 – 100 for Fe, and ≈ 84 – 100 for Mn removal efficiency. Greater than 80% sulphate removal efficiency was observed at the evaluated concentration ranges. The pH remained above 10 in all concentration gradients meaning that 30 minutes of agitation and 1g of the composite would be adequate for neutralization and removal of contaminates from AMD under these conditions. At low concentration of metal species, more surfaces are available for adsorption and at high concentration more surfaces are occupied by pollutants. At low concentration, there is less acidity to be neutralised so the pH remain alkaline (>10). Removal of Al and Fe may be due to ion exchange of base cations (Mg, Ca, Na and K) from the composite interlayers, dissolution of magnesite leading to precipitation and co-precipitation of metal species with an increase in pH. The presence of exchangeable base metals was shown by CEC, SEM-EDS and XRF studies (**Table 5.2 and 5.6).** Dissolution of calcite, periclase and magnesite as shown by XRD contribute to an increase in pH that will precipitate metals as hydroxide and oxyhydrosulphates as shown by SEM-EDS point analysis.

5.3.1.6 Adsorption isotherms and thermodynamics

The relationship between the amount of ions adsorbed and the ion concentration remaining in solution is described by an isotherm. The two most common isotherm models for describing this type of system are the Langmuir and Freundlich adsorption isotherms. These models describe adsorption processes on a homogenous (monolayer) or heterogeneous (multilayer) surface, respectively. The most important model of monolayer adsorption came from Langmuir. This isotherm is given as follows:

$$q_e = \frac{Q_0 b C_e}{1 + b C_e} \tag{5.18}$$

The constant Q_0 and b are characteristics of the Langmuir equation and can be determined from a linearized form of equation 4.11. The Langmuir isotherm is valid for monolayer sorption due to a surface with finite number of identical sites and can be expressed in the following linear form:

$$\frac{Ce}{Q_e} = \frac{1}{Q_m b} + \frac{Ce}{Q_m} \tag{5.19}$$

The essential characteristics of the Langmuir isotherm can be expressed in terms of a dimensionless constant separation factor or equilibrium parameter, R_L , which is defined as:

$$R_L = \frac{1}{1 + bC_o} \quad (5.20)$$

Where, Ce = equilibrium concentration (mg L^{-1}), qe = amount adsorbed at equilibrium (mg g^{-1}), Qm = Langmuir constants related to adsorption capacity (mg g^{-1}) and b = Langmuir constants related to energy of adsorption (L mg^{-1}). A plot of Ce versus Ce/Qe should be linear if the data conforms to the Langmuir isotherm. The value of Qm is determined from the slope and the intercept of the plot. It is used to derive the maximum adsorption capacity and b is determined from the original equation and represents the degree of adsorption.

The Freundlich adsorption isotherm describes the heterogeneous surface energy by multilayer adsorption. The Freundlich isotherm is formulated as follows:

$$q_e = kCe^{1/n} \quad (5.21)$$

The equation may be linearized by taking the logarithm of both sides of the equation and can be expressed in linear form as follows:

$$log\, q_e = \frac{1}{n} log\, C + log\, K \quad (5.22)$$

Where Ce = equilibrium concentration (mg L^{-1}), q_e = amount adsorbed at equilibrium (mg g^{-1}), K = Partition Coefficient (mg g^{-1}) and n = degree of adsorption. A linear plot of log Ce versus log q_e indicates whether the data is described by the Freundlich isotherm. The value of K implies that the energy of adsorption on a homogeneous surface is independent of surface coverage and n is an adsorption constant which reveals the rate at which adsorption is taking place. In order to fully understand the nature of adsorption the thermodynamic parameters such as free energy change (ΔG) could be calculated. It was possible to estimate these thermodynamic parameters for adsorption reaction by considering the equilibrium constant under the experimental conditions. The Gibbs free energy change of adsorption was calculated using the following equation:

$$\Delta G = -RT\, ln\, K_c \quad (5.23)$$

Where, R is gas constant (8.314 J mg^{-1} K^{-1}), T is temperature and Kc is the equilibrium constant ($K_c = q_e/c_e$). The positive ΔG value indicates that the sorption process is spontaneous in nature and also feasible whereas the negative value indicates that the reaction is spontaneous and feasible. The parameters of Langmuir and Freundlich adsorption isotherms

are shown in **Table 5.3.** These two constants are determined from the slope and intercept of the plot of each isotherm. The parameters of Langmuir and Freundlich adsorption isotherms are shown in **Table 5.3.**

Table 5.3: Parameters of Langmuir and Freundlich adsorption isotherm and thermodynamics

	Langmuir					**Freundlich**		
Element	**R^2**	**R_L**	**b (L mg^{-1})**	**Q_{max}**	**$\Delta G/1000$ (kJ/mg)**	**R^2**	**n**	**K_f(mg g^{-1})**
Al	0.71	0.031	0.3	8.9	53.32	0.96	2.1	149
Fe	0.45	0.049	0.1	15.7	73.81	0.85	2.8	7.07
Mn	0.66	0.046	0.1	200	-137.89	0.82	2.5	1.95
SO_4^{2-}	0.55	0.062	0.002	588.2	62.80	0.92	2.3	2.4

The results showed better fit to Freundlich adsorption isotherm than Langmuir adsorption isotherm hence confirming multilayer adsorption. Q_{max} and b were determined from the slope and intercept of the plot and were found to be 8.9, 15.7, 200, 588.2 mg/g and 0.3, 0.1, 0.1, 0.002 L/mg for Mn, Al, Fe and sulphate, respectively. According to Sparks (2003), R_L values between 0 and 1 indicate favourable adsorption. The R_L were found to range from 0.031 to 0.062 hence showing that it was favourable. K_f and n were calculated from the slopes of the Freundlich plots. The constants were found to be K_f = 149, 7.07, 1.95, 2.4 and n = 2.1, 2.8, 2.5, 2.3 for Mn, Al, Fe and sulphate, respectively. According to Langmuir (1997), n values between 1 and 10 represent beneficial adsorption. This showed that adsorption of ions from aqueous solution by the composite was favourable. Gibbs free energy model predicted that the reaction is not spontaneous in nature for Al, Fe and sulphate except for Mn.

5.3.2 Variation of pH with an increase in Fe^{3+} concentration

The variation of pH profile with varying concentration of Fe^{3+} as representative of the inorganic contaminants in the SAMD is shown in **Figure 5.8.**

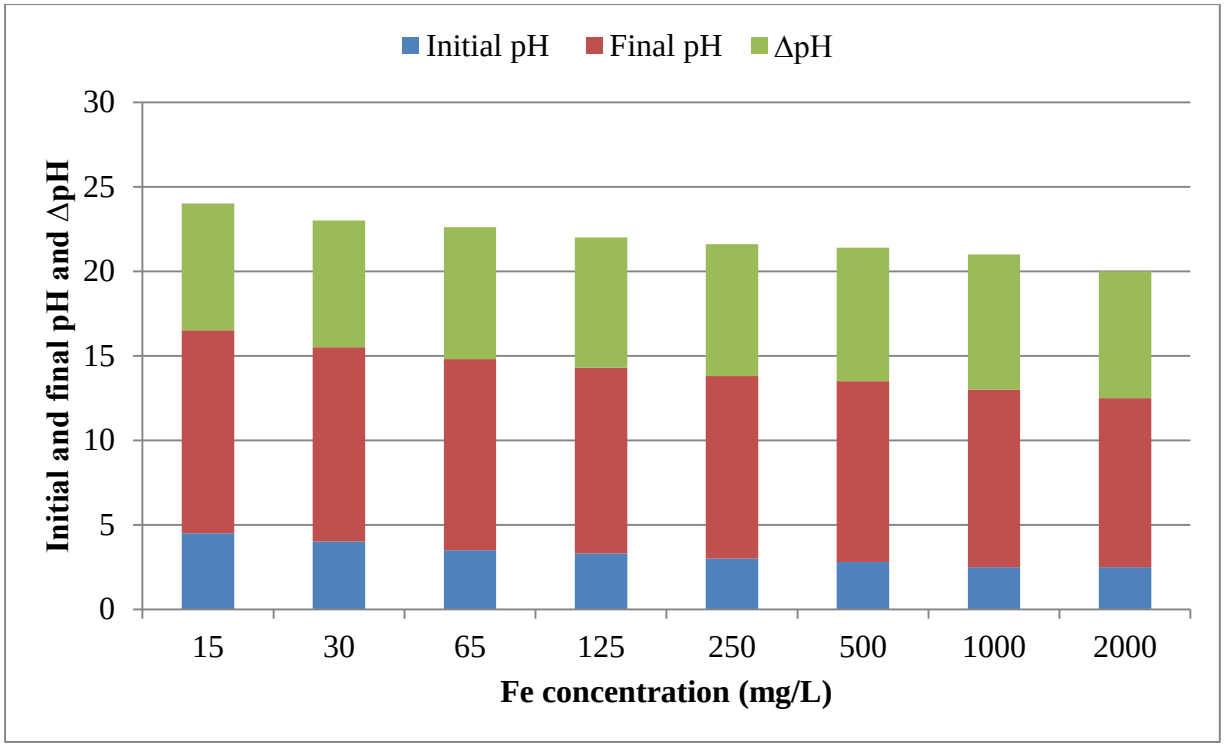

Figure 5.8: Variation of pH gradient with varying sulphate concentrations.

As the metal concentration increases, the initial pH was gradually decreasing, this may be attributed to hydrolysis of metal cations with the release of H^+ cations.

$$Fe^{3+} + H_2O \rightarrow Fe(OH)_{3(s)} + H^+ \quad 5.24$$

$$Al^{3+} + H_2O \rightarrow Al(OH)_{3(s)} + H^+ \quad 5.25$$

$$Mn^{2+} + H_2O \rightarrow Mn(OH)_{2(s)} + H^+ \quad 5.26$$

As shown in **Figure 5.8**, drastic increases in final pH were observed at varying Fe concentrations. Increases in pH were attributed to dissolution of calcite, periclase and magnesite, and release of base metal species from the clay matrices to aqueous solution. Adsorption of sulphate onto clay matrices with release of hydroxyl groups may also have contributed to increases in pH of the aqueous solutions.

5.4 Treatment of field AMD at optimized conditions

The results of AMD treatment with bentonite clay, magnesite and the composite are shown in **Table 5.4.**

Table 5.4: Chemical composition of raw AMD before and after treatment (chemical species in mg L^{-1})

Parameter	Field AMD	DWAS Guidelines	Bentonite treated AMD	Magnesite treated AMD	Composite treated AMD
pH	2.3	6 - 10	6	10.3	11.1
TDS	10237	0 - 1200	9872	4345.2	1145
EC	22713	0 - 700	16425	4635.6	2635
Na	171	0 - 50	316	164	223
K	18	NA	17	17	15
Mg	183	0 - 30	192	402	350
Ca	762	0 - 32	566	302	379
Al	190	0 – 0.9	1.1	< 0.03	< 0.03
Fe	259	0 – 0.1	15	<0.02	0.01
Mn	40	0 – 0.05	35	0.04	0.001
Cu	7.80	0 – 1	0.1	< 0.05	< 0.005
Zn	7.90	0 – 0.5	6.3	0.1	< 0.01
Pb	6.30	0 – 0.01	0.1	0.2	< 0.01
Co	41.30	NA	44.7	0.2	< 0.01
Ni	16.60	0 - 0.07	24.4	0.5	< 0.01
As	20	0.001	0.05	<0.01	<0.01
B	5	0.01	0.2	<0.01	<0.01
Cr	20	0.01	0.1	<0.01	<0.01
Mo	16	0.01	0.6	<0.01	<0.01
Se	17	0.02	0.9	<0.01	<0.01
Si	1.49	NA	5.29	5.7	0.6
SO_4^{2-}	4000	0 - 500	3454	1913	916

Note: DWAS stand for Department of Water Affairs and Sanitation

In field AMD the major ions are Ca, Mg, Na, Al, Fe and sulphate. After treatment, the resultant water had an increased pH with reduced metal species and sulphate concentrations. The composite treatment yielded water to within the DWAS Water Quality Guidelines. Bentonite showed insignificant increase in pH and a slight reduction in metal species. This

showed that the treatment is effective for wastewater with low metal concentrations and as such it can be used as a polishing process. Contact of cryptocrystalline magnesite at optimised conditions produced water conforming to the DWAS Water Quality Guidelines except for pH, EC, TDS, Mg and sulphate. A combination of magnesite and bentonite clay treatment increased the pH of the solution significantly and yielded water conforming to DWAS Guidelines. The pH was > 11, major metals removal was > 99%, oxyanions of As, B, Cr, Mo, Se and sulphate were also removed significantly (> 90%) while alkali and alkaline earth metals were also moderately removed (> 60%) hence indicating the superiority of the composite in the acid effluent treatment.

5.5 Characterisation

5.5.1 X-ray diffraction (XRD) analysis

The mineralogical composition of magnesite (1), bentonite clay (2), composite (3) and AMD-reacted composite (4) are shown in **Figure 5.9.**

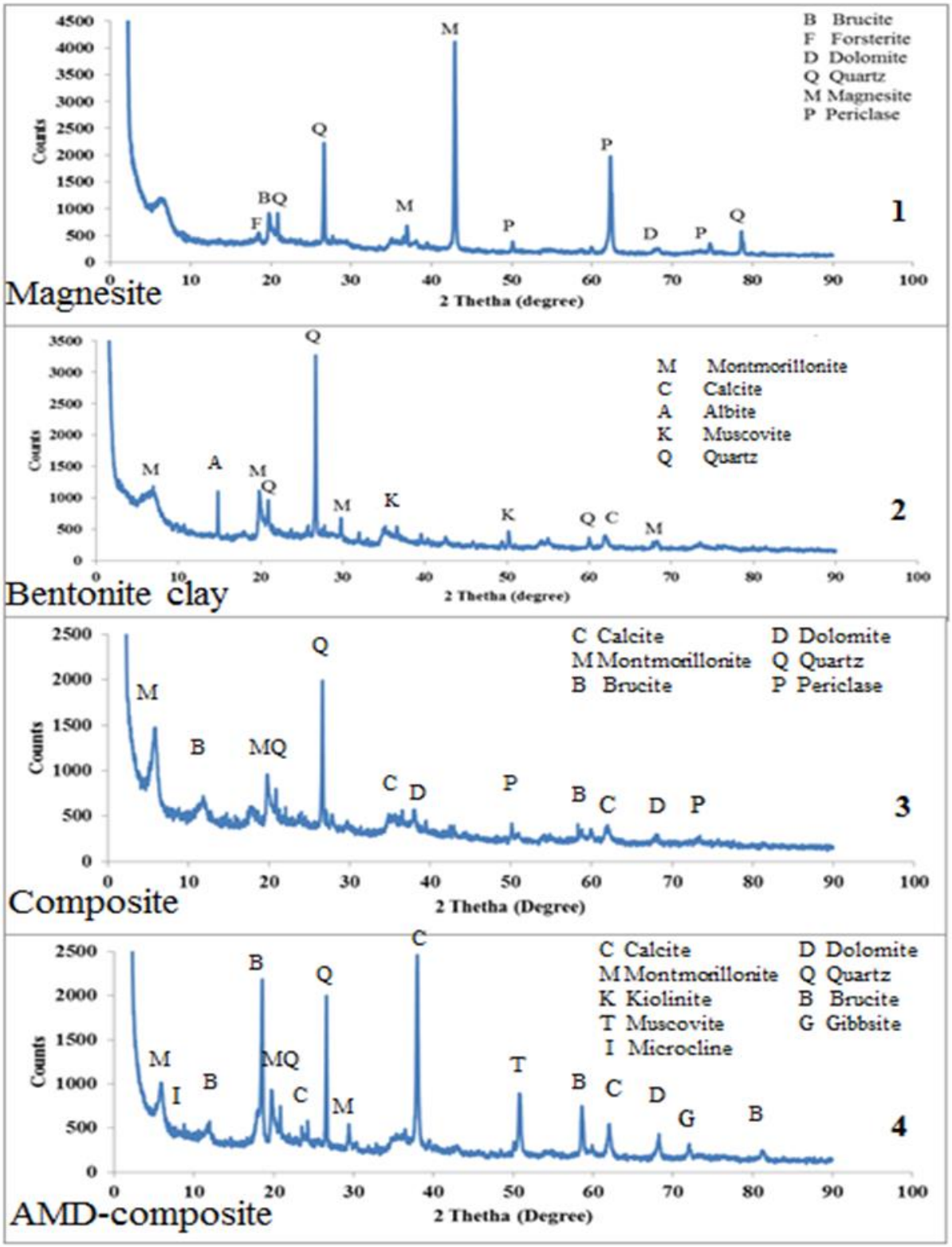

Figure 5.9: XRD patterns of cryptocrystalline magnesite (1), bentonite clay (2), composite (3) and AMD-reacted composite (4).

XRD analysis showed that magnesite consists of magnesite, periclase, brucite, quartz and forsterite as the main mineral phases**.** Bentonite clay was observed to contain

montmorillonite, quartz, calcite and muscovite**.** The composite was reported to contain montmorillonite, quartz, dolomite, calcite, brucite, periclase and muscovite**.** The mechanochemical synthesis of the bentonite clay in the presence of cryptocrystalline magnesite led to an amorphization of the magnesite and bentonite clay in the composite that was revealed through widening, as well as the reduction in the number and intensity of the reflection [**Figure 9(3)**]. AMD-reacted composite was observed to be constituted of montmorillonite, kaolinite, microcline, quartz, dolomite, brucite, calcite, gibbsite and muscovite [**Figure 9(4)**]**.** Quantitative mineralogical compositions of cryptocrystalline magnesite (1), bentonite clay (2), composite (3) and AMD-reacted composite (4) are shown in **Table 5.5.**

Table 5.5: Quantitative mineralogical compositions of bentonite clay, magnesite, composite and AMD-composite (Wt%)

Mineralogy	Magnesite (%)	Bentonite clay (%)	Composite (%)	AMD-composite (%)
Periclase	82		35	
Brucite	15	Ball milling		5
Forsterite	3			
Smectite		69	47	58
Quartz		19	10 + AMD =	
Calcite		4		8
Muscovite		4	2	17
Plagioclase		4		
Gibbsite			6	
Microcline				6

5.3.2 X-ray fluorescence (XRF) analysis

The elemental compositions of raw and AMD-reacted composite are shown in **Table 5.6 and 5.7.**

Table 5.6: Elemental compositions of raw and AMD-reacted composite

Element (Wt %)	Raw composite	AMD-reacted composite
SiO_2	29.97	27.12
TiO_2	0.22	0.19
Al_2O_3	6.64	6.05
Fe_2O_3	1.72	3.82
MnO	0.032	0.517
MgO	51.11	36.57
CaO	1.56	4.35
Na_2O	1.14	0.35
K_2O	0.51	0.43
P_2O_5	0.039	0.033
Cr_2O_3	0.012	0.020
SO_3	0.5	5
LOI	6.23	14.91
Total	99.23	99.35
H_2O-	3.57	2.99

Bentonite clay is mainly comprised of Al and Si confirming that the material under study is an alumino-silicate. The presence of Fe, Mg, Ca, Na and K on clay interlayers is indicating that these are the main exchangeable cations in bentonite clay matrices. Availability of Mg, Ca, Na and K will aid in the neutralisation of AMD. Magnesite is dominated by MgO. These results corroborated with the results obtained by Nasedkin et al. (2001) who suggested that cryptocrystalline magnesite is composed of close to 90% of MgO. The composite was dominated by Al, Mg and Si hence showing that the material is a combination of magnesite and a clay mineral. After contacting AMD with the composite, there was a drastic reduction in Na and K on the composite matrices. This may be described by an increase in Na and K is product water post treatment. Ca, SO_3, Mn and Fe were observed to increase in the secondary residue. This may be better explained by reduction of those chemical species in treated AMD (**Table 5.10**). Notable reduction in Na, K and Mg indicate that these are the exchangeable elements on composite galleries. After interaction with AMD, the resultant solid residue was shown to be enriched with chemical species that are prevalent in AMD, showing that the composite was scavenging chemical species from AMD.

Table 5.7: Trace elemental composition of raw and reacted composite

Elements (ppm)	Raw composite	AMD-reacted composite
As	<4	10
Ba	<5	99
Br	16	<2
Ce	<10	29
Co	1.2	1.2
Cr	6.9	8.6
Cs	104	<5
Cu	7.6	5.7
Ga	8.3	8.7
Hf	6	<3
La	<10	12
Mo	13	<2
Nb	163	8.6
Nd	35	16
Ni	79	80
Pb	11	14
Rb	<2	5.5
Sc	<3	3.5
Se	445	<1
Sm	17	<10
Sr	33	41
Ta	18	<2
Th	5.3	8.6
Tl	4.2	<3
Y	11	9
Zn	8.2	19
Zr	<2	60

Traces of Co, Cr, Cu, Ni, Pb and Zn were observed to be present in the secondary residues post treatment of AMD. This indicates that those elements were removed from AMD to secondary residues. Trace elements (**Table 5.7**) were also observed to be present at notable

levels in the secondary residues hence justifying less conductivity in the composition of the product water.

5.5.3 Fourier Transforms Infrared Spectrometry analysis

The functional groups in raw and AMD-reacted composite are shown in **Figure 5.10**.

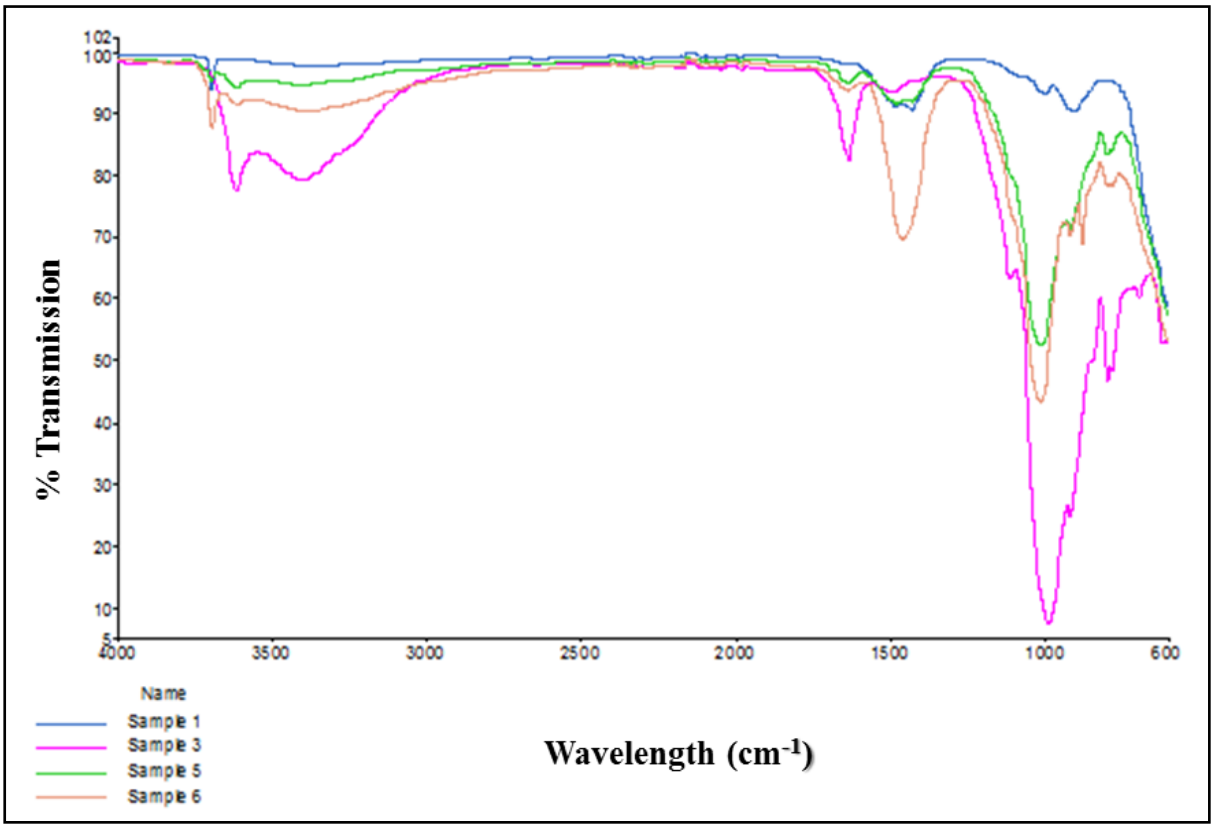

Figure 5.10: Fourier transforms infrared spectrometry **(**FTIR) Spectra for magnesite (sample1), bentonite clay (sample 3), composite (sample 5) and AMD-reacted composite (sample 6)

Raw magnesite (**Figure 5.10, sample 1**) is characterised of brucite bending corresponding to band 3702 cm^{-1}, periclase stretches corresponding to band 1500 and 950 cm^{-1} and magnesite stretching vibration corresponding to bands 1680, 1450, 850 cm^{-1}. The doublet at 1490, 1419 cm^{-1} corresponds to asymmetric stretching vibrations of carbonate. The reason for the split of this peak into a doublet could be due to the formation of new carbonates such as $CaCO_3$ and $MgCO_3$. The band at 1117 cm^{-1} correspond to symmetric stretching of carbonate, and those at 886, 795 cm^{-1} are assigned to in plane and out-of-plane bending vibrations of carbonate ion. The presence of carbonates in raw magnesite suggests the presence of Magnesite and calcite. Sharp peak at 1039 cm^{-1} belonged to the stretching of Si-O-Si bond in montmorillonite

tetrahedral sheet (**Figure 5.10, sample 3**). Peak at 3698 cm^{-1} was due to vibration of –OH in Mg-OH, while the vibration and bending of water molecule appeared at 3450 and 1654 cm^{-1} respectively. Sharp peak at 3616 cm^{-1} was assigned to the asymmetric stretching of Al-OH-Al in the aluminosilicate sheets of pristine montmorillonite (**Figure 5.10, sample 5**). Sharp peak at 1039 cm^{-1} is attributed to the stretching of Si-O-Si bond in montmorillonite tetrahedral sheet. Peak at 3698 cm^{-1} is attributed to vibration of –OH in Mg-OH, while the vibration and bending of OH in water molecule appeared at 3450 and 1654 cm^{-1} respectively. Spectroscopy results also showed that there was Si-O stretching at 1023 cm^{-1} and Al-OH-Al bending at 917 cm^{-1}. OH stretching at region 3628 – 3260 cm^{-1} shows the presence of hydroxyl groups on the composite. This will also contribute to an increase in pH during ion exchange. Moreover, the OH band at 3623 cm^{-1} indicates the coordination of Al^{3+} with OH group. Bands in 875 cm^{-1} and 836 cm^{-1} correspond to $Fe^{2+/3+}$ and Mg^{2+}. The stretching at 1500 cm^{-1} is corresponding to CO_3 stretching for calcite and magnesite. AMD-reacted composite shows CO_3 stretches were observed to be present hence indicating the formation of carbonates (**Figure 5.10, sample 6**). Majority of characteristic absorption bands of both bentonite clay and magnesite were also present in the composite spectra, suggesting a successful blend of the material.

5.5.4 Scanning Electron Microscope and Electron Dispersion X-ray

In order to better understand the mode of interaction of AMD and magnesite-bentonite clay composite and the formation of mineral phases, SEM was utilized to depict the change in morphology of the secondary solid residues as compared with the magnesite-bentonite clay composite (**Figure 5.11 - A, C and E**) and AMD-reacted magnesite-bentonite clay composite (**Figure 5.11 - B, D and F).**

The surface morphology of raw composite (**Figure 5.11 – A, C and E**) are showing that the composite contains leafy like structures and horny comb like structure meshed together. The structural morphology of AMD-reacted composite (**Figure 5.11 – B, D and F**) are showing the leafy like structures with rod like shapes been compacted together. This indicates that contacting the composite with AMD did not alter the morphological properties of clay.

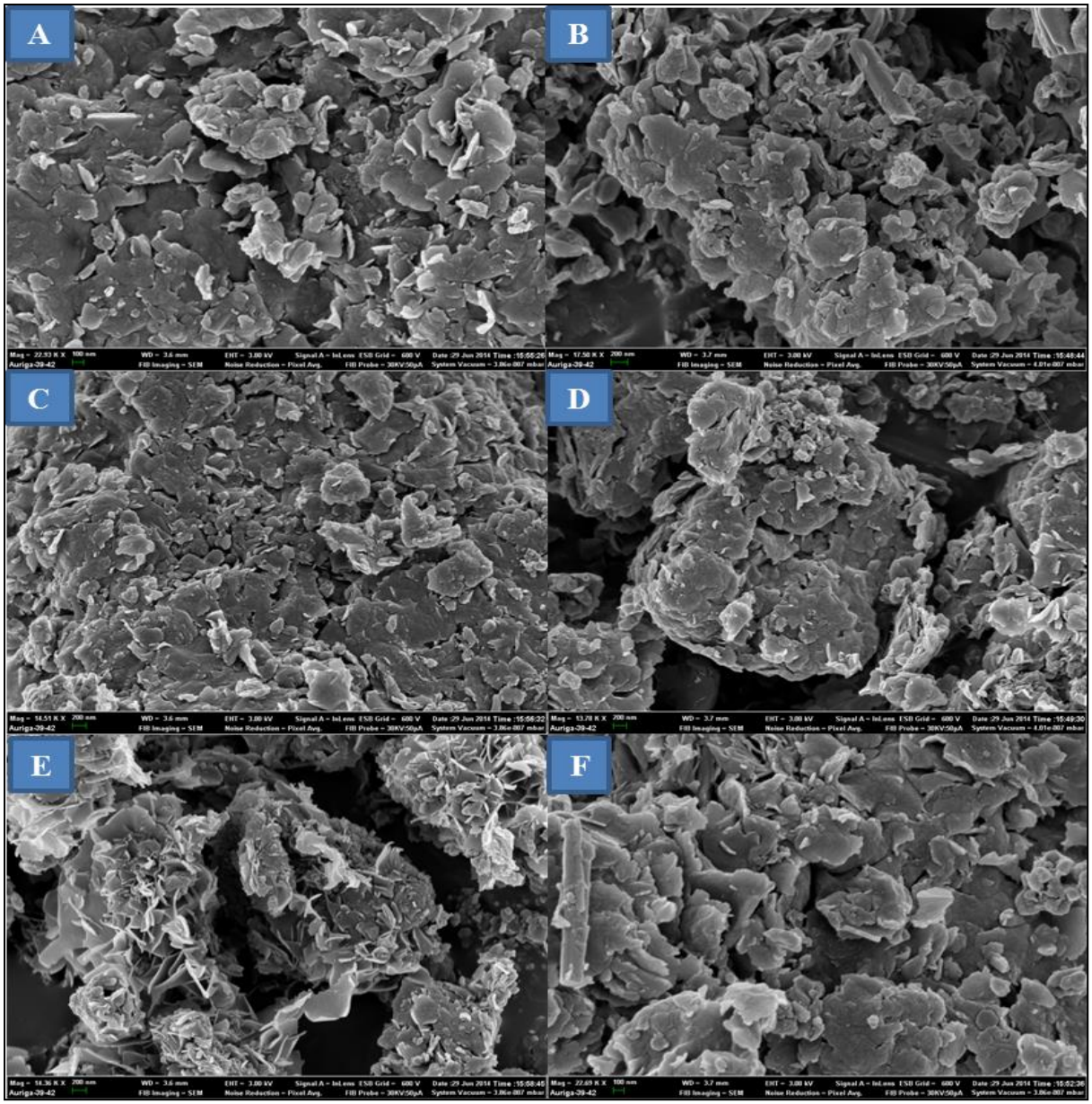

Figure 5.11: Morphological properties of magnesite-bentonite clay composite (**Figure 5.12 - A, C and E**) and AMD-reacted magnesite-bentonite clay composite (**Figure 5.11 - B, D and F).**

The morphologies of magnesite **Figure 5.12 (1)**, bentonite clay **Figure 5.12 (2)**, and magnesite-bentonite clay composite **Figure 5.12 (3)** are shown in **Figure 5.12.** SEM-EDX was utilized to semi-quantitatively identify the elemental constituent in individual minerals. Spot EDS analysis was done on selected solid residue samples (**Figure 5.12**).

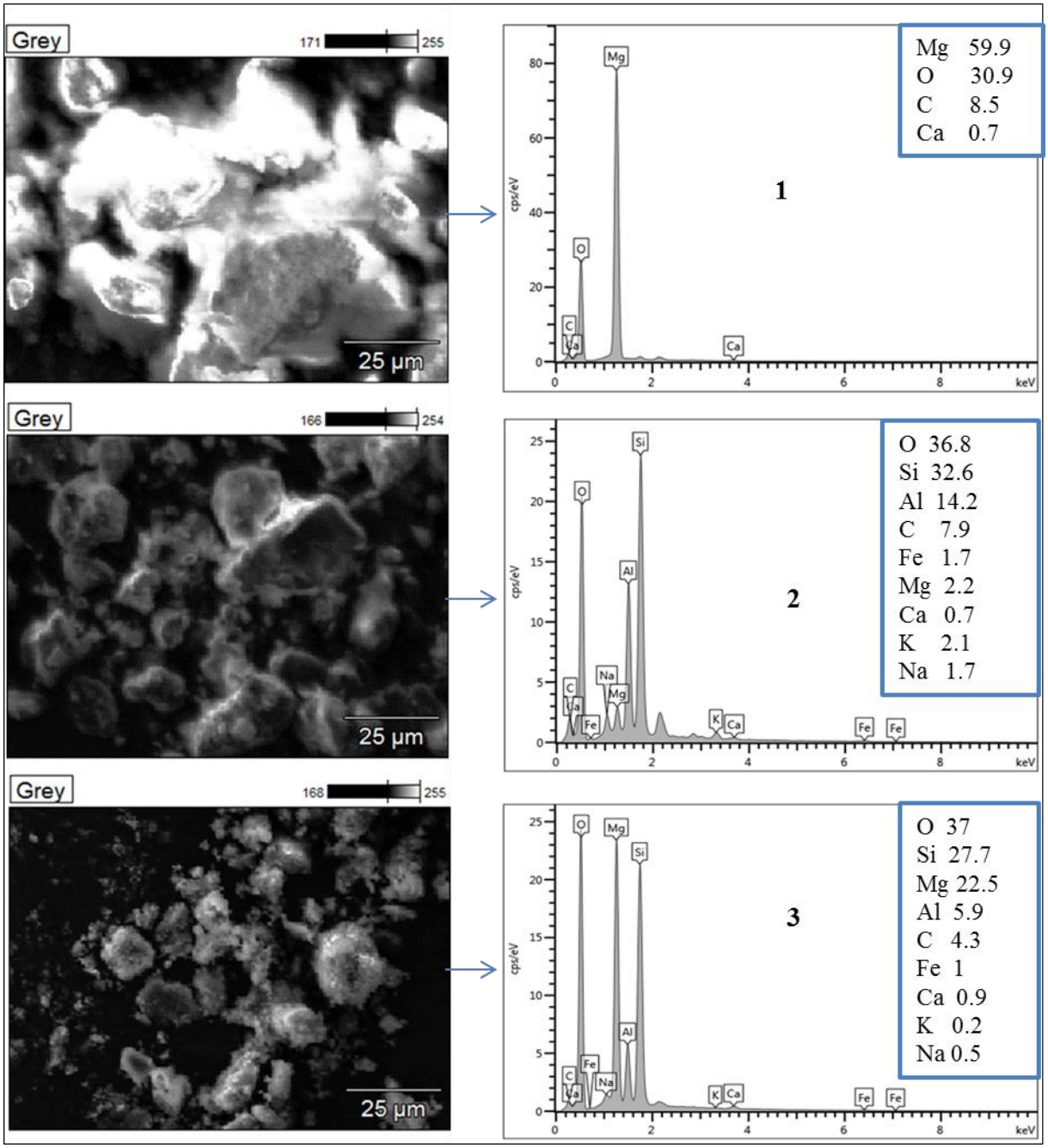

Figure 5.12: SEM-EDS elemental composition of cryptocrystalline magnesite (1), bentonite clay (2) and the composite (3).

The SEM results **(Figure 5.12)** provide important information about the morphology of magnesite, bentonite clay and the composite samples. **Figure 5.12 (1)** shows spherical aggregates on the surface of magnesite structure. EDS revealed the presence of C, O and Mg with trace of Ca.

The SEM-EDS in **Figure 5.12: (2)** showed that bentonite clay has sharp edges typically representing the presence of crystalline structures in raw bentonite clay. The EDS shows the presence of Al and Si at notable concentration hence indicating that they are the major species in bentonite clay structure. Fe, Mg, Ca, Na and K were observed to be presence hence indicating that these are the exchangeable cations.

The SEM-EDS in **Figure 5.12: (3)** shows that the raw composite of irregular (heterogeneous) in shape and size, and tend to be in the form of agglomerated clusters of small particles. The EDS shows that Al, Si and Mg are the major chemical species with traces of Fe, Ca, Na and K. The presence of Na, Mg, Ca and K indicates that these are the exchangeable cations on the composite interlayers. The present results corroborate results obtained by XRF.

The morphology of AMD-reacted composite are shown in **Figure 5.13.** SEM-EDX was utilized to semi-quantitatively identify the mineral phases resulting from the adsorption and neutralization reactions. Spot EDS analysis was done on selected solid residue samples

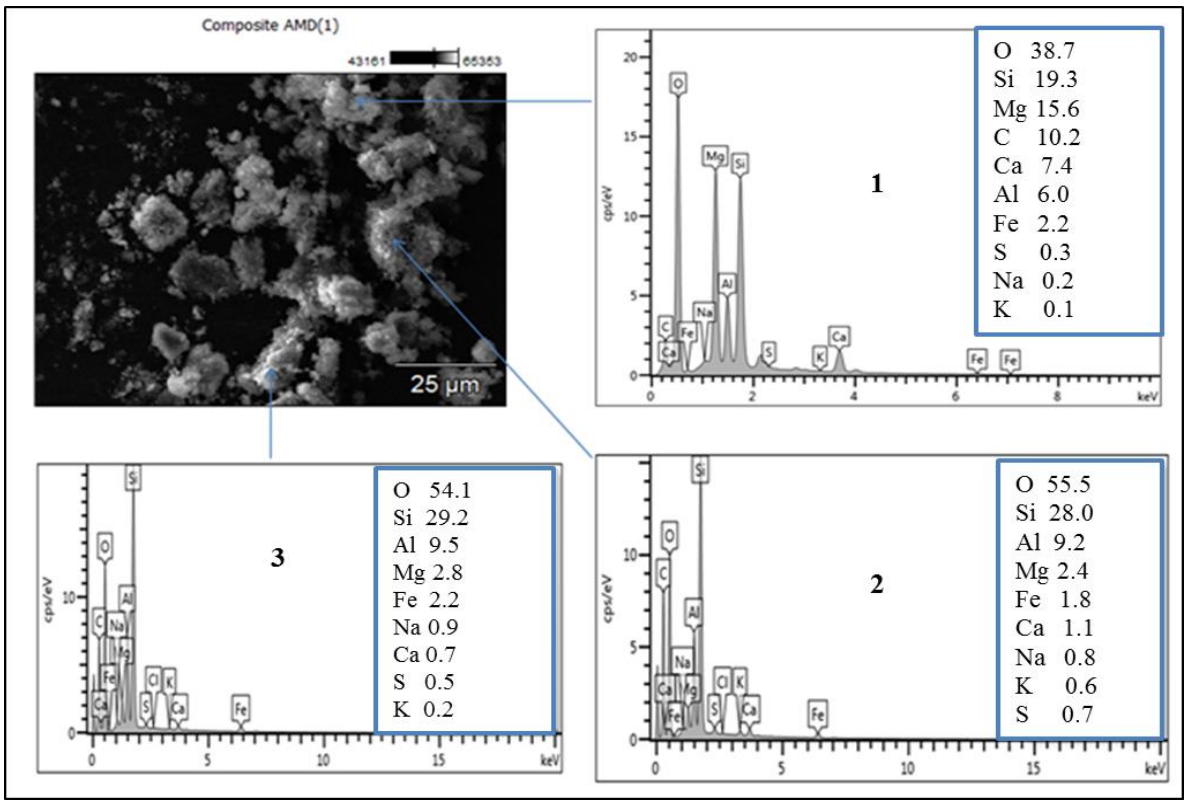

Figure 5.13: SEM-EDS elemental composition of AMD-reacted magnesite-bentonite clay composite.

The SEM image (Figure 5.5) shows that the particles are of the order of micrometres and have irregular shapes with sharp edges. The agglomerates were observed to contain flowery lumps suspended on the surface of reacted composite.

Spot 1 (Figure 5.13), revealed an increase in Al, Ca and Fe on the solid residues. This indicates that the species are removed from wastewater to solid residues. This confirmed by the reduction of those chemical species in the product water chemistry. The levels of Na, K and Mg were observed to have decreased. This indicates that these are the chemical species which are removed from composite interlayers when AMD is reacting with the composite since they are exchangeable cations. A decrease in Si is due to solubilisation on contact with AMD. This again indicated that bentonite clay is a sink for Fe; this was borne out by a significant reduction in levels of Fe in the product water showing that it had been adsorbed by the bentonite clay and ion exchange (release of Na, Mg, Ca and K ions) or precipitation during the dissolution of alkaline and earth alkali metals. There was a large decrease in Na on the AMD-reacted magnesite-bentonite clay composite (**Figure 5.13**) and an increase in Na concentration in the product water (**Table 5.10**) demonstrating that it is a highly exchanged cation. Ca was observed to increase, confirming the XRD results which showed the presence of calcite in the AMD-reacted magnesite-bentonite clay composite. This indicated that calcite was being formed as AMD reacted with AMD-reacted magnesite-bentonite clay composite. Sulphur was also present in the AMD-reacted magnesite-bentonite clay composite complex indicating that the composite is a sink for sulphate from AMD, mainly as oxyhydroxysulphates or gypsum on the composite micro-surfaces. The presence of Fe, Al, Ca, Mg, C and O suggest minerals such as Fe, Al oxide, metals hydroxides, Fe carbonate, gypsum, Al and Fe oxyhydrosulphates. The PHREEQC simulation also predicted precipitation of mineral phases bearing these metal species.

Spot 2 (Figure 5.13), revealed an increase in Al, Ca and Fe on the solid residues. This indicates that the species are removed from wastewater to solid residues. This confirmed by the reduction of those chemical species in the product water chemistry. The levels of Na, K and Mg were observed to have decreased. This indicates that these are the chemical species which are removed from composite interlayers when AMD is reacting with the composite since they are exchangeable cations. A decrease in Si is due to solubilisation on contact with AMD. This again indicated that bentonite clay is a sink for Fe; this was borne out by a significant reduction in levels of Fe in the product water showing that it had been adsorbed by the bentonite clay and ion exchange (release of Na, Mg, Ca and K ions) or precipitation

during the dissolution of alkaline and earth alkali metals. There was a large decrease in Na on the AMD-reacted magnesite-bentonite clay composite (**Figure 5.13**) and an increase in Na concentration in the product water (**Table 5.10**) demonstrating that it is a highly exchanged cation. Ca was observed to increase, confirming the XRD results which showed the presence of calcite in the AMD-reacted magnesite-bentonite clay composite. This indicated that calcite was being formed as AMD reacted with AMD-reacted magnesite-bentonite clay composite. Sulphur was also present in the AMD-reacted magnesite-bentonite clay composite complex indicating that the composite is a sink for sulphate from AMD, mainly as oxyhydroxysulphates or gypsum on the composite micro-surfaces. The presence of Fe, Al, Ca, Mg, C and O suggest minerals such as Fe, Al oxide, metals hydroxides, Fe carbonate, gypsum, Al and Fe oxyhydrosulphates. The PHREEQC simulation also predicted precipitation of mineral phases bearing these metal species.

Spot 3 (Figure 5.13), revealed the presence of an increase in Al, Ca and Fe on the solid residues. This indicates that the species are removed from wastewater to solid residues. This confirmed by the reduction of those chemical species in the product water chemistry. The levels of Na, K and Mg were observed to have decreased. This indicates that these are the chemical species which are removed from composite interlayers when AMD is reacting with the composite since they are exchangeable cations. A decrease in Si is due to solubilisation on contact with AMD. This again indicated that bentonite clay is a sink for Fe; this was borne out by a significant reduction in levels of Fe in the product water showing that it had been adsorbed by the bentonite clay and ion exchange (release of Na, Mg, Ca and K ions) or precipitation during the dissolution of alkaline and earth alkali metals. There was a large decrease in Na on the AMD-reacted magnesite-bentonite clay composite (**Figure 5.13**) and an increase in Na concentration in the product water (**Table 5.10**) demonstrating that it is a highly exchanged cation. Ca was observed to increase, confirming the XRD results which showed the presence of calcite in the AMD-reacted magnesite-bentonite clay composite. This indicated that calcite was being formed as AMD reacted with AMD-reacted magnesite-bentonite clay composite. Sulphur was also present in the AMD-reacted magnesite-bentonite clay composite complex indicating that the composite is a sink for sulphate from AMD, mainly as oxyhydroxysulphates or gypsum on the composite micro-surfaces. The presence of Fe, Al, Ca, Mg, C and O suggest minerals such as Fe, Al oxide, metals hydroxides, Fe carbonate, gypsum, Al and Fe oxyhydrosulphates. The PHREEQC simulation also predicted precipitation of mineral phases bearing these metal species.

5.5.4 Brunauer-Emmett-Teller and point of zero charge analysis

The results for surface area and pH_{PZC} for magnesite, bentonite clay, the composite and AMD-reacted composite are shown in **Table 5.8**.

Table 5.8: Surface are and point of zero charge (PZC) of magnesite, bentonite clay, magnesite-bentonite clay composite and AMD-reacted composite

Parameters	Magnesite	Bentonite clay	Raw composite	AMD-composite
Surface area (m^2/g)				
Single point surface area	16.64	37.05	18.33	15.94
BET surface area	16.76	37.21	18.36	16.17
Adsorption cumulative surface area pore	10.67	20.32	10.57	12.58
Pore volume (cm^3/g)				
Single point pore volume	0.079	0.08	0.07	0.072
Cumulative volume of pores	0.099	0.08	0.09	0.083
Pore size (nm)				
Adsorption average pore width	18.80	8.98	15.75	17.78
Adsorption average pore diameter	37.26	16.49	35.11	26.39
Point of Zero Charge (pH_{PZC})	10	8	10	10

Blending magnesite and bentonite clay resulted to a decrease in the surface area of the composite as compared to bentonite clay alone. The synthesized composite was determined to contain a surface area of 18.36 which decreased to 16.17 m^2/g after contacting the AMD hence indicating that the vacant surfaces on composite surfaces are occupied with specs of precipitating mineral phases which would block the pores of the composite reducing its surface area. This indicates the possible adsorption and deposition of materials to clay surfaces. The pH_{pzc} gives an insight on the type of chemical species that are more likely to be removed from aqueous solution during the reaction. When pH_{pzc} is greater than the supernatant pH, the adsorbent will adsorb anions. When the pH of the supernatant is above the pH_{pzc} the adsorbent will adsorb cations from the solution. A study by Masindi et al. (2014a) pointed out that aluminium and iron oxides have high pH_{PZC} values (≈ 8). The high pH_{PZC} of bentonite clay is due to the presence of aluminium and iron oxides or hydroxides in the clay matrix. The pH_{pzc} value of a material is a reflection of the individual pH_{pzc} values of the components present. Clay and oxide contents increase the pH_{pzc} of the material. Chemical

interaction could have occurred through multidentate ligands with the surface hydroxyl groups hence leading to inner and outer layer complexes.

5.4 Calculation of Saturation Indices (SI) for various mineral phases

The results for calculation of mineral precipitation at various pH values during treatment of simulated AMD with magnesite-bentonite clay composite are presented in **Table 5.9**.

Table 5.9: Calculation of SI for selected mineral phases at various pH

Mineral phase	**pH and saturation indices (SI)**					
	3	**4**	**6**	**8**	**10**	**11**
Alkalinity (eq/Kg)	$-3.6x10^{-2}$	$1.5x10^{-2}$	$6.4x10^{-2}$	$3x10^{-1}$	$-3x10^{-1}$	3.5
$Al(OH)_3$	-0.9	3.5	2.9	1.2	-0.1	-1.5
Boehmite (AlOOH)	-0.5	7	5	3.4	2.1	0.7
Basaluminite $Al_4(OH)_{10}SO_4$	-0.8	23	17.4	6	-1.4	-10.2
Brucite $Mg(OH)_2$	-11	-9	-6.6	-2	0.6	3.6
Calcite	-11	-2.3	-1.5	1.8	3.4	4
Aragonite	-8.6	-2.5	-0.2	1.7	3.7	3.8
Diaspore (AlOOH)	-0.9	8.3	6.8	5.1	3.1	2
Dolomite $CaMg(CO_3)_2$	-6	-2.5	-1.3	4.9	6.9	8
Epsomite	-7	-4	-2	-1.8	-1.8	-1.8
$Fe(OH)_3$	5	4.4	3.7	4.6	3.2	3.1
Gibbsite $Al(OH)_3$	0.3	6.7	5.5	3.7	1.8	0.8
Geothite (FeOOH)	6	8	9.7	10.5	9.1	9
Gypsum ($CaSO_4.H_2O$)	-0.1	-0.2	-0.2	4	5	8
Jarosite H $(H_3O)Fe_3(SO_4)_2(OH)_6$	5	3.2	2.9	-3.7	-16	-20
Jurbanite ($AlOHSO_4$)	1	5	2.5	-3.6	-9.8	-12.8
Rhodochrosite ($MnCO_3$)	-8.75	-0.9	-0.4	0	0	0
Manganite MnOOH	-8.1	-5.3	-2.9	4	6	8
Pyrochroite $Mn(OH)_2$	-8	-7.1	-6.4	0.2	0.9	2.2

As shown in **Table 5.8**, Fe could precipitate as hydroxides at pH > 3. Al could precipitate as hydroxides at pH > 4. Mn could precipitates as hydroxide at pH > 10 and rhodochrosite at pH > 8. Sulphate-bearing minerals could precipitates at pH 6 – 8 (basaluminite), pH > 8 (gypsum), pH 6 (jarosite and jurbanite). PHREEQC predicted mineral phases to precipitate as metal hydroxides, hydroxysulphates and oxyhydroxysulphates. However, sulphates were removed from solution together with Al, Fe and Ca. This corroborate the SEM-EDX and XRF detected Al, Fe, Mn and S rich mineral phases were deposited to solid residues. This indicates that the Al, Fe, Mn and S rich mineral phases were too amorphous to be detected by XRD or the concentration was below the detection limits. To be particular, the presence of Mn, Fe, Al, Ca, Mg, C and O suggest precipitation of minerals such as Mn, Fe, Al oxide, metals hydroxides, Mn and Fe carbonate, gypsum, Al and Fe oxyhydrosulphates, this was validated by PHREEQC geochemical model and SEM-EDS.

5.5 Conclusion

The vibratory ball mill was successfully used for the synthesis of the cryptocrystalline magnesite and bentonite clay composite. Milling blended the two materials hence increasing the surface area and making the materials more amorphous. The pronounced efficiencies in neutralization and attenuation of inorganic contaminants from AMD were observed to be superior as compared to bentonite clay and cryptocrystalline magnesite used individually. It was observed that the best conditions for synthesis of the composite are 1:1 wt%. Milling improved the physicochemical properties of the composite hence making the composite an excellent material for neutralization and attenuation of inorganic contaminants simultaneously. This makes the present study to conclude that the magnesite-bentonite composite has the capacity to neutralize AMD and remove potentially toxic chemical species. Optimization experiments revealed that 20 min of equilibration and 1 g of composite dosage were the optimum conditions under these laboratory conditions for treatment of AMD at 1:100 S/L ratios. Four processes were observed to govern the removal of inorganic contaminants from AMD using the composite, namely, (1) adsorption, (2) ion-exchange (3) precipitation and (4) co-precipitation. The adsorption process fitted to pseudo-second-order kinetics rather than pseudo-first-order kinetics, confirming that the step governing chemical reaction is chemisorption. In adsorption modelling the data conformed better to the Freundlich adsorption isotherm than Langmuir adsorption isotherm hence confirming multilayer adsorption. An increase in the levels of base cations in the product water as shown by ICP-MS and a decrease in the secondary residue as shown by XRF, and SEM-EDS

indicates that ion exchange was one of the mechanisms that were taking place during the removal of metal species from contaminated water bodies. PHREEQC geochemical model, revealed that Fe, Al, Mn, and Ca formed sulphate-bearing minerals. SEM-EDS, disclosed that the presence of Fe, Al, Ca, Mg, C and O suggest minerals such as Fe, Al oxide, metals hydroxides, Fe carbonate, gypsum, Al and Fe oxyhydrosulphates are formed as precipitates or co-precipitates. From modelling simulations, the formation of these phases follow a selective precipitation sequence with Fe^{3+} at pH > 6, Al^{3+} at pH > 6, Fe^{2+} at pH > 8, Mn^{2+}, Ca^{2+} and Mg^{2+} at pH >10. The composite proved to be effective for treatment of AMD as compared to traditional wastewater treatment methods such as limestone, magnesite, clays, lime and bentonite blend. It also produced water of useable standard for industrial and agricultural purposes. This study showed that magnesite and bentonite clay composite can be an efficient and effective technology for treatment of AMD.

REFERENCES

Achterberg, E. P., Herzl, V. M. C., Braungardt, C. B. & Millward, G. E. 2003. Metal behaviour in an estuary polluted by acid mine drainage: the role of particulate matter. *Environmental Pollution,* 121**,** 283-292.

Agboola, O., Schoeman, J. J., Maree, J., Mbaya, R. & Kolesnikov, A. 2012. Performance of an acid stable nanofiltration membrane for nickel removal from centration, solution pH and ionic strength aqueous solutions: Effects of con. *WIT Transactions on Ecology and the Environment,* 163**,** 415-424.

Anawar, H. M. 2013. Impact of climate change on acid mine drainage generation and contaminant transport in water ecosystems of semi-arid and arid mining areas. *Physics and Chemistry of the Earth, Parts A/B/C,* 58–60**,** 13-21.

Atekwana, E. A. & Fonyuy, E. W. 2009. Dissolved inorganic carbon concentrations and stable carbon isotope ratios in streams polluted by variable amounts of acid mine drainage. *Journal of Hydrology,* 372**,** 136-148.

Baker, B. J. & Banfield, J. F. 2003. Microbial communities in acid mine drainage. *FEMS Microbiology Ecology,* 44**,** 139-152.

Bhattacharyya, K. G. & Gupta, S. S. 2008. Adsorption of a few heavy metals on natural and modified kaolinite and montmorillonite: A review. *Advances in Colloid and Interface Science,* 140**,** 114-131.

Bhattacharyya, K. G. & Gupta, S. S. 2011. Removal of Cu(II) by natural and acid-activated clays: An insight of adsorption isotherm, kinetic and thermodynamics. *Desalination,* 272**,** 66-75.

Bhattacharyya, K. G. & Sen Gupta, S. 2006. Pb(II) uptake by kaolinite and montmorillonite in aqueous medium: Influence of acid activation of the clays. *Colloids and Surfaces A: Physicochemical and Engineering Aspects,* 277**,** 191-200.

Blowes, D. W., Ptacek, C. J., Jambor, J. L., Weisener, C. G., Paktunc, D., Gould, W. D. & Johnson, D. B. 2014. 11.5 - The Geochemistry of Acid Mine Drainage. *In:* TUREKIAN, H. D. H. K. (ed.) *Treatise on Geochemistry (Second Edition).* Oxford: Elsevier**,** 131-190.

Bologo, V., Maree, J. P. & Carlsson, F. 2012. Application of magnesium hydroxide and barium hydroxide for the removal of metals and sulphate from mine water. *Water SA,* 38**,** 23-28.

Bortnikova, S. B., Smolyakov, B. S., Sidenko, N. V., Kolonin, G. R., Bessonova, E. P. & Androsova, N. V. 2001. Geochemical consequences of acid mine drainage into a natural reservoir: Inorganic precipitation and effects on plankton activity. *Journal of Geochemical Exploration,* 74**,** 127-139.

Candeias, C., Ávila, P. F., Ferreira Da Silva, E., Ferreira, A., Salgueiro, A. R. & Teixeira, J. P. 2014. Acid mine drainage from the Panasqueira mine and its influence on Zêzere river (Central Portugal). *Journal of African Earth Sciences,* 99, Part 2**,** 705-712.

Chockalingam, E. & Subramanian, S. 2009. Utility of Eucalyptus tereticornis (Smith) bark and Desulfotomaculum nigrificans for the remediation of acid mine drainage. *Bioresource Technology,* 100**,** 615-621.

Couceiro, M. a. A. & Schettini, C. a. F. 2010. Assessment of the suspended sediment dynamics of the Araranguá river estuary (SC): Possible effects of acid drainage from the coal mining activity. *Geociencias,* 29**,** 251-266.

Courtin-Nomade, A., Grosbois, C., Bril, H. & Roussel, C. 2005. Spatial variability of arsenic in some iron-rich deposits generated by acid mine drainage. *Applied Geochemistry,* 20**,** 383-396.

Cruz Viggi, C., Pagnanelli, F., Cibati, A., Uccelletti, D., Palleschi, C. & Toro, L. 2010. Biotreatment and bioassessment of heavy metal removal by sulphate reducing bacteria in fixed bed reactors. *Water Research,* 44**,** 151-158.

Denicola, D. M. & Stapleton, M. G. 2002. Impact of acid mine drainage on benthic communities in streams: The relative roles of substratum vs. aqueous effects. *Environmental Pollution,* 119**,** 303-315.

Djukić, A., Jovanović, U., Tuvić, T., Andrić, V., Grbović Novaković, J., Ivanović, N. & Matović, L. 2013. The potential of ball-milled Serbian natural clay for removal of heavy metal contaminants from wastewaters: Simultaneous sorption of Ni, Cr, Cd and Pb ions. *Ceramics International,* 39**,** 7173-7178.

Druschel, G. K., Baker, B. J., Gihring, T. M. & Banfield, J. F. 2004. Acid mine drainage biogeochemistry at Iron Mountain, California. *Geochemical Transactions,* 5**,** 13-32.

Đukić, A. B., Kumrić, K. R., Vukelić, N. S., Dimitrijević, M. S., Baščarević, Z. D., Kurko, S. V. & Matović, L. L. 2015. Simultaneous removal of Pb(II), Cu(II), Zn(II) and Cd(II) from highly acidic solutions using mechanochemically synthesized montmorillonite–kaolinite/TiO2 composite. *Applied Clay Science,* 103**,** 20-27.

España, J. S., Pamo, E. L., Santofimia, E., Aduvire, O., Reyes, J. & Barettino, D. 2005. Acid mine drainage in the Iberian Pyrite Belt (Odiel river watershed, Huelva, SW Spain):

Geochemistry, mineralogy and environmental implications. *Applied Geochemistry,* 20**,** 1320-1356.

Falayi, T. & Ntuli, F. 2014. Removal of heavy metals and neutralisation of acid mine drainage with un-activated attapulgite. *Journal of Industrial and Engineering Chemistry,* 20**,** 1285-1292.

Ferreira Da Silva, E., Bobos, I., Xavier Matos, J., Patinha, C., Reis, A. P. & Cardoso Fonseca, E. 2009. Mineralogy and geochemistry of trace metals and REE in volcanic massive sulfide host rocks, stream sediments, stream waters and acid mine drainage from the Lousal mine area (Iberian Pyrite Belt, Portugal). *Applied Geochemistry,* 24**,** 383-401.

Gaikwad, R. W. 2010. Review and research needs of active treatment of acid mine drainage by ion exchange. *Electronic Journal of Environmental, Agricultural and Food Chemistry,* 9**,** 1343-1350.

Galan, E., Carretero, M. I. & Fernandez-Caliani, J. C. 1999. Effects of acid mine drainage on clay minerals suspended in the Tinto river (Rio Tinto, Spain). An experimental approach. *Clay Minerals,* 34**,** 99-108.

Gammons, C. H., Duaime, T. E., Botsford, W. S., Parker, S. R. & Grant, T. Geochemistry and hydrogeology of acid mine drainage in the Great Falls-Lewistown coal field, Montana. 7th International Conference on Acid Rock Drainage 2006, ICARD - Also Serves as the 23rd Annual Meetings of the American Society of Mining and Reclamation, 2006. 630-647.

Ghosh, S., Moitra, M., Woolverton, C. J. & Leff, L. G. 2012. Effects of remediation on the bacterial community of an acid mine drainage impacted stream. *Canadian Journal of Microbiology,* 58**,** 1316-1326.

Gitari, M., Petrik, L., Etchebers, O., Key, D., Iwuoha, E. & Okujeni, C. 2006. Treatment of acid mine drainage with fly ash: Removal of major contaminants and trace elements. *Journal of Environmental Science and Health - Part A Toxic/Hazardous Substances and Environmental Engineering,* 41**,** 1729-1747.

Gitari, W. M. 2014. Attenuation of metal species in acidic solutions using bentonite clay: implications for acid mine drainage remediation. *Toxicological and Environmental Chemistry*.

Gray, N. F. & Delaney, E. 2010. Measuring community response of bentic macroinvertebrates in an erosional river impacted by acid mine drainage by use of a simple model. *Ecological Indicators,* 10**,** 668-675.

Groudev, S., Georgiev, P., Spasova, I. & Nicolova, M. 2008. Bioremediation of acid mine drainage in a uranium deposit. *Hydrometallurgy,* 94**,** 93-99.

Grout, J. A. & Levings, C. D. 2001. Effects of acid mine drainage from an abandoned copper mine, Britannia Mines, Howe Sound, British Columbia, Canada, on transplanted blue mussels (Mytilus edulis). *Marine Environmental Research,* 51**,** 265-288.

Gupta, S. S. & Bhattacharyya, K. G. 2006. Removal of Cd(II) from aqueous solution by kaolinite, montmorillonite and their poly(oxo zirconium) and tetrabutylammonium derivatives. *Journal of Hazardous Materials,* 128**,** 247-257.

Gupta, S. S. & Bhattacharyya, K. G. 2011. Kinetics of adsorption of metal ions on inorganic materials: a review. *Adv. Colloid Interface Sci.,* 162**,** 39-58.

Hallberg, K. B. 2010. New perspectives in acid mine drainage microbiology. *Hydrometallurgy,* 104**,** 448-453.

Hamzaoui, R., Muslim, F., Guessasma, S., Bennabi, A. & Guillin, J. 2015. Structural and thermal behavior of proclay kaolinite using high energy ball milling process. *Powder Technology,* 271**,** 228-237.

Hlabela, P., Maree, J. & Bruinsma, D. 2007. Barium carbonate process for sulphate and metal removal from mine water. *Mine Water and the Environment,* 26**,** 14-22.

Johnson, D. B. & Hallberg, K. B. 2005. Acid mine drainage remediation options: a review. *Science of The Total Environment,* 338**,** 3-14.

Kim, W., Kim, K., Lee, H., Shin, M. & Kim, S. 2013. Mechanochemical activation on the preparation of β-eucryptite from powder mixture of pyrophyllite, gibbsite and lithium carbonate. *Materials Transactions,* 54**,** 380-383.

Levings, C. D., Varela, D. E., Mehlenbacher, N. M., Barry, K. L., Piercey, G. E., Guo, M. & Harrison, P. J. 2005. Effect of an acid mine drainage effluent on phytoplankton biomass and primary production at Britannia Beach, Howe Sound, British Columbia. *Marine Pollution Bulletin,* 50**,** 1585-1594.

Macedo-Sousa, J. A., Gerhardt, A., Brett, C. M. A., Nogueira, A. J. A. & Soares, A. M. V. M. 2008. Behavioural responses of indigenous benthic invertebrates (Echinogammarus meridionalis, Hydropsyche pellucidula and Choroterpes picteti) to a pulse of Acid Mine Drainage: A laboratorial study. *Environmental Pollution,* 156**,** 966-973.

Mapanda, F., Nyamadzawo, G., Nyamangara, J. & Wuta, M. 2007. Effects of discharging acid-mine drainage into evaporation ponds lined with clay on chemical quality of the surrounding soil and water. *Physics and Chemistry of the Earth, Parts A/B/C,* 32**,** 1366-1375.

Maree, J. P., Bosman, D. J. & Jenkins, G. R. 1989. Chemical removal of sulphate, calcium and heavy metals from mining and power station effluents. *Water Sewage Effluent,* 9**,** 10-25.

Maree, J. P., De Beer, M., Strydom, W. F., Christie, A. D. M. & Waanders, F. B. 2004. Neutralizing coal mine effluent with limestone to decrease metals and sulphate concentrations. *Mine Water and the Environment,* 23**,** 81-86.

Maree, J. P., Dingemans, D., Van Tonder, G. J. & Mtimkulu, S. 1998. Biological iron(II) oxidation as pre-treatment to limestone neutralisation of acid water. *Water Science and Technology,* 38**,** 331-337.

Maree, J. P., Mujuru, M., Bologo, V., Daniels, N. & Mpholoane, D. 2013. Neutralisation treatment of AMD at affordable cost. *Water SA,* 39**,** 245-250.

Martins, N., Bollinger, C., Harper, R. M. & Ribeiro, R. 2009. Effects of acid mine drainage on the genetic diversity and structure of a natural population of Daphnia longispina. *Aquatic Toxicology,* 92**,** 104-112.

Masindi, V., Gitari, M. W., Tutu, H. & De Beer, M. 2014a. Application of magnesite–bentonite clay composite as an alternative technology for removal of arsenic from industrial effluents. *Toxicological and Environmental Chemistry,* 96**,** 1435-1451.

Masindi, V., Gitari, M. W., Tutu, H. & De Beer, M. 2014b. Application of magnesite–bentonite clay composite as an alternative technology for removal of arsenic from industrial effluents. *Toxicological & Environmental Chemistry***,** 1-17.

Masindi, V., Gitari, W. M. & Ngulube, T. 2014c. Defluoridation of drinking water using Al3+-modified bentonite clay: optimization of fluoride adsorption conditions. *Toxicological & Environmental Chemistry***,** 1-16.

Masukume, M., Onyango, M. S. & Maree, J. P. 2014. Sea shell derived adsorbent and its potential for treating acid mine drainage. *International Journal of Mineral Processing,* 133**,** 52-59.

Mitrović, A. & Zdujić, M. 2014. Preparation of pozzolanic addition by mechanical treatment of kaolin clay. *International Journal of Mineral Processing,* 132**,** 59-66.

Motsi, T., Rowson, N. A. & Simmons, M. J. H. 2009. Adsorption of heavy metals from acid mine drainage by natural zeolite. *International Journal of Mineral Processing,* 92**,** 42-48.

Narayanan, D. L. & Lueking, A. D. 2007. Mechanically milled coal and magnesium composites for hydrogen storage. *Carbon,* 45**,** 805-820.

Nasedkin, V. V., Krupenin, M. T., Safonov, Y. G., Boeva, N. M., Efremova, S. V. & Shevelev, A. I. 2001. The comparison of amorphous (cryptocrystalline) and crystalline magnesites. *Mineralia Slovaca,* 33**,** 567-574.

Netto, E., Madeira, R. A., Silveira, F. Z., Fiori, M. A., Angioleto, E., Pich, C. T. & Geremias, R. 2013. Evaluation of the toxic and genotoxic potential of acid mine drainage using physicochemical parameters and bioassays. *Environmental Toxicology and Pharmacology,* 35**,** 511-516.

Nkonyane, T., Ntuli, T. & Muzenda, E. 2012. Treatment of acid mine drainage using unactivated bentonite and limestone. *World Academy of Science, Engineering and Technology,* 68**,** 139-144.

Pagnanelli, F., De Michelis, I., Di Muzio, S., Ferella, F. & Vegliò, F. 2008. Bioassessment of a combined chemical–biological treatment for synthetic acid mine drainage. *Journal of Hazardous Materials,* 159**,** 567-573.

Paik, B., Walton, A., Mann, V., Book, D., Jones, I. P. & Harris, I. R. 2010. Microstructure of ball milled MgH2 powders upon hydrogen cycling: An electron microscopy study. *International Journal of Hydrogen Energy,* 35**,** 9012-9020.

Parkhurst, D. L. & Appelo, C. a. J. 1999. Users guide to Phreeqc (Version 2) - A computer program for speciation, batch-reactions, one-dimensional transport and inverse geochemical calculations. *Water-Resources Investigations Report 99-4259.*

Ramírez-Paredes, F. I., Manzano-Muñoz, T., Garcia-Prieto, J. C., Zhadan, G. G., Shnyrov, V. L., Kennedy, J. F. & Roig, M. G. 2011. Biosorption of heavy metals from acid mine drainage onto biopolymers (chitin and α (1,3) β-D-glucan) from industrial biowaste exhausted brewer's yeasts (Saccharomyces cerevisiae L.). *Biotechnology and Bioprocess Engineering,* 16**,** 1262-1272.

Rusmin, R., Sarkar, B., Liu, Y., Mcclure, S. & Naidu, R. 2015. Structural evolution of chitosan–palygorskite composites and removal of aqueous lead by composite beads. *Applied Surface Science,* 353**,** 363-375.

Sankaranarayanan, S., Jayalakshmi, S. & Gupta, M. 2011. Effect of ball milling the hybrid reinforcements on the microstructure and mechanical properties of Mg–(Ti(II);n-Al2O3) composites. *Journal of Alloys and Compounds,* 509**,** 7229-7237.

Sarkar, B., Xi, Y., Megharaj, M., Krishnamurti, G. S. R., Rajarathnam, D. & Naidu, R. 2010. Remediation of hexavalent chromium through adsorption by bentonite based Arquad® 2HT-75 organoclays. *Journal of Hazardous Materials,* 183**,** 87-97.

Sheoran, A. S. & Sheoran, V. 2006. Heavy metal removal mechanism of acid mine drainage in wetlands: A critical review. *Minerals Engineering,* 19**,** 105-116.

Shou, J., Jiang, C., Wang, F., Qiu, M. & Xu, Q. 2015. Fabrication of Fe3O4/MgAl-layered double hydroxide magnetic composites for the effective decontamination of Co(II) from synthetic wastewater. *Journal of Molecular Liquids,* 207**,** 216-223.

Simate, G. S. & Ndlovu, S. 2014. Acid mine drainage: Challenges and opportunities. *Journal of Environmental Chemical Engineering,* 2**,** 1785-1803.

Şimşek, S., Baybaş, D., Koçyiğit, M. C. & Yildirim, H. 2014. Organoclay modified with lignin as a new adsorbent for removal of Pb(II) and UO(II) . *Journal of Radioanalytical and Nuclear Chemistry,* 299**,** 283-292.

Sracek, O., Choquette, M., Gélinas, P., Lefebvre, R. & Nicholson, R. V. 2004. Geochemical characterization of acid mine drainage from a waste rock pile, Mine Doyon, Québec, Canada. *Journal of Contaminant Hydrology,* 69**,** 45-71.

Tutu, H., Mccarthy, T. S. & Cukrowska, E. 2008. The chemical characteristics of acid mine drainage with particular reference to sources, distribution and remediation: The Witwatersrand Basin, South Africa as a case study. *Applied Geochemistry,* 23**,** 3666-3684.

Wade, C., Dold, B. & Fontboté, L. Geochemistry and mineralogy of the Quiulacocha tailings impoundment from the polymetallic Zn-Pb-(Ag-Bi-Cu) deposit Cerro de Pasco, Peru. 7th International Conference on Acid Rock Drainage 2006, ICARD - Also Serves as the 23rd Annual Meetings of the American Society of Mining and Reclamation, 2006. 2199-2206.

Yesilnacar, M. I. & Kadiragagil, Z. 2013. Effects of acid mine drainage on groundwater quality: A case study from an open-pit copper mine in eastern Turkey. *Bulletin of Engineering Geology and the Environment,* 72**,** 485-493.

Yuan, G. D., Theng, B. K. G., Churchman, G. J. & Gates, W. P. 2013. Chapter 5.1 - Clays and Clay Minerals for Pollution Control. *In:* FAÏZA, B. & GERHARD, L. (eds.) *Developments in Clay Science.* Elsevier**,** 587-644.

Zänker, H., Moll, H., Richter, W., Brendler, V., Hennig, C., Reich, T., Kluge, A. & Hüttig, G. 2002. The colloid chemistry of acid rock drainage solution from an abandoned Zn-Pb-Ag mine. *Applied Geochemistry,* 17**,** 633-648.

Zhang, M. 2011. Adsorption study of Pb(II), Cu(II) and Zn(II) from simulated acid mine drainage using dairy manure compost. *Chemical Engineering Journal,* 172**,** 361-368.

Zhao, F., Cong, Z., Sun, H. & Ren, D. 2007. The geochemistry of rare earth elements (REE) in acid mine drainage from the Sitai coal mine, Shanxi Province, North China. *International Journal of Coal Geology,* 70**,** 184-192.

Zhao, H., Xia, B., Qin, J. & Zhang, J. 2012. Hydrogeochemical and mineralogical characteristics related to heavy metal attenuation in a stream polluted by acid mine drainage: A case study in Dabaoshan Mine, China. *Journal of Environmental Sciences,* 24**,** 979-989.

Zhao, Y., Qi, W., Chen, G., Ji, M. & Zhang, Z. 2015. Behavior of Cr(VI) removal from wastewater by adsorption onto HCl activated Akadama clay. *Journal of the Taiwan Institute of Chemical Engineers,* 50**,** 190-197.

Zhao, Y., Zhang, L.-Y., Ni, F., Xi, B., Xia, X., Peng, X. & Luan, Z. 2011. Evaluation of a novel composite inorganic coagulant prepared by red mud for phosphate removal. *Desalination,* 273**,** 414-420.

Zhuang, G., Zhang, Z., Guo, J., Liao, L. & Zhao, J. 2015. A new ball milling method to produce organo-montmorillonite from anionic and nonionic surfactants. *Applied Clay Science,* 104**,** 18-26.

Zhuravleva, K., Bönisch, M., Scudino, S., Calin, M., Schultz, L., Eckert, J. & Gebert, A. 2014. Phase transformations in ball-milled Ti–40Nb and Ti–45Nb powders upon quenching from the ß-phase region. *Powder Technology,* 253**,** 166-171.

Zipper, C. E. & Skousen, J. G. 2010. Influent water quality affects performance of passive treatment systems for acid mine drainage. *Mine Water and the Environment,* 29**,** 135-143.

CHAPTER SIX

CONCLUSIONS AND RECOMMENDATIONS

6.1 Conclusion

This study was designed with an attempt to answer the following questions pertaining to the application of cryptocrystalline magnesite-bentonite clay composite for neutralisation of acidity and attenuation of chemical species concentration from gold mine waters.

- What are the chemical compositions of AMD from the Witwatersrand Western Basin, Gauteng, South Africa?
- What are the physicochemical and mineralogical properties of cryptocrystalline magnesite, bentonite clay and the composite before and after interaction?
- What is the chemistry of processed water after interacting AMD with the cryptocrystalline magnesite?
- What is the chemistry of processed water after interacting AMD with the ball milled bentonite clay?
- What is the chemistry of the processed water after interacting AMD with magnesite/bentonite clay composite?
- What is the chemical composition of the processed water is after interaction of AMD with cryptocrystalline magnesite and the composite as compared to department of water affairs and sanitation (DWAS) water quality guidelines?

6.1.1 Characterization of aqueous solution

Analysis of chemical composition of AMD by ICP-MS revealed that the AMD from the Witwatersrand basin contains on average 4635 mg/L sulphate, pH 2.3, TDS of 10237 mg/L, EC of 22713 µS/cm, 248.4 mg/L of Na^{+}, 21.6 mg/L of K^{+}, 2.3 mg/L of Mg^{2+}, 710.8 mg/L of Ca^{2+}, 1243 mg/L of total Fe, 134.4 mg/L of Al^{3+}, 91.5 mg/L of Mn^{2+}, 41.3 mg/L of Co^{2+}, 7.8 mg/L of Cu^{2+}, 16.6 mg/L of Ni^{2+}, 6.3 mg/L of Pb^{2+}, 7.9 mg/L of Zn^{2+}, 2.3 mg/L of Mg^{2+}, 16.6 mg/L of Ni^{2+}, some radioactivity and 200 mg/L acidity (as CaCO3). Oxyanionic species were observed as follows 20 mg/L of As, 5 mg/L of B, 20 mg/L of Cr, 16 mg/L of Mo and 17

mg/L of Se. This results proves that AMD is a highly polluted water that can pose hazardous impact to living organisms on exposure.

6.1.2 Characterization of magnesite

Magnesite was reported to contain brucite, forsterite, dolomite, quartz, magnesite and periclase as the mineral phases. After interacting with AMD, brucite, calcite, dolomite, forsterite, quartz and magnetite were observed to be present in the secondary residues. This could be explained by a decrease of those chemical species in AMD. FTIR showed the availability of brucite, magnesite, and carbonate stretches on raw magnesite. After contacting AMD with raw magnesite, brucite and carbonate stretches hence indicating the formation of siderite, rhodochrosite, calcite and dolomite. SEM-EDS showed that the morphology of cryptocrystalline magnesite contains spherical, leafy like and rod shaped structures hence indicating that the material is heterogeneous. EDS revealed high levels of C, O, and Mg with traces of Ca hence confirming that it is magnesium carbonate. After contacting AMD with magnesite the leafy like, spherical and sheet structures have disappeared after reaction hence indicating the dissolution of magnesite on contact with AMD. Appearance of rod like structures and aggregated lump-like structures indicates formation of new mineral phases in the solid residues. Raw magnesite was observed to contain MgO as the major component with traces of Si and Ca. The levels of Al, Fe, Mg, Ca, Mn and S were observed to increase in the resultant solid residues indicating formation of new phases. ELTRA analytical technique revealed that magnesite contains 6% of carbon on raw material and 8% elemental composition post interaction with AMD. This shows that the material understudy is a carbonate and it sink more carbonate when reacting with carbon rich solution. Sulphur content was recorded to be 0.002% on raw magnesite and 0.97% on reacted magnesite hence confirming that magnesite is a sink of sulphur from AMD.

6.1.3 Characterization of bentonite clay

Al and Si were observed to be present at notable levels hence the name aluminosilicate. The presence of Fe and sulphur indicates possible adsorption of Fe and S during geological deposition. MgO, CaO, Na_2O and K_2O show that these are the main exchangeable cations in the bentonite clay matrices. The chemical composition of AMD-reacted bentonite clay showed an increase in the contents of Al, Fe, Mn, Ca and SO_3 indicating the adsorption and retention of inorganic contaminants from AMD. A decrease in Na, K and Mg indicated that polycations of Al, Fe and Mn were exchanged by those polycations through isomorphous

substitution. Montmorillonite, quartz, muscovite, calcite, and dolomite were observed to be the mineral phases which are present in bentonite clay matrices. The AMD-reacted bentonite clay contained montmorillonite, quartz, muscovite, calcite, dolomite and magnetite. This indicated that there was mineralogical transformation during contact with AMD. The SEM micrographs showed the presence of spherical agglomerates on the bentonite clay matrices. After contacting AMD the SEM micrographs showed a slight alteration in the morphology of bentonite clay since the spherical agglomerates were still intact indicating that the mechanical structure of bentonite clay was not affected by the reaction of bentonite clay and AMD. FTIR showed the presence of Si-O, Al-Al-OH, OH, Al-Al-OH, Al-Fe-OH, Al-Mg-OH, CO_3 stretches were observed to be present in bentonite clay. The surface area of ball milled bentonite clay was observed to be 37.1 m^2/g which increased to 70 m^2/g hence indicating that the materials are being deposited to the surfaces of clay mineral. CEC was observed to be independent of pH. It was observed to decrease from 280.8 to 163 meq/100g after reacting bentonite clay with AMD, thus, indicating the exchange of low density species with high density species.

6.1.4 Characterization of the composite

The composite was reported to contained montmorillonite, quartz, dolomite, calcite, brucite, periclase and muscovite**.** AMD-reacted composite was observed to be constituted of montmorillonite, kaolinite, microcline, quartz, dolomite, brucite, calcite, gibbsite and muscovite**.** The presence of gibbsite, periclase and quartz showed that the material has been mineralogically transformed. The presence of kaolinite, microcline, quartz, dolomite, brucite, calcite, gibbsite and muscovite indicate the adsorption, precipitation and co-precipitation of Al, Fe, Mn, Ca, Mg, K and Na which are the main culprit in AMD. Elementally, the composite was dominated by Al, Mg and Si hence showing that the material is a combination of magnesite and a clay mineral. After contacting AMD with the composite, there was a drastic reduction in Na and K on the composite matrices. This may be described by an increase in Na and K in product water post treatment. Ca, SO_3, Mn and Fe were observed to increase in the secondary residue. The raw composite is characterised of irregular (heterogeneous) shape and size, and tend to be in the form of agglomerated clusters of small particles. The EDS showed that Al, Si and Mg are the major chemical species with traces of Fe, Ca, Na and K. The presents of Na, Mg, Ca and K indicates that these are the exchangeable cations on the composite interlayers. SEM micro image is showing that the particles are of the order of micrometres and have irregular shapes with sharp edges. The

agglomerates were observed to contain flowery lumps suspended on the surface of reacted composite. FTIR showed the presence of MgO, Si-O, Al-Al-OH, OH, Al-Al-OH, Al-Fe-OH, Al-Mg-OH, CO_3 stretches were observed to be present in bentonite clay. The surface area was observed to decrease from 18.3 to 15.9 m^2/g. CEC was determined to be independent of pH since it was 437 and 442 meq/ 100g at pH 5 and 7 respectively.

6.1.5 Treatment of AMD with cryptocrystalline magnesite

Contact of AMD with magnesite led to an increase in pH and a notable reduction in metal and sulphate concentrations. Removal of Al, Mn, Fe and other metals was maximized after 60 min of agitation for a S: L ratio of 1 g: 100 mL and particle size ranging from 0.1 – 125 µm. Under these conditions, the pH achieved was >10, an ideal regime for metal removal. Using geochemical modelling, it was shown that most metals e.g. Fe, Al, Mn, and Ca formed sulphate-bearing minerals. From modelling simulations, the formation of these phases follow a selective precipitation sequence with Fe^{3+} at pH > 6, Al^{3+} at pH > 6, Fe^{2+} at pH > 8, Mn^{2+}, Ca^{2+} and Mg^{2+} at pH >10. This study has pointed to the efficiency of magnesite in neutralizing and attenuating metals from AMD and metalliferous industrial effluents. A disadvantage of this technology is that most of earth alkali and alkaline earth metals remain in solution which means a post treatment processes such as ion exchange or reverse osmosis might be required for polishing the product water.

6.1.6 Treatment of AMD with a vibratory ball milled bentonite clay

The use of vibratory, ball-milled bentonite clay for neutralisation of acidity and removal of heavy metals from acidic and metalliferous mine effluents has delivered good results in treating AMD on a laboratory-scale. Contact of AMD with ball milled bentonite clay led to an increase in pH and large decreases in major metal concentrations. EC and TDS were observed to increase following treatment of AMD with bentonite clay, indicating possible release of basic cations to the aqueous solution through ion-exchange processes. Optimum conditions using bentonite clay for AMD treatment at bench scale were determined to be 1 g of adsorbent to 100 mL of AMD with 30 mins of equilibration with shaking. Even though major cations were removed from AMD there is a need to further “polish” treated AMD to lower the residual concentration of sulphate. However, ball-milled bentonite clay treatment resulted in water that met some of the water quality guidelines requirements as compared to the poorer performance of mortar-and-pestle milled bentonite.

6.1.7 Treatment of AMD with cryptocrystalline magnesite-bentonite clay composite

Optimization experiments revealed that 20 min of equilibration and a 1 g of composite dosage were the optimum conditions under these laboratory conditions for treatment of AMD with magnesite-bentonite clay composite at 1:100 S/L ratios. The adsorption process fitted pseudo-second-order kinetics rather than pseudo-first-order kinetics, confirming that the step governing chemical reaction is chemisorption. In adsorption modelling the data conformed best to the Freundlich adsorption isotherm than Langmuir adsorption isotherm hence confirming multilayer adsorption. Four processes were observed to govern the treatment of AMD using the composite, namely, (1) adsorption, (2) precipitation, (3) co-precipitation and (4) ion-exchange. The composite proved to be effective for treatment of AMD as compared to traditional wastewater treatment methods such as limestone, magnesite, clays, lime and bentonite blend. It also produced water to potable standard. This study showed that magnesite and bentonite clay composite can be an efficient and effective technology for treatment of AMD. Nonetheless, more studies need to be carried out using AMD from various sources to test the capacity of the composite to treat AMD of various geochemical origins.

6.1.8 Overall significance of the study and hypothesis

This study proved that magnesite-bentonite clay composite is better candidate as compared to magnesite and bentonite clay individually. The mechanochemically modified composite managed to reclaim water to usable standards as stipulated by the water quality guidelines hence making it a replacement for conventional methods that are used for AMD treatment. Magnesite and bentonite clay individually showed some good performances however they were not fully effective. This suggests that magnesite can be used as a pre-treatment step for a number of treatment technologies that are proven to work. Bentonite clay can be used as a polishing technology for pre-treated mine water due to poor adsorption capacities at elevated concentrations.

This study successfully proved the hypothesis which state that magnesite-bentonite clay composite is a better candidate for acid mine drainage treatment as compared to cryptocrystalline magnesite and bentonite clay individually.

6.2 Recommendations

The application of magnesite and bentonite clay blends for remediation of AMD showed promise for AMD treatment and remediated water to almost within DWAF Water Quality Guidelines standards. However, further research studies are needed in this area if this technology is to be employed on a larger scale. As such, this study identified several research areas that could be pursued:

- Ability of magnesite and its composite to neutralize and remove inorganic contaminants from AMD was tested against one type of AMD from a gold mine in the Western Basin. Further investigations are needed to be carried out to establish the effectiveness of the composite and magnesite to treat AMD from different sources including neutral drainage.

- This study only focused on batch laboratory experiments and validation of experimental results using a geochemical model. AMD formation is a natural process that can take place in abandoned underground workings as well as surface tailings dumps. Column studies that can simulate natural processes under the force of gravity need to be carried out in attempts to study the effectiveness of magnesite or the composite to stabilize tailings dumps, neutralize acidity and remove inorganic contaminants from tailings leachates.

- Magnesite has been successfully employed in treating acidic and metalliferous mine drainage, further research can be pursued with the aim to explore the possibility of using magnesite mine-tailings for the treatment of AMD, stabilization of gold- and coal-mine tailings and recovery of metals.

- Pilot test and large scale test need to be developed and performed to determine the efficiency of the material at a large scale set up.

- Hybrid systems that can be used in integration with magnesite and magnesite bentonite clay composite need to be developed to further polish the water to required standards for myriad of defined uses.

APPENDICES

Appendix A: Schematic presentation of a proposed treatment plant

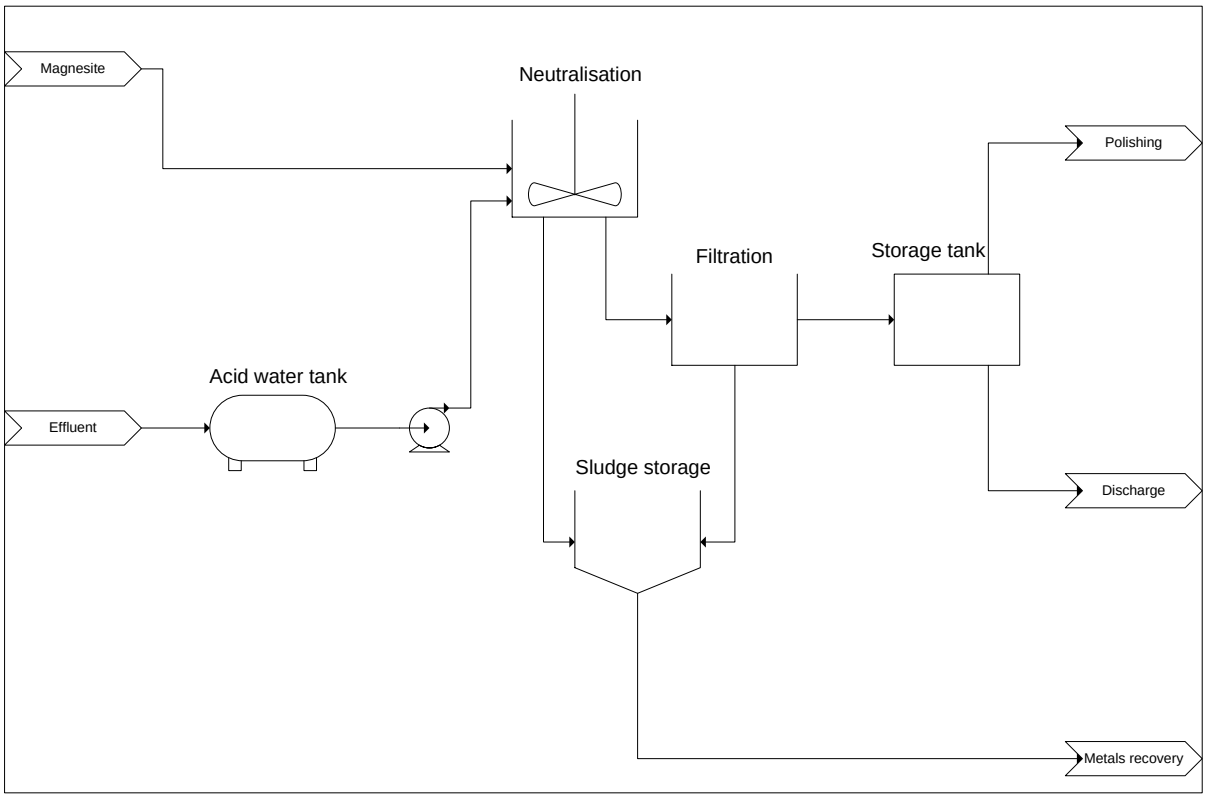

Appendix B: Experimental results

Table B1: Effect of contact time on treatment of acid mine drainage using cryptocrystalline magnesite

Effect of time										
	Al	STDV	Mn	STDV	Fe	STDV	Sulphate	STDV	pH	STDV
1	95	±2.52	92	±1.53	99	±0.58	59	±5.20	7	±0.15
10	100	±0.10	98	±1.76	100	±0.25	69	±3.46	9	±0.36
20	100	±0.40	100	±0.06	100	±0.10	75	±1.55	9	±0.17
60	100	±0.03	100	±0.00	100	±0.06	75	±1.15	10	±0.23
120	100	±0.05	100	±0.06	100	±0.00	75	±1.15	10	±0.10
180	100	±0.00	100	±0.05	100	±0.05	75	±0.58	10	±0.00
240	100	±0.01	100	±0.12	100	±0.03	75	±6.35	10	±0.00
300	100	±0.02	100	±0.06	100	±0.03	75	±0.58	10	±0.00
400	100	±0.05	100	±0.12	100	±0.05	75	±5.00	10	±0.50

Table B2: Effect of magnesite dosage on treatment of acid mine drainage using cryptocrystalline magnesite

Effect of dosage										
	Al	STDV	Mn	STDV	Fe	STDV	Sulphate	STDV	pH	STDV
0.1	76	±3.21	70	±1.00	97	±1.31	20	±10.000	7	±0.500
0.5	97	±0.25	100	±0.15	100	±0.15	33	±2.887	8	±0.153
1	100	±0.12	100	±0.03	100	±0.02	75	±0.000	10	±0.500
2	100	±0.02	100	±0.00	100	±0.01	83	±5.774	11	±0.289
4	100	±0.06	100	±0.03	100	±0.00	93	±6.351	11	±1.041
6	100	±0.00	100	±0.03	100	±0.01	97	±1.732	11	±0.764
8	100	±0.00	100	±0.06	100	±0.58	99	±7.095	11	±0.361

Table B3: Effect of particle size on treatment of acid mine drainage using cryptocrystalline magnesite

Effect of particle size										
	Al	STDV	Mn	STDV	Fe	STDV	Sulphate	STDV	pH	STDV
1	100	±0.28	100	±0.06	100	±0.000	81	±5.00	11	±0.00
32	100	±0.10	100	±0.52	100	±0.003	79	±4.04	11	±0.29
125	100	±0.16	100	±1.10	100	±0.263	80	±2.89	11	±0.76
250	100	±1.09	73	±3.61	100	±0.113	60	±5.00	8	±0.50
500	100	±0.56	40	±0.00	100	±0.574	50	±2.89	7	±0.76
2000	86	±1.00	21	±3.61	95	±1.528	20	±2.89	5	±0.32

Table B4: Effect of chemical species concentration on treatment of acid mine drainage using cryptocrystalline magnesite

Effect of chemical species concentration													
Al	**% removal**	**STDV**	**Mn**	**% removal**	**STDV**	**Fe**	**% removal**	**STDV**	**Sulphate**	**% removal**	**STDV**	**pH**	**STDV**
2	100	±0.035	1	100	±0.153	16	100	±0.006	47	100	±0.015	12	±0.3
3	100	±0.015	2	100	±0.115	31	100	±0.006	94	100	±0.032	12	±0.15
6	100	±0.015	3	100	±0.404	63	100	±0. 023	188	100	±0.456	12	±0.75
13	100	±0.032	6	100	±0.021	125	100	±0.012	375	100	±4.041	11	±1.00
25	100	±0.469	13	100	±0.406	250	100	±0.032	750	94	±2.887	12	±0.50
50	100	±0.317	25	100	±0.045	500	100	±0.546	1500	80	±6.028	11	±0.50
100	100	±0.010	50	100	±0.041	1000	100	±0.000	3000	61	±20.000	11	±0.50
200	100	±0.046	100	100	±0.234	2000	100	±0.000	6000	40	±55.076	10	±0.29

Table B5: Effect of contact time on treatment of acid mine drainage using bentonite clay

Effect of contact time										
	Al	**STDV**	**Mn**	**STDV**	**Fe**	**STDV**	**Sulphate**	**STDV**	**pH**	**STDV**
1	10	±0.764	5	±1.000	8	±1.000	20	±5.033	3	±0.500
5	20	±1.155	10	±1.000	15	±1.528	26	±1.000	4	±0.321
10	70	±2.646	5	±2.000	80	±7.638	33	±2.517	5.5	±0.451
15	80	±2.517	20	±2.887	90	±4.041	35	±3.606	5.5	±0.200
20	85	±5.000	30	±2.517	90	±6.028	35	±1.000	5.5	±0.289
30	85	±5.000	40	±2.646	90	±1.528	35	±2.517	5.5	±0.379
60	85	±1.000	40	±3.215	90	±1.528	35	±1.000	5.5	±0.252
180	85	±1.155	40	±2.082	90	±5.000	35	±2.000	5.5	±0.208
360	85	±1.528	40	±2.646	90	±3.606	35	±3.000	5.5	±0.300

Table B6: Effect of bentonite clay dosage on treatment of acid mine drainage using bentonite clay

Effect of adsorbent dosage										
	Al	**STDV**	**Mn**	**STDV**	**Fe**	**STDV**	**Sulphate**	**STDV**	**pH**	**STDV**
0.1	5	±1.000	2	±0.252	3	±1.000	10	±2.000	3.5	±0.289
0.5	40	±1.000	20	±2.082	30	±0.577	30	±2.646	4	±0.100
1	70	±1.528	40	±2.082	65	±2.000	35	±1.528	6	±0.265
2	85	±2.082	80	±1.528	90	±1.528	75	±1.528	7	±0.100
4	95	±2.000	88	±1.000	99	±1.000	80	±1.000	7.5	±0.265
6	99	±1.000	90	±1.528	99	±0.577	85	±1.000	8	±0.265
8	99	±1.000	94	±1.000	99	±1.000	90	±1.528	8.5	±0.321

Table B7: Effect of chemical species concentration on treatment of acid mine drainage using bentonite clay

Effect of chemical species concentration													
Al	**% removal**	**STDV**	**Mn**	**% removal**	**STDV**	**Fe**	**% removal**	**STDV**	**Sulphates**	**% removal**	**STDV**	**pH**	**STDV**
2	100	±0.500	1	99	±1.000	15	100	±1.136	50	96	±2.884	7	±0.321
2.5	100	±0.300	2	100	±0.500	30	100	±1.509	100	98	±1.311	6.5	±0.361
5	100	±0.529	2.5	100	±0.503	65	100	±2.640	200	98	±2.082	6	±0.115
15	100	±1.136	5	100	±0.408	125	100	±0.996	375	98	±1.026	6	±0.153
25	100	±1.510	15	100	±0.543	250	100	±1.526	750	99	±1.046	6	±0.265
50	100	±0.572	25	100	±0.461	500	100	±0.999	1500	90	±2.517	6	±0.153
100	100	±0.995	50	100	±0.468	1000	100	±0.955	3000	67	±1.347	5.5	±0.416
200	100	±1.719	100	99	±0.551	2000	100	±1.405	6000	33	±2.269	5.5	±0.252

Table B8: Effect of contact time on treatment of acid mine drainage using cryptocrystalline magnesite-bentonite clay composite

Effect of contact time										
	Al	**STDV**	**Mn**	**STDV**	**Fe**	**STDV**	**Sulphate**	**STDV**	**pH**	**STDV**
1	75	±2.89	70	±2.52	90	±2.52	10	±42.72	6	±0.31
5	100	±0.10	89	±0.76	98	±1.00	15	±6.35	8	±0.25
10	100	±0.23	99	±0.00	100	±0.15	24	±1.15	10	±0.25
15	100	±0.05	100	±0.06	100	±0.02	50	±7.51	11	±0.25
20	100	±0.01	100	±0.04	100	±0.04	50	±25.17	11	±1.00
30	100	±0.01	100	±0.02	100	±0.02	50	±6.08	11	±0.32
60	100	±0.05	100	±0.04	100	±0.04	48	±103.64	11	±0.26
180	100	±0.02	100	±0.03	100	±0.02	53	±31.75	11	±0.10
360	100	±0.02	100	±0.06	100	±0.04	53	±3.79	11	±0.33

Table B9: Effect of composite dosage on treatment of acid mine drainage using cryptocrystalline magnesite-bentonite clay composite

Effect of adsorbent dosage										
	Al	**STDV**	**Mn**	**STDV**	**Fe**	**STDV**	**Sulphate**	**STDV**	**pH**	**STDV**
0.1	82	±1.53	39	±2.65	95	±0.76	85	±1.02	6	±0.32
0.5	99	±0.55	79	±3.21	99	±0.54	92	±1.11	8	±0.25
1	100	±0.50	98	±2.08	100	±1.09	99	±1.04	10	±0.00
2	100	±0.57	100	±0.01	100	±0.06	100	±0.43	11	±0.06
4	100	±0.00	100	±1.00	100	±0.12	100	±0.68	12	±0.50
6	100	±0.00	100	±0.63	100	±0.52	100	±0.58	12	±0.17
8	100	±0.00	100	±0.11	100	±0.29	100	±0.12	12	±0.46
10	100	±0.00	100	±0.01	100	±0.35	100	±1.21	12	±0.46

Table B10: Effect of bentonite clay to cryptocrystalline magnesite ratio on treatment of acid mine drainage

Effect of dosage to dosage ratio										
	Al	**STDV**	**Mn**	**STDV**	**Fe**	**STDV**	**Sulphate**	**STDV**	**pH**	**STDV**
0.1: 1	100	±0.50	99	±0.55	100	±0.58	85	±0.51	10	±0.90
0.2: 1	100	±0.45	100	±0.87	100	±1.52	93	±1.71	11	±0.29
1:1	100	±0.15	100	±0.05	100	±0.58	99	±0.41	11	±0.25
2:1	100	±0.00	100	±6.30	100	±1.15	100	±0.25	12	±0.29
3:1	100	±0.56	100	±1.10	100	±0.57	100	±0.88	12	±0.21
4:1	100	±0.00	100	±1.21	100	±0.63	100	±1.17	12	±0.23

Table B11: Effect of chemical species cocentration on treatment of acid mine drainage using cryptocrystalline magnesite-bentonite clay composite

Effect of chemical species concentration													
Al	**% removal**	**STDV**	**Mn**	**% removal**	**STDV**	**Fe**	**% removal**	**STDV**	**Sulphate**	**% removal**	**STDV**	**pH**	STDV
2	100	±0.115	1	100	±0.577	16	100	±0.500	47	100	±0.577	11	±0.289
3	100	±0.462	2	100	±0.265	31	100	±1.000	94	100	±0.115	11	±0.500
6	100	±0.115	3	100	±0.346	63	100	±2.309	188	100	±1.155	11	±0.416
13	100	±0.346	6	100	±0.529	125	100	±0.608	375	100	±2.309	11	±0.404
25	100	±2.082	13	100	±0.462	250	100	±1.000	750	100	±0.252	11	±0.115
50	100	±0.529	25	100	±1.674	500	100	±0.115	1500	98	±0.058	11	±0.115
100	100	±0.300	50	100	±1.155	1000	100	±0.577	3000	95	±1.015	11	±0.603
200	100	±0.577	100	100	±0.468	2000	100	±0.361	6000	90	±1.000	10	±1.127

Appendix C: Papers

Paper 1

Passive remediation of acid mine drainage using cryptocrystalline magnesite: A batch experimental and geochemical modelling approach.

Vhahangwele Masindi[1,2]*, Mugera Wilson Gitari[1], Hlanganani Tutu[3] and Marinda De Beer[4]

[1]*Environmental Remediation and Water Pollution Chemistry Research Group, Department of Ecology and Resources Management, School of Environmental Science, University of Venda, P/bag X5050, Thohoyandou, 0950, South Africa*

[2]*Molecular Sciences Institute, School of Chemistry, University of the Witwatersrand, P/Bag X4, WITS, 2050, Johannesburg, South Africa*

[3]*CSIR (Council of Scientific and Industrial Research), Built Environment, Building Science and Technology (BST), P.O Box 395, Pretoria, 0001, South Africa*

[4]*DST/CSIR National Centre for Nano-Structured Materials, Council for Scientific and Industrial Research, P.O Box 395, Pretoria, 0001, South Africa*

ABSTRACT

Acid mine drainage is generated when mining activities expose sulphidic rock to water and oxygen leading to generation of sulphuric acid effluents rich in Fe, Al, SO_4 and Mn with minor concentrations of Zn, Cu, Mg, Ca, Pb depending on the geology of the rock hosting the minerals. These effluents must be collected and treated before release into surface water bodies. Mining companies are in constant search for cheaper, effective and efficient mine water treatment technologies. This study assessed the potential of applying magnesite as an initial remediation step in an integrated acid mine drainage (AMD) management system. Neutralization and metal attenuation was evaluated using batch laboratory experiments and simulations using geochemical modelling. Contact of AMD with cryptocrystalline magnesite for 60 min at 1 g: 100 mℓ S/L ratio led to an increase in pH, and a significant increase in metals attenuation. Sulphate concentration was reduced to ≈1 910 mg/ℓ. PH redox equilibrium (in C language) (PHREEQC) geochemical modelling results showed that metals precipitated out of solution to form complex mineral phases of oxy-hydroxysulphates, hydroxides, gypsum and dolomite. The results of this study showed that magnesite has potential to neutralize AMD, leading to the reduction of sulphate and precipitation of metals.

Keywords: acid mine drainage, cryptocrystalline magnesite, toxic metals, geochemical modelling, water treatment

INTRODUCTION

The aftermath of gold and coal mining has triggered serious environmental problems that need urgent attention prior to degradation of terrestrial and aquatic ecosystems and their ability to foster life (Jooste et al., 1999; Luís et al., 2009; Raymond et al., 2009; Equeenuddin et al., 2010). Mining of the aforementioned minerals exposes sulphide-bearing minerals to oxidising conditions. During rainfall and underground working, sulphide minerals react with water and oxygen leading to the formation of highly acidic mine effluent known as acid mine drainage (AMD). The acidity in AMD promotes the leaching of heavy metals from the surrounding geology (Johnson et al., 2005; Sheoran et al., 2006; Cheng et al., 2009; Simate et al., 2014; Amos et al., 2015; Delkash et al., 2015). The equation below shows the formation of acid mine drainage using pyrite as an example (Simate et al., 2014):

$$4FeS_2 + 15O_2 + 14H_2O \xrightarrow{\text{bacteria}} 4Fe(OH)_3 + 8SO_4^{2-} + 16H^+ \quad (1)$$

In the Witwatersrand gold ores of South Africa, for instance, up to 70 minerals have been identified, including gold, pyrite, uraninite (U_3O_8), sphalerite (ZnS), galena (PbS) and various silicates among others (Tutu et al., 2008, 2009). Numerous technologies have been developed for remediation of acid mine drainage (Gitari et al., 2008; Delkash et al., 2015; Lakovleva et al., 2015). The commonly used technologies include ion exchange (Buzzi et al., 2013), reverse osmosis (Johnson et al., 2005), adsorption (Gitari, 2014; Lakovleva et al., 2015), biosorption (Sheoran et al., 2006) and precipitation (Bologo et al., 2012; Maree et al., 2013). However, generation of secondary sludge, toxicity, high operation costs, poor efficiency and demand for large expanses of land limit the application of the majority of developed technologies (Johnson et al., 2005; Kalin et al., 2006; Sheoran et al., 2006, Simate et al., 2014).

The Witwatersrand Basin produces approximately 340 Mℓ/day of mine water (Bologo et al., 2012) and this has been reported to impair the quality of water downstream (Jooste et al., 1999). Treatment of large volumes of mine effluents requires a very effective and efficient technology. In South Africa, limestone has been widely used as the main chemical agent for neutralization and removal of metals in acid mine waters (Maree et al., 1994, 2004, 2013). However, the use of limestone has the limitation of precipitating toxic metals with gypsum and raising pH > 7 (Maree et al., 1993).

* To whom all correspondence should be addressed.
☎ + 2712 841 4107, E-mail: VMasindi@csir.co.za; masindivhahangwele@gmail.com

Received: 26 November 2014; accepted in revised from 15 September 2015

http://dx.doi.org/10.4314/wsa.v41i5.10
Available on website http://www.wrc.org.za
ISSN 1816-7950 (On-line) – Water SA Vol. 41 No. 5 October 2015
Published under a Creative Commons Attribution Licence

Paper 2

G Model
JECE 1022 No. of Pages 11

ARTICLE IN PRESS

Journal of Environmental Chemical Engineering xxx (2015) xxx–xxx

Contents lists available at ScienceDirect

Journal of Environmental Chemical Engineering

journal homepage: www.elsevier.com/locate/jece

Fate of inorganic contaminants post treatment of acid mine drainage by cryptocrystalline magnesite: Complimenting experimental results with a geochemical model

Vhahangwele Masindi[a,c,*], Mugera W. Gitari[a], Hlanganani Tutu[b], Marinda De Beer[d]

[a] Environmental Remediation and Pollution Chemistry Research Group, Department of Ecology and Resources Management, School of Environmental Science, University of Venda, Pvbag X5050, Thohoyandou, 0950, South Africa
[b] Molecular Sciences Institute, School of Chemistry, University of the Witwatersrand, Pvbag X4, WITS, 2050, Johannesburg, South Africa
[c] CSIR (Council of Scientific and Industrial Research), Built Environment, Building Science and Technology (BST), P.O. Box 395, Pretoria, 0001, South Africa
[d] DST/CSIR National Centre for Nano-Structured Materials, Council for Scientific and Industrial Research, P.O. Box 395, Pretoria, 0001, South Africa

ARTICLE INFO

Article history:
Received 13 November 2015
Received in revised form 17 February 2016
Accepted 11 March 2016
Available online xxx

Keywords:
Acid mine drainage
Magnesite
Toxic metals
Sulphate
Neutralization
Geochemical modelling

ABSTRACT

This study assessed the fate of inorganic contaminants post treatment of acid mine drainage by cryptocrystalline magnesite. To accomplish that, neutralization and metal attenuation were evaluated and complemented with simulations using geochemical modeling. Mineral phase formation and changes during the reaction of magnesite and AMD were also evaluated. The geochemical computer code PHREEQC and WATEQ4 database was used for geochemical modelling of the process water. Interaction of AMD with magnesite at an optimum solid: liquid ratio of 1:100 and contact time of 60 min led to an increase in pH, reaching a maximum pH of 10, resulting in significant precipitation of most metal species. Increase of pH in solution with contact time caused the removal of the metal ions mainly by precipitation, co-precipitation and adsorption. Sulphate concentration was lowered from 4640 down to 1910 mg/L. Fe was mainly removed as $Fe(OH)_3$, goethite, and jarosite, Al as basaluminite, boehmite and jurbanite, Al $(OH)_3$ and as gibbsite and diaspore. Al and Fe precipitated as iron (oxy)-hydroxides and aluminium (oxy)-hydroxides. Mn precipitated as rhodochrosite and manganite. Ca was removed as gypsum. Sulphate was removed as gypsum, and Fe, Al hydroxyl sulphate minerals. Mg was removed as brucite and dolomite. Cryptocrystalline magnesite effectively neutralized AMD and attenuated concentration of inorganic species to within department of water affairs and sanitation (DWAS) water quality guidelines.

© 2016 Elsevier Ltd. All rights reserved.

1. Introduction

Mining contributes significantly to the gross domestic product and, consequently, to the economy of South Africa. However, it has been reported to impair the quality of terrestrial and aquatic ecosystems and their integrities to foster life due to generation of acid mine drainage (AMD). AMD is a common legacy in most gold and coal mines and results from the oxidation of pyrite (FeS_2) in the host rock [1–8]. AMD is formed when sulphide minerals such as pyrite are exposed to oxygen and water leading to the formation of iron hydroxide, sulphate and acid as indicated in Equation (1).

$$4FeS_2 + 15O_2 + 14H_2O \xrightarrow{bacteria} 4Fe(OH)_3 + 8SO_4^{2-} + 16H^+ \quad (1)$$

This acid promotes weathering and leaching of toxic elements such as Al, Fe, As, B, Ba, Co, Cr, Cu, Mo, Ni, Sr, Zn and Mn contained in the host rock [2–11]. In the Witwatersrand basin gold mines in South Africa, close to 70 minerals have been identified in the host rock including gold, pyrite, uraninite (U_3O_8), sphalerite (ZnS), galena (PbS) and various silicates [2,4–6,8,10].

In the last decades, AMD has received great attention due to the devastating impacts that it can impose onto aquatic and terrestrial ecosystems. Currently, a total volume of 360 ML/d is generated by gold mines in Johannesburg which is decanting to adjacent aquatic ecosystem and accelerating the degradation of waterbodies downstream. Out of that, 20 ML/d of contaminated water flows into the Tweelopies Spruit near Randfontein (Western Basin). Research studies also pointed out that, by 2015, a further 60 ML/d will decant near Boksburg (Central Basin) and a further 120 ML/day

* Corresponding author at: Environmental Remediation and Pollution Chemistry Research Group, Department of Ecology and Resources Management, School of Environmental Science, University of Venda, Pvbag X5050, Thohoyandou, 0950, South Africa.
E-mail address: VMasindi@csir.co.za (V. Masindi).

http://dx.doi.org/10.1016/j.jece.2016.03.020
2213-3437/© 2016 Elsevier Ltd. All rights reserved.

Please cite this article in press as: V. Masindi, et al., Fate of inorganic contaminants post treatment of acid mine drainage by cryptocrystalline magnesite: Complimenting experimental results with a geochemical model, J. Environ. Chem. Eng. (2016), http://dx.doi.org/10.1016/j.jece.2016.03.020

Paper 3

Journal of Water Process Engineering 8 (2015) 227–240

Contents lists available at ScienceDirect

Journal of Water Process Engineering

journal homepage: www.elsevier.com/locate/jwpe

Efficiency of ball milled South African bentonite clay for remediation of acid mine drainage

Vhahangwele Masindi [a,c,*], Mugera W. Gitari [a], Hlanganani Tutu [b], Marinda DeBeer [d]

[a] Environmental Remediation and Water Pollution Chemistry Research Group, Department of Ecology and Resources Management, School of Environmental Science, University of Venda, Pjbag X5050, Thohoyandou 0950, South Africa
[b] Molecular Sciences Institute, School of Chemistry, University of the Witwatersrand, Pjbag X4, WITS, 2050 Johannesburg, South Africa,
[c] CSIR (Council of Scientific and Industrial Research), Built Environment, Building Science and Technology (BST), P. O. Box 395, Pretoria 0001, South Africa,
[d] DST/CSIR National Centre for Nano-Structured Materials, Council for Scientific and Industrial Research, P. O. Box 395, Pretoria 0001, South Africa

ARTICLE INFO

Article history:
Received 30 May 2015
Received in revised form 22 October 2015
Accepted 5 November 2015

Keywords:
Acid mine drainage
Bentonite clay
Ball-milling
Neutralization
Heavy metals
Adsorption

ABSTRACT

The feasibility of using vibratory ball milled South African bentonite clay for neutralization and attenuation of inorganic contaminants from acidic and metalliferous mine effluents has been evaluated. Treatment of acid mine drainage (AMD) with bentonite clay was done using batch laboratory assays. Parameters optimized included contact time, adsorbent dosage and adsorbate concentration. Ball milled bentonite clay was mixed with simulated AMD at specific solid: liquid (S/L) ratios and equilibrated on a table shaker. Contact of AMD with bentonite clay led to an increase in pH and a significant reduction in concentrations of metal species. At constant agitation time of 30 min, the pH increased with the increase in dosage of bentonite clay. Removal of Mn^{2+}, Al^{3+}, and Fe^{3+} was greatest after 30 min of agitation. The adsorption affinity obeyed the sequence: SO_4^{2-} (221.8 mg g^{-1}) > Mn (30.7 mg g^{-1}) > Al (30.5 mg g^{-1}) > Fe (30.2 mg g^{-1}). The pH of reacted AMD ranged from ≈3 to 6. Bentonite clay showed high adsorption capacities for Al and Fe at concentration <500 mg/L, while the capacity for Mn was lower. Adsorption capacity for sulphate was >50%. Adsorption kinetics revealed that the suitable kinetic model describing data was pseudo-second-order hence confirming chemisorption. Adsorption isotherms indicated that removal of metals fitted the Langmuir adsorption isotherm for Fe and sulphate and the Freundlich adsorption isotherm for Al and Mn, respectively. Ball-milled bentonite clay showed an excellent capacity in neutralizing acidity and lowering the levels of inorganic contaminants in acidic mine effluents.
© 2015 Elsevier Ltd. All rights reserved.

1. Introduction

Exposure of sulphide bearing minerals to water and oxygen during and following mining activities accelerates the formation of acid mine drainage (AMD) which is very acidic and metalliferous. The acidity in AMD promotes the leaching of heavy metals from the surrounding geology. Due to its acidic nature and high loads of heavy metals, AMD has high electrical conductivity (EC) and total dissolved solids (TDS) concentration which are considerably above the recommended limits for effluents to be discharged into rivers. Thus mine effluent needs to be contained and managed prior to release to the environment as an initial step in preventing environmental degradation [1–4].

Discharge of AMD to the environment can reduce the ability of any ecosystem to support life. It lowers water quality rendering it unfit for defined uses such as for domestic and agricultural purposes [5,6]. It also leads to iron sedimentation in aquatic ecosystems due to precipitation of iron hydroxide (yellow boy sludge). The suspended flocs also lead to reduced hunting abilities of fish due to poor visibility in water bodies [7]. Toxic chemical species in AMD pose hazards to terrestrial and aquatic organisms [8]. Acidity in water leads to the migration of certain species less tolerant to acidic conditions affecting the integrity of the ecosystem to support life due to reduced biodiversity [7,9–19]. This has emphasized the need to develop pragmatic solutions to treat AMD by neutralizing the acidity and removing heavy loads of dissolved metals and sulphate.

Due to their high surface areas, cation-exchange capacity (CEC), swelling ability, low cost, abundance and versatility, clays have

* Corresponding author at: Council for Scientific and Industrial Research (CSIR), Built Environment, Building Science and Technology (BST), P. O. Box 395, Pretoria 0001, South Africa.
E-mail addresses: VMasindi@csir.co.za, masindivhahangwele@gmail.com (V. Masindi).

http://dx.doi.org/10.1016/j.jwpe.2015.11.001
2214-7144/© 2015 Elsevier Ltd. All rights reserved.

Paper 4

G Model
JWPE-206; No. of Pages 16
ARTICLE IN PRESS
Journal of Water Process Engineering xxx (2015) xxx–xxx
Contents lists available at ScienceDirect
Journal of Water Process Engineering
journal homepage: www.elsevier.com/locate/jwpe

Synthesis of cryptocrystalline magnesite–bentonite clay composite and its application for neutralization and attenuation of inorganic contaminants in acidic and metalliferous mine drainage

Vhahangwele Masindi[c,*], Mugera W. Gitari[a], Hlanganani Tutu[b], Marinda DeBeer[d]

[a] Environmental Remediation and Water Pollution Chemistry Research Group, Department of Ecology and Resources Management, School of Environmental Science, University of Venda, Pjbag X5050, Thohoyandou 0950, South Africa
[b] Molecular Sciences Institute, School of Chemistry, University of the Witwatersrand, Pjbag X4, WITS, 2050 Johannesburg, South Africa
[c] CSIR (Council of Scientific and Industrial Research), Built Environment, Building Science and Technology (BST), P.O Box 395, Pretoria 0001, South Africa
[d] DST/CSIR National Centre for Nano-Structured Materials, Council for Scientific and Industrial Research, P.O. Box 395, Pretoria 0001, South Africa

ARTICLE INFO

Article history:
Received 23 April 2015
Received in revised form
12 November 2015
Accepted 22 November 2015
Available online xxx

Keywords:
Acid mine drainage
Neutralization
Magnesite–bentonite clay composite
Inorganic contaminants
Adsorption modelling

ABSTRACT

The primary aim of this study was to synthesize cryptocrystalline magnesite–bentonite clay composite by mechanochemical activation and evaluate its usability as low cost adsorbent for neutralization and attenuation of inorganic contaminants in acidic and metalliferous mine drainage. The composite was synthesized at 1:1 weight to weight ratio. The capacity of the composite to neutralize acidity and remove toxic chemical species from synthetic and field AMD was evaluated at optimized conditions. Interaction of the composite with AMD led to an increase in pH (pH> 11) and lowering of metal concentrations. The removal of chemical species was optimum at 20 min of equilibration and 1 g of dosage. The composite removed ≈99% (Al^{3+}, Fe^{3+}, and Mn^{2+}) and ≈90% (SO_4^{2-}) from raw mine effluent. Adsorption kinetics fitted better to pseudo-second-order kinetic than pseudo-first-order kinetic hence confirming chemisorption. Adsorption data fitted better to Freundlich adsorption isotherm than Langmuir hence confirming multisite adsorption. Gibbs free energy model predicted that the reaction is spontaneous in nature for Al, Fe and sulphate except for Mn. Geochemical model indicated that Fe was removed as $Fe(OH)_3$, goethite, and jarosite, Al as basaluminite, boehmite and jurbanite, $Al(OH)_3$ and as gibbsite and diaspore. Al and Fe precipitated as iron (oxy)-hydroxides and aluminium (oxy)-hydroxides. Mn precipitated as rhodochrosite and manganite. Ca was removed as gypsum. Sulphate was removed as gypsum, and Fe, Al hydroxyl sulphate minerals. Mg was removed as brucite and dolomite. It was concluded that the composite has the potential to neutralize acidity and attenuate potentially toxic chemical species from acidic and metalliferous mine drainage.

© 2015 Elsevier Ltd. All rights reserved.

1. Introduction

Acidic and metalliferous drainage originating from metal mining activities can cause serious environmental pollution [1]. On release to receiving aquatic ecosystems, acid mine drainage (AMD) can cause major ecological impacts which have the capability to compromise the integrity of terrestrial and aquatic ecosystems to sustain life [2]. In South Africa, AMD is generated by oxidation of pyrite associated with coal and gold seams [3]. During mining processes, pyrite is exposed to water and oxygen and this promotes the formation of AMD post oxidation [4]. During rainfall on tailings dumps and rising groundwater in disused mineshafts, water and oxygen interacts with pyrite leading to the formation of acidic effluent. The resultant acidic water accelerates leaching of metals from surrounding rock strata or tailings [2]. The release of metals to effluent waters makes the water metalliferous. In most instances, the formation of AMD can be represented by the following chemical equations [5]:

$$2FeS_{2(s)} + 7O_{2(g)} + 2H_2O \xrightarrow{bacteria} 2Fe^{2+}_{(aq)} + 4H^{+}_{(aq)} + 4SO^{2-}_{4(aq)} \quad (1)$$

$$4Fe^{2+}_{(aq)} + O_{2(g)} + 4H^{+}_{(aq)} \rightarrow 4Fe^{3+}_{(aq)} + 2H_2O_l \quad (2)$$

$$FeS_{2(s)} + 14Fe^{3+} + 8H_2O \rightarrow 15Fe^{2+} + 2SO^{2-}_{4(l)} + 16H^{+} \quad (3)$$

* Corresponding author.
E-mail addresses: VMasindi@csir.co.z.a, masindivhahangwele@gmail.com (V. Masindi).

http://dx.doi.org/10.1016/j.jwpe.2015.11.007
2214-7144/© 2015 Elsevier Ltd. All rights reserved.

Please cite this article in press as: V. Masindi, et al., Synthesis of cryptocrystalline magnesite–bentonite clay composite and its application for neutralization and attenuation of inorganic contaminants in acidic and metalliferous mine drainage, J. Water Process Eng. (2015), http://dx.doi.org/10.1016/j.jwpe.2015.11.007

Appendix C: Awards and Pictures

Award

Picture 1: Handing over of award

Picture 2: Winners and management

Picture 3: Prof Mugera Wilson Gitari and Dr Vhahangwele Masindi (*Pr. Sci. Nat.*)